THE UNIVERSITY OF WARWICK

Library Declaration and Deposit Agreement

1. **STUDENT DETAILS**

Please complete the following:
Full name: …….
University ID number: ……

2. **THESIS DEPOSIT**

2.1 I understand that under my registration at the University, I am required to deposit my thesis with the University in BOTH hard copy and in digital format. The digital version should normally be saved as a single pdf file.

2.2 The hard copy will be housed in the University Library. The digital version will be deposited in the University's Institutional Repository (WRAP). Unless otherwise indicated (see 2.3 below) this will be made openly accessible on the Internet and will be supplied to the British Library to be made available online via its Electronic Theses Online Service (EThOS) service.
[At present, theses submitted for a Master's degree by Research (MA, MSc, LLM, MS or MMedSci) are not being deposited in WRAP and not being made available via EthOS. This may change in future.]

2.3 In exceptional circumstances, the Chair of the Board of Graduate Studies may grant permission for an embargo to be placed on public access to the hard copy thesis for a limited period. It is also possible to apply separately for an embargo on the digital version. (Further information is available in the *Guide to* Examinations for Higher Degrees by Research.)

2.4 *If you are depositing a thesis for a Master's degree by Research, please complete section (a) below.*
For all other research degrees, please complete both sections (a) and (b) below:

(a) Hard Copy

I hereby deposit a hard copy of my thesis in the University Library to be made publicly available to readers (please delete as appropriate) EITHER immediately OR after an embargo period of ……..... months/years as agreed by the Chair of the Board of Graduate Studies.

I agree that my thesis may be photocopied. YES / NO (*Please delete as appropriate*)

(b) Digital Copy

I hereby deposit a digital copy of my thesis to be held in WRAP and made available via EThOS.

Please choose one of the following options:

EITHER My thesis can be made publicly available online. YES / NO (*Please delete as appropriate*)

OR My thesis can be made publicly available only after…..[date] (Please give date)
YES / NO (*Please delete as appropriate*)

OR My full thesis cannot be made publicly available online but I am submitting a separately identified additional, abridged version that can be made available online.
YES / NO (*Please delete as appropriate*)

OR My thesis cannot be made publicly available online. YES / NO (*Please delete as appropriate*)

3. GRANTING OF NON-EXCLUSIVE RIGHTS

Whether I deposit my Work personally or through an assistant or other agent, I agree to the following:

Rights granted to the University of Warwick and the British Library and the user of the thesis through this agreement are non-exclusive. I retain all rights in the thesis in its present version or future versions. I agree that the institutional repository administrators and the British Library or their agents may, without changing content, digitise and migrate the thesis to any medium or format for the purpose of future preservation and accessibility.

4. **DECLARATIONS**

(a) I DECLARE THAT:

I am the author and owner of the copyright in the thesis and/or I have the authority of the authors and owners of the copyright in the thesis to make this agreement. Reproduction of any part of this thesis for teaching or in academic or other forms of publication is subject to the normal limitations on the use of copyrighted materials and to the proper and full acknowledgement of its source.

The digital version of the thesis I am supplying is the same version as the final, hard-bound copy submitted in completion of my degree, once any minor corrections have been completed.

I have exercised reasonable care to ensure that the thesis is original, and does not to the best of my knowledge break any UK law or other Intellectual Property Right, or contain any confidential material.

I understand that, through the medium of the Internet, files will be available to automated agents, and may be searched and copied by, for example, text mining and plagiarism detection software.

(b) IF I HAVE AGREED (in Section 2 above) TO MAKE MY THESIS PUBLICLY AVAILABLE DIGITALLY, I ALSO DECLARE THAT:

I grant the University of Warwick and the British Library a licence to make available on the Internet the thesis in digitised format through the Institutional Repository and through the British Library via the EThOS service.

If my thesis does include any substantial subsidiary material owned by third-party copyright holders, I have sought and obtained permission to include it in any version of my thesis available in digital format and that this permission encompasses the rights that I have granted to the University of Warwick and to the British Library.

5. **LEGAL INFRINGEMENTS**

I understand that neither the University of Warwick nor the British Library have any obligation to take legal action on behalf of myself, or other rights holders, in the event of infringement of intellectual property rights, breach of contract or of any other right, in the thesis.

Please sign this agreement and return it to the Graduate School Office when you submit your thesis.

Student's signature: .....……
Date: .....

The *in situ* analysis of the microbial community associated with footrot of sheep

By

Luci Ann Witcomb

A THESIS SUBMITTED TO THE UNIVERSITY OF WARWICK FOR THE DEGREE OF
DOCTOR OF PHILOSOPHY

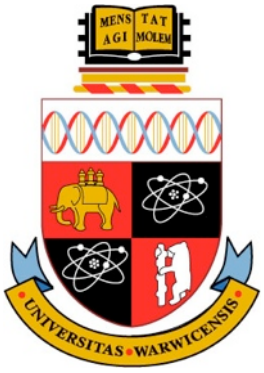

School of Life Sciences
University of Warwick

September 2012

CONTENTS

ACKNOWLEDGEMENTS

I would like to thank my supervisors Prof. Elizabeth Wellington and Prof. Laura Green for their advice and help throughout my time at Warwick. I would also like to thank all past and present members of the CEDFAS project; Dr. Leo Calvo-Bado, Dr. Atiya Ul-Hassan, Dr. Jasmeet Kaler, Dr. Claire Russell, and Dr. Edward Smith, Prof. Graham Medley and Dr. Rose Grogono-Thomas for their help with data analysis and assistance in the lab and in the field.

I would also like to thank all members of lab C123 for their help and support. Additionally, I would like to thank my two lovely housemates Tanya and Hannah for their support. I also want to thank my good friend Poppy and Stone Monkey Yoga Cafe for helping me relax during a rather stressful period. I particularly want to thank Mike, for his massive amount of support (emotional and professional!) and for always being their for me.

And finally, I would like to thank my parents for their support; my mum for her support throughout my school and University years and my dad, who sadly passed away during the writing of this thesis, for his urging me to finish on time.

DECLARATION

The results presented in this thesis are the work of the author unless otherwise stated in the text. None of this work has been previously submitted for a degree application. All sources of information presented in this thesis have been acknowledged by a reference.

ABSTRACT

Footrot (FR) is a highly infectious and debilitating disease of sheep, which has a significant economic impact on the sheep farming industry, in the UK and worldwide and causes significant suffering of sheep. Despite some recent advances, FR remains a scientifically challenging disease to understand. To help improve our understanding of disease pathogenesis, two culture-independent techniques were developed to examine the microbial succession events between the causative agent, *Dichelobacter nodosu*s and an accessory agent, *Fusobacterium necrophorum*, the latter also postulated to be involved in disease initiation. The two populations were monitored in relation to disease initiation and progression during a longitudinal study and disease presentation in tissue biopsies (*in situ*). Finally, the distribution of these two species of bacteria in the environment was examined to highlight possible sources of infection.

The work in this thesis has demonstrated that FR is a disease where expression is related to *D. nodosus* load present in the ovine interdigital space. *D. nodosus* (*rpoD*) load increased from that on a healthy foot to one presenting with interdigital dermatitis (ID) and feet with a higher *D. nodosus* (*rpoD*) load were more likely to go on to develop FR one week later. FISH analysis of the *D. nodosus* population present within the epidermis also revealed similar findings; *D. nodosus* cell counts increased during stages of ID, but the organism was less frequently detected in biopsies from feet with FR. Suggesting that ID might be the most infectious stage of the disease process. A fact that needs to be highlighted to farmers to encourage treatment at this stage of disease. In contrast, *F. necrophorum* (*rpoB*) load did not correlate with ID presentation or prior to the development of FR, but increased the week of FR onset. FISH analysis also revealed that *F. necrophorum* cell counts were higher in feet with FR than those with ID. It is possible therefore that *F. necrophorum* may thrive in the altered environment of a foot presenting with FR, possibly contributing to disease persistence and severity. Finally, both pathogens were detected in a range of environmental samples from a farm with endemic FR, highlighting possible sources of infection and material, which once contaminated with *D. nodosus* and *F. necrophorum* may contribute to the spread of FR.

This study has provided an improved understanding of the microbial population dynamics involved in the development of ID and FR in sheep, which may have implications for control and treatment practices not only in the UK, but world-wide.

ABBREVIATIONS

ANOVA	Analysis of variance
ARB	Antibiotic resistant bacteria
B	Bedding
BBQ	Black Berry Quencher
BE	Blank Extraction
BFR	Benign Footrot
BH	Bedding Hoof
BLAST	Basic Local Alignment
bp	base pair
BSA	Bovine Serum Albumin
cDNA	Complementary deoxyribonucleic acid
CI	Confidence Interval
CF	Concrete floor
CODD	Contagious ovine interdigital dermatitis
D	Dermis
DAPI	4’,6-diamidino-2-phenylindole
DES	DNase/Pyrogen Free Water
DNA	Deoxyribonucleic acid
dNTP	Deoxyribonucleoside triphosphate
DOPE	Double labelling of oligonucleotide probes
DP	Dermal Papillae
dsDNA	Double-stranded deoxyribonucleic acid
E	Epidermis
EB	Elution Buffer
EDB	Epidermal-Boundary
EP	Epidermal Peg
F	Faeces
FAM	6-Carboxy-fluorescein
FF	Feaces Floor
FH	Faeces Hoof
FISH	Fluorescence *in situ* Hybridisation
FITC	Fluorescein isothiocyanate

FMD	Foot and mouth disease
FOV	Field of View
FR	Footrot
GFP	Green Fluorescent Protein
H	Healthy
ha	Hectare
H&E	Haematoxylin & Eosin (stain)
HF	Hair Follicle
HH	Hoof Horn Agar
HPA	Health Protection Agency
hv_{EX}	Excitation photon
hv_{EM}	Emission photon
IFR	Intermediate Footrot
ID	Interdigital Dermatitis
JOE	6-carboxy-4', 5'Dichloro-2', 7'-Dimethoxyfluorescein, Succinimidyl Ester
kb	kilobase pairs
LF	Left Front (foot)
LH	Left Hind (foot)
LB	Luria-Bertani Agar
LOD	Limit of Detection
LPS	Lipopolysaccharide
MHC	Major Histocompatibility Complex
NCS	Negative clinical spike
NFQ	Non-Fluorescent Quencher
NIC	No Inhibition Control
NTC	Non-template Control
OC	Oral Cavity
OR	Odds Ratio
OTU	Operational taxonomic unit
PBS	Phosphate-Buffered Saline
PCR	Polymerase Chain Reaction
PFA	Paraformaldehyde
p.i.	post-inoculation

qPCR	Quantitative Polymerase Chain Reaction
RBC	Red Blood Cell
RD4	Region of Deletion 4
RF	Right Front (foot)
RH	Right Hind (foot)
ROX	5-Carboxy-X-rhodamine (passive reference dye)
RPM	Rounds Per Minute
rRNA	Ribosomal ribonucleic acid
S	Soil
SB	Stratum Basale
SC	Stratum Corneum
SDS	Sodium Dodecyl Sulphate
SD	Standard Deviation
SEM	Standard Error of the Mean
SG	Stratum Granulosum
SS	Stratum Spinosum
TAE	Tris base, acetic acid and EDTA (buffer)
TDL	Theoretical Limit of Detection
UC	Undiluted culture
US	Undiluted spike
VFR	Virulent Footrot
VLA	Veterinary Laboratories agency
v/v	Volume to volume
WC	Wilkins-Chalgren Agar
[wet wt]	Wet weight
w/o	Without
w/v	Weight to volume

C_T	Threshold cycle Cycle number at which fluorescence passes the threshold.
ΔC_T	Delta C_T The difference in the C_T value of a sample compared to that of the no inhibition control (NIC).
ΔRn	Delta Rn Magnitude of signal generated by specific PCR conditions.

LIST OF TABLES

LIST OF FIGURES

CHAPTER 1

1. General introduction.

1.1. Introduction to ovine footrot (FR).

Footrot (FR) is a highly infectious and debilitating disease of sheep and is the main cause of lameness in the UK (Grogono-Thomas and Johnston, 1997; Kaler and Green, 2008). Lameness in sheep causes pain and discomfort, resulting in weight loss, poor wool growth, lower fertility in rams, poor milk production and lower lamb growth rates (Marshall, et al., 1991; Wassink, et al., 2010a) and thus is an important and challenging welfare issue (Fitzpatrick, et al., 2006). In addition to this, FR has been estimated to cost the sheep-farming industry in the UK approximately £24 million per annum on lost production, treatment, control and prevention according to Nieuwhof and Bishop, (2005). However a more recent study demonstrated this value may be higher, at £6 per sheep, i.e. £84 million per annum across the total population (Wassink, et al., 2010b) and with current (2012) lamb prices, the losses are likely to be considerably higher.

Footrot (FR) has been estimated to cause approximately 82 % of lameness cases with 39 % presenting with under-running and 43 % with interdigital dermatitis (ID), a precursor to the disease. The remaining 18 % of cases are caused by a number infectious and non-infectious conditions (Figure 1.1.) (Grogono-Thomas and Johnston, 1997; Moore, et al., 2005a; Kaler and Green, 2008). In the UK, over 90 % of farmers reported lame sheep presenting with either ID or FR on their farms (Wassink, et al., 2010b) and estimated that between 8-10 % of sheep within their flocks were affected by this disease (Wassink, et al., 2003; Goddard, et al., 2006). FR therefore remains a significant problem.

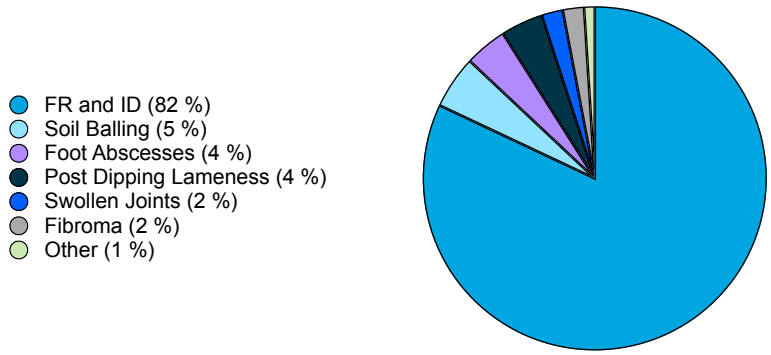

Figure 1.1. Royal Veterinary College survey (1997) of 547 farms quantifying causes of lameness in the UK. Footrot (FR) and interdigital dermatitis (ID) are the primary causes of lameness in sheep. Figure modified from the MAFF (Ministry of Agriculture, Fisheries and Food) Final Report (Grogono-Thomas and Johnston, 1997).

1.2. History of footrot (FR).

Footrot (FR) was first reported in 1791 in France (Chabert, et al., 1791) and was suggested to be infectious after a flock suffered an outbreak of FR following the introduction of two rams into a healthy flock (Gohier, 1813-1816). The disease was also reported in other countries within Europe around the same time; Germany, Italy and the UK, and even in parts of northern America, following the importation of sheep from France (Youatt, 1837). Control measures such as quarantine and treatments such as foot-paring and foot-bathing were recommended as early as 1818 (Mohler and Washburn, 1905) and these whole flock treatments are still widely used for treating lame sheep in the UK (Wassink, et al., 2003; 2004).

It was not known initially whether FR was an infectious disease and to complicate matters further it was often confused with foot and mouth disease (FMD) or other diseases of the foot/hoof; in fact even today it is still confused with other diseases, such as contagious ovine digital dermatitis (CODD) (Moore, et al., 2005b). However, the

disease was finally reproduced in healthy sheep, when a part of a diseased hoof was rubbed against a scarified section of skin belonging to a healthy ovine foot (de Gasparin, 1821). This was then replicated in the early 1900s, by applying either (i) purulent matter from a diseased foot or (ii) bouillon culture inoculated with exudate from the diseased foot, to the scarified interdigital skin of a healthy ovine foot (Mohler and Washburn, 1905). The contagion however, was not identified until 1938 (Beveridge, 1941), when the postulated causative agent was applied to the scarified interdigital space of healthy ovine feet, which induced FR lesions.

1.3. Geographical distribution.

Footrot (FR) is one of the top five diseases of sheep worldwide and has been reported in many countries in Europe, including Spain, Portugal, Norway, Germany, Sweden and Italy (Píriz, et al., 1990c; Hurtado, et al., 1998; Jiménez, et al., 2003; Ganter, 2008; König, et al., 2011, Vatn, et al., 2012). It has also been reported in countries with larger sheep-farming industries, such as Australia (Beveridge, 1941), New Zealand (Zhou and Hickford, 2000) and India (Wani, et al., 2004). The disease has even been reported in parts of Canada (Olson, et al., 1998) and the USA (Gradin, et al., 1993).

1.4. Clinical signs, aetiology and pathogenesis.

Disease begins as an inflammation of the interdigital space (interdigital dermatitis, ID), which in some circumstances may be followed by the separation (under-running) of the hoof horn from the sensitive underlying tissue (Beveridge, 1941) (Figure 1.2.). Under-running of the hoof horn begins at the skin-horn junction and can extend along the sole and heel and can spread laterally and anteriorly until the infection has reached the

abaxial wall/toe (Abbott and Lewis, 2005). These signs are usually accompanied by a characteristic foul smell and grey/white exudate (Beveridge, 1941). The severity of disease is thought to be exacerbated by the host's acute inflammatory response to infection, causing the sloughing of necrotic tissue (Egerton, et al., 1969). The disease has been reported in other ruminants, such as goats (Ghimire, et al., 1999; Egerton, et al., 2002), cattle and deer (Egerton, 1989) and has even been reported in pigs (Píriz, et al., 1996), although the severity of disease varies by host species (Ghimire, et al., 1999)

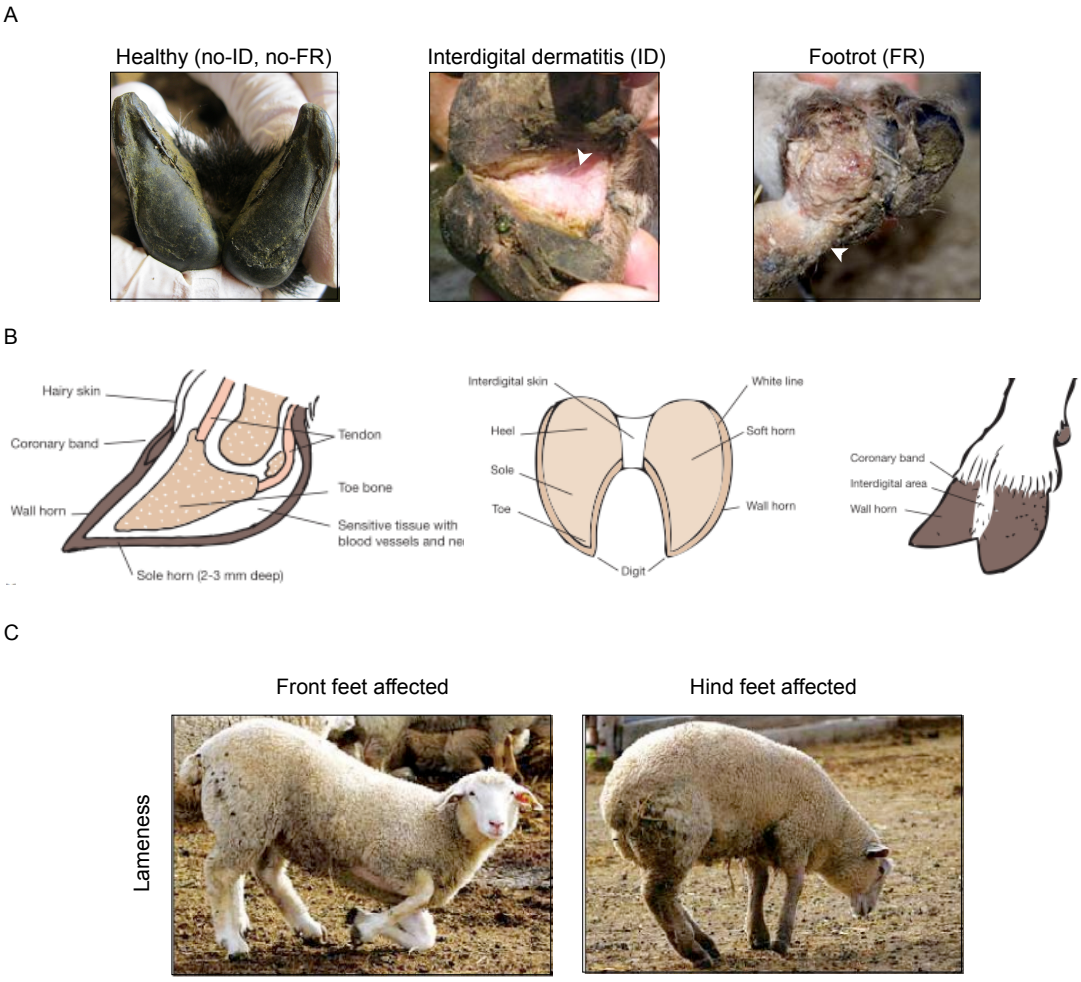

Figure 1.2. Ovine hoof anatomy and clinical signs of FR. A healthy ovine foot and feet presenting with ID and FR are shown (A) (author observation). Ovine foot anatomy (B) (EBLEX Ltd. Sheep BRP Manual 7) and signs of lameness (front and hind feet) (C) (Hagedorn, 2007). Arrows indicate areas of inflammation and under-running.

Damage to the interdigital skin may arise by both physical and chemical means, such as wet conditions (maceration), coarse grass, poor surface conditions, soil-balling and post-dipping (Moore, et al., 2005a; Green and George, 2008). Damage to the epithelium of the interdigital skin is considered a prerequisite to disease; disrupting the skin's barrier function, allowing opportunistic infection to occur (Beveridge, 1941). The disease is thought to be caused by the synergistic action of *Dichelobacter nodosus* and *Fusobacterium necrophorum*. *D. nodosus* is the causative agent (Beveridge, 1941; Kennan, et al., 2001; 2010), whilst *F. necrophorum* is an accessory agent thought to be involved in the initiation of disease and/or disease persistence or severity (Beveridge, 1941; Egerton, et al., 1969; Bennett. et al., 2009), however its precise role remains unclear.

Egerton, et al., (1969) postulated that the damaged epidermis is invaded initially by *F. necrophorum*, which via the action of its virulence factors is thought to generate a more anaerobic microenvironment, suitable for the growth and survival of more fastidious anaerobes, such as *D. nodosus*. *D. nodosus* is then thought to colonise and invade the epidermis and via the action of its virulence factors, along with *F. necrophorum,* contributes to the destruction of the epidermal matrix. *F. necrophorum* is also reported, on occasion, to enter the dermal layers after this initial process (Egerton, et al., 1969). *D. nodosus* has been shown to be the causative agent of FR in sheep virulence trials (Beveridge, 1941; Roberts and Egerton, 1969; Kennan, et al., 2001; 2010), being the only microorganism able to reproduce typical FR lesions. However, *F. necrophorum* has been reported to cause a self-limiting interdigital dermatitis (ID) that does not cause lameness in experimentally infected sheep (Parsonson, et al., 1967), providing some

confusion.

It is postulated that the damage to the skin causes a shift in the bacterial community structure, which may then aid the growth *D. nodosus* and *F. necrophorum* within the epidermis of the interdigital space (Roberts and Egerton, 1969; Calvo-Bado, et al., 2011b). A recent study examined and compared the changes in the bacterial community structures present on the ovine interdigital space between healthy feet, feet with ID and feet with FR, using deep-sequencing of the 16S rRNA gene (Calvo-Bado, et al., 2011b). It was observed that although the bacterial community structures differed by flock, there were greater differences by disease state. In addition, a core community structure was observed between healthy and diseased (ID and FR) sheep, but sheep with ID had an increased OTU (operational taxonomic unit) richness and were significantly associated with the presence of corynebacteria. This work highlights the importance of bacterial community shifts in disease development.

1.5. Disease nomenclature in the UK and Australia.

In the international literature, ID and FR are usually considered as different stages of the same disease process (Moore, et al., 2005a; Calvo-Bado, et al., 2011b), however in the UK veterinary and farming community, ID and FR are instead regarded as separate diseases, with ID thought to be primarily caused by environmental factors, such as weather and pasture quality (Wassink, et al., 2005). Consequently in the UK, treatment and control regimes are different for each condition. In contrast, Australian literature describes the conditions as ‘benign FR’ (BFR) and ‘virulent FR’ (VFR), corresponding to the clinical presentations of ID and FR, respectively (Green and George, 2008;

Kennan, et al., 2010). In addition, the term ‘intermediate FR’ (IFR) is sometimes used to describe outbreaks of FR of moderate severity (Abbott and Egerton, 2003).

A specific diagnostic test (the gelatin gel test) is often used to determine strain virulence (Section 1.8.2.2.), it is thought that *D. nodosus* strains, which cause less severe FR (or ‘benign’ FR) are in fact less virulent than those strains causing ‘virulent’ FR (Depiazzi, et al., 1991; Palmer, 1993). Despite these classifications, the majority of strains in the UK are virulent using this diagnostic test, whether isolated from feet with ID or those with FR (Moore, et al., 2005a) and so the classifications using this diagnostic assay are not informative in the UK. In light of this, the clinical presentations, ID and FR, are used in this thesis to describe the spectrum of disease severity and the virulence of the bacterium will not be discussed.

1.6. Importance of environmental factors in disease expression.

Footrot (FR) is reported to commonly occur under warm (> 10^{o}C) and damp conditions (Graham and Egerton, 1968; Cross, 1978). However, a recent longitudinal study examining ID and FR in sheep, which took place during October 2010 to August 2011 indicated that the temperature at which these diseases occur within UK may in fact be much lower (author observation). The disease is commonly thought to be seasonal, particularly in Australia, where there are more predictable periods of transmission (Green and George, 2008), however in the UK, no seasonality is observed for FR (Wassink, et al., 2003).

Despite this, a number of environmental factors are thought to influence distribution,

clinical expression and persistence of the disease and so these may vary from country to country (Abbott and Egerton, 2003). Studies in the UK have highlighted a number of environmental and/or management practices as potential risk factors, including; high rainfall, lowland farms, high stocking densities, winter-housing and coarse grass (Wassink, et al., 2003; 2004; Moore, et al., 2005a).

1.7. Treatment of ovine footrot (FR).

1.7.1. Overview.

Sheep do not develop long-term immunity to FR (*D. nodosus*) and the immunity acquired decreases over time and sheep then become susceptible to disease (Green and George, 2008; Dhungyel and Whittington, 2009). This type of response is common for endemic bacterial pathogens and has a number of implications for control, because development of vaccines is difficult and standard vaccines are only partially effective (Green and George, 2008). As previously discussed, whole flock treatments have historically been used to prevent lameness, ID and FR in the UK (Morgan, 1987) and treatments and management practices have included combinations of the following; routine foot-trimming, foot-bathing, culling of non-responders, vaccination, the use of clean well-drained pastures and the selection of FR resistant sheep (Winter, 2008). However, recent studies have demonstrated that some of the more traditionally-used treatments may not be effective and some may even be detrimental (Wassink, et al., 2003; 2004; Green, et al., 2007; Kaler and Green, 2009). Targeted individual treatment with antibiotic injection and topical antibiotic spray have instead been shown to be the most effective at combating ID and FR in sheep (Wassink, et al., 2010b; Kaler, et al., 2012).

1.7.2. Treatments; whole-flock versus the individual.

Foot-bathing and routine foot-trimming have been used in the past and are still used by some farmers today to prevent and treat lameness at whole flock level (Grogono-Thomas and Johnston, 1997; Wassink, et al., 2010a). One hypothesis proposed indicated that foot-trimming or -paring removed excess hoof horn that may trap mud and harbour bacteria (Abbott and Lewis, 2005), however there is no evidence that foot-trimming prevents FR, but rather, FR infection leads to misshapen feet (Stewart, 1989; Kaler, et al., 2010). Similarly, foot-bathing with 10-20 % (w/v) zinc sulphate or 3-5 % (v/v) formalin, is believed to provide cure rates of 61-72 % (Parajuli and Goddard, 1989; Grogono-Thomas, et al., 1994; Winter, 2008), but these solutions are reported to also cause hardening of the hoof and keratinisation of the interdigital skin (Abbott and Lewis, 2005). Despite these reports, foot-trimming and foot-bathing are both included in the top five FR treatments used by UK farmers (Wassink, et al., 2010a).

A number of observational and experimental studies have demonstrated that routine foot-trimming (≥ once a year) and foot-bathing are associated with a significantly increased prevalence of ID and FR in the UK (Wassink, et al., 2003; 2004; Green, et al., 2007; Kaler and Green, 2009; Wassink, et al., 2010a) and that foot-trimming sheep with FR is associated with a longer time to healing when compared to using antibiotics (Green and Kaler, 2011). The hypothesis is that foot-trimming may instead result in the removal of healthy horn and damage the foot and so delay healing. In addition, exposing the underlying tissues may increase the risk of infection to an individual or via the shedding of contaminated material may increase *D. nodosus* environmental burden from an infected individual and thus transmission between sheep. In addition, gathering

of sheep for whole-flock management and/or treatments may increase transmission events between infected and uninfected individuals because of close contact (Green, et al., 2007). In support of this, an increased ID prevalence was associated with a stocking density of > 8 ewes / ha (Kaler and Green, 2009).

The isolation of lame or brought-in sheep from the flock and the individual treatment of diseased sheep with either parenteral or topical antibiotics were associated with a decrease in FR prevalence (Wassink, et al., 2003; 2004; Kaler and Green, 2008; 2009). This is supported by the fact that farmers satisfied with their current treatment practices had ≤ 5 % lameness on their farms and rapidly caught and treated lame sheep with parenteral antibiotics, whereas farmers dissatisfied with their practices, reported > 5 % lameness within their flocks and instead employed routine foot-trimming and foot-bathing (Wassink, et al., 2010a), which have been shown to be less effective.

Parenteral long-acting antibiotics are administered intramuscularly and topical antibiotic sprays are instead applied to the affected areas of the foot surface (Green and George, 2008). Antibiotic treatment decreases inflammation and results in > 95 % recovery from ID and FR and feet normally recover within 3-4 days, with a median recovery of 2 days for feet with ID and 4 days for feet with FR, if the feet are not trimmed (Egerton and Parsonson, 1966; Wassink, et al., 2003; 2004; Kaler, et al., 2010). It has also been demonstrated that if sheep are treated with antibiotics on an individual basis, it is associated with a low flock prevalence of FR (2.6 % compared to 15 %) (Wassink, et al., 2005) and injectable antibiotic has been shown to be most effective (Kaler, et al., 2010). However, individual treatments such as these are considered to take time to do

and are tedious to implement by farmers, despite their therapeutic and economic benefits (Wassink, et al., 2010b).

Prevention of FR is of course preferable, as it limits animal suffering and provides economic benefits, however, prevention is not always possible and antibiotics remain one of the primary treatment methods (Wassink, et al., 2010b). Unfortunately the overuse of antibiotics has played a key role in the rise in the number of antibiotic resistant bacteria (ARB) over the last few years (Cartlet, et al., 2012; Hughes, et al., 2012), complicating matters further. There are a number of published studies examining antibiotic resistance in *D. nodosus* and *F. necrophorum* strains isolated from cases of caprine and ovine footrot (Píriz, et al., 1990a; 1990b, 1991; Jiménez, et al., 2004). Both pathogens were observed to be resistant to a number of β-lactams, but the levels of *D. nodosus* resistance were much lower and less frequent than those exhibited by *F. necrophorum* (Píriz, et al., 1990a). In all cases, both *D. nodosus* and *F. necrophorum* demonstrated some resistance to the tetracyclines (tetracycline and oxytetracycline) (Píriz, et al., 1990b; Jímenez, et al., 2004). However, antibiotics such as the tetracyclines are still used to effectively treat ovine FR in the field (Green and Kaler, 2011; Kaler, et al., 2012).

A similar study by Lechtenberg and colleagues (1998), reported that *F. necrophorum* isolates, obtained from cases of bovine hepatic absecesses, were resistant to (i) aminoglycosides (gentamicin, kanamycin, neomycin and streptomycin), (ii) ionophores (excluding narasin) and (iii) peptides (avoparcin, polymyxin and thiopeptin), however *F. necrophorum* isolates were again sensitive to the tetracyclines (chlortetracycline and

oxytetracycline).

1.7.3. History of vaccination of ovine footrot (FR).

There have been a number of attempts to generate an effective FR vaccine, the first of which was produced in 1969; the vaccine consisted of monovalent whole *D. nodosus* cells emulsified in an oil adjuvant (Egerton and Burrell, 1970; Egerton and Roberts, 1971). It has now been demonstrated however, that there are a total of ten serogroups (A-I and M), which consist of eighteen further serotypes, which are discussed in more detail in Section 1.8.2.1. Multi-serogroup infections can occur at the flock and even at the individual level (Claxton, et al., 1983; Moore, et al., 2005a). Multivalent vaccines containing nine serogroups (A-I) were only protective for approximately 12 weeks, whereas the monovalent formulations were protective for slightly longer, with approximately 16 weeks protection (Raadsma, et al., 1994; Hunt, et al., 1996).

A single dose (1 ml) of the current vaccine (Footvax^{TM}) consists of 10 μg of each recombinant fimbriae (*Pseudomonas aeruginosa*) of serogroups A, B1, B2, C, D, E, F, G, H and 5 x 10^8 inactivated *D. nodosus* cells belonging to serogroup I, in an oil adjuvant. This vaccine does not provide long-lasting heterologous protection between serogroups and this is thought to occur because of a phenomenon known as antigenic competition; whereby as the number of antigens increases, the responsiveness to the individual antigens significantly decreases (Schwartzkoff, et al., 1993; Hunt, et al., 1996; Raadsma, et al., 1994). It is thought that antigens compete for the major-histocompatibility complex (MHC) binding sites and T-cell antigen presentation is therefore biased between serogroups of *D. nodosus.* It has been shown that there is a

linear decrease in $\log_2$ antibody titre and protection over a range of vaccine types; from monovalent to decavalent formulations (ten serogroups) (Raadsma, et al., 1994; Dhungyel and Whittington, 2009).

In summary, vaccination using the multivalent recombinant fimbrial vaccine does not protect equally against all strains of *D. nodosus* (Raadsma, et al., 1994), but does provide some benefit. In view of this, specific monovalent vaccines have been prepared and implemented for flock-based vaccination, when a single serogroup predominates within a flock. Specific FR vaccination was first used in cases of ovine and caprine FR in Nepal, which had a 25-year history of FR. Two serogroups were found to predominate within the study flock and a bivalent recombinant fimbrial vaccine was subsequently produced. Vaccination started in 1992 and continued for four years, followed by seven years surveillance. Non-responders were culled and VFR was successfully eliminated (no cases of VFR observed after November 1993). An anamnestic test also demonstrated that there was no serological evidence of on-going infection (Egerton, et al., 2002). This type of targeted elimination programme was also successful in Bhutan using a whole cell serogroup B vaccine (Gurung, et al., 2006) and in Australia using two whole cell vaccines, one targeting a flock with a serogroup F infection and the other targeting a flock with a serogroup C infection (Dhungyel, et al., 2008), both studies stated that the clinical signs of VFR had been eliminated, however cases of BFR still persisted.

This type of specific-flock based vaccination is unlikely to be possible for flocks within the UK, because of the presence of multi-serogroup infections within flocks (Moore, et

al., 2005a).

1.7.4. Control and elimination.

As previously discussed, elimination of FR in the UK is unlikely and prevention and control are the most practical options for farmers. Control aims to minimise the impact of disease, whilst not eliminating the pathogen, whereas elimination deals with the removal of a pathogen from an individual flock or even country (Green and George, 2008). Elimination of FR from a flock requires the individual farmer to be strict and adhere to guidelines, such as quarantine, isolation and culling, all of which are associated with a decrease in FR prevalence (Wassink, et al., 2003; 2004). The farm must also have very good security and well-defined boundaries. The high annual rainfall, unpredictable periods of non-transmission, a reluctancy to cull lame sheep and a lack of biosecurity make elimination in the UK difficult (Green and George, 2008; Wassink, et al., 2006; 2010b).

Elimination has however been successful in parts of Australia, which has a mediterranean climate and predictable periods of hot and dry weather. In Western Australia (W.A.) they have observed a significant decrease in VFR and a similar protocol for elimination was used in New South Wales (N.S.W.), where a reduction in prevalence of flocks with VFR was observed, from 50 % to only 4 % of premises affected (from 1988 to 2003). It was postulated that the programme was slightly less successful in N.S.W., because of differing climatic conditions (increased rainfall and shorter dry period) (Green and George, 2008).

1.8. *D. nodosus*: the causative agent of ovine footrot (FR).

1.8.1. Overview.

D. nodosus is a large (0.6-0.8 μm wide by 3-10 μm in length) Gram negative anaerobic rod, with characteristic enlarged ends (Beveridge, 1941), it produces small (0.5-3.0 mm) translucent colonies with raised centers (author observation). It is the first member of the order Cardiobacteriales (γ-Proteobacteria) to have its genome sequenced, which consists of a single circular chromosome of approximately 1.4 Mb (1, 389, 350 bp) and is one of the genetically smallest anaerobic non-intracellular pathogens described to date (Myers, et al., 2007).

1.8.2. Virulence factors.

The understanding of how bacterial pathogens interact with their hosts and cause disease is of fundamental importance. The ability of bacterial pathogens to cause disease is usually mediated by a number of virulence factors, which are often involved in direct interactions with the host (Wu, et al., 2008). *D. nodosus* has a number of virulence factors that are important for disease, which include type IV fimbriae (Kennan, et al., 2001), twitching motility (Han, et al., 2007; 2008), a number of extracellular proteases (gelatinase, fibrogenase, collagenase, caseinase and elastase) (Palmer, 1993; Parker, et al., 2006; Kennan, et al., 2010), outer membrane proteins (Moses, et al., 1995; Ghimire and Egerton, 1999) and a number of virulence-associated gene regions (Katz, et al., 1994; Cheetham, et al., 1995; Billington, et al., 1996; Cheetham, et al., 2006; Tanjung, et al., 2009; Calvo-Bado, et al., 2011a).

1.8.2.1. Type IV fimbriae.

Fimbriae are proteinaceous structures that protrude from the bacterial cell surface and usually mediate adhesion and twitching motility (van der Woude, et al., 2004). The fimbriae exhibit a highly conserved N-terminal domain, containing an N-methylphenylalanine residue, polar distribution and twitching motility and are therefore classified into the type IV group (Billington, et al., 1996). The N-terminal domain is also highly homologous with fimbriae from *Pseudomonas aeruginosa*, *Neisseria gonorrhoaea* and *Moraxella nonliquefaciens* (McKern, et al., 1983).

The type IV fimbriae of *D. nodosus* are highly immunogenic, are the major immunoprotective antigens and form the basis of the *D. nodosus* classification system (Kennan, et al., 2003) as previously discussed. The serological diversity observed is due to sequence variation within the fimbrial subunit (FimA) protein and sequence analysis has revealed that usually more than 35 amino acids differ between serogroups and up to 15 between serotypes (Mattick, et al., 1991; Zhou and Hickford, 2000). Ten serogroups (designated A-I and M) have been identified and further subdivided into nineteen serotypes; A1, A2, B1, B2, B3, B4, B5, B6, C1, C2, D, E1, E2, F1, F2, G1, G2, H1, H2 (Claxton, 1989; Bhat, et al., 2012). The ten serogroups are categorised based on the agglutination reactions obtained from antisera raised against *D. nodosus*. The K-type agglutination reaction is described as being “distinctive” whereby the formation of “a coarse....loosely coherent sediment” is observed (Egerton, 1973). In addition, there is evidence that *D. nodosus* can undergo seroconversion *in vitro* and that this therefore may be one way in which *D. nodosus* evades the host’s immune response to infection (Ghimire, et al., 1998; Kennan, et al., 2003). *D. nodosus* cells are highly fimbriated

(Figure 1.3.) (Kennan, et al., 2001) and an increase in the number of fimbriae is associated with an increase in virulence (Billington, et al., 1996). The type IV fimbriae are not only essential for virulence but for natural transformation, protease secretion and twitching motility (Kennan, et al., 2001). It was shown that *fimA* (fimbrial subunit gene) mutants which were generated by allelic exchange were avirulent in sheep virulence trials. The *fimA* mutants (JIR3727 and JIR3728) were also unable to produce fimbriae (Figure 1.3.) and thus unable to exhibit twitching motility. In contrast, the *fimB* (encoding a putative fimbrial assembly protein) mutant (JIR3737) retained the wild-type phenotype and virulence characteristics.

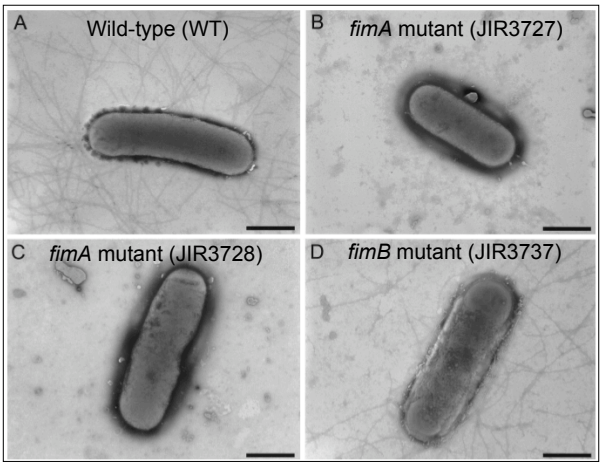

Figure 1.3. Transmission electron micrographs of *D. nodosus* (VCS1703A) cells; wild-type (A) and *fimA* (B and C) and *fimB* mutants (D). Wild-type cells and *fimB* mutants remain highly fimbriated, whereas *fimA* mutants become de-fimbriated. Scale bars: 1 μm. Modified from Figure 3 - Kennan, et al., (2001).

In addition to this, *fimA* mutants did not secrete the extracellular proteases; although the proteases were produced, they remained within the periplasm and were not secreted (Kennan, et al., 2001). It is postulated therefore that the type IV fimbriae of *D. nodosus* expel the synthesised extracellular proteases from the perisplasm into the extracellular milieu, acting as a secretion portal, via the action of fimbrial extension and retraction.

D. nodosus does not have any other type of secretory machinery (such as a type II secretion system), but there are several putative type IV fimbrial biogenesis genes that exhibit similarity to genes of the type II secretion system (Han, et al., 2007; Myers, et al., 2007). In addition, the mutation of the *pilE* gene (pilin-like protein gene) and *fimN*, *fimO* and *fimP* (fimbrial biogenesis genes) also resulted in an absence of surface fimbriae (Han, et al., 2007). In contrast, *pilT* and *pilU* mutants were able to produce fimbriae, but did not exhibit twitching motility and were avirulent in sheep infection studies (Han, et al., 2008). The fimbriae are therefore an important virulence factor of *D. nodosus*.

1.8.2.2. Extracellular subtilisin-like proteases.

D. nodosus strains produce three closely related extracellular subtilisin-like proteases; which vary in their activity. A diagnostic test was developed to examine the thermostability of these proteases. Heat-stable proteases (those able to hydrolyse gelatin after heating to 68^{o}C were associated with virulent *D. nodosus* strains, whereas heat-labile proteases (those which lose gelatinase activity after heating) were associated with benign *D. nodosus* strains (Palmer, 1993); this diagnostic test is commonly used in states of Australia, but not in the UK. Two acidic protease isoenzymes 2 and 5; AprV2, AprV5 and one basic protease BprV are produced by virulent strains and corresponding enzymes are produced by benign strains; AprB2, AprB5 and BprB. The virulent strain isoenzymes exhibit greater thermostability and elastase activity than the benign strain isoenzymes and it was recently shown that there is only a single amino acid difference between AprV2 and AprB2 and AprV5 and AprB5 and that BprV and BprB exhibited a 96 % sequence similarity (Kennan, et al., 2010).

Mutants of the six aforementioned protease genes were generated using allelic exchange (Kennan, et al., 2010) and it was demonstrated in sheep challenge trials, that the *aprV2*, *aprV5* and *bprV* mutants were avirulent in sheep, but upon complementation of *aprV2*, virulence was restored, thus fulfilling Koch's molecular postulates (Kennan, et al., 2010). In addition, AprV2 was shown to degrade type I keratin, serum albumin and the β-subunit of haemaglobin, demonstrating a direct role in destroying the keratin within the ovine hoof (Kennan, et al., 2010).

1.8.2.3. Other virulence factors.

In addition to the above major virulence factors, *D. nodosus* also has four outer membrane protein genes (*omp1A*, *omp1B*, *omp1C* and *omp1D*), which are structurally linked variants. These genes exhibit short cross-over site sequences at the 5' region, suggesting that site-specific DNA inversion may occur, causing the rearrangement of the *omp1* gene, to form the structural variants. It was postulated that this genetic capability may allow *D. nodosus* to switch the antigenic specificity of one of its major outer membrane proteins, which may in turn allow the bacterium to evade the host's immune system (Moses, et al., 1995; Ghimire and Egerton, 1999).

A number of loci that are associated with virulence have also been identified using comparative hybridisations on plasmid libraries from a virulent *D. nodosus* isolate (A198) and a benign *D. nodosus* isolate (C305). From this comparative study, two regions were preferentially associated with virulent isolates, which were designated virulence-associated protein (*vap*) region and the virulence-related locus (*vrl*). Of 800 *D. nodosus* isolates, 95 % of virulent/high intermediate isolates, 88 % of intermediate

isolates and 38 % of low intermediate/benign strains contained *vap* sequences. In conjunction with this, 77 % of virulent/high intermediate strains had *vrl* sequences, whereas only 13 % and 7 % of intermediate and low intermediate/benign strains had *vrl* sequences. These loci represent the major differences between virulent and benign strain genomes (Katz, et al., 1994; Cheetham, et al., 1995; Billington, et al., 1996). There have been reports that there is a correlation between the thermostability of proteases, the ability of a strain to cause VFR in sheep and the presence of the *intA* gene (Cheetham, et al., 2006) and the presence of the *pgrB* gene in strains isolated from BFR in Western Australia (W.A.) (Calvo-Bado, et al., 2011a). Similarly, the *intD* gene was primarily associated with benign *D. nodosus* strains (Tanjung, et al., 2009). In summary, the currently used virulence/diagnostic tests provide limited epidemiological information and do not always correlate with clinical presentation (Cheetham, et al., 2006; Calvo-Bado, et al., 2010a).

1.8.3. The causative agent of ovine footrot (FR).

Proving cause and effect in infectious disease research is essential. Scientists attempt to fulfill Koch's postulates and more recently Koch's molecular postulates (Falkow, 2004), but these criteria may not apply to all diseases. One such category has been termed the 'microbiota shift diseases' or polymicrobial diseases, which are not necessarily caused by one microorganism, but rather by a shift in the microbial population (Salyers and Whitt, 2002), where co-infections appear to cause disease, such as in bacterial vaginosis, periodontal disease, otitis media, rhinosinusitis and chronic wound infections (Sbordone and Bortolaia, 2003; Verstraelen, et al., 2004; Harro, et al., 2010). For these types of disease the model for pathogenesis is far more complex than for those diseases

caused by a lone pathogen.

D. nodosus mutants in *fimA* and *aprV2*, as described previously, were shown to be avirulent in sheep infection studies (Kennan, et al., 2001; 2010) and in addition the complementation of *aprV2*, restored virulence and sheep developed FR lesions (Kennan, et al., 2010), thus fulfilling Koch's molecular postulates. In contrast, *F. necrophorum* was only able to cause a mild to severe inflammation, with no under-running, in experimentally infected sheep (Parsonson, et al., 1967). This provides conclusive evidence that *D. nodosus* is the primary causative agent of ovine FR, but that *D. nodosus* may be initially aided by environmental conditions, damage to the skin, a shift in the commensal microbial community (Calvo-Bado, et al., 2011b) and/or by the action of *F. necrophorum* (Egerton, et al., 1969), complicating the situation.

1.8.4. Survival of *D. nodosus* in the environment.

Disease has to be transmitted between sheep indirectly via contaminated pasture or flooring. However, *D. nodosus* is not thought to persist in the environment for long periods of time, but under optimal conditions (warm and damp) is reported to survive a maximum of no more than two weeks on pasture (Beveridge, 1941; Whittington, 1995). A study reported the transmission of FR between a diseased flock (< 1 % prevalence of FR lesions) and a healthy flock, by exposing the healthy flock to the yard, in which the diseased flock were held, one hour previously (Whittington, 1995). It has also been postulated that *D. nodosus* may be able to survive in a latent (viable, but non-culturable) stage within the ovine foot asymptomatically and disease may only occur once the environment becomes favourable for transmission (Beveridge, 1941), as *D. nodosus* has

previously been detected using PCR from healthy ovine feet (Moore, et al., 2005a).

In addition, a study by Depiazzi and colleagues (1998) reported that 8 % (19/237) healthy feet were positive for *D. nodosus* by culture. This observational data supports the hypothesis that *D. nodosus* may survive asymptomatically on ovine feet, until environmental conditions become conducive for pathogen transmission.

1.9. *F. necrophorum*: accessory agent to ovine footrot (FR).

1.9.1. Overview.

F. necrophorum is a Gram negative non-spore forming anaerobe, which belongs to the Bacteroidaceae family. The organism exhibits extensive pleomorphism and has been recognised as a pathogen of animals since the late 1800s (Langworth, 1977), despite this its genome is not yet sequenced. *F. necrophorum* is classified into three subspecies or biovars; *F. necrophorum* subsp. *necrophorum* (biovar A), *F. necrophorum* subsp. *funduliforme* (biovar B) and *F. pseudonecrophorum* (biovar C). *F. necrophorum* is a commensal of the alimentary of tract of both humans and animals (Tan, et al., 1996), is the predominant *Fusobacterium* species in human faecal material (Ohtani, 1970) and is part of the normal microflora of the human oral cavity and female genital tract (Gorbach and Bartlett, 1974). However, it is also an opportunistic pathogen which causes a number of necrotic disease conditions of animals, such as bovine hepatic abscesses, bovine mastitis, ruminant foot abscesses and calf diphtheria (Langworth, 1977; Tan, et al., 1996). Of the three *F. necrophorum* biovars, *F. necrophorum* subsp. *necrophorum* (biovar A) is reported to be the more pathogenic of the two (Tan, et al., 1996), whereas *F. pseudonecrophorum* (biovar C) is non-pathogenic and according to 16S-23S

intergenic spacer region sequence analysis is identical to *F. varium* (Nagaraja, et al., 2005).

Despite the many morphological, biochemical and biological differences demonstrated between the biovars, many publications have not identified the specific subspecies (possibly due to a lack of genomic information) and as such, it is sometimes not known, which subspecies is primarily involved in the disease process in question (Kristensen and Prag, 2000). Despite this, there is some evidence that *F. necrophorum* subsp. *necrophorum* (biovar A) is mainly involved in diseases of animals, whereas *F. necrophorum* subsp. *funduliforme* (biovar B) is mainly responsible for human disease (Hall, et al., 1997; Smith and Thornton, 1997). One such human disease is Lemierre's syndrome; a rare, but life-threatening disease usually affecting healthy young adults. It is an oropharyngeal infection, which consists of pharyngitis, bacteraemia and thrombophlebitis of the interjugular vein, which is often complicated by metastatic septic emboli (Ramirez, et al., 2003; Riordan, 2007).

1.9.2. Virulence factors.

The pathogenesis of *F. necrophorum* is complicated and there are several virulence factors that have been identified and have been implicated in the disease process (Langworth, 1977; Tan, et al., 1996; Hofstad, 2006). Some of these virulence factors include; endotoxin, leukotoxin, haemolysin, haemagglutinin, capsule, adhesins, platelet aggregation factor and number of extracellular enzymes. Of these the endotoxin and leukotoxin have been extensively studied.

1.9.2.1. Endotoxin.

The outer membrane of Gram negative bacteria contains the endotoxic lipopolysaccharide (LPS) (Munford, 2008). The LPS of *F. necrophorum* has been shown to be lethal to mice, rabbits and chicken embryos and to cause erythema and oedema when subcutaneously inoculated into rabbit skin. The composition of LPS also differs between subspecies of *F. necrophorum*, in particular *F. necrophorum* subsp. *necrophorum* (biovar A) is reported to have a higher LPS and lipid A content and to be more potent than the LPS belonging to *F. necrophorum* subsp. *funduliforme* (biovar B) (Inoue, et al., 1985). The LPS generally induces a necrotic effect, which in turn generates an anaerobic microenvironment and assists *F. necrophorum* dissemination (Hofstad, 2006).

1.9.2.2. Leukotoxin.

Leukotoxins are a group of exotoxins that exhibit activity against leukocytes and therefore are a mechanism used to manipulate the host immune response (Narayanan, et al., 2002). Leukotoxins are cytotoxic to immune cells (neutrophils, macrophages), hepatocytes and ruminal epithelial cells (Tan, et al., 1994). The leukotoxic ability of *F. necrophorum* was first reported in 1967, when leukocyte migration was inhibited and leukocytes were killed, when an *F. necrophorum* culture filtrate was injected intradermally into sheep (Roberts, 1967). It has been demonstrated that *F. necrophorum* subsp. *necrophorum* (biovar A) produced approximately eighteen times more leukotoxin than *F. necrophorum* subsp. *funduliforme* (biovar B) (Tan, et al., 1996; Zhang, et al., 2006), although strain variation can also occur. The leukotoxin is also highly toxic to bovine and ovine neutrophils, only slightly toxic to equine neutrophils and swine and

rabbit neutrophils remained unaffected (Tan, et al., 1994), demonstrating a specificity for ruminant immune cells. The ability of this toxin to modulate the host's innate immune response is an important mechanism and may in fact contribute to the synergistic behaviours commonly observed between *F. necrophorum* and other bacteria in a number of disease processes (Ruder, et al., 1981; Smith, et al., 1989).

1.9.2.3. Haemolysin and haemagglutinin.

Most pathogenic bacteria require iron as a growth factor, however, iron is usually at a low concentration within the mammalian host and therefore pathogens employ certain mechanisms by which to obtain iron (Tan, et al., 1992). *F. necrophorum* has both a haemolysin and a haemagglutinin; the haemolysin has two roles, the first to provide *F. necrophorum* with iron via the lysis of the host's erythrocytes and secondly it likely also generates an anaerobic microenvironment, because the lysis of RBCs decreases oxygen transport to the site of infection. The haemagglutinin has a similar role in the creation of anaerobic environment, but does this by promoting RBC clotting, which may also aid adherence of *F. necrophorum* to ruminal epithelial cells (Tan, et al., 1996). Again, *F. necrophorum* subsp. *necrophorum* (biovar A) is reported to produce a higher agglutination titre than *F. necrophorum* subsp. *funduliforme* (biovar B) (Nagai, et al., 1984).

1.9.2.4. Other virulence factors.

Other virulence factors include; capsule, adhesins, platelet aggregation factor and proteolytic enzymes, however their role in disease pathogenesis remains to be examined in detail.

1.9.3. Survival of *F. necrophorum* in the environment.

In contrast to *D. nodosus*, *F. necrophorum* is reported to be ubiquitous in the environment and able to survive in soil (Marsh and Tunnicliff, 1934; Garcia, et al., 1971; Langworth, 1977), although evidence for this is lacking. *F. necrophorum* is a coloniser of the alimentary tract and so faecal material is reported to provide the primary source of infection for ovine FR (and other animal necrobacilloses) (Roberts and Egerton, 1969; Handeland, et al., 2010). However, contradictory reports suggest that this microorganism is in fact rarely excreted in animal faeces (Smith, et al., 1991; 1993b; Nagaraja, et al., 2005) and only usually when the gut microflora has been perturbed (Smith, et al., 1993a). *F. necrophorum* has however been detected in the rumen and ruminal contents of sheep (Smith, et al., 1993b; Edwards, et al., 2005).

1.9.4. Brief summary and comparison of *D. nodosus* and *F. necrophorum* traits.

D. nodosus appears to exhibit a highly specific host-range, reservoir and suite of enzymes, suitable for the degradation of the epidermal-matrix, whereas *F. necrophorum* has a broader host-range, with a number of nonspecific virulence factors (largely inflammatory) and appears to be implicated in a wide range of mammalian diseases (Table 1.1.). *F. necrophorum* also has a number of virulence factors, which may aid or assist *D. nodosus* (and other microbes) by generating a more anaerobic environment and this is possibly one of the reasons *F. necrophorum* is commonly involved in synergistic bacterial relationships (Ruder, et al., 1981; Smith, et al., 1989). *D. nodosus* appears to be specialised and highly adapted to the ovine/ruminant foot, whereas *F. necrophorum* appears to exhibit traits of a generalist or opportunist (Dykhuizen and Davies, 1980; Taylor, et al., 2004; Agosta, et al., 2010; Christie-Oleza, et al., 2012).

Table 1.1. Comparison of *D. nodosus* and *F. necrophorum* traits.

	D. nodosus	***F. nerophorum***
Diseases caused/ implicated in	Interdigital dermatitis (ID), footrot (FR).	Interdigital dermatitis (ID), footrot (FR), bovine hepatic abscesses, calf diphtheria, ruminant foot abscesses, bovine mastitis, Lemierre's syndrome.
Reservoirs	Ruminant feet.	Faeces, soil, animal and human alimentary tract, female genital tract, ruminant feet.
Host range	Ruminants, pigs.	Ruminants, humans.
Virulence factors	Gelatinase, collagenase, fibrogenase, caseinase, elastase.	LPS (endotoxin), leukotoxin, haemolysin, haemaglutinin.

1.10. New approaches to study the microbial ecology of ovine footrot (FR).

Despite the recent advances in understanding particular virulence mechanisms of *D. nodosus* (Kennan, et al., 2001; Han, et al., 2007, Parker, et al., 2006; Myers, et al., 2007; Han, et al., 2008; Kennan, et al., 2010) and in determining effective treatments (Wassink, et al., 2003; 2004; Green, et al., 2007; Kaler and Green, 2009; Wassink, et al., 2010b), the precise series of microbial succession events, between *D. nodosus* and *F. necrophorum*, leading to the initiation and development of ID and FR have not been determined, despite some recent advances (Calvo-Bado, et al., 2011b). In addition, the distribution of *D. nodosus* and *F. necrophorum* in the environment has yet to be determined.

A number of studies have detected *D. nodosus* and *F. necrophorum* in relation to disease presentation, however these studies were cross-sectional, non-quantitative and some used culture-dependent techniques, despite the fastidious nature of *D. nodosus* and *F. necrophorum* (Moore, et al., 2005a; Wani, et al., 2007; Bennett, et al., 2009). In addition, culture-dependent techniques have been shown to be less sensitive than PCR-

based methods for the detection of *D. nodosus* from ovine foot swabs (Moore, et al., 2005a). A number of reports have highlighted the difficulties associated with studying microorganisms in their natural environments, due to limited bacterial morphologies and the inability to grow certain microorganisms in a laboratory environment (Prosser, et al., 2007; Rogers, et al., 2009). In light of this, a series of culture-independent techniques were selected for the current study.

1.10.1. Culture-independent techniques; quantitative real-time PCR (qPCR).

Real-time quantitative PCR (qPCR) is a culture-independent, specific, sensitive and reproducible method for the detection and quantification of nucleic acids. It has revolutionised a number of fields, including molecular diagnostics and microbial ecology, because of its high-throughput and automated nature (Arya, et al., 2005). It has been used for a variety of clinical and environmental studies and for a wide range of sample types, including; soil, faeces, milk, water, tissue and swabs (Nogva, et al., 2000; Buttner, et al., 2001; Fujita, et al., 2002; Stelzel, et al., 2002; Kawaji, et al., 2011; Fredericks, et al., 2009; Pontiroli, et al., 2011; Calvo-Bado, et al., 2011b). It is a highly specific and sensitive approach and has been shown to be more sensitive than culture when detecting bacteria (Saukkoriipi, et al., 2003; Moore, et al., 2005a; Rampersad, et al., 2008). In addition, bacterial and viral loads have been shown to correlate temporally with disease development and presentation (Hill, et al., 2000; Hackett, et al., 2002; Dormans, et al., 2004; Sha, et al., 2005; Smith-Vaughan, et al., 2006). Despite this, bacterial DNA-based detection methods, such as qPCR, may overestimate bacterial load, by quantifying dead/membrane-compromised or dormant bacterial cells (Castillo, et al., 2006; Pathak, et al., 2012).

1.10.2. Culture-independent techniques; fluorescence *in situ* hybridisation (FISH).

FISH is another culture-independent method for the *in situ* detection, identification, quantification and phylogenetic analysis of microbes. It was first introduced in the late 1980s and since then it has become one of the most widely used methods for examining microbial community composition *in situ* (Amann, et al., 1990; Amann and Fuchs 2008). A number of adaptations to FISH have been introduced, some using different gene targets; double labelling of oligonucleotide probes (DOPE-FISH) (Stoecker, et al., 2010), 16S rRNA gene clones (clone-FISH) (Schramm, et al., 2002), peptic nucleic acid probes (PNA-FISH) (Perry-O'Keefe, et al., 2001), combining microautoradiography with FISH (MAR-FISH) (Chua, et al., 2006) and using catalysed reporter deposition (CARD-FISH) (Eickhorst and Tippkötter, 2008), demonstrating the many applications of this method.

Despite this, the majority of FISH studies continue to target ribosomal RNA (rRNA) with fluorescently labelled oligonucleotide probes (Amann and Fuchs, 2008). The rRNA molecules are ideal targets because (i) each bacterial target cell contains many ribosomes and so are naturally amplified, (ii) they are more evolutionary conserved and (iii) by using rRNA as the target, one can link microbial ecology with microbial evolution. Using this method, bacterial classification is no longer based on morphology or physiology. In contrast to qPCR, FISH may provide information on the physiological state of microorganisms, because rRNA content has been shown to be directly correlated with growth rate (Kemp and LaRoche, 1993; Wallner, et al., 1993; Poulsen, et al., 1993), providing an advantage over qPCR.

The FISH procedure for bacterial targets consists of three basic steps (Figure 1.4.); cell fixation, whereby cells are penetrated with a fixative (such as paraformaldehyde or ethanol), which retains cells morphology and structure and also permeabilises the cell membranes. Permeabilisation allows the labelled oligonucleotide probe to diffuse and bind to its intracellular targets during hybridisation (usually 1-4 hours), the specific hybrid formed is a heteroduplex (rRNA:DNA). Excess or unbound probe is then washed away and labelled cells are visualised or quantified by a variety of methods (Amann and Fuchs, 2008).

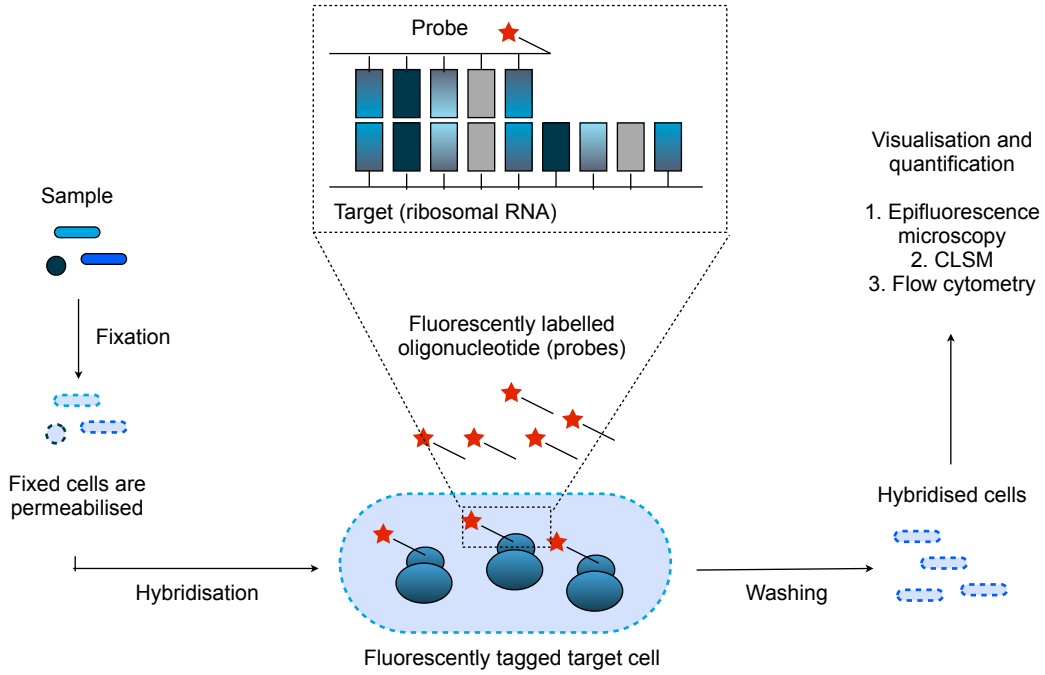

Figure 1.4. Outline of the core steps involved in fluorescence *in situ* hybridisation (FISH). The steps include fixation, permeabilisation, hybridisation, washing and visualisation. Modified from Figure 1 from Amann and Fuchs (2008).

FISH has been employed for a variety of clinical and environmental studies and has been used on a number of samples types; faecal material, mammalian and plant tissue, soil, swabs and water, to name some (Harmsen, et al., 1999; Takada, et al., 2004;

Ainsworth, et al., 2006; Kutter, et al., 2006; Boye, et al., 2006; Lefmann, et al., 2006 Klitgaard, et al., 2008; Whiley, et al., 2011), demonstrating again a broad range of applications. It is therefore suitable for the *in situ* detection, identification, localisation and quantification of bacterial species and complements the use of a DNA-based detection method, such as qPCR.

1.11. Concluding remarks.

Ovine FR remains a significant problem in the UK in terms of sheep welfare, productivity and cost to farmers. It is complicated disease, which demonstrates aspects of both 'microbiota shift diseases' and traditional infectious diseases, with a single causative agent. Despite FR being first recognised as early as 1791 and the infectious agent first isolated in 1941, the causative nature of *D. nodosus* was not fully demonstrated until it was shown to fulfil Koch's molecular postulates. The role of the total bacterial community and particularly *F. necrophorum*, in the initiation and/or persistence of disease, despite some recent advances, remains unclear. A number of advances have been made with regards to effective treatments and determining key virulence factors, however the treatments are time-consuming and provide no long-lasting treatment or cure for ovine FR. Attempting to control an infectious disease, where disease pathogenesis and role of the environment are not fully understood can therefore be extremely difficult.

1.12. Aims and hypotheses.

Aims:

1. To elucidate the temporal patterns associated with *D. nodosus* and *F. necrophorum* load in relation to the initiation and development of ID and FR in sheep, in order to define the roles of the causative and accessory agents more precisely.
2. To determine the localisation patterns and microbial succession events involving *D. nodosus* and *F. necrophorum in situ*, in relation to the general microbial population and disease presentation (ID and FR).
3. To examine the distribution and load of *D. nodosus* and *F. necrophorum* in a variety of environmental samples, to highlight potential sources of infection and to what extent contaminated material may contribute to the spread of disease.

Hypotheses:

1. *D. nodosus* and *F. necrophorum* will be more frequently detected in diseased (ID and FR) sheep by qPCR and FISH analysis. But, *F. necrophorum* load will increase prior to the development of ID (in line with its reported inflammatory and initiatory role) and *D. nodosus* load will instead increase prior to the development of FR (in line with its causative role).
2. Both *D. nodosus* and *F. necrophorum* loads will decrease after FR development, possibly due to sloughing of necrotic tissue.
3. *D. nodosus* and *F. necrophorum* cells will localise mainly within the layers of epidermis (stratum corneum, stratum spinosum), but may during cases of FR, penetrate deeper layers, possibly entering the dermis.
4. Faecal material will act as the primary source of *F. necrophorum* infection as previously reported. *D. nodosus* will instead be primarily associated with the ovine foot, but may contaminate material in the surrounding environment to act as a transitory source of infection.

CHAPTER 2

2. Materials and Methods.

2.1. General laboratory reagents.

General laboratory reagents were purchased from Sigma-Aldrich Ltd. (Poole, Dorset, UK) and were of analytical grade, unless otherwise stated.

2.2. Bacterial strains and control DNA samples.

Bacterial strains and DNA samples were obtained from variety of sources and countries. Control DNA samples were primarily used for specificity screening purposes, all strains are listed in Tables 2.1, 2.2 and 2.3.

Table 2.1. *Dichelobacter nodosus* strains and control DNA samples.

Bacterial species	Strain id.	Host	Sample type	Country / Source
D. nodosus	VCS1703A (NC_009446)	Ovine	Isolate	Australia/MONASH
D. nodosus	A198	Ovine	Isolate	Australia/MONASH
D. nodosus	C305	Ovine	Isolate	Australia/MONASH
D. nodosus	Serogroup A	Ovine	Isolate	Australia/MONASH
D. nodosus	Serogroup B	Ovine	Isolate	Australia/MONASH
D. nodosus	Serogroup C	Ovine	Isolate	Australia/MONASH
D. nodosus	Serogroup D	Ovine	Isolate	Australia/MONASH
D. nodosus	Serogroup E	Ovine	Isolate	Australia/MONASH
D. nodosus	Serogroup F	Ovine	Isolate	Australia/MONASH
D. nodosus	Serogroup G	Ovine	Isolate	Australia/MONASH
D. nodosus	Serogroup H	Ovine	Isolate	Australia/MONASH
D. nodosus	Serogroup I	Ovine	Isolate	Australia/MONASH
D. nodosus	Serogroup M	Ovine	Isolate	Australia/MONASH

Bacterial species	Strain id.	Host	Sample type	Country / Source
D. nodosus	BS-1 to BS-30	Ovine	Isolate	UK/University of Bristol
D. nodosus	C809	Bovine	DNA	MONASH Australia
D. nodosus	C810	Bovine	DNA	MONASH Australia

Table 2.2. *Fusobacterium* sp. strains and control DNA (for screening purposes).

Bacterial species	Strain id.	Host	Sample type	Country / Source
F. necrophorum	BS-1	Ovine	Isolate	UK/University of Bristol
F. necrophorum subsp. *necrophorum*	D146	Ovine	Isolate	VLA[a]
F. necrophorum subsp. *necrophorum*	D213	Ovine	Isolate	VLA[a]
F. necrophorum subsp. *necrophorum*	D306	Ovine	Isolate	VLA[a]
F. necrophorum subsp. *necrophorum*	D332	Ovine	Isolate	VLA[a]
F. necrophorum subsp. *necrophorum*	D514	Ovine	Isolate	VLA[a]
F. necrophorum subsp. *necrophorum*	D555	Ovine	Isolate	VLA[a]
F. necrophorum subsp. *necrophorum*	D745	Ovine	Isolate	VLA[a]
F. necrophorum subsp. *necrophorum*	D797	Ovine	Isolate	VLA[a]
F. necrophorum subsp. *necrophorum*	D809	Ovine	Isolate	VLA[a]
F. necrophorum subsp. *necrophorum*	NCTC 10576	-	DNA	HPA[b]
F. necrophorum subsp. *necrophorum*	ATCC 25286	-	DNA	HPA[b]
F. necrophorum subsp. *necrophorum*	B575	-	DNA	HPA[b]
F. necrophorum subsp. *necrophorum*	B579	-	DNA	HPA[b]
F. necrophorum subsp. *funduliforme*	B571	-	DNA	HPA[b]
F. necrophorum subsp. *funduliforme*	ATCC 51357	-	DNA	HPA[b]
F. necrophorum	R17807	-	DNA	HPA[b]
F. nucleatum	ATCC 25886	-	DNA	HPA[b]
F. simiae	ATCC 33568	-	DNA	HPA[b]
F. varium	AR17443	-	DNA	HPA[b]

[a] Veterinary Laboratories Agency (VLA), UK

[b] Health Protection Agency (HPA), UK

Table 2.3. Other bacterial and yeast strains and control DNA.

Bacterial species	Strain id.	Host	Form	Country / Source
Aermonas hydrophila	-	River water	Isolate	UK/G.C.A. Amos
Aermonas media	-	River water	Isolate	UK/G.C.A. Amos
Arcanobacterium pyogenes	DS7M 20 - 630	Ovine foot	Isolate	UK/University of Bristol
Bacillus circulans	WL-12	Soil	Isolate	UK/A. Johnson-Rollings
Citrobacter freundii	-	River water	Isolate	UK/G.C.A. Amos
Escherichia coli	K-12	-	Isolate	UK/N. Kyratsous
Klebsiella pneumoniae	-	River water	Isolate	UK/G. C. A. Amos
Macrococcus caseolyticus	87	Bovine Milk	Isolate	UK/C. O'Neill
Corynebacterium amycolatum	-	Ovine foot	DNA	Australia/N. Buller
Corynebacterium urealyticum	-	Ovine foot	DNA	Australia/N. Buller
Enterococcus spp.	-	Ovine foot	DNA	Australia/N. Buller
Lactococcus garvieae	-	Ovine foot	DNA	Australia/N. Buller
Mycobacterium bovis	-	Ovine foot	DNA	Australia/N. Buller
Pseudomonas putida	-	Ovine foot	DNA	Australia/N. Buller
Staphylococcus aureus	-	Ovine foot	DNA	Australia/N. Buller
Staphylococcus simulans	-	Ovine foot	DNA	Australia/N. Buller
Streptococcus spp.	-	Ovine foot	DNA	Australia/N. Buller
Streptomyces spp.	-	Ovine foot	DNA	Australia/N. Buller
Schizosaccharomyces pombe	-		Isolate	UK/M.E. Bond
Saccharomyces cerevisiae	-		Isolate	UK/M.E. Bond

2.3. Media and Reagents.

2.3.1. Wilkins-Chalgen Agar (WC).

Ingredients (g l^{-1})

Casein enzymatic hydrolysate	10
Peptic digest of animal tissue	10

Yeast extract	5
Dextrose	1
Sodium chloride	5
L-Arginine	1
Sodium pyruvate	1
Hemin	0.005
Menadione	0.0005
Agar	10

2.3.2. Hoof-Horn Agar (HH).

Ingredients (g l^{-1})	
Proteose peptone	10
NaCl	5
Beef extract	4
Yeast extract	1
Finely ground ovine hoof	15
Agar (2 %) (maintenance)	20

2.3.3. Luria-Bertani Agar (LB).

Ingredients (g l^{-1})	
Peptone	10
Yeast extract	5
NaCl	10
Agar	10

2.3.4. Yeast extract Agar (YE).

Ingredients (g l^{-1})	
Yeast extract	10
Glucose	30
Adenine	0.05
Leucine	0.25
Uracil	0.25
Agar	17

All growth media were autoclaved at 121^{o}C for 15 m.

2.3.5. Paraformaldehyde (PFA) solution (4 % (w/v)).

For a 50 ml solution, 2 g of PFA (BDH Chemicals Ltd., Poole, UK) were added to 33 ml of sterile distilled H_2O (heated to 65^{o}C) and NaOH added until the PFA was completely dissolved. A volume of 16.6 ml of 3x PBS was then added to the solution and left to cool. The pH of the solution was adjusted to 7.2-7.4. The PFA solution was then filter-sterilised (0.2 μm filter), and stored in 1 ml aliquots at -20^{o}C.

Table 2.4. Buffer solutions.

Buffer	Constituents
1 M Tris-HCl (pH 8.0)	Tris (hydroxymethyl)methylamine 201.9 g l^{-1} (pH 8.0).
50x TAE	Tris base 242 g l^{-1}, glacial acetic acid 57.1 g l^{-1} and 0.5 M EDTA (pH 8.0) 100 ml l^{-1}.
Transport buffer (pH 8.0) (Moore, et al., 2005a)	1x sterile PBS containing 20 mM Na_2EDTA (pH 8.0).

Table 2.5. Fluorescence *in situ* hybridisation (FISH) hybridisation buffers (HB).

	Formamide (%)									
	0	**5**	**10**	**15**	**20**	**25**	**30**	**35**	**40**	**45**
5 M NaCl	180	180	180	180	180	180	180	180	180	180
1 M Tris/HCl	20	20	20	20	20	20	20	20	20	20
ddH_2O	799	749	699	649	599	549	499	449	399	349
Formamide	0	50	100	150	200	250	300	350	400	450
10 % SDS	1	1	1	1	1	1	1	1	1	1

Volumes listed in µl (total volume 1000 µl).

Table 2.6. Fluorescence *in situ* hybridisation (FISH) wash buffers (WB).

	Formamide (%)									
	0	**5**	**10**	**15**	**20**	**25**	**30**	**35**	**40**	**45**
5 M NaCl	9.00	6.30	4.50	3.18	2.15	1.49	1.02	0.70	0.46	0.30
1 M Tris/HCl	1	1	1	1	1	1	1	1	1	1
0.5 M EDTA	0	0	0	0	0.5	0.5	0.5	0.5	0.5	0.5
ddH_2O	up to 50 ml	up to 50 ml	up to 50 ml	up to 50 ml	up to 50 ml	up to 50 ml	up to 50 ml	up to 50 ml	up to 50 ml	up to 50 ml

Volumes listed in ml (total volume 50 ml).

2.4. Bacterial growth conditions.

2.4.1. Anaerobic bacterial species.

All anaerobic microorganisms were grown and handled in an anaerobic cabinet (Don Whitley Mk.III anaerobic cabinet; 80 % N_2, 10 % CO_2 and 10 % H_2, Don Whitley Scientific Ltd., Shipley, UK) at 37^{o}C. *D. nodosus* strains were grown on HH agar under anaerobic conditions at 37^{o}C for 3-4 days (Thomas, 1958; Skerman, 1975). *F. necrophorum* strains and *A. pyogenes* (isolate DS7M 20-630) were grown on WC agar under anaerobic conditions at 37^{o}C for 48 h and 24 h, respectively. All isolates were

stored in 20 % (v/v) glycerol and kept at -80^{o}C.

2.4.2. Aerobic bacterial and yeast species.

E. coli (K-12), *M. caseolyticus* (87), *Ae. media*, *Ae. hydrophilia*, *C. freundii* and *K. pneumoniae* were grown at 37^{o}C for 24-48 h on LB agar. LB agar was also used for the growth of. *B. circulans* (WL-12), which was grown at 30^{o}C for 48 h. Isolates were stored in 20 % (v/v) glycerol and kept at -80^{o}C. *S. cerevisiae* and *Sz. pombe* were grown at 30^{o}C for 24 h on YE agar.

2.4.3. *F. necrophorum* stress response growth conditions.

Petri dishes containing 20 ml Wilkins-Chalgren (WC) agar were supplemented with 2 ml 1 M NaCl solution (final concentration 0.1 M). The solution was spread onto the agar surface and left to diffuse into the agar. *F. necrophorum* isolates were then grown as previously described (Section 2.4.1.) or until growth was visible.

2.4.4. Category I and II microorganisms.

Category I and II microorganisms were used for this study and relevant safety procedures were followed as appropriate.

2.5. Collection of clinical/environmental samples.

2.5.1. Collection of ovine foot swabs (Longitudinal study) (Chapter 3).

Sheep were turned using a turning crate (Figure 2.1.) and all four feet of eighteen ewes, were examined each week for five weeks. The ewes were individually identified and their feet coded as - healthy (H); no signs of clinical disease (sheep n = 3, foot

observations/swabs n = 54), ID; inflammation of the interdigital skin with no separation of the hoof horn (sheep n = 7, foot observations/swabs n = 138) and FR: separation of the hoof horn from the sensitive underlying tissue (under-running with or without ID) (sheep n = 8, foot observations/swabs n = 157). On all but eleven occasions, a sterile cotton swab (EUROTUBO collection swab; Delta lab, Rubi, Spain) was used to sample the most severe point of damage on each foot each week. Sampling and ID and FR severity scores were carried out by a single trained researcher as described by Kaler, et al., 2011, in order to reduce sample/score variation. The study was approved by the university local ethical committee. All swabs were stored in 500 µl sterile transport buffer (Table 2.4.) (Moore, et al., 2005a). The swabs were then maintained at 4^{o}C and transferred to -20^{o}C within 24 h and stored until required. Flock information detailed in Section 3.3.1. *Dr. J. Kaler is acknowledged for the collection of samples and foot severity scoring (Kaler, et al., 2011).

2.5.2. Collection of ovine foot swabs and interdigital space biopsies (Cohort study) (Chapter 4).

All four feet of three ewes (ewe ids. 97, 112 and 126) and three lambs (lamb ids. 293, 200 and 358) from the Cohort study flock (2) were scored using the severity scoring system previously discussed (Kaler, et al., 2011) and sampled using sterile cotton swabs (EUROTUBO collection swab; Delta lab, Rubi, Spain) to examine the interdigital space. The three lambs were culled 15/07/2011, Ewe 97 was culled 04/11/2010 and Ewes 112 and 126 were culled 25/08/2011. Punch biopsies were taken from the interdigital space of all feet after culling, using disposable sterile Biopsy Punches (8

mm in diameter) (Stiefel Laboratories, (UK) Ltd., Woodburn Green, UK). Biopsies were taken from all four feet from each sheep (n = 24). Healthy (control) feet were sourced from the EU-licensed red meat abattoir at the Bristol Veterinary School, University of Bristol, Langford, UK. Healthy sheep, sheep with ID and sheep with ID and FR were instead euthanised and punch biopsies then collected from all feet. Severity scores were taken prior to culling to avoid postmortem complications and punch biopsies were collected immediately after culling. *Dr. C. Russell and Dr. E. Smith are acknowledged for the collection of some of the interdigital space biopsies.

2.5.3. Collection of soil (S) and faecal (F) samples.

Bulk soil samples (n = 20) were collected from pasture occupied by the cohort study flock (2) in March 2011 using a sterilised trowel and put into 50 ml falcon tubes (Becton Dickinson Labware, Cowley, Oxford, UK) (Figure 2.1.). Faecal (F) samples were taken (i) directly from ewes (i.e. before coming into contact with the pasture using faecal collecting bags) (n = 20), (ii) from the floor (FF) of a housed-area (n = 35) (Figure 2.1.) and (iii) from the hoof (FH) (compacted within interdigital space) (n = 7) using sterile cotton swabs (EUROTUBO collection swab; Delta lab, Rubi, Spain). After collection, soil and faecal samples were transported at 4^{o}C and were stored at -20^{o}C until required for DNA extraction. *Dr. M. Krsek is acknowledged for collection of faecal samples (F) (n = 20).

2.5.4. Collection of bedding (B) samples.

Bedding (B) (straw) samples were collected (n = 20) from a housed-area (under-cover) that had been recently occupied by sheep (Cohort study flock (2)) (Figure 2.1.).

Samples were collected using sterilised tweezers and put into 50 ml tubes (Becton Dickinson Labware, Cowley, Oxford, UK), transported at 4°C and DNA extracted within 24 h. *Dr. L. Calvo-Bado is acknowledged for collecting some of the bedding samples.

2.5.5. Collection of concrete floor (CF) swabs.

Concrete floor swabs (CF) (n = 42) (EUROTUBO collection swab; Delta lab, Rubi, Spain) were submerged briefly into sterile transport buffer (Table 2.4.) and then used to sample the concrete flooring (approx. 10 x 10 cm area) (Figure 2.1.) (Buttner, et al., 2001). The swabs were then maintained in the transport buffer at 4°C and transferred to -20°C within 24 h and stored until required.

Figure 2.1. Environmental sampling sites. Sheep were turned using turning crates and swabs taken from all four feet (A). Concrete floor swabs and faeces floor samples (B), bedding samples (C) and soil samples (D) were collected from a farm with a flock suffering with endemic FR. Arrows indicate faeces collected from the floor (FF).

2.5.6. Collection of oral cavity (OC) swabs.

Oral cavity (OC) swabs swabs (cotton and buccal) (EUROTUBO collection swab; Delta lab, Rubi, Spain) taken from around the lower gums (gingiva) and teeth from the front of the mouth towards the back (n = 35) and put into sterile transport buffer (Table 2.4.) and stored at -20^{o}C until required. Additionally, sterile buccal swabs (Epicentre Biotechnologies, Madison, WI, USA) were also taken from the same site for fluorescence *in situ* hybridisation (FISH) analysis.

2.6. DNA extraction methods.

2.6.1. NucleoSpin Blood kit.

2.6.1.1. NucleoSpin Blood kit for bacterial culture.

Chromosomal DNA was isolated from cells (up to 5.00 x 10^6 cells in a final volume of 200 µl PBS) using the NucleoSpin Blood kit (Macherey-Nagel, ABgene, Epsom, UK) according to the manufacturer's instructions. All timed incubations were carried out for the maximum amount of time stated and new collection tubes were always used (collection tubes were not re-used, in order to avoid the increased risk of cross-contamination). DNA was then eluted into 100 µl (maximum volume) of EB (elution buffer).

2.6.1.2. NucleoSpin Blood kit for swabs (ovine foot, concrete floor, oral cavity).

After sampling, swabs were submerged in 500 µl transport buffer (Table 2.4.) and stored at -20^{o}C until required. Swabs were then thawed on ice, vortexed briefly to resuspend swab material and 200 µl used for DNA extraction (Moore, et al., 2005a). Blank Extraction (BE) control swabs (sterile swabs with sterile buffer) were included for each

set of extractions.

2.6.1.3. NucleoSpin Blood kit for bedding samples.

The bedding samples were thawed, the weight recorded and 40 ml transport buffer (Table 2.4.) was added to each sample. The samples were then put on a shaker for 1 h at 37^{o}C. The liquid was then removed and centrifuged for 15 m at 12, 000 rpm at 4^{o}C. The supernantant was then decanted and the pellet resuspended in 2 ml 1x sterile PBS, of this 200 µl was then used for the DNA extraction using the NucleoSpin Blood kit, according to the manufacturer's instructions, and DNA eluted into 40 µl EB (Calvo-Bado, unpublished). Blank Extraction (BE) control samples using sterile bedding (autoclaved 121^{o}C for 15 m - two cycles) were included for each set of extractions.

2.6.2. FastDNA Spin kit for Soil.

2.6.2.1. FastDNA Spin kit for Soil - soil samples.

DNA was extracted from soil samples (n = 20) using the FastDNA Spin kit for Soil according to the manufacturer's instructions (QBiogene, Carlsbad, CA, USA). A total of 500 mg of soil was used for the extraction protocol and all timed incubations were carried out for the maximum amount of time stated. DNA was then eluted into 100 µl DES (DNase/Pyrogen Free Water). Blank Extraction (BE) control samples using sterile soil (autoclaved 121^{o}C for 15 m - two cycles, after cooling) were included for each set of extractions.

2.6.2.2. FastDNA Spin kit for Soil - faecal samples.

Individual bulk faecal samples (n = 62) were weighed and were diluted with sterile H_2O

in a ratio of 1:1 (w/v), tubes were then inverted for 1 m and further diluted 10^{-1} by adding 900 µl sterile H_2O to 100 µl pre-diluted faecal slurry (Layton, et al., 2006). A volume of 300 µl diluted faecal slurry was then used for the DNA extraction using the FastDNA Spin kit for Soil according to the manufacturer's instructions. All timed incubations were carried out for the maximum amount of time stated and DNA was then eluted into 100 µl DES (DNase/Pyrogen Free Water). Blank Extraction (BE) samples using sterile faecal material (autoclaved 121^{o}C for 15 m - two cycles, after cooling) were included for each set of extractions.

2.7. DNA quantification.

DNA sample purity and quantity was determined using a NanoDrop® (ND-1000) spectrophotometer (Labtech International Ltd., Luton, UK).

2.8. Polymerase Chain Reaction (PCR).

2.8.1. PCR primers.

The *Fusobacterium* genus primers (*FUSO1* and *FUSO2*) (Nagano, et al., 2007) were synthesised commercially (TIB MOLBIOL GmbH, Berlin, Germany). Primers were supplied as lyophilised powder, briefly centrifuged and resuspended in nuclease-free H_2O (Promega, London, UK) to create stock solutions of 100 µM (100 pmol μl^{-1}). The vector sequencing primers (M13f and M13r) supplied with the TOPO TA Cloning® kit (Invitrogen, Paisley, UK) were also treated as above, to create stock solutions of 100 µM (100 pmol μl^{-1}).

Table 2.7. PCR primers.

Target	Forward (5' to 3')	Reverse (5' to 3')
Fusobacterium genus (16S rRNA)[a]	GAG AGA GCT TTG CGT CC	TGG GCG CTG AGG TTC GAC
M13f and M13r vector primers[b]	GTAAAACGACGGCCAG	CAGGAAACAGCTATGAC

Respective annealing temperatures as determined by gradient PCR [a] 60°C and [b] 55°C.

2.8.2. PCR amplification and cycling parameters.

All PCR amplifications were carried out on an Eppendorf Mastercycler vapo.protect pro machine (Eppdendorf, Hamburg, Germany) using Promega PCR Master Mix (2x) (Promega, London, UK). All PCR reactions had a final reaction volume of 50 µl, containing 25 µl Master mix (50 units ml^{-1} *Taq* (*Thermus aquaticus*) DNA polymerase supplied in a proprietary reaction buffer (pH 8.5), containing deoxyribonucleoside triphosphates (dNTPs); 400 µM dATP, 400 µM dGTP, 400 µM dCTP, 400 µM dTTP and 3 mM $MgCl_2$), 2 µl of both sense and antisense primers (at a working concentration of 10 µM), 2.5 µl filter-sterilised bovine serum albumin (BSA) (10 mg ml^{-1}), with 1-2 µl of template DNA and made up to a final volume of 50 µl with sterile H_2O. PCR cycles consisted of an initial denaturation (1 cycle) step of 95°C for 5 m to ensure complete denaturation of the DNA template. The initial denaturation step was then followed by; a subsequent denaturation step of 95°C for 1 m, an annealing step of between 50-60°C for 1 m, an extension step of 72°C held for 1 m per kb of product (according to the manufacturer's instructions) (35 cycles each). Followed by a final extension step of 72°C for 10 m (1 cycle). Gradient PCRs were used to determine optimal annealing temperatures for each primer set.

2.9. Quantitative real-time PCR (qPCR).

2.9.1. The TaqMan® Probe chemistry.

For this study the TaqMan® Probe chemistry was used (Applied Biosystems, Warrington, UK), which employs a 5'-fluorescently-labelled oligonucleotide probe to enable specific detection of a PCR product as it accumulates during PCR. The probe was also labelled at the 3'-end with a non-fluorescent quencher (NFQ), which is cleaved by the the 5'-nuclease activity of the hot-start DNA polymerase (Applied Biosystems, Warrington, UK) during extension. This cleavage separates the reporter dye from the quencher, allowing the fluorescent dye emission to increase and be detected.

2.9.2. qPCR primer and probe sets.

Primer and probe sets were designed using the Primer Express® software v3.0 (Applied Biosystems, Warrington, UK), the first targeting a 61 bp sequence within the *rpoD* gene (RNA polymerase sigma subunit) of *D. nodosus* VCS1703A (accession no. NC_009446/Gene ID 5122738) (Calvo-Bado, et al., 2011b). The second targeting an 86 bp sequence within the partial *rpoB* gene (RNA polymerase beta subunit) of *F. necrophorum* subsp. *necrophorum* (accession no. AF527637.1). Primer and probe sets were selected based on the low penalty score and low amplicon size allocated by the software. The TaqMan probe® was selected first and the primers were then selected as close as possible to the probe sequence. The G/C content was kept within the 30-80 % range and identical runs of nucleotides (especially guanine) should be avoided if possible. Primer sequences had expected T_m of 58-60^{o}C and no more than two G and/or C bases were present at the 3'-ends. TaqMan probes® had a T_m of 68-70^{o}C (approx. 10^{o}C higher than that of the primers) and guanine residues at the 5'-ends were avoided.

The primer and probe sets were synthesised and purified (HPLC; high performance liquid chromotography) commercially (TIB MOLBIOL GmbH, Berlin, Germany). The TaqMan probes® were labelled at the 5'-end with the fluorescent dye FAM (6-carboxy-fluorescein) and at the 3'-end with a non-fluorescent quencher BBQ (Black Berry Quencher).

Table 2.8. qPCR primer and TaqMan® probe sets for the detection of *D. nodosus* (*rpoD*) and *F. necrophorum* (*rpoB*).

	Gene Target (5' to 3')	
	rpoD (***Dichelobacter nodosus***)	***rpoB*** (***Fusobacterium necrophorum***)
Forward	[1547] GCTCCCATTTCGCGCATAT [1565]	[103] AACCTCCGGCAGAAGAAAAATT [124]
Reverse	[1607] CTGATGCAGAAGTCGGTAGAACA [1585]	[189] CGTGAGGCATACGTAGAGAACTGT [166]
TaqMan® probe[ab]	[1567] 6FAM-CATTCTTACCGGA+T+C +CG-BBQ [1583]	[164] 6FAM-TCGAACATCTCTCGCTTTTTCCCCGA-BBQ [139]

[a] 6FAM (6 carboxy-fluorescein), BBQ (Black Berry Quencher).
[b] + indicates positions of LNA bases or 'locked' nucleotide bases, which increase stability of hybridisation to target sequence (Simeonov, et al., 2002).

2.9.3. Construction of standard curves.

The real-time qPCR method used (absolute quantification) required the construction of standard curves. Chromosomal DNA isolated from *D. nodosus* (VCS1703A) and *F. necrophorum* (clinical isolate BS-1) was quantified and the number of gene copies were then estimated using the dsDNA copy number calculator (http://www.uri.edu/research/gsc/resources/cndna.html). The calculation requires the DNA concentration (ng μl^{-1}) and the genome size (bp) of the microorganism (calculation presented in Section 2.21.1.). The *D. nodosus* (VCS1703A) genome (NC_009446) size is 1, 389, 350 bp (Myers, et

al., 2007), however the *F. necrophorum* genome has not yet been fully sequenced, and the calculation relies on the assumption that it is of a similar molecular size to the fully-sequenced *F. nucleatum* subsp. *nucleatum* genome (accession no. NC_003454) (2, 174, 500 bp) and that *F. necrophorum* also contains a single copy of the *rpoB* gene per cell (Aliyu, et al., 2004). Bacterial genomes normally only have one rpoB copy each (Case, et al., 2007).

For the longitudinal study (Chapter 3), serial dilutions of *D. nodosus* and *F. necrophorum* chromosomal DNA were then prepared to provide an estimated 2.04 to 2.04 x 10^6 *rpoD* copies μl^{-1} and 2.47 to 2.47 x 10^7 *rpoB* copies μl^{-1}, respectively. For environmental screening (Chapter 5) a second set of standards had to be prepared providing an estimated 7.89 to 7.89 x 10^6 *rpoD* copies μl^{-1} and 1.44 to 1.44 x 10^7 *rpoB* copies μl^{-1} for the *D. nodosus* (*rpoD*) and *F. necrophorum* (*rpoB*) assays, respectively.

2.9.4. qPCR amplification and cycling parameters.

The real-time qPCR assays were performed using an Applied Biosystems 7500 Fast Real-time detection system (Applied Biosystems, Warrington, UK). PCR master mix preparation and DNA manipulations were carried out in separate designated rooms with separate pipetting devices to avoid contamination. Each sample was run in technical triplicate and each amplification run was set up using the 96-well plate format (MicroAmp 96-Well Reaction Plate, Applied Biosystems). Each well contained a final volume of 25 µl; consisting of 12.5 µl of 2x TaqMan Universal Master Mix (Applied Biosystems, Warrington, UK), 2.5 µl Bovine Serum Albumin (BSA) (10 mg ml^{-1}), the final concentration of each primer was 900 nM and the final concentration of the probe

was 250 nM, with 1 µl of undiluted DNA extract used as template. A contamination control was also included in the form of nuclease-free water, i.e. non-template control (NTC). The Applied Biosystem rapid assay development guidelines were adhered to. A final concentration of 900 nM forward and reverse primer and 250 nM of TaqMan® probe provides a highly reproducible and sensitive assay when using cDNA or DNA as the assay template.

The cycling parameters for the *D. nodosus* (*rpoD*) real-time qPCR assay were: one cycle of denaturation at 95°C for 20 s followed by 40 cycles of amplification at 95°C for 3 s and at 55°C for 30 s. The cycling parameters for the *F. necrophorum* (*rpoB*) real-time assay were: 95°C for 20 s followed by 40 cycles of amplification at 95°C for 3 s and at 61°C for 30 s, as instructed by the manufacturer's set protocol. Modifications to the standard Applied Biosystem protocol; annealing temperatures were adjusted to 55°C and 61°C for the *D. nodosus* and *F. necrophorum* assays, respectively. The annealing temperature for the *D. nodosus* (*rpoD*) assays was decreased, in order to increase target detection (ΔRn), whilst retaining specificity. The annealing temperature for the *F. necrophorum* (*rpoB*) assay was instead increased in order to eliminate non-target detection (data not shown). The Applied Biosystems instrument calculates the increase in fluorescence in each reaction well. An increase in fluorescence above a calculated background threshold (ROX passive dye) indicates amplification of the target sequence. If no increase in the fluorescence signal is observed after 40 cycles, the sample is defined as 'undetectable' (below the limit of detection). The results were then analysed using the 7500 Fast System SDS software (Applied Biosystems); in the Analysis Settings, the Auto C_t option was selected to calculate the C_T values.

2.9.5. Analytical specificity.

The specificity of both assays was established by screening chromosomal DNA from a panel of microorganisms that had previously been detected on the ovine foot by either pyrosequencing methods (Calvo-Bado, et al., 2011b) or by isolation from the ovine foot (Nicky Buller, personal communication). For the *D. nodosus* (*rpoD*) real-time assay a total of twenty-three *D. nodosus* strains and fourteen negative controls were screened and for the *F. necrophorum* (*rpoB*) real-time assay a total of fourteen *F. necrophorum* (consisting of both subspecies) strains and fifteen negative controls were screened. PCR amplicon size and specificity (production of a single band) were determined by using gel electrophoresis on a 3 % (w/v) agarose gel (VWR International, Ltd., Lutterworth, UK). In addition, PCR products from both assays were cloned into the TOPO 2.1 vector system (Invitrogen Ltd., Paisley, UK), the inserts sequenced and the blastn algorithm used to confirm their identity in GenBank. PCR products could not be sequenced directly due to their small sizes (61 bp and 86 bp, respectively).

2.9.6. Analytical sensitivity.

The theoretical detection limit (TDL) for both assays was determined by using two separate methods. Firstly, the standard curves generated for each assay showed the lowest detected standard, which could then be extrapolated to estimate the TDL. The TDL for each sample type (swab, soil, faeces and bedding) was then determined using a series of spiking experiments.

2.9.6.1. Spiking of swab samples (estimation of TDL).

Sterile cotton swabs (EUROTUBO collection swab; Delta lab, Rubi, Spain) were spiked

with 500 µl undiluted and serially diluted *D. nodosus* (VCS1703A) culture (dilutions ranging from 10^{-1} to 10^{-7}) in sterile transport buffer (Table 2.4.) and *F. necrophorum* (clinical isolate BS-1) culture (ranging from 10^{-1} to 10^{-7}), prior to DNA extraction. This experiment was carried out twice; for the first, DNA was eluted into 100 µl EB and for the second, the DNA was eluted into 60 µl EB, to determine if decreasing the elution volume could increase the TDL significantly. In addition, clinical swabs (CS) (n = 4) (negative for either *D. nodosus* and/or *F. necrophorum* by qPCR taken from the ovine foot) were also spiked with the 10^{-1} and 10^{-2} dilutions of *D. nodosus* and *F. necrophorum* cultures, respectively, as performed by Lund and colleagues (2004). The clinical swabs (CS) were spiked to determine if lesion exudate / contaminating material (e.g. soil / faecal matter) present on the swab, interfered with the PCR reaction. Samples were then screened with both qPCR assays (*rpoD* and *rpoB*).

2.9.6.2. Spiking of faeces, soil and bedding (estimation of TDLs).

Bulk soil (Langford, Bristol, UK), bulk ovine faeces and bulk bedding samples were sterilised by autoclaving for 15 m at 121^{o}C (two cycles, after cooling). The samples were then setup to do a DNA extraction (as previously described), but prior to extraction were spiked with 50 µl or 1000 µl of either *D. nodosus* (VCS1703A) or *F. necrophorum* (clinical isolate BS-1) undiluted or serially diluted culture for soil/faeces and bedding samples, respectively. The dilution series ranged from 10^{-1} to 10^{-6} for faecal samples and 10^{-1} to 10^{-7} for soil and bedding samples. DNA was then extracted (as previously described) and samples screened using both qPCR assays (*rpoD* and *rpoB*).

2.10. Internal inhibition control.

An internal inhibition control reaction was used on environmental samples (soil, faecal, bedding) to determine if a sample was affected by inhibition and the extent of that inhibition. The protocol used an inhibition control plasmid (RD4-GFPpCR®2.1); TOPO pCR®2.1 plasmid (Invitrogen, Paisley, UK) containing a cloned green fluorescent protein (GFP) sequence (residues 61-120) flanked by *Mycobacterium bovis* region of deletion four (RD4) region primer sites. The internal inhibition control assays were performed as described (Pontiroli, et al., 2011) on a an Applied Biosystems 7500 Fast Real-time detection system (Applied Biosystems, Warrington, UK). Primer and probe sequences listed in Table 2.9. All wells (except three) were spiked with 1 µl of RD4-GFPpCR®2.1 plasmid (2.7 ng μl^{-1}) and 1 µl of undiluted DNA (sample) extract. Samples were run in technical triplicate and a 'no inhibition control' (NIC) was also included (in technical triplicate per 96-well plate). The NIC (containing the plasmid, without sample DNA) passed the threshold (C_T) at cycle number 21. A difference in sample C_T value compared to the NIC value of 21, was termed Delta C_T (ΔC_T). Inhibition was detected when ΔC_T values were > 0 and a ΔC_T value of 1 theoretically indicated a 2-fold decrease in RD4 detection (Pontiroli, et al., 2011).

Table 2.9. qPCR primer and TaqMan® probe set for the detection of the RD4-GFPpCR®2.1 plasmid. Plasmid contains a green fluorescent protein (GFP) sequence flanked by *Mycobacterium bovis* RD4 region primer sites (Pontiroli, et al., 2011).

Forward (5' to 3')	Reverse (5' to 3')	TaqMan® probe (5' to 3')[ab]
TGTGAATTCATACAAGCCGTAG TCG	CCCGTAGCGTTACTGAGAAAT TGC	JOE-ATATGAAA+CAG+CATGA +CTTT—BBQ

[a] JOE (6-carboxy-4', 5'-Dichloro-2',7'-Dimethoxyfluorescein, Succinimidyl Ester), BBQ (Black Berry Quencher). [b] + indicates positions of LNA bases or 'locked' nucleotide bases, which increase stability of hybridisation to target sequence (Simeonov, et al., 2002).

2.11. Gel Electrophoresis.

PCR products were analysed by electrophoresis on 1-3 % agarose (w/v) (VWR International Ltd., Lutterworth, UK) gels (depending on size of PCR products) containing 0.5 μg ml^{-1} ethidium bromide. Electrophoresis was performed at 120 volts for 45 m. Agarose gels were visualised and photographed using Gene Flash (Syngene Bio Imaging, Cambridge, UK). Fermentas O'GeneRuler™ 1 kb and 100 bp DNA ladders were used (Fermentas Life Sciences, York, UK).

2.12. Purification of PCR products.

PCR products were purified using the QIAquick Gel Extraction kit (Qiagen, West Sussex, UK) using the PCR Purification Spin Protocol according to the manufacturer's instructions. Centrifugation steps were carried out for the maximum amount of time stated and the DNA was eluted into a final volume of 50 μl EB.

2.13. Gel extraction.

If multiple bands were present on a gel, bands of the expected size were excised and DNA extracted using the QIAquick Gel Extraction kit (Qiagen, West Sussex, UK) using the Gel Extraction Spin Protocol according to the manufacturer's instructions. Incubation and centrifugation steps were carried out for the maximum amount of time stated and the DNA was eluted into a final volume of 50 μl EB.

2.14. TOPO TA Cloning®.

2.14.1. TOPO TA Cloning® reaction (ligation).

The TOPO TA Cloning® kit (Invitrogen Ltd., Paisley, UK) was used to clone *rpoD* and

rpoB PCR products using the aforementioned assays. The cloning procedure used fresh PCR products (with 3'- deoxyadenosine (A) overhangs) and the TOPO TA Cloning® reactions set-up according to the manufacturer's instructions and incubated at room temperature (22-23^{o}C) for the maximum amount of time stated (30 m).

2.14.2. Transformation of One Shot® TOP10 competent cells (*E. coli*).

The transformations were carried out using the chemically competent (TOP10) *E. coli* cells (Invitrogen Ltd., Paisley, UK). Kanamycin (50 μg ml^{-1}) was used as the selective agent for the regular chemical transformation protocol. All subsequent incubations were done using the maximum amount of time stated. In addition, the control TOPO® Cloning reaction, using the 750 bp control PCR product, was included for every set of reactions.

2.14.3. Analysing transformants.

Possible transformants (white or light blue colonies) were selected and (i) streaked onto LB plates containing kanamycin (50 μg ml^{-1}) for maintenance and storage and (ii) put into a well on a 96-well plate (each well containing 50 μl sterile H_2O) for downstream PCR screening, 1 μl of this was then used as template for PCR 'colony' screens. PCR screens were set-up as previously described, using the vector/sequencing primers (M13f and M13r). Vectors containing *rpoD* inserts and *rpoB* inserts produced single bands of 262 bp and 287 bp, respectively. Empty vectors (false positives) produced a single band of 201 bp. M13f and M13r PCR products (containing inserts, either *rpoD* or *rpoB*) were sent for sequencing.

2.15. Sequencing.

DNA was sequenced by the Molecular Biology Service at the University of Warwick. Sequencing reactions used Big Dye Terminator 3.1 chemistry (Applied Biosystems, Warrington, UK) and were run on a 3100 Genetic Analyser (Applied Biosystems, Warrington, UK). Sequences were then analysed using the blastn algorithm (Altschul, et al., 1997), and aligned using ClustalW2 (http://www.ebi.ac.uk/Tools/msa/clustalw2/) program using the default parameters.

2.16. Fluorescence *in situ* hybridisation (FISH).

2.16.1. FISH probes and dyes.

The EUB338-I (Alm, et al., 1996), EUB338-II (Daims, et al., 1999), EUB338-III (Daims, et al., 1999) and EUK1195 (Giovannoni, et al., 1988) oligonucleotide probes were synthesised commercially (Eurofins MWG-Biotech, Ebersberg, Germany) and each EUB338 probe labelled at the 5'-end with Cy3 (cyanine) and the EUK1195 probe labelled at the 5'-end with FITC (fluorescein). The *D. nodosus* and *F. necrophorum* (Boye, et al., 2006) oligonucleotide probes were also synthesised commercially (TIB MOLBIOL, GmbH., Berlin, Germany) and labelled at the 5'-end and 5'- and 3'-ends with Cy3, respectively. The *D. nodosus* oligonucleotide probe (Table 2.10.) was derived from the *D. nodosus* Cc primer (LaFontaine, et al., 1993). The oligonucleotide probes were received as lyophilised powder, were briefly centrifuged and resuspended using sterile distilled H_2O to create stock solutions of 100 µM (100 pmol μl^{-1}) and stored at -20^{o}C (in the dark) until required. Probes were then diluted to 10-12 µM (10-12 pmol μl^{-1}) to obtain working solutions of 50-60 ng μl^{-1} (as required).

In addition, 4',6-diamidino-2-phenylindole (DAPI) (VectaShield® Mounting Medium with DAPI H-1200, Vector Laboratories Inc., Burlingham, CA, USA) was used to stain nucleic acids (primarily used for the visualisation of epithelial cell nuclei). The fluorescence spectrum of each dye/fluorophore (DAPI, FITC, Cy3) was evaluated using Fluorescence Spectrum Viewer (BD Bioscience), in order to assess excitation and emission bandwidths. This determined if and where spectral overlap occurred. The set of dyes/fluorophores were chosen based on well-separated emission spectra.

Table 2.10. Oligonucleotide (FISH) probes with fluorescent labels and additional dyes.

Probe/dye name	Target	Sequence (5' to 3')	Fluorescent label (Max Ex/Em)
EUB338-I	90 % domain Bacteria (16S rRNA position 338-355)	GCT GCC TCC CGT AGG AGT	5' - Cy3 (550/564 nm)[a]
EUB338-II	Planctomycetales (16S rRNA position 338-355)	GCA GCC ACC CGT AGG TGT	5' - Cy3 (550/564 nm)
EUB338-III	Verrucomicrobiales (16S rRNA position 338-355)	GCT GCC ACC CGT AGG TGT	5' - Cy3 (550/564 nm)
EUK1195	Eukarya (18S rRNA position 1195 - 1210)	GGG CAT CAC AGA CGT G	5' - FITC (495/520 nm)[a]
D. nodosus	*Dichelobacter nodosus* (16S rRNA (position 821 - 840)*	TCG GTA CCG AGT ATT TCT AC	5' - Cy3 (550/564 nm)
F. necrophorum	*Fusobacterium necrophorum* (fnn, fnf) (16S rRNA)	GAT TCC TCC ATG CGA AAA	5' and 3' - Cy3 (550/564 nm) (also with Alexa Fluor® 594 (584/616 nm)[a]
DAPI	Nucleic acid	n/a	DAPI (360/460 nm)[b]

[a] Max Ex/Em (nm) as listed by IDT Integrated DNA Technologies (Coralville, IA, USA)

[b] DAPI Max Ex/Em (nm) as listed by Vector Laboratories Inc., (Burlingham, CA, USA)

* Nucleotide position in the *D. nodosus* 16S rRNA sequence (Dewhirst, et al., 1990; La Fontaine, et al., 1992)

2.16.2. Fixation protocols.

2.16.2.1. Fixation of Gram negative bacteria.

Gram negative cells were fixed with ice-cold 4 % PFA (w/v) in a ratio of 3 vol. PFA to 1 vol. sample and incubated at 4^{o}C for 3-12 h. The sample was then centrifuged at 4^{o}C at 12,000 rpm for 5 m and the supernatant was replaced with ice-cold 1x PBS, this procedure was carried out 2-3 times to remove residual fixative. Finally, the sample was resuspended in 1 vol. ice-cold 1x PBS to 1 vol. 96 % (v/v) ethanol. Samples were stored at -20^{o}C until required. (Amann, et al., 1990).

2.16.2.2. Fixation of Gram positive bacteria.

Gram positive cells were fixed with ice-cold 96 % (v/v) ethanol, in a ratio of 1:1 with the sample. Samples were stored at -20^{o}C until required. (Amann, et al., 1990).

2.16.2.3. Fixation of yeast cells (*Sz. pombe* and *S. cerevisiae*).

Two yeast species (*Schistosaccharomyces pombe* and *Saccharomyces cerevisiae*) were fixed with ice-cold 4 % PFA (w/v) in a ratio of 3 vol. PFA to 1 vol. sample and incubated at 4^{o}C for 4 h (Wallner, et al., 1993; Inácio, et al., 2010) and processed as described in Section 2.16.2.1.

2.16.2.4. Fixation and processing of tissue biopsies.

Immediately after collection, biopsies were submerged into 10 % (w/v) neutral buffered formalin (NBF) (Fisher Scientific, Leicestershire, UK) (containing 3.8-4.0 % formaldehyde in PBS) to fix for 24 h, to prevent autolysis and bacterial cell decomposition. The fixative volume was 15-20 times larger than the tissue volume

(Knoblaugh, et al., 2012) and fixed biopsies were sent to the Veterinary Pathology Department, Division of Veterinary Pathology, Infection and Immunity, School of Veterinary Science, University of Bristol, Langford, UK for processing. Biopsies were placed into labelled plastic cassettes and processed using an automatic tissue processor (Leica Histokinette®, Leica Instruments GmbH, Germany) on an 18 h schedule. The biopsies were subjected to a series of dehydration steps; 70 % alcohol for 1 h (1 cycle), 90 % alcohol for 1 h (1 cycle) and 100 % alcohol - 1 h 30 m (4 cycles), to remove any aqueous fixative and any tissue water content. The biopsies were then submerged into clearing fluid; Histo-Clear for 1 h 45 m (2 cycles), Histoclear 1 h 30 m (1 cycle) and then into molten paraffin wax for 2 h 30 m (60-65^{o}C) for embedding (carried out in a Tissue Tek® embedding centre). After cooling, the tissue blocks were trimmed and sections were cut from each block (approx. 4-5 µm thick) using a rotary microtome. Using a water bath (pre-heated) the wax-embedded sections were then floated and lifted onto glass microscope slides (to remove any creases) and left to dry.

Approximately six slides were produced for each individual punch biopsy, with 2-4 sections floated onto each slide. Sections were then collected and stored at 4^{o}C (embedded in wax) at the University of Warwick until required.

2.16.2.5. Fixation of oral cavity swab material.

Oral cavity buccal swabs (Epicentre Biotechnologies, Madison, WI, USA) were submerged into 300 µl ice-cold sterile 1x PBS, to which 900 µl of ice-cold 4 % (w/v) filter-sterilised PFA (ratio 1:3) was then added and gently pipetted up and down to resuspend swab material. Swabs were then incubated in the PBS:PFA mix at 4^{o}C for

3-12 h. The samples followed the same processing as for Gram negative bacteria (Section 2.16.2.1.).

2.16.3. FISH optimisation (*in vitro*).

2.16.3.1. Hybridisation stringency.

The correct hybridisation stringency (ensuring a probe is specific) was achieved by altering the formamide concentration (%) in the hybridisation buffer (Table 2.5.). The EUB338 probe set (-I, -II and -III) has a published optimal formamide concentration range of 0-50 % (Alm, et al., 1996; Daims, et al., 1999). However, the probe set was tested on four positive bacterial controls (two Gram negative and two Gram positive: *D. nodosus*, *E. coli*, *A. pyogenes*, *M. caseolyticus*) to confirm this. The *D. nodosus* probe was tested on three positive controls (*D. nodosus* strains: VCS1703A, Serogroup A and A198) and three negative controls (*E. coli*, *F. necrophorum* and *B. circulans*). The *F. necrophorum* probe (Boye, et al., 2006) was tested on three positive controls (*F. necrophorum*: BS-1, D213 and D555) and three negative controls (*E.coli*, *D. nodosus* and *B. circulans*). A more in-depth specificity screen then followed.

2.16.3.2. FISH probe specificity.

The *in silico* specificity of *D. nodosus* and *F. necrophorum* oligonucleotide probes was first checked using probeCheck (http://www.microbial-ecology.net/probecheck) (Loy, et al., 2008). The EUB338 probe set (-I, -II and -III) have been well studied and their specificity confirmed, therefore only positive controls were screened (*D. nodosus* VCS1703A, *M. caseolyticus*, *A. pyogenes*, *E. coli*, *B. circulans*, *F. necrophorum* (BS-1 clinical isolates and D809) to determine if any target organisms of interest (e.g. *F.*

necrophorum and *D. nodosus*) were not detected by this screen. The *D. nodosus* probe was screened against five positive controls (*D. nodosus* strains VCS1703A, Serogroup A, A198, BS-1 and BS-6) and nine negative controls (*B. circulans*, *A. pyogenes*, *E. coli*, *F. necrophorum*, *M. caseolyticus*, *Ae. media*, *Ae. hydrophila*, *K. pneumoniae* and *C. freundii*). The *F. necrophorum* probe was screened against seven positive controls (*F. necrophorum* BS-1 and *F. necrophorum* subsp. *necrophorum* (D146, D213, D306, D514, D555, D809) and seven negative controls (*B. circulans*, *A. pyogenes*, *E. coli*, *D. nodosus* (VCS1703A), *M. caseolyticus*, *Ae. media*, *Ae. hydrophila*, *K. pneumoniae* and *C. freundii*). In addition, Boye and colleagues (2006) demonstrated that the *F. necrophorum* probe also detected *F. necrophorum* subsp. *necrophorum* (ATCC 25286) and did not detect *F. nucleatum* (ATCC 25586).

2.16.3.3. Lysozyme pre-treatment.

Gram-positive cells required an additional lysozyme pre-treatment step to permeabilise the outer membrane, increasing the accessibility of the oligonucleotide probe. The lysozyme pre-treatment step was optimised using three Gram-positive bacteria (*A. pyogenes*, *M. caseolyticus* and *B. circulans*) and three Gram-negative bacteria (*E. coli*, *D. nodosus*, *F. necrophorum*) as negative controls. The positive and negative controls were incubated at 37^{o}C with lysozyme (10 mg ml^{-1}) over a time series; 0 m, 30 s, 1 m, 2 m, 3 m, 4 m, 10 m and 20 m. After lysozyme treatment the slides were submerged into sterile distilled H_2O for 2-3 s to remove the lysozyme and then left to air-dry in a drying rack. The FISH procedure was followed once the slides were dried. All cells were screened with the EUB338 (-I, -II and -III) probe set (except *F. necrophorum*, which was screened with the *F. necrophorum*-specific probe (Boye, et al., 2006)) and target

cell fluorescence measured using ImageJ (Abramoff, et al., 2004) (http:// rsb.info.nih.gov/ij/). Lysozyme experiments were performed in duplicate.

2.16.3.4. Proteinase K pre-treatment for tissue sections.

Tissue sections were pre-treated with proteinase-K (5 µg ml^{-1}) at room temperature (22-23^{o}C) for 10 m and washed in sterile distilled H_2O, as described by Peters, et al., (2011). This pre-treatment step was tested on a number of bacterial cells (*D. nodosus*, *F. necrophorum*, *A. pyogenes*) to determine it's effect on bacterial cells. Proteinase K experiments were performed in duplicate.

2.16.4. FISH optimisation (*in situ*).

2.16.4.1. FISH sensitivity using tissue.

Biopsies were taken from the interdigital space of healthy feet (H); no signs of clinical disease (obtained from the EU-licensed red meat abattoir at the Bristol Veterinary School, University of Bristol, Langford, UK). The biopsies (n = 32) were then subcutaneously inoculated using sterile 25 gauge (G) needles (BD Microlance™ 3, BD, Drogheda, Ireland) to inject each biopsy with either *F. necrophorum* (clinical isolate BS-1) or *D. nodosus* (VCS1703A). Biopsies were inoculated at multiple sites in an attempt to evenly distribute the inocula. Individual punch biopsies were inoculated with 100 µl undiluted and serial diluted culture (10^{-2}, 10^{-4} and 10^{-6}), which were made using sterile H_2O. The biopsies were then incubated in sterile petri dishes for 1 h and 24 h at 37^{o}C under (i) aerobic conditions and (ii) anaerobic conditions. Biopsies were then processed as previously described and screened using the *D. nodosus*, *F. necrophorum* and EUB338 (-I, -II, -III) probe sets. DNA was extracted from undiluted cultures as

described in Section 2.6.1.1. and quantified using the aforementioned qPCR assays (Section 2.9.4.) to quantify the number of *rpoD* and *rpoB* copies present, to provide an estimated bacterial load (*rpoD* or *rpoB* copies ml^{-1}) for the undiluted inocula prior to spiking the biopsies and therefore can only be considered semi-quantitative.

2.16.4.2. FISH sensitivity using swabs.

One Gram negative (*E. coli*) and one Gram positive (*M. caseolyticus*), representing the PFA-fixation and ethanol-fixation methods, respectively, were used to test the sensitivity of FISH using swabs. Initial cultures were diluted 10^{-2} with 1x sterile PBS and cells concentrations determined using a haemocytometer using the following calculation:

$$\text{mean cells per square}^{*} \times \text{dilution factor} \times 10^{4} = \text{cells ml}^{-1}$$

* bacterial cells were counted in a total of five 1 mm^2 squares, to calculate the mean.

The undiluted *E. coli* (K-12) and *M. caseolyticus* (87) cultures were determined to have 3.02 x 10^8 and 3.17 x 10^8 cells ml^{-1}, respectively. Cultures were then serially diluted (10^{-1} to 10^{-7}) using 1x sterile PBS and 300 µl of each samples was then aliquoted into 2.0 ml tubes containing sterile cotton swabs. Undiluted and serially diluted *E. coli* (K-12) swab samples were fixed with 900 µl 4 % (v/v) PFA (1:3) at 4°C for 3-12 h. Cells were then washed as described in Section 2.16.2.1. and cell pellets resuspended and stored in 300 µl 1x PBS and 300 µl 96 % (v/v) ethanol (1:1) at -20°C. Undiluted and serially diluted *M. caseolyticus* (87) swab samples were fixed with 300 µl 96 % (v/v) ethanol (1:1) and stored at -20°C. Fixed *E. coli* (K-12) and *M. caseolyticus* (87) cells were spotted (20 µl) onto Poly-Prep slides and the FISH procedure performed as

described in Section 2.16.5. using the EUB338 (-I, -II, -III) probe set.

2.16.5. FISH protocol.

2.16.5.1. FISH protocol - bacterial cells and ovine oral cavity material.

Fixed bacterial cells were spotted (2-35 µl depending on cell density) onto Poly-Prep Slides (coated with poly-L-lysine) and left to air-dry. Gram positive cells were pre-treated with lysozyme (10 mg ml^{-1}) as previously described. The slides were then subjected to an ethanol gradient (dehydration series); 50 %, 80 % and 96 % ethanol (v/v) for 3 m each. After dehydration, the slides were left to air-dry on a drying rack. Once dry, 10 µl of hybridisation buffer (Table 2.5.), containing 30-50 ng $µl^{-1}$ of target probe(s) was spotted on top of the bacterial smear. The remaining hybridisation buffer was poured onto folded tissue paper and put inside a 50 ml falcon tube (Becton Dickinson Labware, Cowley, Oxford, UK), to create a humid hybridisation chamber, the slide was then inserted into the same tube and left to incubate for 4 h at 46^{o}C. The slides were then removed, rinsed briefly and then submerged into the corresponding (matching formamide percentage) wash buffer (Table 2.6.) for 15 m at 48^{o}C. The slides were then removed and dipped briefly (2-3 s) in ice cold sterile distilled H_2O and dried with pressurised air (Dust-Pro®). The samples were then mounted with VectaShield® Mounting Medium H-1000 (Vector Laboratories Inc., Burlingham, CA, USA) and a coverslip placed on top.

2.16.5.2. FISH protocol - interdigital space biopsies.

The tissue samples were stored as paraffin-embedded sections mounted on glass slides at 4^{o}C. The selected slides were dewaxed in Histo-Clear (National Diagnostics, Atlanta,

GA, USA) for 10 m, followed by a second wash in fresh Histo-Clear for 5 m. Slides were then rinsed with sterile distilled H_2O for 2-3 s before being rehydrated in an ethanol gradient; 100 % ethanol and 70 % ethanol (v/v) for 10 m each. The tissue sections were then air-dried and subjected to a proteinase K pre-treatment step, in order to reduce intrinsic tissue autofluorescence and aid probe penetration (Peters, et al., 2011), as previously described. The slides were dehydrated using an ethanol series - 70 % and 100 % ethanol (v/v) for 6 m each and left to air-dry in a drying rack (Peters, et al., 2011). Samples to be screened with the general bacterial probes (EUB338-I, -II and -III) were also pre-treated with the aforementioned lysozyme step to increase target detection. Samples to be screened with the *D. nodosus* or the *F. necrophorum* probes did not require lysozyme pre-treatment. The FISH procedure was then continued as described previously (Section 2.16.5.1.). The samples were then mounted with VectaShield® Mounting Medium with DAPI H-1200 (Vector Laboratories Inc., Burlingham, CA, USA) and a coverslip placed on top.

2.17. Haematoxylin and Eosin staining (tissue).

Haematoylin and eosin is the most commonly used staining in anatomical pathology worldwide (Churukian, 2009). Tissue samples were dewaxed using Histo-Clear (National Diagnostics, Atlanta, GA, USA) as previously described (Section 2.16.5.2.) and rinsed in ethanol and then sterile distilled H_2O. Sections were covered with Harris' Haematoxylin stain and left for 10 m and then rinsed in sterile distilled H_2O for 1 m (blueing). A few drops of 1.0 % HCl (v/v) in 70 % ethanol (v/v) were then applied to the top of the section for 10 s for differentiation and rinsed again using sterile distilled H_2O (for 5 m). Surface water was then removed and the back of the slide dried with tissue

paper. Eosin Y 1 % (w/v) stain was then added for 4 m and the slide rinsed again in sterile distilled H_2O. The sections were then dehydrated using a few drops of 100 % ethanol (v/v) for 30 s and rinsed with sterile distilled H_2O. Finally, the slides were mounted xylene and coverslips applied (Kumar and Kiernan, 2010).

2.18. Image acquisition.

2.18.1. Light microscopy.

Bacterial cells were examined using a light microscope (Unilux-11, Kyowa, Tokyo, Japan) using the x100 objective (oil immersion) prior to and after fixation to confirm purity of the culture and to examine cell density.

2.18.2. Confocal-laser scanning microscopy (CLSM).

Tissue sections and oral cavity slides were examined using a True Confocal Scanner Leica TCS SP5 microscope (Leica Microsystems Ltd., Milton Keynes, UK) using the 100x objective (oil immersion). The Blue Diode (405 nm), Argon gas (488 nm), Ti sapphire (561 nm) and Orange HeNe (596 nm) lasers were used for this study. Z-series were taken for all images.

2.19. Image analysis.

All image processing was carried out using the open source software ImageJ (http://rsb.info.nih.gov/ij/) (Abramoff, et al., 2004). Average pixel intensity and cell length measurements were recorded by ImageJ and bacterial cell counts were carried out using the Cell Counter plug-in (Kurt De Vos, University of Sheffield; kurt.devos@iop.kcl.ac.uk).

2.19.1. Measuring pixel intensity.

Colour images were converted to 8-bit images, which can display 256 (2^8) grey levels; a grey level range of 0-255. Individual pixel intensity is assigned an arbitrary value based on this range; a value of 0 would indicate absence of signal/noise and a value of 255 would indicate complete pixel saturation. The average pixel intensity of selected objects was measured using ImageJ (http://rsb.info.nih.gov/ij/) (Abramoff, et al., 2004).

2.19.2. Bacterial quantification using FISH.

Each biopsy section was screened using the three different oligonucleotide probes (EUB338-I, -II, -III, *D. nodosus* and *F. necrophorum*_183) and a total of twelve images taken for each screen; three from the epidermis (E), three from the epidermal-dermal boundary (EDB) and three from the dermis (D). The three images from each tissue layer (E, EDB, and D) were taken randomly. Each image or field of view (FOV) was standardised to 25 μm^2 (Davenport and Curtis, 2008). Bacterial counts were then +1 $\log_{10}$ transformed for downstream analysis.

2.20. Multinomial model construction in MLwiN 2.21.

Real-time qPCR data obtained from the longitudinal study were analysed using an unordered multinomial mixed effects model accounting for repeated observations and samples of feet clustered within ewes using MLwiN 2.21 [www.bristol.ac.uk/cmm/software/mlwin/] (Rabash, et al., 2005). The outcome variables were healthy H-, ID- and FR-affected feet in a week clustered by repeated measures of feet and sheep. The explanatory variables were *D. nodosus* (*rpoD*) and *F. necrophorum* (*rpoB*) copies $swab^{-1}$, at the week sampled and one week earlier as; undetectable (baseline): below the

LOD (< 10^3 copies swab^{-1}), low: 10^3 to < 10^4 copies swab^{-1}, mid: 10^4 to < 10^5 copies swab^{-1}, high: 10^5 to < 10^6 copies swab^{-1} and highest: ≥ 10^6 copies swab^{-1}. The 'high' category for *F. necrophorum* was instead categorised as ≥ 10^5 *rpoB* copies swab^{-1}. Healthy feet were classified as the baseline. The effect of *D. nodosus* (*rpoD*) and *F. necrophorum* (*rpoB*) were considered separately (univariate) and together (multivariable). The model outputs a coefficient and a standard error of the mean (SEM), from which, the odds ratios (ORs) and 95 % confidence intervals (CI) were calculated. Statistical significance of $p < 0.05$ was assumed when the 95 % CI and OR did not overlap with a value of 1 (null hypothesis, i.e. no association) (von Wissman, et al., 2012). *Prof. L. E. Green is acknowledged for the construction of the multinomial model.

2.21. Data and statistical analysis.

2.21.1. DNA standard curve calculation (copy number).

$$\text{number of genome copies} = \frac{(\text{amount} \times 6.022 \times 10^{23})}{(\text{genome size} \times 1 \times 10^{9} \times 650)}$$

Amount: ng of DNA, 6.022×10^{23}: Avogadro's constant, genome size: expressed in bp, 1×10^{9}: to express as ng and 650: average weight of a bp (650 daltons).

2.21.2. Calculation of TDL.

This calculation is dependent on the sample size, dilution factors used at various stages of the procedure and DNA elution volume (Pontiroli, et al., 2011). The TDL was determined using the following calculation:

$$TDL = (1/TV) \times (1/w) \times (D) \times (E)$$

TV: volume (µl) of template DNA used for the PCR reaction, w: weight/volume (g)/(µl) of sample used for DNA extraction, D: dilution factor and E: elution volume (µl).

2.21.3. Statistical analysis using GraphPad Prism.

Statistical analyses were performed using GraphPad Prism software (version 4.0 for Windows; GraphPad Software, San Diego, California, USA [www.graphpad.com]). Correlation data for $\log_{10}$ *D. nodosus* and *F. necrophorum* load by disease state and $\log_{10}$ red blood cell (RBC) counts by $\log_{10}$ bacterial cells counts were analysed using Pearson's correlation test. Bacterial and RBC counts obtained from FISH analysis were +1 $\log_{10}$ transformed and were either analysed using a one-way ANOVA, followed by a Bonferroni's post-hoc test for pairwise comparisons or using an unpaired t-test. P-values of < 0.05 were considered significant. Contingency tables were used to analyse percentage positive results; results were first analysed using a 3x2 contingency table with Chi-squared test, followed by 2x2 contingency tables with Fishers exact test for pairwise comparison by disease state (H, ID, FR). P-values of < 0.05 were considered significant.

2.21.4. Calculation of SEM in Apple iWork Numbers '09 software.

= (STDEV(**A1:A2**) / (SQRT(COUNT(**A1:A2**)))[a]

[a] **A1:A2** refer to range of data selection

CHAPTER 3

3. The longitudinal detection and quantification of *D. nodosus* and *F. necrophorum* from a flock with a history of endemic footrot.

3.1. Introduction.

Footrot (FR) is characterised by two clinical presentations; inflammation of the interdigital space (interdigital dermatitis, ID), which in some circumstances is followed by separation of the hoof horn from the sensitive under-lying tissue (footrot, FR) (Beveridge, 1941). Damage to the epithelium of the interdigital space is a prerequisite for the initiation of disease (Beveridge, 1941), which allows the damaged epidermis to be invaded by *F. necrophorum*, in turn facilitating the invasion of *D. nodosus*, the causative agent of ovine FR (Roberts and Egerton, 1969). *D. nodosus* is primarily responsible for the under-running of the hoof horn and has been shown to cause FR in experimentally infected sheep (Beveridge, 1941; Roberts and Egerton, 1969; Kennan, et al., 2001; 2010). *F. necrophorum*, however, is only reported to cause a mild to severe ID in sheep that have been experimentally infected (Parsonson, et al., 1967). In contrast, Bennett, et al., (2009) reported that *D. nodosus* and *F. necrophorum* were more likely to be co-detected by PCR in cases of FR and postulated that both organisms therefore contributed to the disease process.

The study of microbial communities and succession with regards to infectious disease development is vitally important, as changes in the total or subsets of that community may play a role in facilitating pathogen invasion (Mao-Jones, et al., 2010). A recent

study (Calvo-Bado, et al., 2011b) examined changes in the total ovine foot microbiome ('ovine pedome') in relation to ID and FR in sheep and found that there were profound differences in the bacterial community structures by clinical condition, possibly demonstrating the importance of community shifts in supporting the colonisation and growth of *F. necrophorum* and *D. nodosus*. The authors also detected *D. nodosus* from interdigital space biopsies over all three disease states (healthy, ID and FR) using a nested PCR approach. The *F. necrophorum* population, however, was not examined.

A number of other studies have also investigated the presence of *D. nodosus* and *F. necrophorum* in sheep in relation to clinical presentation (La Fontaine, et al., 1993; Moore, et al., 2005a; Bennett, et al., 2009). However, the cross-sectional nature of these studies prevents extrapolation to disease initiation and progression and therefore determining when the *F. necrophorum* and *D. nodosus* populations become important, is difficult. In line with this problem, a number of criteria have been established to help distinguish causation from association (Hill, 1965) (Table 3.1.).

Table 3.1. Study criteria to help differentiate causation from association[a].

Criterion	Definition
Temporality	The cause (in this case the causative agent) must precede the effect.
Strength of association	Strong associations will increase confidence.
Dose response	Responses that increase as a result of increased exposure (biological gradient).
Consistency	Correlates with other scientific reports.
Biological plausibility	Results are consistent with the biological understanding of the disease.

[a] Hill, 1965

The first criterion describes that for the relationship to be causal, the causative agent (in this case *F. necrophorum* or *D. nodosus*) must precede the effect (the development of ID or FR) and therefore longitudinal sampling is essential. The second criterion indicates that the strength of an association (likelihood) is also an important factor when considering causality. An odds ratio (OR) is one way of assessing the relative measure of risk or strength of an association; comparing the odds of an event occurring (e.g. disease) if a particular factor/biological agent is present. The OR compares the risk of this event occurring in one group to the risk of it occurring in another group. An OR of 1 therefore indicates that the event is just as likely to occur in both groups (reference and test groups), whereas an OR of > 1 implies that the event is more likely to occur in the test group. In addition, a dose-response (or biological gradient) describes that individuals with a greater exposure to an agent are more likely to have an effect - this criterion is supportive of a causal relationship. Finally, the last two criteria represent whether the data found are consistent with what is thought to occur biologically and whether it is consistent with other published data (Hill, 1965). Together, these factors strengthen studies that assess causality and risk. In addition, regression analysis is useful for discovering or disentangling relationships in complex data sets (Freedman, 1997).

Despite a number of experimental infection studies (Beveridge, 1941; Roberts and Egerton, 1969; Kennan, et al., 2001; 2010) that clearly demonstrate *D. nodosus* as the causal agent of ovine FR, a number of authors suggest that *F. necrophorum* is responsible for or at least contributes to the disease process (ID/FR) (Parsonson, et al., 1967; Roberts and Egerton, 1969; Bennett, et al., 2009).

3.2. Aims.

The temporal patterns associated with *F. necrophorum* and *D. nodosus* load were therefore elucidated, to determine the key microbial succession events involved in the initiation and development of ID and FR in sheep.

The hypotheses were that (i) *D. nodosus* and *F. necrophorum* would be more frequently detected in diseased sheep, as previously found by standard PCR or culture techniques (Moore, et al., 2005a; Bennett, et al., 2009), (ii) that *F. necrophorum* load would increase prior to the development of ID (in line with its reported inflammatory/initiatory role) (Roberts and Egerton, 1969), (iii) that *D. nodosus* load would instead increase prior to the development of FR, in line with its causal nature (Beveridge, 1941; Roberts and Egerton, 1969; Kennan, et al., 2001; 2010) and that (iv) after the development of FR, *D. nodosus* and *F. necrophorum* loads would decrease, possibly due to the sloughing of necrotic tissue (Beveridge, 1941).

3.3. Results.

3.3.1. Study flock (1) information.

The study flock (n = 570) was located on lowland pastures in Oxfordshire, England, which during the sampling period (October 2006) was recorded to have a high rainfall and an average temperature of 10-12^{o}C. The The flock consisted of Mule and Suffolk cross-breeds and had a long history of endemic FR. The flock were monitored during a period of high transmission, when environmental conditions (rainfall, temperature) were conducive for transmission. From this flock a subset (n = 60) of ewes were monitored and of these, eighteen were selected for further analysis (presenting with a range of non-

experimentally induced disease states). Ovine foot swabs and ID and FR severity scores were collected from these eighteen sheep from every foot once a week for five weeks, as described in Section 2.5.1, resulting in a total of 349 individual foot swabs and severity scores. The sheep selected had a range of non-experimentally induced disease states (Table 3.2.) and during the sampling period study flock (1) had a 30.53 % prevalence of ID and a 4.75 % prevalence of FR.

Table 3.2. Information regarding the selected eighteen ewes from study flock (1). Sheep categorised into healthy, ID and FR groups. Sheep identification numbers followed by numbers of swabs collected in brackets. Foot swabs and severity scores were collected from the eighteen sheep below from every foot (RF, LF, RH, LH), once a week during a five week study. On eleven occasions a swab could not be collected.

H (n = 3)[a]	**ID** (n = 7)[b]	**FR** (n = 8)[c]
2685 (n = 16)	2208 (n = 20)	2290 (n = 20)
2720 (n = 19)	2223 (n = 20)	2650 (n = 19)
2229 (n = 19)	2274 (n = 20)	2613 (n = 20)
	2620 (n = 20)	2211 (n = 20)
	2705 (n = 19)	2225 (n = 20)
	2314 (n = 19)	2610 (n = 19)
	2301 (n = 20)	2714 (n = 19)
		2234 (n = 20)

[a] Healthy sheep - all four feet remained healthy (no ID/no FR) during the five week study. [b] Sheep with ID - one or more feet had ID during the five week study (other feet were healthy). [c] Sheep with FR - one or more feet had FR during the five week study (other feet were healthy or had ID).

3.3.2. The development of two TaqMan® real-time qPCR assays for the detection and quantification of *D. nodosus* and *F. necrophorum.*

As described in Section 2.9.2., the Primer Express® (v3.0) software was used to design two primer and TaqMan® probe sets (Table 2.8.). The first set targeted a 61 bp sequence

within the *rpoD* gene (RNA polymerase sigma subunit) of *D. nodosus* VCS1703A (accession no. NC_009446) and an 86 bp sequence within the partial *rpoB* gene (RNA polymerase beta subunit) of *F. necrophorum* subsp. *neccrophorum* (accession no. AF527637.1). The *rpoD* and *rpoB* genes were selected based on their house-keeping status and because the *rpoD* gene was present in 1 copy per *D. nodosus* genome, making quantification analysis simpler. In addition, the *rpoB* gene has previously been used for quantification of *F. necrophorum* from clinical samples (Aliyu, et al., 2004), making it an ideal candidate. The default Applied Biosystems amplification and cycling parameters, as detailed in Section 2.9.4, were used for both assays. However, the annealing temperatures of the *D. nodosus* (*rpoD*) and *F. necrophorum* (*rpoB*) assays were adjusted to 55^{o}C and 61^{o}C, respectively. The annealing temperatures were altered, in order to increase target detection (signal magnitude) (ΔRn) for the *D. nodosus* (*rpoD*) assay and to decrease any non-target detection to below the threshold for the *F. necrophorum* (*rpoB*) assay (data not shown).

3.3.3. Analytical specificity.

The analytical specificity of both assays was then assessed by screening positive control strains of *D. nodosus* and *F. necrophorum*, in order to determine if any amplicon sequence variation occurred. A panel of negative control microorganisms, which had previously been detected on the ovine foot, either by pyro-sequencing methods (Calvo-Bado, et al., 2011b) or by isolation techniques (Nicky Buller, personal communication), were also screened. Both assays amplified all tested positive strains of their respective targets, indicating that little or no amplicon variation occurred (Table 3.3. and 3.4.).

Table 3.3. Analytical specificity of *D. nodosus* (*rpoD*) assay.

***D. nodosus* strain**	**Result**	**Negative controls**	**Result**
Serogroups		*Arcanobacterium pyogenes* (DS7M20-630)	-
Serogroup A	+	*Corynebacterium amycolatum*	-
Serogroup B	+	*Corynebacterium urealyticum*	-
Serogroup C	+	*Enterococcus* sp.	-
Serogroup D	+	*Escherichia coli*	-
Serogroup E [a]	+	*Fusobacterium necrophorum* (BS-1)	-
Serogroup F	+	*Fusobacterium nucleatum* (ATCC 25286)	-
Serogroup H	+	*Lactococcus garvieae*	-
Serogroup I	+	*Mycobacterium bovis*	-
Control strains		*Pseudomonas putida*	-
VCS1703A ('virulent'[b] control) [a]	+	*Staphylococcus aureus*	-
C305 ('benign'[b] control) [a]	+	*Staphylococcus simulans*	-
Clinical isolates (ovine)		*Streptococcus* sp.	-
BS-1	+	*Streptomyces* sp.	-
BS-2	+		
BS-4	+		
BS-6	+		
BS-10	+		
BS-13	+		
BS-18 [a]	+		
BS-19	+		
BS-23	+		
BS-27	+		
BS-30	+		
Clinical isolates (bovine)			
C809	+		
C810	+		

[a] *D. nodosus rpoD* PCR products from these strains were cloned and sent for sequencing to confirm their identities. [b] Virulent and benign controls refer to positive/negative results on the gelatinase gel test (Palmer, 1993).

Table 3.4. Analytical specificity of *F. necrophorum* (*rpoB*) assay.

***F. necrophorum* strain**	**Result**	**Negative controls**	**Result**
Reference strains (HPA)		*Arcanobacterium pyogenes* (DS7M20-630)	-
NCTC 10576 *F. necrophorum* subsp. *necrophorum* [a]	+	*Corynebacterium amycolatum*	-
ATCC 25286 *F. necrophorum* subsp. *necrophorum*	+	*Corynebacterium urealyticum*	-
ATCC 51357 *F. necrophorum* subsp. *funduliforme* [a]	+	*Dichelobacter nodosus* (VCS1703A)	-
Clinical isolates (HPA & Bristol)		*Enterococcus* sp.	-
BS-1 *F. necrophorum* [a]	+	*Escherichia coli*	-
R17807 *F. necrophorum*	+	*Fusobacterium nucleatum* (ATCC 25286)	-
B571 *F. necrophorum* subsp. *funduliforme* [a]	+	*Fusobacterium simiae* (ATCC 33568)	-
B575 *F. necrophorum* subsp. *necrophorum*	+	*Fusobacterium varium* (AR17443)	-
B579 *F. necrophorum* subsp. *necrophorum*	+	*Lactococcus garvieae*	-
Clinical isolates (VLA)		*Mycobacterium bovis*	-
D213 *F. necrophorum* subsp. *necrophorum*	+	*Pseudomonas putida*	-
D332 *F. necrophorum* subsp. *necrophorum*	+	*Staphylococcus aureus*	-
D514 *F. necrophorum* subsp. *necrophorum*	+	*Staphylococcus simulans*	-
D555 *F. necrophorum* subsp. *necrophorum*	+	*Streptococcus* sp.	-
D745 *F. necrophorum* subsp. *necrophorum*	+	*Streptomyces* sp.	-
D797 *F. necrophorum* subsp. *necrophorum*	+		

[a]*F. necrophorum rpoB* PCR products from these strains were cloned and sent for sequencing to confirm their identities.

In addition, no signal was detected when screening non-target microorganisms (Table 3.3. and Table 3.4.) or the non-template controls (NTC), indicating that the assays were

specific for their respective targets and that contamination did not occur. Both assays produced single bands of the expected sizes (when examined by gel electrophoresis) and non-specific spurious bands were not observed (Figure 3.1.).

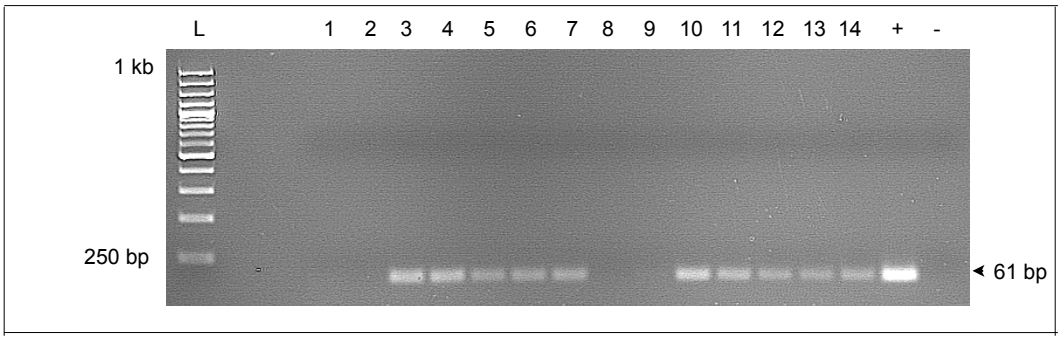

Figure 3.1. *D. nodosus* (*rpoD*) qPCR products on a 3 % (w/v) agarose gel. The production of a single discrete band (61 bp) was observed. Ladder (L) - Fermentas O'GeneRuler 1 kb DNA ladder with 1 kb and 250 bp markers indicated. 1-14: a selection of ovine foot swabs taken during the longitudinal study, +: *D. nodosus* positive control (strain A198) and -: negative control (sterile H_2O). Blank lanes indicate samples as negative or below the theoretical detection limit (TDL) (as described in Section 3.3.4.). Similar gels were run for *F. necrophorum* (*rpoB*) qPCR products (data not shown) and single discrete bands of 86 bp were observed.

The *rpoD* and *rpoB* PCR products were then cloned using the TOPO TA Cloning® kit as described in Section 2.14, transformants were screened for inserts (Figure 3.2.) using the M13f and M13r vector primers (Table 2.7.) and PCR products were sent for sequencing and analysed as described in Section 2.15. The *rpoD* and *rpoB* PCR products could not be sent directly for sequencing, because of the small amplicon sizes (61 bp and 86 bp, respectively) and therefore cloning was required. A total of seven *rpoD* amplicons were cloned and sequenced, from four lab isolates (Table 3.3.) and three ovine foot swabs. A total of six *rpoB* amplicons were cloned and sequenced from four lab isolates (Table 3.4.) and two ovine foot swabs.

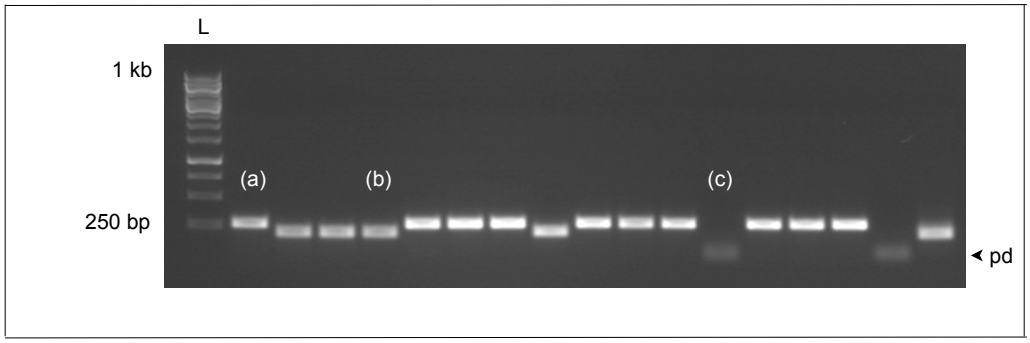

Figure 3.2. Colony screen (using M13f and M13r vector primers) for *rpoD* inserts on a 1 % (w/v) agarose gel. Products appear as either (a) vector with *rpoD* insert (262 bp) (or 287 bp for *rpoB* inserts), (b) vector without insert (201 bp) or (c) failed PCR/no PCR product observed, arrow highlights faint primer dimer (pd). Ladder (L) - Fermentas O'GeneRuler 1 kb DNA ladder with 1 kb and 250 bp markers indicated. Negative control (sterile H_2O) included, but not shown on this row. Similar screens were run for cloned *F. necrophorum* (*rpoB*) PCR products (data not shown).

The *rpoD* sequences revealed a 100 % sequence similarity to the *D. nodosus rpoD* sequence with no other matches. The *rpoB* sequences from *F. necrophorum* (BS-1) and subsp. *necrophorum* (NCTC 10576) revealed a 97 % sequence similarity, due to a deletion (position 129) and an insertion (position 137), that were not observed in the partial GenBank sequence (accession no. AF527637.1). However, the two sequence differences were uniform in the seven cloned sequences, suggesting that the partial GenBank sequence was incomplete/incorrect. The *rpoB* gene sequences for subsp. *funduliforme* instead revealed at 96 % sequence similarity, due to an additional mismatch at position 130, this mismatch was not present in either the primer or probe binding sites and thus would not have affected binding or amplification efficiency (Figure 3.3.).

***D. nodosus* (*rpoD*) cloned sequences**

```
GenBank sequence  F >                Probe >                              < R
VCS1703A        1547GCTCCCATTTCGCGCATATACATTCTTACCGGATCCGTTGTTCTACCGACTTCTGCATCAG1607
Lab strains
VCS1703A          GCTCCCATTTCGCGCATATACATTCTTACCGGATCCGTTGTTCTACCGACTTCTGCATCAG
C305               GCTCCCATTTCGCGCATATACATTCTTACCGGATCCGTTGTTCTACCGACTTCTGCATCAG
BS-18              GCTCCCATTTCGCGCATATACATTCTTACCGGATCCGTTGTTCTACCGACTTCTGCATCAG
SgE                GCTCCCATTTCGCGCATATACATTCTTACCGGATCCGTTGTTCTACCGACTTCTGCATCAG
Longitudinal study
2208 RF 30/10/06  GCTCCCATTTCGCGCATATACATTCTTACCGGATCCGTTGTTCTACCGACTTCTGCATCAG
2650 RF 04/10/06  GCTCCCATTTCGCGCATATACATTCTTACCGGATCCGTTGTTCTACCGACTTCTGCATCAG
2211 RF 30/10/06  GCTCCCATTTCGCGCATATACATTCTTACCGGATCCGTTGTTCTACCGACTTCTGCATCAG
                  ************************************************************
```

***F. necrophorum* (*rpoB*) cloned sequences**

```
GenBank sequence F >                                                  < Probe
FNF_AF527637.1  103AACCTCCGGCAGAAGAAAAATTACTGGCGAGCTA-TTTCGGGGAAAAAGCGAGAGATGTTC
Lab strains
FNF_ATCC 51357    AACCTCCGGCAGAAGAAAAATTACTG-AGAGCTATTTTCGGGGAAAAAGCGAGAGATGTTC
FNF_B571          AACCTCCGGCAGAAGAAAAATTACTG-AGAGCTATTTTCGGGGAAAAAGCGAGAGATGTTC
FNN_NCTC 10576    AACCTCCGGCAGAAGAAAAATTACTG-CGAGCTATTTTCGGGGAAAAAGCGAGAGATGTTC
FN_BS-1           AACCTCCGGCAGAAGAAAAATTACTG-CGAGCTATTTTCGGGGAAAAAGCGAGAGATGTTC
Longitudinal study
2301 RF 23/10     AACCTCCGGCAGAAGAAAAATTACTG-CGAGCTATTTTCGGGGAAAAAGCGAGAGATGTTC
2211 RF 30/10     AACCTCCGGCAGAAGAAAAATTACTG-CGAGCTATTTTCGGGGAAAAAGCGAGAGATGTTC
                  *************************  ****** **************************

GenBank sequence                          < R
FNF_AF527637.1    GAGACAGTTCTCTACGTATGCCTCACG189
Lab strains
FNF_ATCC 51357    GAGACAGTTCTCTACGTATGCCTCACG
FNF_B571          GAGACAGTTCTCTACGTATGCCTCACG
FNN_NCTC 10576    GAGACAGTTCTCTACGTATGCCTCACG
FN_BS-1           GAGACAGTTCTCTACGTATGCCTCACG
Longitudinal study
2301 RF 23/10/06  GAGACAGTTCTCTACGTATGCCTCACG
2211 RF 30/10/06  GAGACAGTTCTCTACGTATGCCTCACG
                  **************************
```

Figure 3.3. Cloned *rpoD* and *rpoB* PCR product sequence alignments. The cloned *rpoD* sequences included four *D. nodosus* lab strains: VCS1703A, C305, BS-18 and Serogroup E and three samples from the longitudinal study: 2208 RF 30/10/06, 2650 RF 04/10/06, 2211 RF 30/10/06. The cloned *rpoB* sequences included four lab strains from *F. necrophorum,* subsp. *necrophorum* (FNN) and subsp. *funduliforme* (FNF) (ATCC 51357, B571, NCTC 10576, BS-1) and two samples from the longitudinal study (2301 RF 23/10/06 and 2211 RF 30/10/06). Primer sequences in bold, TaqMan® probe sequences in red, mismatches/deletions/insertions when compared to the GenBank sequence highlighted in grey and asterisks (*) indicate consensus to GenBank sequences NC_009446 and AF527637.1, respectively.

3.3.4. Analytical sensitivity.

The *D. nodosus* (*rpoD*) and *F. necrophorum* (*rpoB*) qPCR assays each had a set of serially diluted DNA standards ranging from 2.04 to 2.04 x 10^6 *rpoD* copies μl^{-1} and 2.47 to 2.47 x 10^7 *rpoB* copies μl^{-1}, respectively. The lowest detected standards for both assays were 2.04 x 10^2 *rpoD* copies μl^{-1} and 2.47 x 10^2 *rpoB* copies μl^{-1}. Calibration standards for the *D. nodosus* (*rpoD*) and *F. necrophorum* (*rpoB*) assays generated R^2 values of ≥ 0.995 and mean slope values of -3.6 (SEM ± 0.04) and -3.7 (SEM ± 0.04), respectively.

The theoretical detection limit (TDL) for both assays was also determined by setting up a series of spiking experiments as detailed in Section 2.9.6.1. Two sets of spiking experiments were carried out using *D. nodosus* (VCS1703A) and *F. necrophorum* (BS-1) cells. For the first set, DNA was extracted and eluted into 100 µl elution buffer (EB) (Figure 3.4.) and for the second set, DNA was extracted and instead eluted into 60 µl (Figure 3.5.) EB, to determine if decreasing the elution volume could increase target detection as reported by DeGraves and colleagues (2003). For the first set of spiking experiments (100 µl EB), swabs were spiked with 500 µl of undiluted *D. nodosus* (VCS1703A) culture and 500 µl of each of the seven 10-fold serial dilutions (10^{-1} to 10^{-7}), resulting in approximately 9.20 x 10^1 to 9.20 x 10^8 *rpoD* copies $swab^{-1}$. Additional swabs were then spiked with 500 µl of undiluted *F. necrophorum* (BS-1) culture and 500 µl of each of the seven 10-fold serial dilutions (10^{-1} to 10^{-7}), resulting in approximately 3.75 x 10^0 to 3.75 to 10^7 *rpoB* copies $swab^{-1}$. The lowest detected spiked samples for the first set of spiking experiments (100 µl elution volume) were the 10^{-6} and 10^{-4} dilutions for the *D. nodosus* (*rpoD*) and *F. necrophorum* (*rpoB*) assays, respectively. This revealed TDLs of 1.74 x 10^3 and 2.55 x 10^3 *rpoD* and *rpoB* copies

swab^{-1}, respectively (Figure 3.4.).

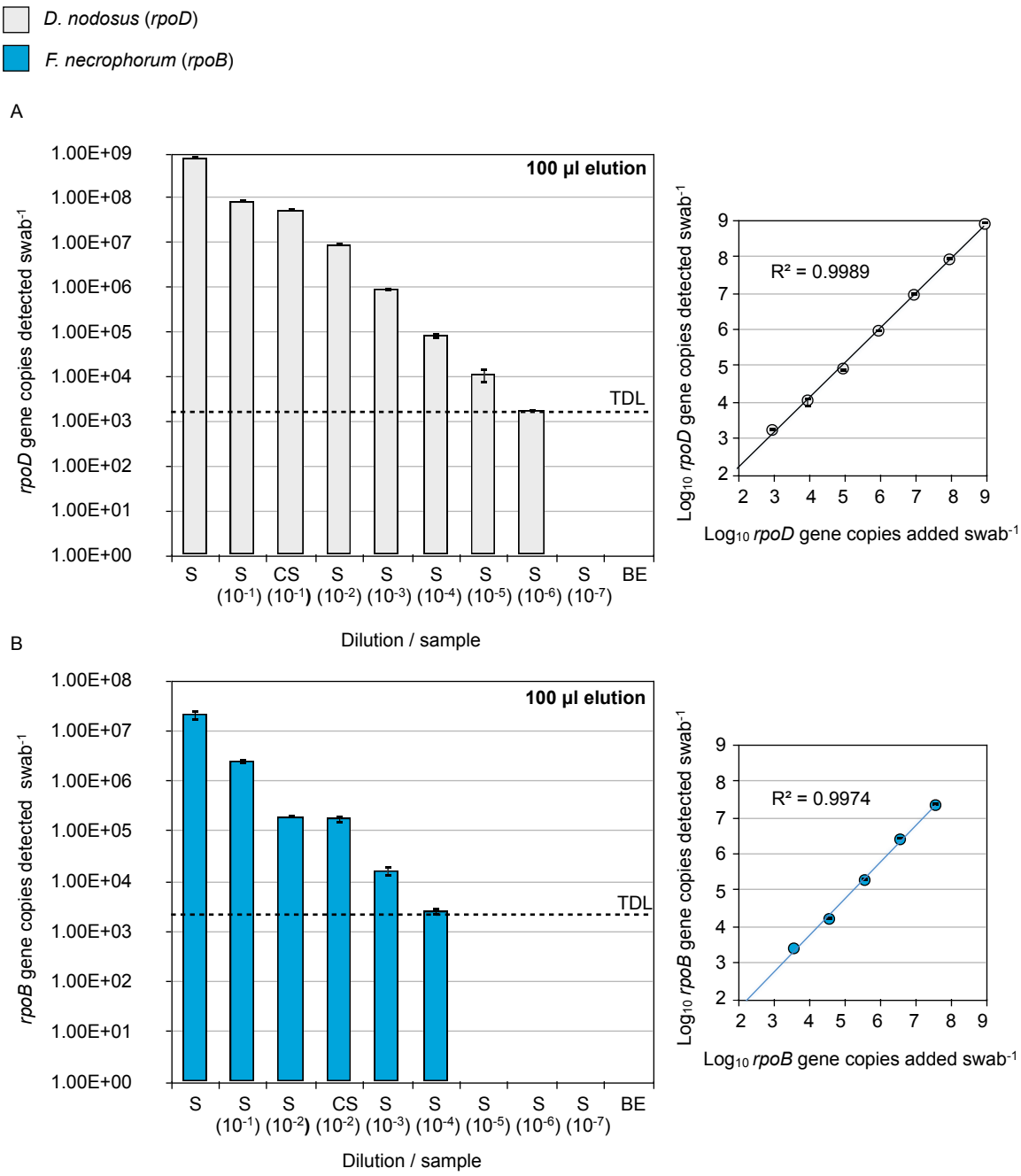

Figure 3.4. Analytical sensitivity of the *D. nodosus* (*rpoD*) (A) and *F. necrophorum* (*rpoB*) (B) assays (100 µl elution volume). Spiking experiments were set up as described in Section 2.9.6.1. Data presented as number of *rpoD* and *rpoB* copies swab^{-1} with approximate TDLs indicated (dashed line) (bar charts). Data also presented as $\log_{10}$ *rpoD* or *rpoB* copies detected swab^{-1} against $\log_{10}$ *rpoD* or *rpoB* copies added swab^{-1} (line graphs). Error bars ± SD of three technical replicates. Serial dilutions ranged from 10^{-1} to 10^{-7}. A blank extraction (BE) (sterile swab with sterile water) was included with each set of DNA extractions. Spiked samples (S) and clinical spiked samples (CS) are shown.

Swabs that were taken from ovine feet were screened for *rpoD* and *rpoB* and four that were negative for both, were then spiked with either diluted *D. nodosus* or *F. necrophorum* culture, as described in Section 2.9.6.1, as detailed by Lund and colleagues (2004). These spiked controls were termed clinical spikes (CS). The CS for both assays exhibited similar C_T values when compared with their sterile buffer counterparts, indicating that lesion exudate and other material present on the CS swabs did not significantly inhibit the PCR reaction (Figure 3.4. and Figure 3.5.).

For the second set of spiking experiments (60 µl EB), swabs were spiked with 500 µl of undiluted *D. nodosus* (VCS1703A) and 500 µl of each of the seven 10-fold serial dilutions (10^{-1} to 10^{-7}), resulting in approximately 1.59 x 10^2 to 1.59 x 10^9 *rpoD* copies swab^{-1}. Additional swabs were then spiked with 500 µl of undiluted *F. necrophorum* (BS-1) and 500 µl of each of the seven 10-fold serial dilutions (10^{-1} to 10^{-7}), resulting in approximately 4.33 x 10^0 to 4.33 to 10^7 *rpoB* copies swab^{-1}. The lowest detected spiked samples for the second set of spiking experiments (60 µl elution volume) were the 10^{-5} and 10^{-4} dilutions for the *D. nodosus* (*rpoD*) and *F. necrophorum* (*rpoB*) assays, respectively. This revealed TDLs of 1.30 x 10^3 and 1.43 x 10^3 *rpoD* and *rpoB* copies swab^{-1}, respectively (Figure 3.4.). Using the decreased elution volume (60 µl) only marginally increased the TDL for both qPCR assays, however a larger elution volume was preferred over the marginal increase in detection limit.

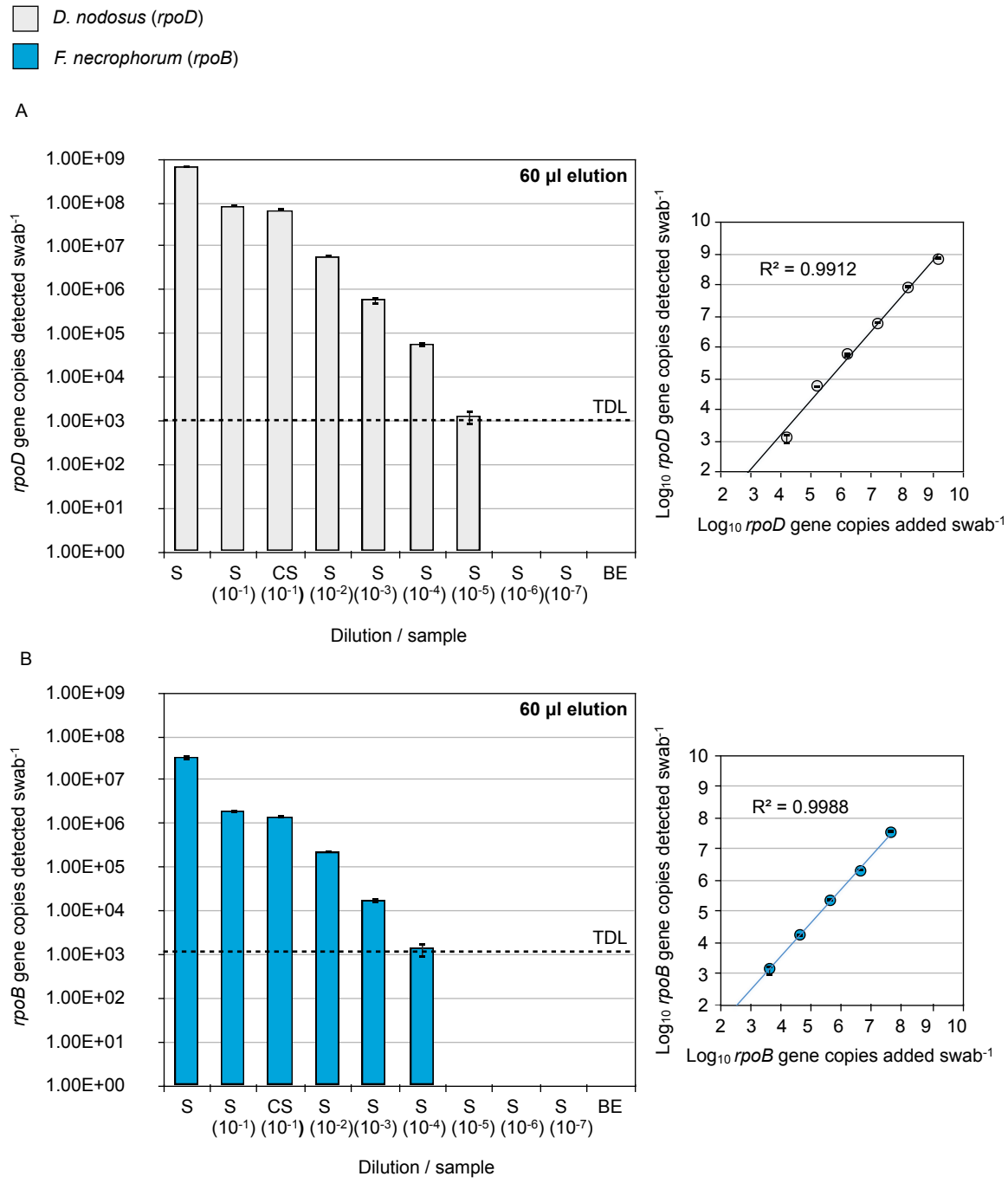

Figure 3.5. Analytical sensitivity of the *D. nodosus* (*rpoD*) (A) and *F. necrophorum* (*rpoB*) (B) assays (60 µl elution volume). Spiking experiments were set up as described in Section 2.9.6.1. Data presented as number of *rpoD* and *rpoB* copies swab^{-1} with approximate TDLs indicated (dashed line) (bar charts). Data also presented as $\log_{10}$ *rpoD* or *rpoB* copies detected swab^{-1} against $\log_{10}$ *rpoD* or *rpoB* copies added swab^{-1} (line graphs). Error bars ± SD of three technical replicates. Serial dilutions ranged from 10^{-1} to 10^{-7}. A blank extraction (BE) (sterile swab with sterile water) was included with each set of DNA extractions. Spiked samples (S) and clinical spiked samples (CS) are shown.

3.3.5. Longitudinal detection and quantification of *D. nodosus* (*rpoD*) and *F. necrophorum* (*rpoB*) from ovine foot swabs.

Data were examined at (i) sheep-level; all feet from healthy sheep, sheep with ID and sheep with FR and at (ii) foot-level; feet examined independently from the individual and based on their individual foot scores. Overall, there was an increase in *D. nodosus* (*rpoD*) detection in swabs from diseased sheep and feet when compared to healthy sheep/feet (Table 3.5.), which is consistent with already published work (Moore, et al., 2005a; Bennett, et al., 2009). Similarly, there was also an increase in *F. necrophorum* (*rpoB*) detection in samples from diseased sheep and feet, again correlating with already published work (Bennett, et al., 2009). However, an increase in *rpoD* and *rpoB* detection was observed for healthy feet (foot-level analysis) when compared to healthy sheep (sheep-level analysis), suggesting that the healthy feet of diseased sheep may become superficially contaminated with *D. nodosus* and *F. necrophorum* during an outbreak of disease.

Table 3.5. Percentage positive swabs for *D. nodosus* (*rpoD*) and *F. necrophorum* (*rpoB*) using both a sheep-level and foot-level analysis.

		H	ID	FR
SHEEP-LEVEL	*D. nodosus* (*rpoD*)	42.6 % (23/54)	84.8 % (117/138)	75.2 % (118/157)
	F. necrophorum (*rpoB*)	51.9 % (28/54)	64.5 % (89/138)	68.2 % (107/157)
FOOT-LEVEL	*D. nodosus* (*rpoD*)	68.4 % (154/225)	86.0 % (86/100)	70.83 % (17/24)
	F. necrophorum (*rpoB*)	62.2 % (140/225)	64.0 % (64/100)	75.0 % (18/24)

D. nodosus (*rpoD*) was significantly more likely to be detected from sheep with ID and FR when compared to healthy sheep ($p < 0.001$) and also significantly more likely to be

associated with sheep with ID than those with FR ($p < 0.05$) (sheep-level analysis). In contrast, *D. nodosus* (*rpoD*) was significantly more likely to be detected from feet with ID than from healthy feet ($p < 0.05$) (foot-level analysis). *F. necrophorum* (*rpoB*) detection was only significantly increased in sheep presenting with FR than those that were healthy ($p < 0.05$) (sheep-level analysis). This demonstrates that *D. nodosus* detection is associated with both ID and FR, although more commonly with ID, whilst *F. necrophorum* is more likely to be detected in feet presenting with FR.

D. nodosus (*rpoD*) and *F. necrophorum* (*rpoB*) loads were then examined over the three foot states (H, ID, FR), firstly on a (i) sheep-level analysis (Figure 3.6.) and then on a (ii) foot-level analysis (Figure 3.7.). *D. nodosus* quantification data were categorised into the following groups: undetectable (below the TDL; $< 10^3$ copies swab^{-1}), low (10^3 to $< 10^4$ copies swab^{-1}), mid (10^4 to $< 10^5$ copies swab^{-1}), high (10^5 to $< 10^6$ copies swab^{-1}) and highest ($\geq 10^6$ copies swab^{-1}) load categories, *F. necrophorum* quantification data were categorised in the same manner, except that the high and highest load categories were combined ($\geq 10^5$ *rpoB* copies swab^{-1}). Data were then expressed as a percentage of samples categorised into each of the groups. The data were handled in this manner to highlight (visually) shifts in community structure.

A shift in the *D. nodosus* community abundance was observed over the three disease states; for samples taken from healthy-sheep, sheep with ID and sheep with FR (sheep-level analysis) (Figure 3.6.). The majority (57.4 % (31/54)) of samples from healthy sheep were ‘undetectable’, indicating that they were below the TDL, with a further 31.5 % (17/54) of samples in the ‘low’ load category. In comparison, the *D. nodosus*

population shifted into the higher categories from samples taken from sheep with ID or FR (Figure 3.6.). For sheep within the ID group, 24.6 % (34/138), 21.7 % (30/138) and 10.1 % (14/138) of samples fell into the 'mid', 'high' and 'highest' categories, respectively. For sheep within the FR group, 21.6 % (34/157), 18.5 % (29/157) and 19.8 % (31/157) of samples fell into the 'mid', 'high' and 'highest' categories, respectively. In contrast, none of the samples from healthy sheep fell into the 'high' or 'highest' categories (Figure 3.6.) (sheep-level analysis). However, when examining feet individually (foot-level analysis), a less dramatic shift was observed (Figure 3.7.). Despite this, there was still an increase in the number of samples falling into the 'high' and 'highest' categories for samples taken from feet presenting with ID and FR. For feet with ID, 25.0 % (25/100) and 23.0 % (23/100) of samples fell into the 'high' and 'highest' categories, respectively. For feet with FR, 16.67 % (4/24) and 20.83 % (5/24) of samples fell into the 'high' and 'highest' categories (Figure 3.7.).

For the *F. necrophorum* population, most of samples for all three disease states fell into the 'undetectable' and 'mid' categories (Figure 3.6.) (sheep-level analysis). For healthy sheep 48.2 % (26/54) and 44.4 % (24/54) of samples fell into the 'undetectable' and 'low' categories and similar results were observed for sheep with ID (35.5 % (49/138) and 40.6 % (56/138), respectively) and for sheep with FR (31.9 % (50/157) and 37.6 % (59/157), respectively) (sheep-level analysis). However, for sheep with ID and FR there was a slight shift from the 'undetectable' group into the 'low' group. In addition, there was also an approximate 3-fold increase in the number of samples within the 'high' load category (15.3 % (24/157)) for sheep with FR (Figure 3.6.). However, when examining the foot-level analysis, the patterns observed were still the similar to that of the sheep-

level analysis, however there was an increase in the number of samples falling into the 'high' category for feet with FR; with 25.0 % (6/24) of samples falling into this category, when compared to only 8.0 % (18/225) and 10.0 % (10/100) for healthy feet and those with ID (Figure 3.7.).

The differences observed in detection frequency and load of *D. nodosus* (*rpoD*) and *F. necrophorum (rpoB*), when examining the data on (i) a sheep-level analysis and (ii) a foot-level analysis, indicates that healthy-feet of diseased sheep may become superficially contaminated with both microorganisms and at an increased load.

SHEEP-LEVEL ANALYSIS

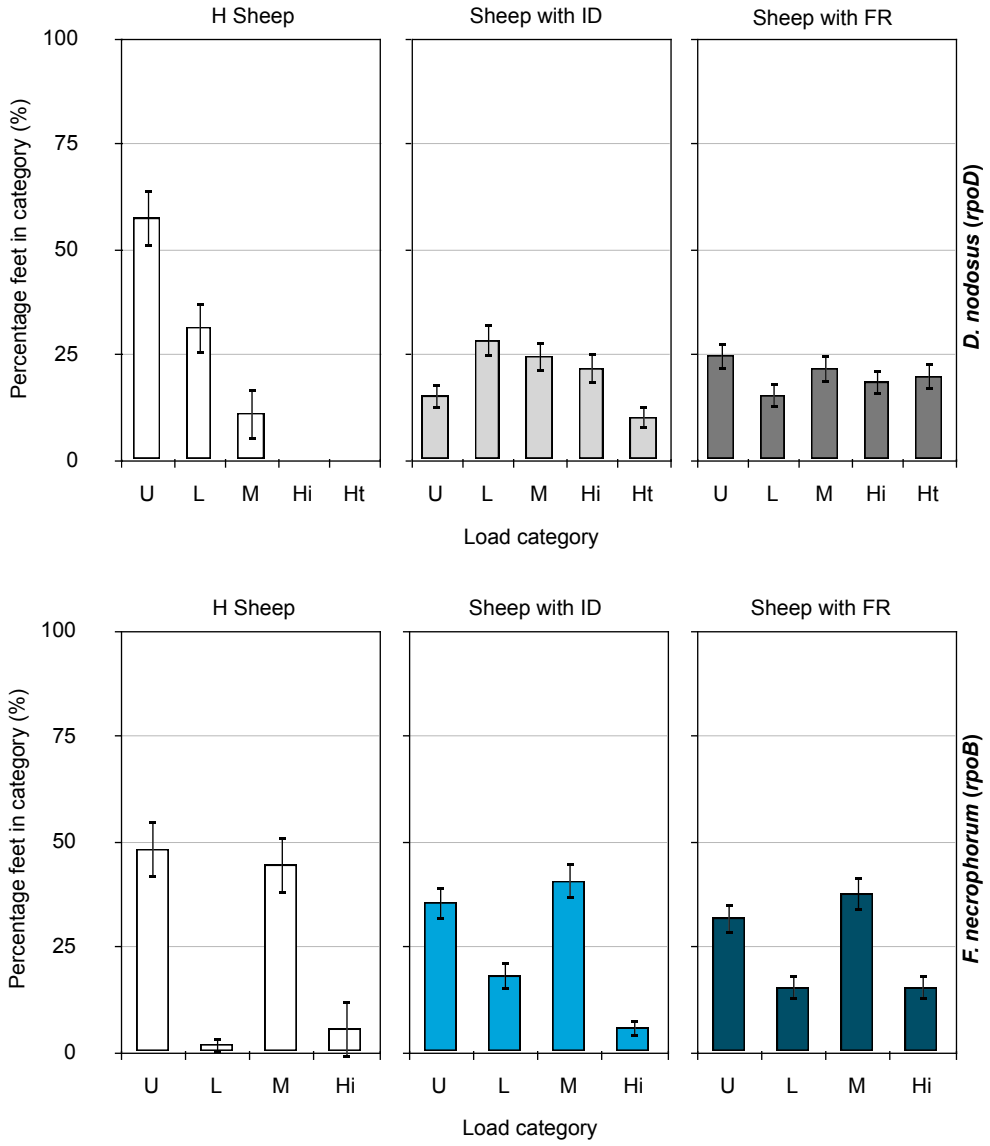

Figure 3.6. Distribution of *D. nodosus* and *F. necrophorum* population abundance in relation to sheep disease status (H, ID, FR) (sheep-level analysis). Quantification data were categorised as the following: 'U' (undetectable): below the TDL < 10^3 copies swab^{-1}, 'L' (low): 10^3 to < 10^4 *rpoD*/*rpoB* copies swab^{-1}, 'M' (mid): 10^4 to < 10^5 *rpoD*/*rpoB* copies swab^{-1}, 'Hi' (high): 10^5 to < 10^6 *rpoD* copies swab^{-1} and 'Ht' (highest): ≥ 10^6 *rpoD* copies swab^{-1}. The 'high' category for *F. necrophorum* data was ≥ 10^5 *rpoB* copies swab^{-1}. Data presented as percentage feet (%) in respective load categories with percentage standard error (SE).

FOOT-LEVEL ANALYSIS

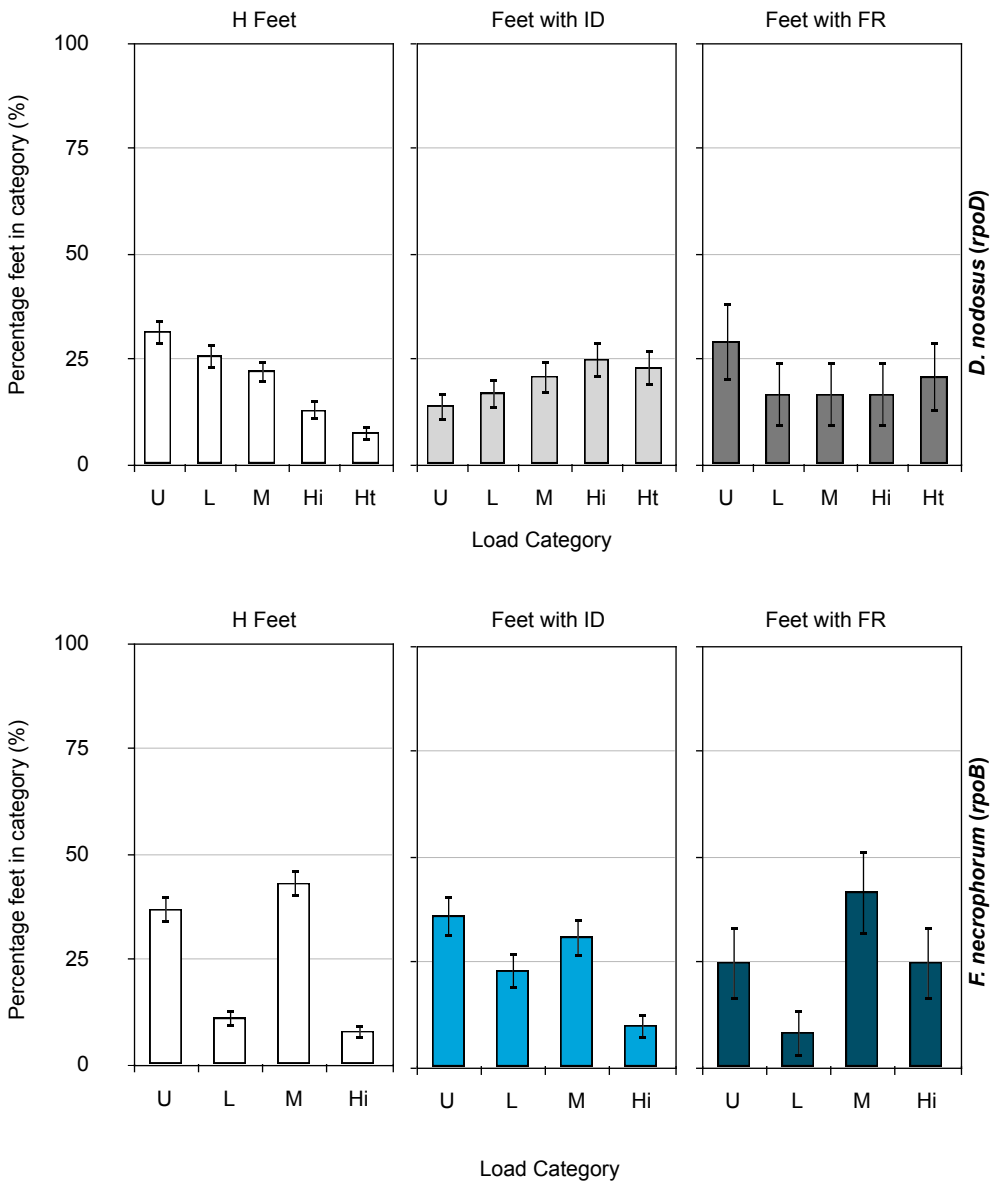

Figure 3.7. Distribution of *D. nodosus* and *F. necrophorum* population abundance in relation to foot disease status (H, ID, FR) (foot-level analysis). Quantification data were categorised as the following: 'U' (undetectable): below the TDL < 10^3 *rpoD*/*rpoB* copies swab^{-1}, 'L' (low): 10^3 to < 10^4 *rpoD*/*rpoB* copies swab^{-1}, 'M' (mid): 10^4 to < 10^5 *rpoD*/*rpoB* copies swab^{-1}, 'Hi' (high): 10^5 to < 10^6 *rpoD* copies swab^{-1} and 'Ht' (highest): ≥ 10^6 *rpoD* copies swab^{-1}. The 'high' category for *F. necrophorum* data was ≥ 10^5 *rpoB* copies swab^{-1}. Data presented as percentage feet (%) in respective load categories with percentage standard error (SE).

The healthy feet of healthy sheep (H-H) and the healthy feet of diseased sheep (termed H-ID and H-FR) were then examined, to determine the extent of superficial contamination with *D. nodosus* and *F. necrophorum*. *D. nodosus* (*rpoD*) was detected on 80.2 % (73/91) of healthy-feet from ID-sheep (H-ID) and 73.8 % (59/80) of healthy-feet from FR-sheep (H-FR), when compared to a detection frequency of 42.6 % (23/54) of healthy-feet from healthy sheep (H-H), indicating a 37.6 % and 31.2 % increase in detection frequency of *D. nodosus* on the healthy-feet of diseased sheep. In conjunction with this, the *D. nodosus* population on the H-ID and H-FR feet also shifted into the higher load categories (Figure 3.8.). Very few samples from H-H feet fell into the 'mid' (11.1 %) category and none within the 'high' or 'highest' categories. However, for samples taken from H-ID feet, 27.5%, 16.5 % and 6.6 % fell into the 'mid', 'high' and 'highest' groups. Likewise, for samples taken from H-FR feet, 22.5 %, 18.8 % and 13.8 % of samples fell into the top three categories, indicative of spatial cross-contamination between feet.

F. necrophorum (*rpoB*) was detected on 51.9 % (28/54) of H-H feet, 63.7 % (58/91) of H-ID feet and 70.0 % (56/80) of H-FR feet, again showing that spatial cross-contamination between feet occurs, demonstrating a 11.8 % and 18.1 % increase on H-ID and H-FR feet, respectively. Despite this, the shift in *F. necrophorum* (*rpoB*) load was not as pronounced as in H-ID and H-FR feet, as a large number of samples still fell into the 'mid' category; 45.1 % and 41.3 %, respectively. However, there was an 11.4 % and 13.2 % increase in the 'low' category for H-ID and H-FR feet when compared to H-H feet and approximately a 2-fold increase in the majority of samples in the 'high' category for H-FR feet (Figure 3.8.). Demonstrating, that although detection frequency

increased on the healthy-feet of diseased-sheep, that changes in the bacterial load (gene copies swab^{-1}) also changed. Changes in the *F. necrophorum* (*rpoB*) load on the healthy feet of diseased sheep were marginal in comparison to those observed for *D. nodosus* (*rpoD*) load.

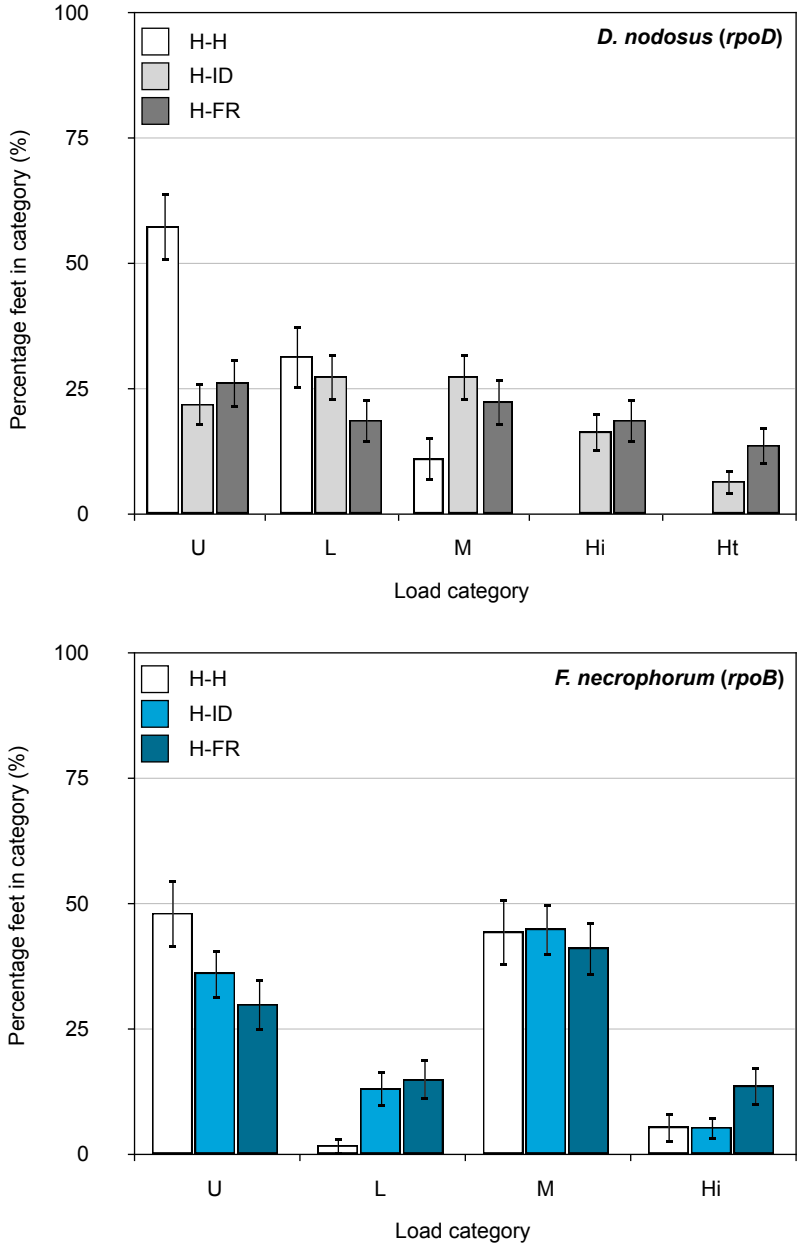

Figure 3.8. Distribution of *D. nodosus* and *F. necrophorum* population abundance on healthy-feet of healthy sheep (H-H) compared to the healthy-feet of diseased sheep (H-ID and H-FR). Quantification data were categorised as the following: 'U' (undetectable): below the TDL < 10^3 *rpoD*/*rpoB* copies swab^{-1}, 'L' (low): 10^3 to < 10^4 *rpoD*/*rpoB* copies swab^{-1}, 'M' (mid): 10^4 to < 10^5 *rpoD*/*rpoB* copies swab^{-1}, 'Hi' (high): 10^5 to < 10^6 *rpoD* copies swab^{-1} and 'Ht' (highest): ≥ 10^6 *rpoD* copies swab^{-1}. The 'high' category for *F. necrophorum* data was ≥ 10^5 *rpoB* copies swab^{-1}. Data presented as percentage feet (%) in respective load categories with percentage standard error (SE) indicated.

The *D. nodosus* (*rpoD*) and *F. necrophorum* (*rpoB*) loads were then compared, to determine when they increased (in relation to disease presentation) on firstly a (a) sheep-level analysis and secondly on a (b) foot-level analysis. *D. nodosus* (*rpoD*) and *F. necrophorum* (*rpoB*) loads were not significantly correlated in feet from healthy sheep or on feet from sheep with ID ($p > 0.05$) (sheep-level analysis). However, *D. nodosus* (*rpoD*) and *F. necrophorum* (*rpoB*) loads in feet from sheep with FR were significantly positively correlated ($r = 0.3040$; $p < 0.01$), with 9.0 % ($r^2 = 0.09$) of the variance explained by the two variables (Figure 3.9.) (sheep-level analysis). *D. nodosus* and *F. necrophorum* were less frequently detected in healthy sheep and when they were detected, samples tended to be in the lower load categories - this is represented by a small tight cluster in the first scatter plot. For sheep with ID, an increase in the *D. nodosus* community abundance was then observed, shifting the scatter plot to the right. In sheep with FR, the scatter plot then migrated upwards, as the *F. necrophorum* community increased in line with the *D. nodosus* population.

However, when feet were analysed individually (irrespective of sheep disease status), a less obvious pattern was observed (Figure 3.9.), with *D. nodosus (rpoD*) and *F. necrophorum* (*rpoB*) loads correlating for healthy-feet ($p < 0.01$) and for feet with FR ($p < 0.05$). The findings from this section (Section 3.3.5.) highlight the difficulties associated with analysing such a complex data set; consisting of longitudinal time points, stages of disease and quantification data for two pathogens. The data therefore required additional analysis, in the form of a statistical model, in order to find significant patterns associated with disease initiation and progression and *F. necrophorum* (*rpoB*) and *D. nodosus* (*rpoD*) load.

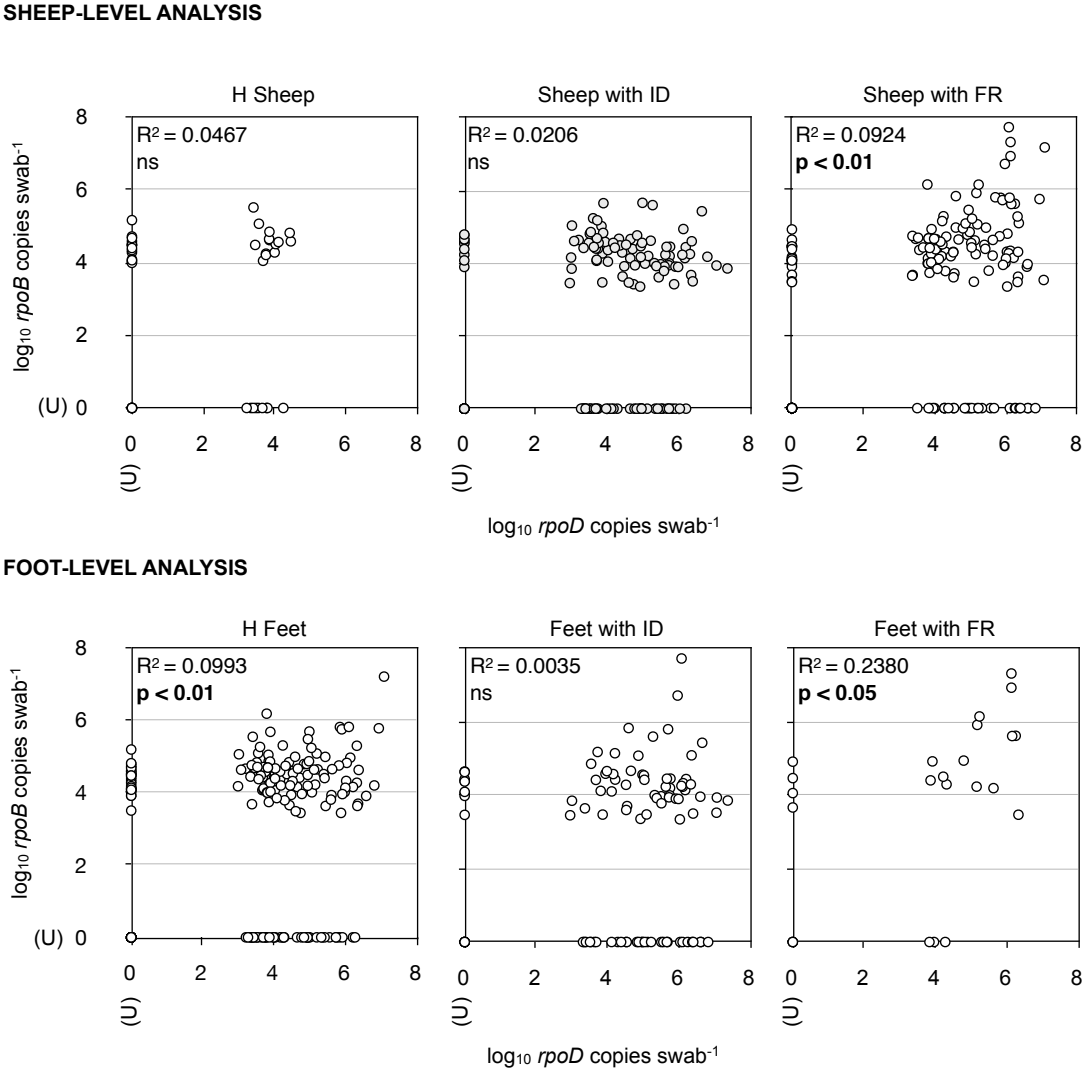

Figure 3.9. Correlation analysis between *D. nodosus* (*rpoD*) and *F. necrophorum* (*rpoB*) load in healthy sheep (H), sheep with ID and sheep with FR (sheep-level analysis) and in healthy feet (H), feet with ID and feet with FR (foot-level analysis). A significant positive correlation was observed between *D. nodosus* and *F. necrophorum* load in sheep with FR ($p > 0.01$) (sheep-level analysis). A less obvious pattern was observed for the foot-level analysis; *D. nodosus (rpoD*) and *F. necrophorum* (*rpoB*) loads appeared to correlate for healthy-feet ($p < 0.01$) and for feet with FR ($p < 0.05$). Quantification data were +1 $\log_{10}$ transformed and analysed using Pearson's correlation test (two-tailed) (GraphPad Prism software). Undetectable (U) values were coded as +1 and then $\log_{10}$ transformed, so that they were represented on the scatter plots (as zero).

3.3.6. Construction of a multinomial regression model to elucidate the temporal patterns of *D. nodosus* (*rpoD*) and *F. necrophorum* (*rpoB*) load associated with the development and presentation of ID and FR in sheep.

The quantitative data obtained from the longitudinal study were also analysed using an unordered multinomial mixed effects model for repeated observations and samples of feet clustered within ewes using MLwiN 2.2.1 as described in Section 2.20. Multiple regression models can incorporate many explanatory variables, in this case the presence of *D. nodosus* and *F. necrophorum* split into load categories one week prior to disease (ID and FR) development and week of disease (ID and FR) onset. Univariate analysis would assume that the response variable (ID and FR) is influenced only by one factor. By using multivariable regression one can take into consideration multiple predictive factors, providing more flexibility and accuracy. Comparison of multivariable and univariate analysis are shown in Table 3.6.

For the multivariable analysis - after accounting for a lack of independence between sheep and sampling events and variability in incidence of disease by week, detection of *D. nodosus* (*rpoD*) at the low (OR: 2.363, 95 % CIs: 1.011-5.217) and mid (OR: 2.547, 95 % CIs: 1.048-6.190) ranges was significantly more likely in feet the week before the onset of ID, however there was then a significant association between the ‘high’ (OR: 3.391, 95 % CIs: 1.401-8.207) and ‘highest’ (OR: 5.613, 95 % CIs: 2.152-14.635) ranges the week of ID onset (Table 3.6/Figure 3.10.). Indicating an increase in *D. nodosus* (*rpoD*) load during the progression from a healthy foot to a foot presenting with ID within one week. In addition, a foot was more likely to develop FR when

D. nodosus (*rpoD*) was detectable one week prior to the development of FR and the strength of this association increased when *D. nodosus* (*rpoD*) load was at its highest (OR: 27.385, 95 % CIs: 3.980-188.414) (i.e. was dose-dependent). Interestingly, no significant association was observed between *D. nodosus* (*rpoD*) load and FR presentation (the week of disease onset) (Table 3.6/Figure 3.10.). In contrast, *F. necrophorum* (*rpoB*) load was not significantly associated with ID or FR, the week prior to disease onset or the week of ID onset (Table 3.6/Figure 3.10.). However, an association between FR and *F. necrophorum* (*rpoB*) was observed, but only after FR had developed (week of disease) with a high (OR: 5.518, 95 % CIs: 1.330-22.896) *F. necrophorum* load being significantly associated with FR presentation. Which is consistent with the descriptive analyses (Section 3.3.5.).

The univariate results (Table 3.6.) demonstrate that by only examining single predictors most associations are found to be significant. However, by examining the effects of *D. nodosus* and *F. necrophorum* load simultaneously in the development of ID and FR, the effect of *D. nodosus* in the progression of a healthy foot to one presenting with ID and in the development of FR is considered significant, whereas *F. necrophorum* load (‘high’ category) is now only significant after lesion (FR) development.

Table 3.6. Output from full multinomial regression model (univariate and multivariable results) for the effect of *D. nodosus* (Dn) (*rpoD*) and *F. necrophorum* (Fn) (*rpoB*) load on the development and presentation of ID and FR. The baselines for each explanatory variable were Dn undetectable (U) and Fn undetectable (U). Quantification data were categorised as the following: 'U' (undetectable): $< 10^3$ copies swab^{-1}, low: 10^3 to $< 10^4$ copies swab^{-1}, mid: 10^4 to $< 10^5$ copies swab^{-1}, high: 10^5 to $< 10^6$ copies swab^{-1} and highest: $\geq 10^6$ *rpoD* copies swab^{-1}. The high category for *F. necrophorum* data was $\geq 10^5$ *rpoB* copies swab^{-1}. Significant associations shown in bold ($p < 0.05$).

	Univariate		Multivariable	
Explanatory variables[a]	ID Odds ratios with 95 % CIs (lower, upper)	FR Odds ratios with 95 % CIs (lower, upper)	ID Odds ratios with 95 % CIs (lower, upper)	FR Odds ratios with 95 % CIs (lower, upper)
Week prior to onset				
Dn undetectable	-	-	-	-
Dn low	**2.389 (1.063, 5.368)**	1.024 (0.220, 4.762)	**2.363 (1.011, 5.217)**	2.255 (0.383, 13.287)
Dn mid	**3.019 (1.344, 6.783)**	2.472 (0.665, 9.191)	**2.547 (1.048, 6.190)**	**8.248 (1.767, 38.496)**
Dn high	**4.108 (1.783, 9.468)**	1.680 (0.359, 7.858)	1.813 (0.693, 4.746)	3.515 (0.545, 22.668)
Dn highest	**3.892 (1.435, 10.555)**	**5.835 (1.440, 23.652)**	2.630 (0.815, 8.492)	**27.385 (3.980, 188.414)**
Fn undetectable	-	-	-	-
Fn low	**3.501 (1.413, 8.675)**	1.423 (0.154, 13.257)	0.745 (0.296, 1.870)	0.302 (0.036, 2.546)
Fn mid	1.844 (0.879, 3.869)	1.210 (0.342, 4.285)	0.726 (0.375, 1.406)	0.526 (0.176, 1.577)
Fn high	**4.674 (1.782, 12.260)**	**5.842 (1.450, 23.537)**	1.326 (0.502, 3.498)	1.272 (0.294, 5.513)
Week of onset				
Dn undetectable	-	-	-	-
Dn low	1.441 (0.659, 3.149)	0.678 (0.191, 2.404)	1.283 (0.560, 2.939)	2.113 (0.558, 7.995)
Dn mid	**2.143 (1.002, 4.584)**	0.816 (0.230, 2.901)	1.968 (0.857, 4.518)	0.407 (0.107, 1.557)
Dn high	**4.166 (1.932, 8.983)**	1.333 (0.373, 4.768)	**3.391 (1.401, 8.207)**	0.489 (0.112, 2.134)
Dn highest	**6.773 (2.997, 15.301)**	2.945 (0.880, 9.849)	**5.613 (2.152, 14.635)**	0.711 (0.158, 3.245)
Fn undetectable	-	-	-	-
Fn low	**2.121 (1.077, 4.179)**	1.107 (0.216, 5.678)	1.770 (0.807, 3.884)	1.564 (0.359, 6.814)
Fn mid	0.729 (0.418, 1.272)	1.412 (0.498, 4.006)	0.907 (0.483, 1.701)	2.228 (0.749, 6.624)
Fn high	1.214 (0.530, 2.782)	**4.371 (1.315, 14.534)**	0.955 (0.374, 2.437)	**5.518 (1.330, 22.896)**
Week	0.445 (0.353, 0.561)	0.107 (0.071, 0.161)	**1.619 (1.240, 2.114)**	**2.018 (1.229, 3.313)**

MULTINOMIAL MODEL OUTPUT (FOOT-LEVEL ANALYSIS)

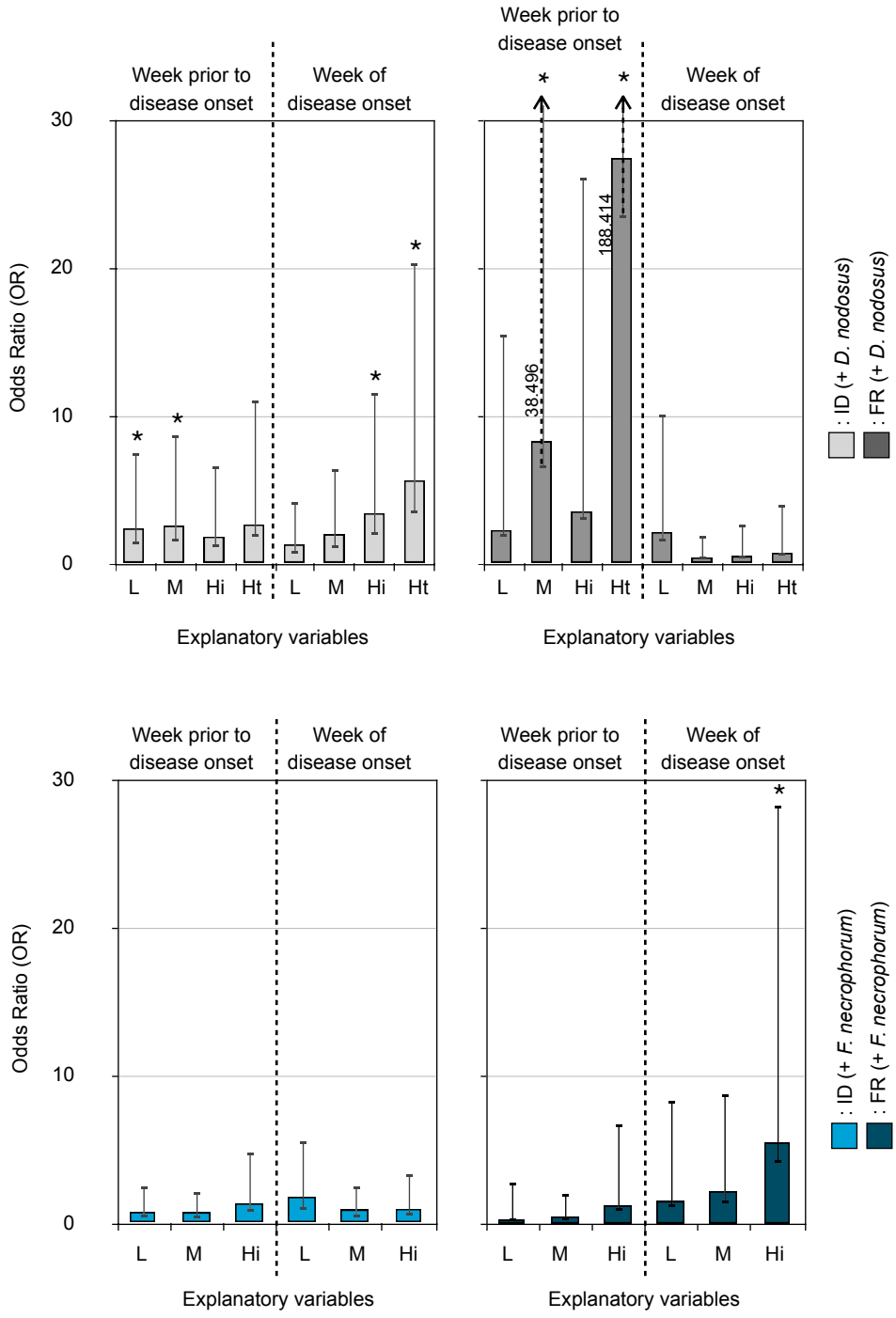

Figure 3.10. Output from full multinomial regression model (multivariable results) for the effect of *D. nodosus* (Dn) (*rpoD*) and *F. necrophorum* (Fn) (*rpoB*) load on the development and presentation of ID and FR. The baselines for each explanatory variable were 'Dn undetectable (U)' and 'Fn undetectable (U)'. Quantification data were categorised as the following: undetectable (U): < 10^3 copies swab^{-1}, low (L): 10^3 to < 10^4 copies swab^{-1}, mid (M): 10^4 to < 10^5 copies swab^{-1}, high (Hi): 10^5 to < 10^6 copies swab^{-1} and highest (Ht): ≥ 10^6 *rpoD* copies swab^{-1}. The high (Hi) category for *F. necrophorum* data was ≥ 10^5 *rpoB* copies swab^{-1}. Asterisks (*) indicate statistically signifiant results ($p < 0.05$), dotted arrows show upper 95 % CI (with values noted).

3.4. Discussion

In this chapter, the temporal patterns of *D. nodosus* (*rpoD*) and *F. necrophorum* (*rpoB*) load in relation to the presentation and development of ID and FR over time have been elucidated, using a multi-disciplinary approach, combining aspects from microbial ecology, epidemiology and applied statistics.

The *D. nodosus* (*rpoD*) and *F. necrophorum* (*rpoB*) assays were both specific and sensitive for their respective targets and had a TDL of 1.70 x 10^3 *rpoD* and 2.55 x 10^3 *rpoB* copies $swab^{-1}$, as determined by a series of spiking experiments. A number of negative controls were also used at various stages, the first being blank extraction (BE) swabs, which were included with each set of DNA extractions and were determined to be negative for the *rpoD* and *rpoB* amplicons, ensuring that no cross-contamination occurred during the extraction procedures. In addition, NTCs (in triplicate) were included for each 96-well plate qPCR experiment and were also negative. Finally, the clinical spiked (CS) swabs (foot swabs taken from the ovine interdigital skin, which were negative for either *D. nodosus* (*rpoD*) or *F. necrophorum* (*rpoB*)) produced similar C_T values when spiked with *D. nodosus* (*rpoD*) and *F. necrophorum* (*rpoB*) compared with their sterile buffer counterparts, indicating that lesion exudate and contaminating material present on the foot swab (such as faeces, soil, blood, etc.) did not inhibit the PCR reaction.

A number of published studies have examined the presence of *D. nodosus* and/or *F. necrophorum* in relation to clinical presentation (ID and/or FR) (La Fontaine, et al., 1993; Moore, et al., 2005a; Bennett, et al., 2009) and have also monitored

experimentally induced infections (Beveridge, 1941; Roberts and Egerton; 1969; Kennan, et al., 2001; 2010), however this is the first longitudinal study to examine the progression of natural disease in relation to *D. nodosus* and *F. necrophorum* burden. The cotton swab is a commonly used method for sampling the ovine interdigital space (a small skin surface area located between the two ovine digits) to obtain DNA and bacterial isolates (Moore, et al., 2005a; Bennett, et al., 2009; Hill, et al., 2010). Replicate samples were consequently not taken from the interdigital space at each sampling point, due to the small surface area. Taking additional swabs from this small site would have produced a dilution effect (with subsequent swabs collecting less material), which would have skewed the mean when calculated. This phenomenon has previously been described for repeated swabs taken from human hands, where the first swab produces the highest yield and has consistently > 10 times the yield of the fourth swab (Chamberlain, et al., 1997). Individual animals/feet were instead considered as biological replicates of the population and multiple samples were taken over time (repeated measures). The determination of bacterial load from swab samples using qPCR is also common practice (Lund, et al., 2004; Jaton, et al., 2006; Fredericks, et al., 2009), particularly when studying disease development over time (Srinivasan, et al., 2010), as it provides a non-invasive strategy to take repeated samples. In addition, invasive sampling strategies (such as punch or needle biopsies) would have predisposed the ovine foot to infection and had severe implications for animal welfare. Sampling and severity scoring variation was minimised by having a single operator.

In summary, a total of 349 foot swabs and corresponding severity scores were collected over a five week study and were individually screened for the *rpoD* and *rpoB*

amplicons. *D. nodosus* (*rpoD*) and *F. necrophorum* (*rpoB*) were more frequently detected in samples from diseased sheep and feet (ID and/or FR) than samples from healthy sheep/feet; which is in agreement with already published work (Moore, et al., 2005a; Bennett, et al., 2009). This study also showed that shifts in the *D. nodosus* community abundance occurred between disease states; demonstrating a shift into the mid, high and highest load categories. This type of shift was not as pronounced for the *F. necrophorum* population for either foot-level or sheep-level analysis, although an increase was observed for samples falling into the 'high' category for feet and sheep with FR, when compared to healthy feet/sheep or those with ID.

This work has also revealed a number of important findings with regard to the burden of infection. Firstly, that FR is a disease where expression is related to the dose of *D. nodosus* present and that *F. necrophorum* load is unlikely to be related to disease development. *D. nodosus* was detected prior to ID development at the low (10^3 to $< 10^4$ copies swab^{-1}) and mid ranges (10^4 to $< 10^5$ copies swab^{-1}), however the population then shifted into the high (10^5 to $< 10^6$ copies swab^{-1}) and highest ($\geq 10^7$ copies swab^{-1}) ranges the week of ID presentation, and these associations were statistically significant ($p < 0.05$). This demonstrates that *D. nodosus* (*rpoD*) load increases significantly during the progression from a healthy foot to a foot presenting with ID within one week. The detection of *D. nodosus* in sheep presenting with ID, as well as those with FR might indicate that these sheep are also highly infectious. As a result, control measures targeted at reducing *D. nodosus* load in sheep with ID and isolating these sheep from the flock might be most successful. The majority of farmers and veterinarians in the UK consider ID to be primarily caused

environmental factors, such as weather and pasture quality, and/or colonisation with *F. necrophorum* (Wassink, et al., 2005) and as a result are currently less likely to treat sheep with ID to prevent the spread of FR. Our model for disease strongly indicates that rapid isolation and treatment of sheep with ID, as well as those with FR, would prevent the environmental accumulation of *D. nodosus* and further sheep to sheep transmission. This correlates with the finding that a high ID prevalence is associated with a stocking density of > 8 ewes / ha (Kaler and Green, 2009). In addition, initiating treatment during the stages of ID, may also prevent sheep from progressing onto more severe and painful stages of disease, which is important when considering animal welfare.

The model also demonstrated that a foot was more likely to develop FR, if *D. nodosus* was detectable one week prior to disease onset, and that this association increased when *D. nodosus* load was in the highest category ($\geq 10^6$ copies swab^{-1}) (although the mid category was also considered significant). The high load one week prior to the development of FR, supports the observation that these same sheep were more lame one week before they developed FR, than those that did not (Kaler, et al., 2011). The increase in severity of lameness and *D. nodosus* load at this time, may indicate that these feet were more inflamed before visible separation of the hoof horn. Interestingly, there was no significant association between FR presentation (week of disease) and *D. nodosus* load. The reason for this is not known, but the highly invasive nature of this pathogen (Beveridge, 1941) could mean that (i) the *D. nodosus* cells are deep within the epithelium and are therefore not detectable using the swabbing method, (ii) the majority of microorganisms have been removed by the sloughing of inflamed necrotic tissue, (iii) because secondary invaders outcompete superficial *D. nodosus* by this stage or (iv) due

to increased exposure to oxygen. This is consistent with the finding that *D. nodosus* (*rpoD*) was not detected by qPCR from DNA extracted from interdigital space biopsies from feet with FR (Calvo-Bado, et al., 2011b). However, examination of the bacterial communities within the epidermis of the interdigital skin (*in situ*) would be required to determine where precisely the *D. nodosus* cells are located if present. However, an increase in *F. necrophorum* (*rpoB*) load was instead observed at this time, after hoof horn separation (FR) had occurred, suggesting that *F. necrophorum* may play a role in secondary invasion, as previously postulated (Roberts and Egerton, 1969); this association was again related to an increase in *F. necrophorum* (*rpoB*) load.

D. nodosus (*rpoD*) and *F. necrophorum* (*rpoB*) loads were also found to be elevated on the healthy-feet of diseased sheep (H-ID and H-FR) when compared to the healthy-feet of healthy sheep (H-H), indicating that spatiotemporal cross-contamination between feet may also occur. Again, if infectiveness is linked to bacterial load, these healthy feet might be at greater risk of becoming diseased, if the epidermis becomes compromised, which is supported by the observation that sheep are more likely to have two feet affected than one (than expected by chance) (Beveridge, 1941; Laura Green, personal communication). In addition, when ewes are with lambs, a clustering of disease in family groups is also observed (Kaler, et al., 2010). This transmission between feet and sheep is thought to occur indirectly via contaminated pasture or housed floors (Beveridge, 1941; Whittington, 1995). There is currently no known source for *D. nodosus* in the environment, but it is thought that infected sheep and goats are the sole reservoir (Whittington, 1995) and it has been shown that asymptomatic infection may also occur (Depiazzi, et al., 1998). For *F. necrophorum*, again no environmental

reservoir is known, but as a coloniser of the alimentary tract, faecal material is thought to provide the primary source of infection (Roberts and Egerton, 1969; Handeland, et al., 2010).

Parallels have been drawn between FR in sheep and periodontal disease in humans (Edwards, et al., 2003); a condition that describes the destruction of the tissue surrounding the teeth at the interface between gum and tooth (periodontium), a similar site to the interdigital skin hoof horn junction. Succession events between members of the microbial community are thought to be responsible for the breakdown of the periodontium ('microbiota shift' disease) (Darveau, 2010) and *Fusobacterium nucleatum*, is thought to be involved in microbial 'bridging' events and in the generation of an anaerobic microenvironment conducive for the growth of more fastidious anaerobes (e.g. *Porphyromonas ginivalis*) (Edwards, et al., 2003). Our findings however, cannot provide any information regarding the role *F. necrophorum* is postulated to play in the initiation of FR or early 'bridging' events, but instead highlights the opportunistic nature of *F. necrophorum*, suggesting that it thrives after FR development, in the altered microenvironment possibly contributing to disease persistence and severity.

Despite the experimental studies (Beveridge, 1941; Roberts and Egerton, 1969; Kennan, et al., 2001; 2010) that have demonstrated *D. nodosus* as the causative agent of ovine FR, there has been some debate regarding the microbial succession events involved in the disease process, particularly with regards to the 'accessory agent' *F. necrophorum* (Bennett, et al., 2009). This study has however provided additional evidence for the

causative role of *D. nodosus*, by demonstrating that an increase in *D. nodosus* load (dose-dependence) is strongly associated with the presentation of ID and development of FR over-time and that *F. necrophorum* load only appears to play a role after the development of FR (under-running).

This work has provided novel insights into the microbial succession events involved in the development of ID and FR in sheep and is consistent with earlier cross-sectional reports. However, one limitation of DNA-based detection methods, such as qPCR, is the overestimation of bacterial load, due to the detection of free DNA from lysed cells (Castillo, et al., 2006; Pathak, et al., 2012). The use of propidium monoazide (PMA) could have been implemented to detect the viable (those with intact membranes) bacterial population (Nocker, et al., 2006; 2007; Kobayashi, et al., 2009), thereby excluding DNA from lysed cells. However, problems have been reported when using PMA with small amplicons (such as those required for TaqMan® assays), due to a decrease in possible DNA intercalation sites (Contreras, et al., 2011). Similar issues were observed for the *rpoD* and *rpoB* assays (data not shown) (author observation). To complement this work however, physiologically active *D. nodosus* and *F. necrophorum* cells were examined *in situ* using FISH (Chapter 4).

In summary, both pathogens have been detected and quantified from natural occurrences of ID and FR using a sensitive culture-independent method, which has provided conclusive evidence that both are present on swabs taken from the ovine foot and that the populations change over time and in relation to disease presentation. In conclusion, this is the first study to examine the temporal patterns of *D. nodosus* and *F.*

necrophorum load over time and to highlight the importance of *D. nodosus* load in the presentation of ID and development of FR, whilst demonstrating the opportunistic nature of *F. necrophorum*. This provides an improved understanding of the population dynamics associated with disease pathogenesis, whilst informing current control and treatment practices.

CHAPTER 4

4. The *in situ* detection and localisation of *D. nodosus*, *F. necrophorum* and the domain Bacteria using fluorescence *in situ* hybridisation (FISH).

4.1. Introduction.

The skin acts as the primary barrier between the body and the environment, thus providing the first line of defense against microbial invasion and physical and chemical damage (Nestle, et al., 2009). Skin has two main compartments; the outer-most layer (the epidermis) and below that, the dermis. The deepest layer of the epidermis is the stratum basale (SB), which contains one layer of undifferentiated epithelial cells (basal keratinocytes). These cells move upwards into the stratum spinosum (SS) (the 'spiny' layer), where they begin to mature and change from columnar to polygonal in shape. Above the stratum spinosum is the stratum granulosum (SG), which contains keratinocytes that synthesise keratin, proteins and lipids. Finally, the outer-most of the four strata is the stratum corneum (SC), which consists of corneocytes; terminally-differentiated keratinocytes (devoid of organelles), forming the skin's protective barrier (Figure 4.1.) (Elias, et al., 2005; Nestle, et al., 2009).

Footrot (FR) is an infectious disease that is triggered by damage to the epithelium of the ovine interdigital skin, which leads to the failure of the skin's barrier function and permits bacteria to invade. The initial stages of disease begin as an inflammation of the interdigital skin (ID), which in some circumstances is followed by the separation of the keratinous hoof layer from the underlying tissue, primarily caused by the degradation of

the epidermis (Beveridge, 1941). This separation is reported to be caused by the host's inflammatory response, rather than by direct bacterial action on the epidermal matrix (Egerton, et al., 1969), although *D. nodosus* has been reported to be able to directly degrade type I keratin (Kennan, et al., 2010). Inflammatory processes, such as mononuclear cell infiltration, increased cell atrophy and haemorrhage, are sometimes evident within ovine interdigital space biopsy sections (Egerton, et al., 1969).

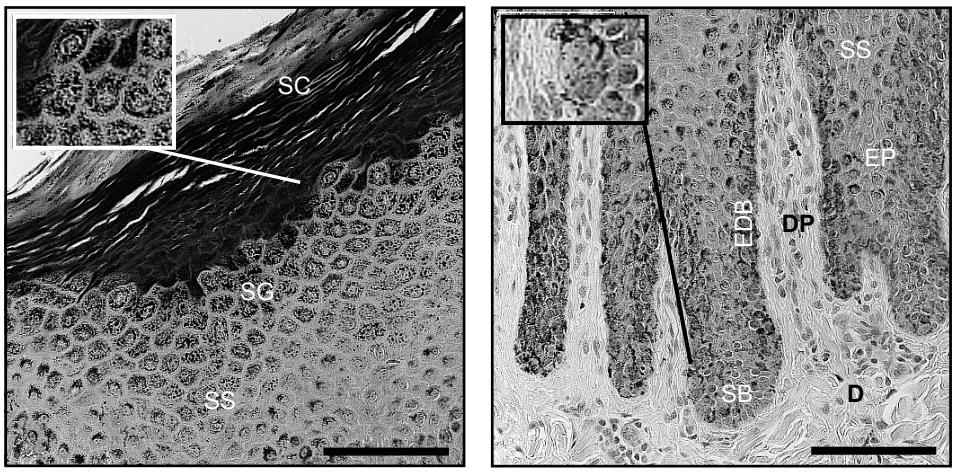

Figure 4.1. Haematoxylin and eosin (H&E) stained section of healthy ovine interdigital skin (bright-field image). Image taken as described in Section 2.18.2. using the 40x objective (oil immersion). Left image: upper epidermal layers (SC: stratum corneum, SG: stratum granulosum, SS: stratum spinosum). Right image: lower epidermal layers, epidermal-boundary and dermal layers (SB: stratum basale, EDB: epidermal-boundary, EP: epidermal pegs, DP: dermal papillae and D: dermis). Scale bars: 100 μm.

The first histopathological study of ovine FR was carried out in the mid 20th Century (Beveridge, 1941). The study reported that FR was a 'poly-microbial' infection, with a primary causative agent "*Fusiformis nodosus* (n.sp.)" (now *Dichelobacter nodosus*) and an accessory agent - the "motile Fusiform", similar to "*Fusiformis necrophorus*" (now *Fusobacterium necrophorum*). Two later studies then examined the aetiology of FR in more detail and assessed, specifically, the pathogenic relationship between *D. nodosus* and *F. necrophorum* (Egerton, et al., 1969; Roberts and Egerton, 1969). It was observed

that *D. nodosus* and *F. necrophorum* were the only two microorganisms seen invading into the damaged tissue, whilst all other bacteria remained localised superficially (Egerton, et al., 1969). Secondly, that colonisation by *D. nodosus* was always preceded by *F. necrophorum* and that once *D. nodosus* became established, *F. necrophorum* could then penetrate deeper layers of tissue, sometimes entering the dermal layers (Egerton, et al., 1969). It was also highlighted that *D. nodosus* was unable to cause disease when applied to normal or scarified feet, but that when faecal material was present (postulated to contain *F. necrophorum*), the feet were rendered susceptible to infection by *D. nodosus*. Roberts and Egerton (1969) also reported that *F. necrophorum* was responsible for the majority of inflammation observed, which they postulated created a favourable environment in which *D. nodosus* could replicate and survive. However, recent infection studies using *D. nodosus* have shown that mutants in a number of virulence genes (*fimA*, *pilT*, *pilU*, *fimO*, *fimN*, *fimP, aprV2, aprV5, bprV*) were avirulent in sheep trials (Kennan, et al., 2001; Han, et al., 2007; 2008, Kennan, et al., 2010). In addition, the complementation of the *aprV2* mutant restored virulence and sheep developed FR lesions, thereby fulfilling Koch's molecular postulates (Kennan, et al., 2010). The studies did not mention the presence of *F. necrophorum*.

It is understandable therefore that the precise series of microbial succession events *in situ* remains unclear, particularly as the early histopathological work relied on the morphology of microorganisms for their identification (Beveridge, 1941; Egerton, et al., 1969; Roberts and Egerton, 1969). This calls into question the reliability of these studies, because of the limited morphological diversity exhibited by bacterial populations. In addition, *F. necrophorum* exhibits marked pleomorphism (Hofstad,

2006; Young, 2006) making identification difficult without a specific staining procedure. Fluorescence *in situ* hybridisation (FISH) is a specific molecular and culture-independent technique, for the identification, detection, quantification and spatial resolution of microorganisms within their natural environments (including within plant and mammalian tissue) (Boye, et al., 2006; Kutter, et al., 2006; Klitgaard, et al., 2008; Schmiedel, et al., 2009) and therefore has a number of advantages over other techniques. Combining this technique with confocal-laser scanning microscopy (CLSM) also has a number of advantages over conventional epifluorescence, including the removal of out-of-focus blur (produced by the focal planes above and below the object of interest), the ability to take horizontal and vertical sections and to produce three-dimensional reconstructions (Caldwell, et al., 1992; Lopez, et al., 2005).

4.2. Aims

A FISH assay was therefore designed for the detection of *D. nodosus*, *F. necrophorum* and other bacterial species present within ovine interdigital space biopsies, in order to determine the *in situ* abundance and colonisation sites of these microorganisms at different stages of disease (H, ID, FR).

The hypotheses were that *D. nodosus* and *F. necrophorum* would be more frequently detected in biopsies from diseased feet (feet with ID and ID and FR), but that bacterial load (cell counts) would correlate with the earlier longitudinal findings (Chapter 3); that *D. nodosus* would increase before the development of FR, that feet with ID represented a significant burden of *D. nodosus* infection and that *F. necrophorum* load would increase after the development of FR. In addition, it was expected that *D. nodosus* and

F. necrophorum cells would be observed primarily within the epidermis, but that during cases of FR, *D. nodosus* may be removed via the sloughing of necrotic tissue, which would explain the lack of an association between *D. nodosus* (*rpoD*) load and FR presentation the week of disease onset (Chapter 3).

4.3. Results.

4.3.1. Study flock (2) information.

The second study flock (Mule and Suffolk cross-breeds n = 99, lambs n = 168) were located in Langford, Bristol, UK and were monitored from October 2010 until August 2011. Routine sampling periods were carried out, where ovine foot swabs, body condition scoring, foot integrity scoring and ID and FR severity scoring were collected. Ovine foot swabs and punch biopsies were collected from three ewes (ewe ids. 97, 112 and 126) and three lambs (lamb ids. 293, 200 and 358) from this flock, as described in Section 2.5.2, for subsequent qPCR and FISH analysis, respectively.

4.3.2. FISH probe evaluation, optimisation and controls.

4.3.2.1. Fluorophore evaluation.

All oligonucleotide probes and their fluorophores used in this study are listed in Table 2.10. and were used as described in Section 2.16.1. Fluorescence is described as a three stage process; (i) excitation, when a fluorophore absorbs a photon of energy (hx_{EX}), which is supplied by an external source, such as a laser. This process generates an excited electronic singlet state (S1'). The excited singlet then has a (ii) lifetime of typically 1-10 nanoseconds, where the fluorophore exhibits a conformational change. The energy of the singlet (S1') is slightly decreased forming a relaxed singlet (S1), from

which the (iii) emission (hv_{EM}) originates and can be detected. The photon released during emission, returns to the ground state (S0) and due to the energy decrease of this photon, it exhibits a longer wavelength than the excited photon (Johnson and Spence, 2010). This three-step process is cyclical, unless the fluorophore is irreversibly damaged (by photo-bleaching); an anti-fadent was therefore used in an attempt to prevent this damage (VectaShield). In addition, low-resolution (512 x 512) scanning was performed until z-series were taken (1024 x 1024), in an attempt to increase the speed when screening sections, thereby decreasing the risk of photo-bleaching. The excitation and emission bandwidths of fluorophores are important when performing multiplex-experiments. The FISH analysis to follow used three separate dyes/fluorophores: DAPI, FITC and Cy3 (or Alexa Fluor 594, which was then later excluded from this study and replaced by Cy3). This represents an ideal combination, because the emission spectra of each dye/fluorophore are well-separated (Figure 4.2.).

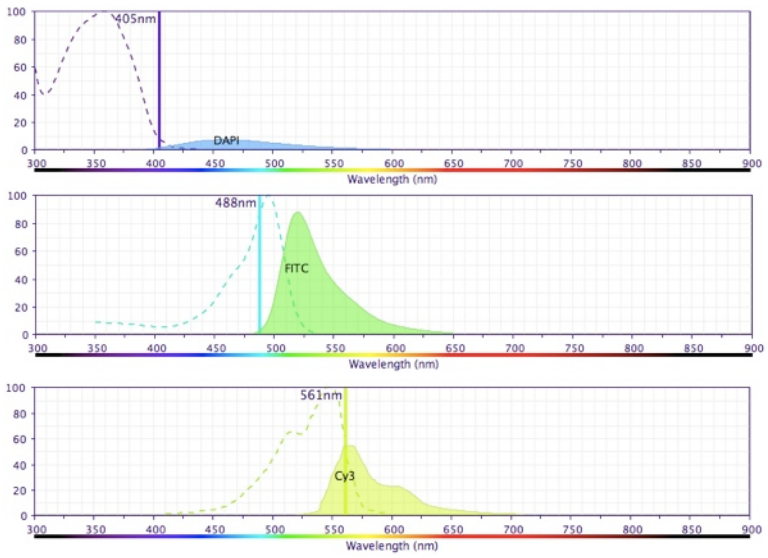

Figure 4.2. BD Fluorescence Spectrum Viewer (BD BioSciences) output for DAPI, FITC and Cy3. Spectral bandwidths for DAPI (blue), FITC (green) and Cy3 (orange); excitation spectra indicated by the dashed line, laser used for excitation highlighted by vertical line (405 nm Blue Diode, 488 nm Argon and 561 nm Ti Sapphire) and emission spectra indicated by filled segments. Y-axis excitation and emission values are expressed as a percentage of maximum values under defined conditions (normalised to 100 %) for each fluorophore/dye (BD BioSciences).

It should be noted that the *D. nodosus*- and *F. necrophorum*-specific probes were tested with single fluorescent labels (5'-Cy3 and 5'-Alexa Fluor 594, respectively) and with two fluorescent labels (DOPE-FISH) (5'- and 3'-Cy3). Empirical optimisation experiments demonstrated that the *D. nodosus* double-labelled (5'- and 3'-Cy3) probe exhibited non-specific binding with non-target organisms (data not shown), in comparison to the single-labelled probe (5'-Cy3). This phenomenon has previously been described (Wallner, et al., 1993), but also disputed (Stoecker, et al., 2010). Adding more than one dye molecule has been reported to significantly increase non-specific fluorescence. This problem therefore is not caused by probe mis-pairing, but by non-specific interactions with the conjugated (fluorescent) molecule. The single-labelled *D. nodosus* probe (5'-Cy3) was therefore selected for downstream experiments.

In contrast, the *F. necrophorum* double-labelled probe (5'- and 3'-Cy3) exhibited the same specificity as the single-labelled version (5'-Alexa Fluor 594), but also increased target cell fluorescence and therefore was selected for all downstream experiments. This difference observed between the two probes highlights the importance of empirical optimisations. Optimisation experiments were then performed on each combination of oligonucleotide probe and fluorescent label, but only results for the final selections are shown. Final selections included; the *D. nodosus* single-labelled probe (5'-Cy3), the *F. necrophorum* double-labelled probe (5'- and 3'-Cy3), the EUB338 (-I, -II, -III) probe set, each individually labelled with a single 5'-Cy3 fluorophore and the EUK1195 single-labelled probe (5'-FITC).

4.3.2.2. FISH probe specificity (*in silico*).

The EUB338 (-I, -II, -III) probe set has been widely used for the detection of the domain Bacteria from a variety of sample types (Pimental-Elardo, et al., 2003; Altmann, et al., 2003; Santelli, et al., 2008). In addition, the EUB338 (-I, -II, -III) probe set is often included as a control for false negatives caused by methodological issues (Moter and Göbel, 2000). Similarly, the *F. necrophorum* probe has received some use and has previously been optimised (Boye, et al., 2006), however additional optimisation was included during this study. The novel *D. nodosus* probe (Table 2.10.) modified from the *Cc* reverse primer (La Fontaine, et al., 1992), however required full evaluation and optimisation.

The *in silico* specificity of the *D. nodosus* (Table 4.1.) and *F. necrophorum* (Table 4.2.) oligonucleotide probes was assessed using probeCheck (Loy, et al., 2008). ProbeCheck is a freely accessible web server, providing rapid specificity and coverage evaluations for probes and primers. The *in silico* analysis revealed that the probes were 100 % specific for their respective targets; zero mismatches were observed for their target organism, whereas non-target organisms had a minimum of two and three mismatches, for the *F. necrophorum* and *D. nodosus* probes, respectively.

Table 4.1. *In silico* evaluation of the specificity of the *D. nodosus*-specific probe using probeCheck. Specific targets (no mismatches) above the grey line, non-specific hits (with mismatches) below the grey line (top five hits shown). Target sequence automatically converted to reverse complement.

Name	Accession no.	Mismatches	ΔG	Sequence (5' to 3') GUAGAAAUACUCGGUACCGA
D. nodosus (VCS1703A)	CP000513	0	-19.32	AGGUGUUGG-==========-AGCUAACGC

Name	Accession no.	Mismatches	ΔG	Sequence (5' to 3') GUAGAAAUACUCGGUACCGA
D. nodosus (VCS1703A)	DQ016291	0	-19.32	AGGUGUUGG-==========-AGCUAACGC
D. nodosus	DQ016290	0	-19.32	AGGUGUUGG-==========-AGCUAACGC
D. nodosus	M35016	0	-19.32	AGGUGUUGG-==========-AGCUAACGC
Soehngenia saccharolytica (n = 5)	AY353956	3	-19.32	AGGUGUCGG-=======u=====g===C-AGCUAACGC
Trepomonas steinii	EF551173	3	-13.70	ACUAAAUCA-==U=====g=g=======-AAGCGUAGU
Unidentified rumen bacterium RF17	AF001749	4	-13.70	UUACAAUGG-=======a===gg==g====-CUGGUGACA
Acinetobacter sp. NF4	EF565936	4	-13.70	CUACAAUGG-=======a===gg==g====-ACAGCGAUG
Trypanosoma cruzi (n = 7)	AF359484	4	-11.64	UAGACCCAC-====g=========g=A=u-UAUUGGUCG

ΔG change in free-energy (the energy that is available from the process) expressed in kcal mol^{-1}, an indication of hybridisation efficiency.

Table 4.2. *In silico* evaluation of the specificity of the *F. necrophorum*-specific probe using probeCheck. Specific targets (no mismatches) above the grey line, non-specific hits (with mismatches) below the grey line (top hit is shown). Target sequence automatically converted to reverse complement.

Name	Accession no.	Mismatches	ΔG	Sequence (5' to 3') UUUUCGCAUGGAGGAAUC
F. necrophorum subsp. *necrophorum*	AB525413	0	-17.84	AUUAUGGUU-==========-AUGAAAGCU
Fusobacterium sp. D213	ACDG0100 0169	0	-17.84	AUUAUGGUU-==========-AUGAAAGCU
F. necrophorum	AF044948	0	-17.84	AUUAUGGUU-==========-AUGAAAGCU
F. necrophorum	AJ867038	0	-17.84	AUUAUGGUU-==========-AUGAAAGCU
F. necrophorum subs	AJ867039	0	-17.84	AUUAUGGUU-==========-AUGAAAGCU
F. necrophorum subsp. *funduliforme*	AM905356	0	-17.84	AUUAUGGUU-==========-AUGAAAGCU
F. necrophorum (n = 12)	DJ390780	0	-17.84	AUUAUGGUU-==========-AUGAAAGCU
F. necrophorum subsp. *funduliforme*	EF447425	0	-17.84	AUUAUGGUU-==========-AUGAAAGCU
F. necrophorum (n = 4)	FJ984622	0	-17.84	AUUAUGGUU-==========-AUGAAAGCU
Paenibacillus sp. YK20	AB091337	2	-13.35	UAGGUGAUU-===C=========g===-AAGAAACAC

ΔG change in free-energy (the energy that is available from the process) expressed in kcal mol^{-1}, an indication of hybridisation efficiency.

4.3.2.3. FISH probe specificity (*in vitro*).

The *in vitro* specificity of the *F. necrophorum* and the *D. nodosus* probes was then determined. In addition, the optimal formamide concentration (for the hybridisation buffer) for all probes then had to be evaluated. The formamide concentration was represented as a percentage (%) of the total hybridisation buffer volume and equates to the hybridisation stringency; the higher the formamide concentration the more stringent/ specific the DNA-rRNA hetero-duplex formation.

Formamide gradients (0-35 %) were then performed for all three oligonucleotide probes (Figure 4.3.) for a series of positive and negative control microorganisms. Strains VCS1703A, A198 and Serogroup A were used as positive controls for the *D. nodosus* probe formamide gradients and strains BS-1, D213 and D555 were used as the positive controls for the *F. necrophorum* probe formamide gradients. *B. circulans* (WL-12), *E. coli* (K-12) and either *F. necrophorum* (BS-1) or *D. nodosus* (VCS1703A) instead acted as the negative controls for the above gradients (data not shown). For the EUB338 (-I, -II, -III) probe set, *B. circulans* (WL-12), *M. caseolyticus* (87), *D. nodosus* (VCS1703A) and *A. pyogenes* (DS7M 20-630) acted as positive controls. *Schizosaccharomyces pombe* and *Saccharomyces cerevisiae* acted as negative controls for EUB338 (-I, -II, -III) probe set (data not shown).

The aim of the formamide gradients was to determine the point at which background or non-specific (cell) fluorescence decreased and when target cell fluorescence was at its highest. Background fluorescence was almost negligible for all images taken, but was usually highest at 0 % formamide (data not shown), correlating with the least stringent

conditions. Non-specific probe-conferred fluorescence was not observed for any of the negative control microorganisms tested over the 0-35 % formamide range for any of the oligonucleotide probes (data not shown).

The formamide gradients for the different bacterial oligonucleotide probes produced varying results (Figure 4.3.), with some working at a broader formamide range than others. Target cell and background fluorescence were measured as described in Section 2.19.1. and were expressed as a mean pixel intensity measurement (arbitrary units (a.u.)). The *D. nodosus* probe (5'-Cy3) exhibited the highest mean target cell fluorescence at 20 % formamide (66.2 a.u.), which then rapidly decreased over 25-35 % formamide range, demonstrating a narrow optimal formamide range (5-20 %). The *F. necrophorum* probe (5'- and 3'-Cy3) had the highest starting mean target cell fluorescence, which was likely because of the presence of the double-label (Stoecker, et al., 2010). The highest mean target cell fluorescence for the *F. necrophorum* probe was observed between 10-25 % formamide (73.7-74.8 a.u.), but the *F. necrophorum* probe also had a broad formamide range. The EUB338 (-I, -II, -III) probe set instead had the lowest overall mean fluorescence, probably due to its variable binding affinities for the different bacterial species selected. The highest mean fluorescence however was between 20-35 % formamide (57.7-59.1 a.u.), which corresponded with published formamide ranges (Amann, et al., 1990; Daims, et al., 1999).

It was therefore decided that all subsequent hybridisations for all probes would be performed using the same formamide concentration for simplicity and a concentration of 20 % was selected.

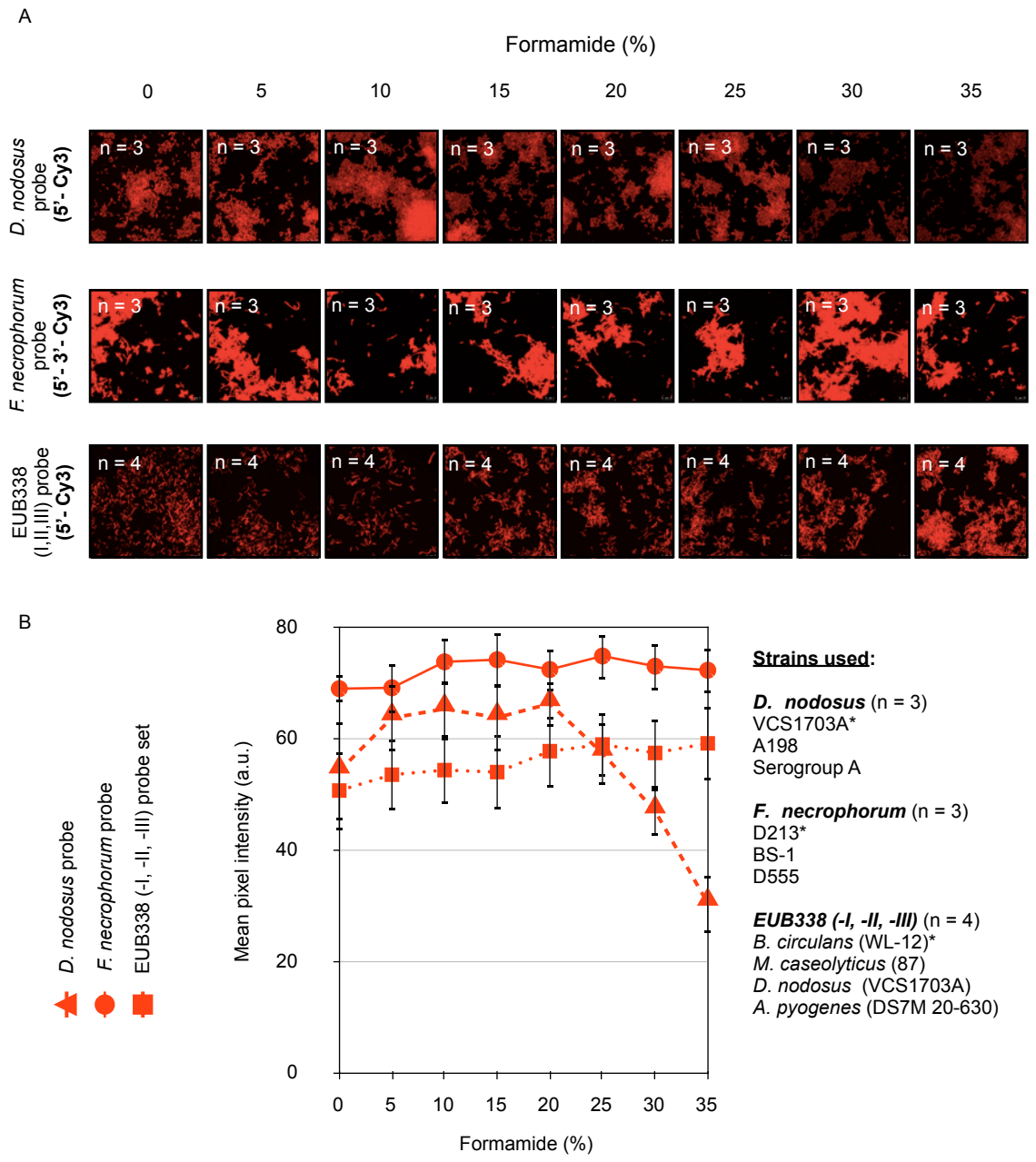

Figure 4.3. Formamide (0-35 %) gradients for the *D. nodosus* and *F. necrophorum* probes and the EUB338 (-I, -II, -III) probe set. Three positive control strains were used for both the *D. nodosus* (n = 24 images) and *F. necrophorum* (n = 24 images) formamide gradients (A). Four positive bacterial controls were used for the EUB338 (-I, -II, -III) formamide gradients (n = 32 images) (A). Total number of images n = 80. Target cell (n = 20 cells per image) and background fluorescence (n = 10 selections per image) were measured as described in Section 2.19.1. and are expressed as mean pixel intensity (a.u.). Background fluorescence was subtracted from target cell fluorescence. Mean target cell fluorescence (representative of three or four strains) is shown with ± SD (B). Asterisks (*) next to bacterial species/ strain highlight which image series is shown in (A). Gram positive bacteria were pre-treated with lysozyme as described in Section 4.3.2.4. Scale bars: 10 µm.

Additional positive and negative controls were then screened with the *D. nodosus* and *F. necrophorum* probes using this selected formamide concentration (20 %). A total of five positive controls were screened with the *D. nodosus*-specific probe and all strains produced a positive fluorescent signal, with little or no background fluorescence (Table 4.3.). Seven positive controls were then screened with the *F. necrophorum*-specific probe and all seven produced positive signals (Table 4.4.). A total of nine negative controls were screened for both the *D. nodosus* and *F. necrophorum* probes and no fluorescent signal was observed. The accessibility of oligonucleotide probes to their site, in this case the 16S rRNA, may be hindered by the three-dimensional structure of the ribosome (Behrens, et al., 2003). The accessibility map using *E. coli* (Fuchs, et al., 1998) was briefly examined, but empirical experimentation determined that the site targeted by the *D. nodosus* probe (modified Cc primer) was accessible (Figure 4.3. and Table 4.3.).

Table 4.3. *In vitro* specificity of the *D. nodosus* oligonucleotide FISH probe.

***D. nodosus* strain (positive controls)** n = 5	**Result**	**Negative controls** n = 9	**Result**
VCS1703A[a]	+	*Aeromonas hydrophila*	-
BS-1	+	*Aeromonas media*	-
BS-6	+	*Arcanobacterium pyogenes* (DS7M 20-630)	-
A198[a]	+	*Bacillus circulans* (WL-12) [a]	-
Serogroup A[a]	+	*Citrobacter freundii*	-
		Escherichia coli (K-12) [a]	-
		Fusobacterium necrophorum (BS-1) [a]	-
		Klebsiella pneumoniae	-
		Macrococcus caseolyticus (87)	-

[a] Strains used for formamide gradients.

Table 4.4. *In vitro* specificity of the *F. necrophorum* oligonucleotide FISH probe.

***F. necrophorum* strain (positive controls)** n = 7	**Result**	**Negative controls** n = 9	**Result**
F. necrophorum (BS-1)[a]	+	*Aeromonas hydrophila*	-
F. necrophorum subsp. *necrophorum* D146	+	*Aeromonas media*	-
F. necrophorum subsp. *necrophorum* D213[a]	+	*Arcanobacterium pyogenes* (DS7M 20-630)	-
F. necrophorum subsp. necrophorum D306	+	*Bacillus circulans* (WL-12) [a]	-
F. necrophorum subsp. necrophorum D555[a]	+	*Citrobacter freundii*	-
F. necrophorum subsp. necrophorum D745	+	*Dichelobacter nodosus* (VCS1703A) [a]	-
F. necrophorum subsp. necrophorum D809	+	*Escherichia coli* (K-12) [a]	-
		Klebsiella pneumoniae	-
		Macrococcus caseolyticus (87)	-

[a] Strains used for formamide gradients.

A number of target microorganisms were also screened with the EUB338 (-I, -II, -III) probe set, to determine if *D. nodosus* or *F. necrophorum* would be detected with this set (Figure 4.4.). The EUB338 (-I, -II, -III) probe set bound to all tested bacterial species and target cell fluorescence (a.u.) was measured. However, the probe set bound poorly to *F. necrophorum* (BS-1), with an average target cell fluorescence intensity of 17.80 (a.u.), which was considerably lower than the other tested bacterial species (*E. coli* (K-12), *A. pyogenes* (DS7M 20-630), *M. caseolyticus* (87) and *B. circulans* (WL-12)). *F. necrophorum* subsp. *necrophorum* (strain D809) was also tested and exhibited similarly poor fluorescence (data not shown). It was concluded therefore that *F. necrophorum* would be unlikely to be detected in the screens using the EUB338 (-I, -II. -III) probe set, because of the low signal to to noise ratio. The EUB338 (-I, -II, -III)

probe set is reported to cover approximately 94 % of bacterial entries within the domain Bacteria (Amann and Fuchs, 2008). It was subsequently decided that quantification protocols (Section 4.3.5.) would therefore not include relative quantification (relative abundance compared to the general population), because *F. necrophorum* would be unlikely to be detected using the general population probe set (EUB338-I, -II, -III).

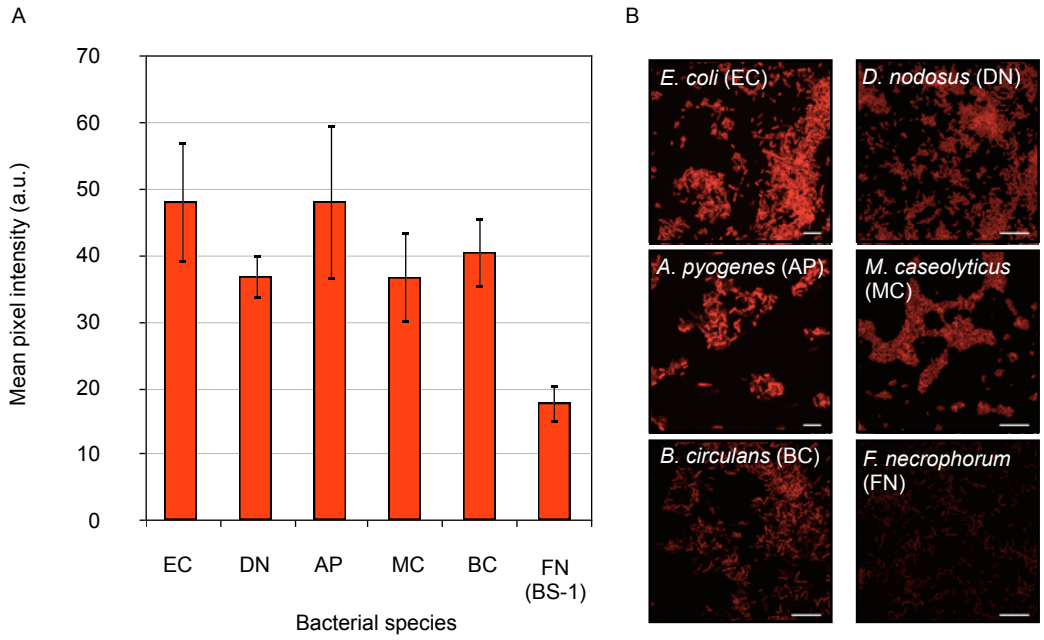

Figure 4.4. Binding efficiency (measured by pixel intensity) of the EUB338 (-I, -II, -III) probe set to a range of target cells. The EUB338 probe set bound to all targets and target cell fluorescence (mean pixel intensity (a.u.)) was measured (A). Target cell (n = 20 cells per image) and background fluorescence (n = 10 selections per image) were measured as described in Section 2.19.1. Data presented as mean pixel intensity of target cells with ± SD. The probe set bound weakly to *F. necrophorum* (BS-1), indicated by the decrease in fluorescence intensity observed and *F. necrophorum* subsp. *necrophorum* (D809) (data not shown). Gram positive bacteria were pre-treated with lysozyme as described in Section 4.3.2.4. Images for *A. pyogenes* (AP) and *E. coli* (EC) - scale bars: 10 µm. Images for *D. nodosus* (DN), *M. caseolyticus* (MC), *B. circulans* (BC) and *F. necrophorum* (FN) - scale bars: 25 µm (B).

4.3.2.4. Lysozyme pre-treatment for Gram positive bacteria.

Bacterial cells, environmental samples and tissue biopsies are usually fixed in formaldehyde or ethanol and then dehydrated (permeabilised) via an ethanol gradient

(from a low to high ethanol concentration). However, the cell wall composition of bacteria and other microorganisms is diverse and as such different permeabilisation steps may be required. For example, some Gram positive bacteria require additional enzymatic pre-treatment, due to their thicker peptidoglycan layer, in order to fully permeabilise their cell wall and allow the labelled oligonucleotide probe access to the target rRNA molecules (Amann and Fuchs, 2008). There is currently no standard permeabilisation method for all microorganisms and empirical optimisations are frequently employed to determine the precise set of pre-treatments required. One of the primary reasons for a lack of fluorescent signal is insufficient probe penetration (Moter and Göbel, 2000) and therefore an appropriate permeabilisation step should be employed. Enzymatic digestion, for example using lysozyme, is frequently used to digest thick peptidoglycan layers (Thurnheer, et al., 2004; Amann and Fuchs, 2008).

Three Gram positive bacteria (*A. pyogenes* (DS7M 20-630), *B. circulans* (WL-12) and *M. caseolyticus* (87)) were therefore selected to assess the effect of incubation with lysozyme (10 mg ml^{-1}) at 37^{o}C for 0.5, 1, 2, 3, 4, 10 and 20 m, as outlined in Section 2.16.3.3. In addition, three Gram negative bacteria (*E. coli* (K-12), *D. nodosus* (VCS1703A) and *F. necrophorum* (BS-1)) were also selected for comparison. Experiments were carried out in duplicate. The effect of lysozyme on target cell fluorescence (mean pixel intensity (a.u.)) was then measured, as described in Section 2.19.1.

Lysozyme greatly increased the mean pixel intensity of *A. pyogenes* and *M. caseolyticus* by 31.6 and 21.9 a.u., respectively, after only a 30 s incubation. The mean target cell

fluorescence of both *A. pyogenes* and *M. caseolyticus* continued to increase until 3 m. A slight decrease in target cell fluorescence was then observed after the 20 m incubation (although this was minimal) (Figure 4.5.). The initial mean target cell fluorescence for *B. circulans* was instead much higher (76.9 (a.u.)) than that of the other two Gram positive bacteria, but *B. circulans* also appeared to be affected less during the time series. However, over time the mean cell fluorescence intensity gradually decreased. This observation may indicate some difference in the peptidoglycan layer compositions between *B. circulans* and *A. pyogenes* and *M. caseolyticus.* Interestingly, a study by Laflamme and colleagues (2009) reported that *B. cereus* cells can be fixed in 4 % PFA and hybridised with the EUB338 probe without an additional permeabilisation step. In addition, *B. cereu*s cells are reported to be more permeable than other Gram positive bacteria to nucleic acid dyes (such as ethidium bromide) (Walberg, et al., 1999). This may suggest that certain species of genus *Bacillus* may be more permeable than other Gram positive bacteria to fluorescently labelled probes and/or dyes. *B. cereus* and *B. subtilis* are also reported to be resistant to lysozyme, because of the presence of deacetylated glucosamine residues in their peptidoglycan layers (Westmacott, et al., 1979; Kobayashi, et al., 2012), providing a possible explanation as to why there was no further increase in *B. circulans* target cell fluorescence after lysozyme treatment (Figure 4.5.)

A comparison of *A. pyogenes* before and after lysozyme treatment is also shown (Figure 4.6.), a large proportion of the cells had only partial uptake of the oligonucleotide probe prior to lysozyme treatment.

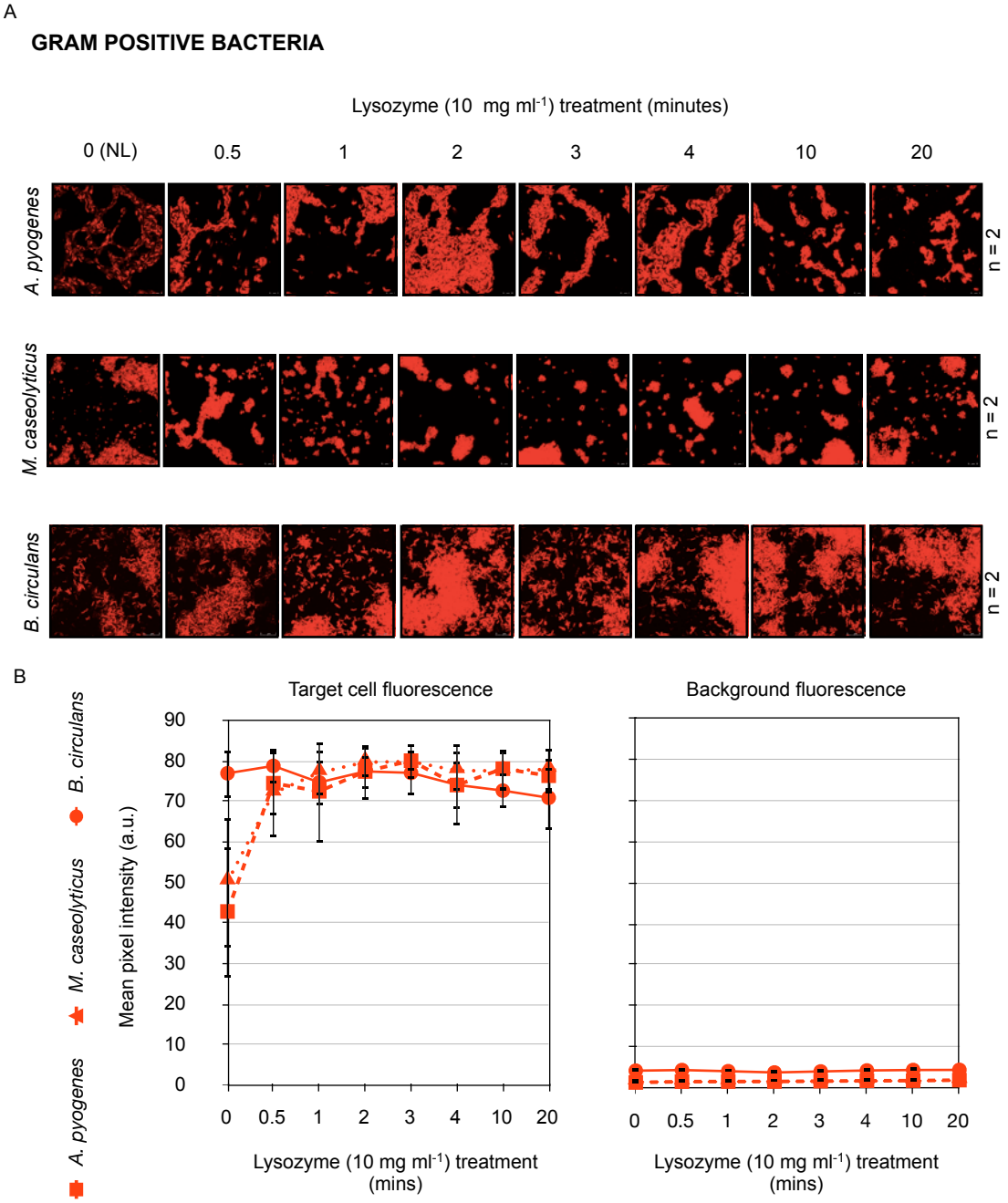

Figure 4.5. Effect of incubation time with lysozyme (10 mg ml^{-1}) at 37^{o}C on the fluorescence intensity (a.u.) of three Gram positive bacteria. The lysozyme pre-treatment was performed as described in Section 2.16.3.3. and target cell (n = 20 cells per image) and background (n = 10 selections per image) fluorescence were measured. Representative images shown (A). A rapid increase in fluorescence intensity was observed, after only 30 s lysozyme treatment for *A. pyogenes* and *M. caseolyticus*. *B. circulans* fluorescence was initially much higher (B). Background fluorescence was negligible. NL: no lysozyme. Error bars ± SD. Lysozyme experiments were carried out in duplicate. *A. pyogenes* and *M. caseolyticus* images- scale bars: 10 µm and *B. circulans*- scale bars: 25 µm (A).

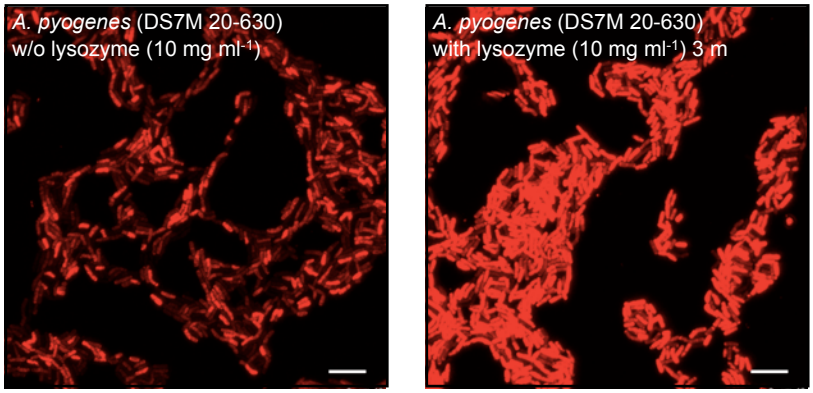

Figure 4.6. Example of effect of lysozyme treatment on the permeability and thus fluorescence intensity of *A. pyogenes* (DS7M 20-630). Before lysozyme treatment and after a 3 m incubation with lysozyme (10 mg ml^{-1}) at 37°C. Scale bars: 10 µm.

The rapid increase in fluorescence intensity after only 30 s incubation with lysozyme for *A. pyogenes* and *M. caseolyticus* was not observed for the three Gram negative bacteria; either a gradual increase was observed followed by a plateau (no change) or a gradual decrease in target cell fluorescence (Figure 4.7.), which has previously been demonstrated (Thurnheer, et al., 2004). No significant negative effect was observed for either the Gram positive or the Gram negative bacterial species tested. The lysozyme pre-treatment step was then used for the all *in vitro* optimisations using Gram positive bacteria and for the EUB338 (-I, -II, -III) screens on tissue biopsies to increase target detection (3 m treatment with lysozyme (10 mg ml^{-1}) at 37°C), it was not required for the *D. nodosus* or *F. necrophorum* biopsy screens. The overall aim was to preserve bacterial cell shape and integrity, whilst permeabilising as many cells as possible, without losing cells via lysis.

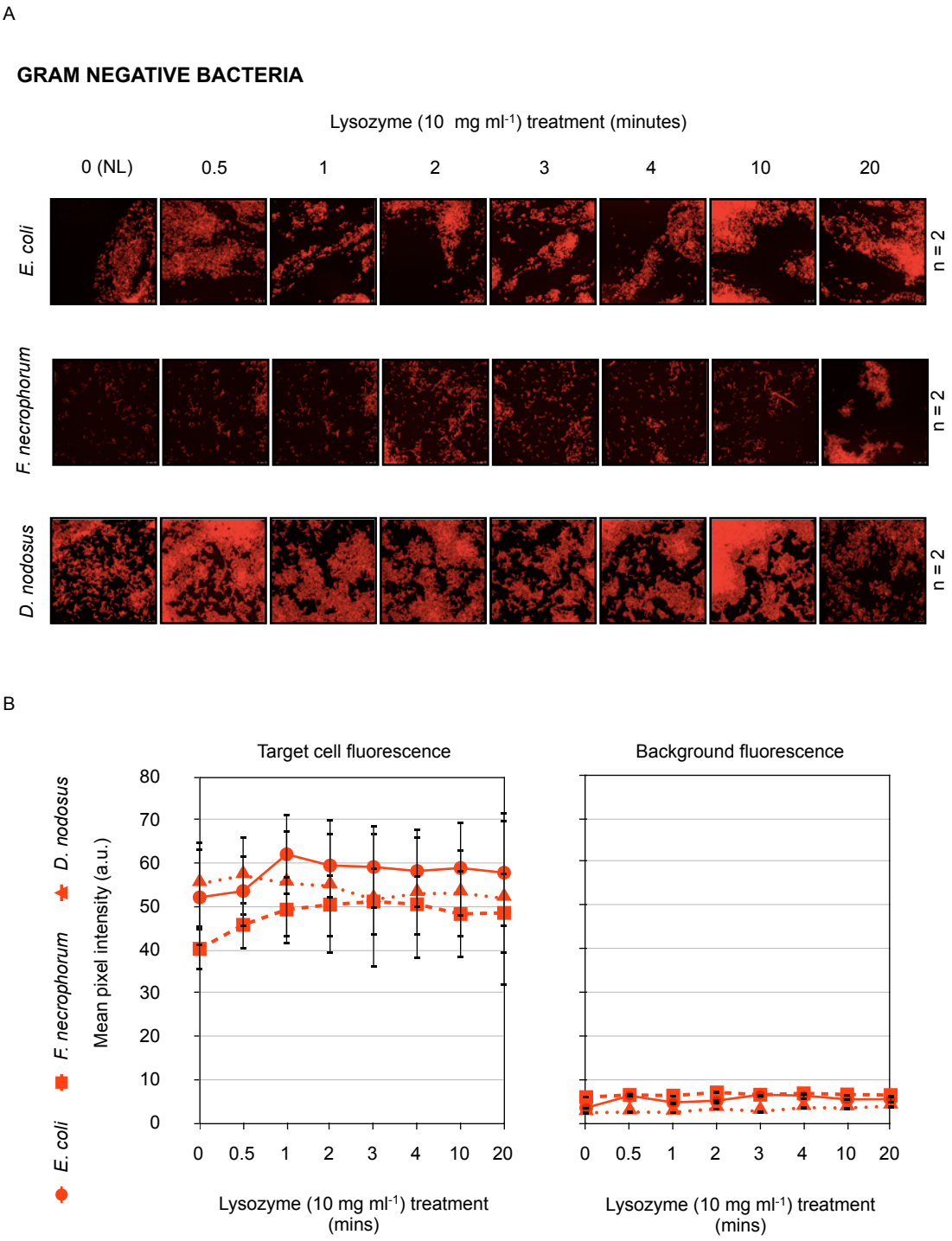

Figure 4.7. Effect of incubation time with lysozyme (10 mg ml^{-1}) at 37^{o}C on the fluorescence intensity (a.u.) of three Gram negative bacteria. The lysozyme pre-treatment was performed as described in Section 2.16.3.3. and target cell (n = 20 cells per image) and background (n = 10 selections per image) fluorescence were measured. Representative images shown (A). A gradual increase in target cell fluorescence was observed (B). Background fluorescence was negligible. NL: no lysozyme. Error bars ± SD of twenty target cell measurements and ten background measurements. Lysozyme experiments were carried out in duplicate. Scale bars: 10 µm.

4.3.3. Ovine interdigital space tissue sections.

4.3.3.1. Visualisation and staining of tissue and ovine epithelial cells.

Tissue biopsies were taken from the interdigital space of clinically healthy ovine feet collected from the EU-licensed abattoir (as described in Section 2.5.2.) and were then fixed and sectioned as described in Section 2.16.2.4. The biopsies were examined (i) prior to FISH, (ii) with DAPI stain only and (iii) with DAPI stain, after hybridisation with the EUK1195 probe. After de-waxing, rehydration and dehydration, the tissue sections were first examined under the 405 nm Blue Diode, the 488 nm Argon and the 561 nm Ti Sapphire laser lines, to act as a negative FISH 'no probe' control (Figure 4.8.). Some intrinsic tissue autofluorescence was observed under the 405 nm and 488 nm laser lines and this was one of the primary reasons for labelling the bacterial probes in the Cy3 fluorophore, in order to prevent masking of target signal. There are many causes of natural autofluorescence in tissue (mammalian and plant) (Neumann and Gabel, 2002) and even in some microorganisms (Glöckner, et al., 1996), due to substances like flavins or porphyrins (such as chlorophyll). In contrast, some autofluorescence may be of value and aid the observer by allowing better orientation within tissue sections (Baschong, et al., 2001).

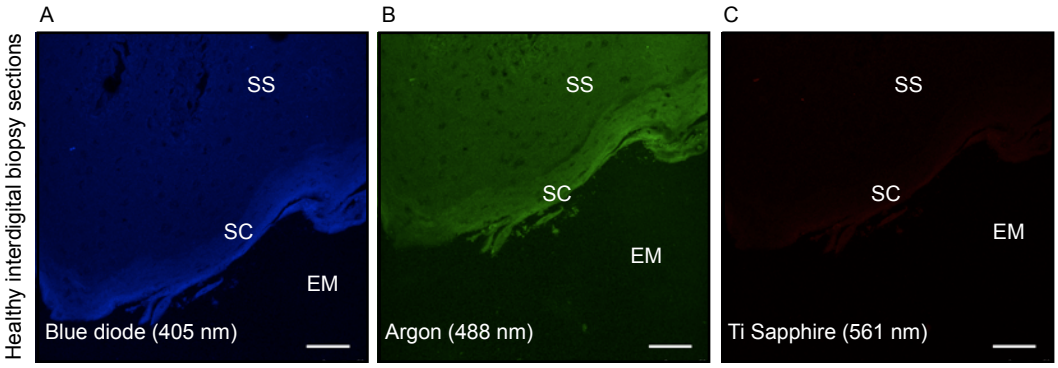

Figure 4.8. 'No-probe' FISH negative control under three laser lines (Blue diode 405 nm (A), Argon 488 nm (B), Ti Sapphire 561 nm (C)). Some intrinsic autofluorescence observed under the 405 nm and 488 nm lasers lines, very little observed under the 561 nm laser. Extracellular milieu (EM), stratum corneum (SC) and stratum spinosum (SS) layers are shown. Scale bars: 50 µm.

The fixed healthy tissue biopsies were then examined with DAPI only (present in the Vecta-Shield anti-fadent) and with DAPI after hybridisation with the EUK1195 oligonucleotide probe (5'- FITC) (Figure 4.9.). A formamide concentration of 20 % was used for the hybridisations, containing the EUK1196 probe. The same formamide concentration had to be used, as for the other bacterial probes, because the EUK1195 and bacterial probes would later be hybridised simultaneously within the same hybridisation buffer. In the DAPI-stained tissue sections, the epithelial nuclei fluoresced intensely under the 405 nm laser line, with some tissue autofluorescence observed in green (488 nm laser line). The tissue sections stained with DAPI after hybridisation with the EUK1195 probe (targeting the 18S rRNA ribosomal gene) highlighted epithelial cell junctions, useful for assessing bacterial localisation and tissue histology.

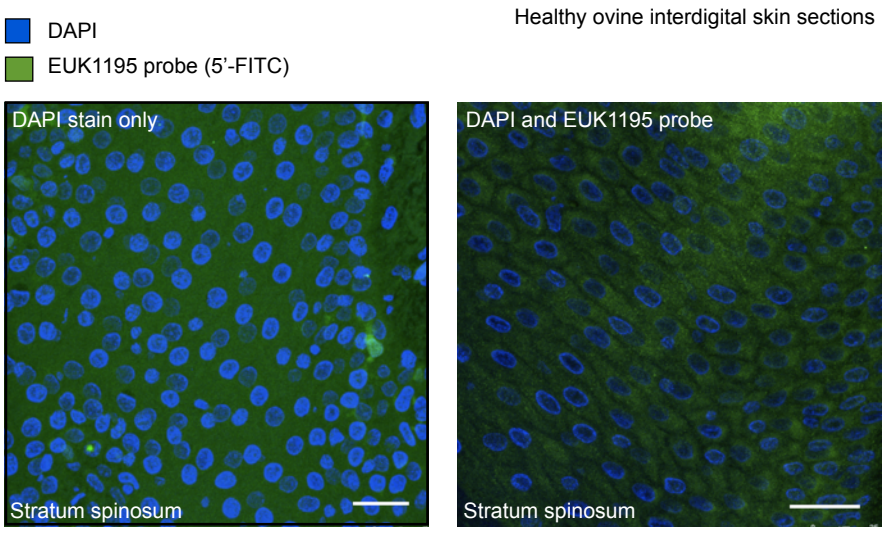

Figure 4.9. Healthy ovine interdigital space tissue stained with DAPI and with DAPI after hybridisation with the EUK1195 probe (5'-FITC). In both sections, the epithelial cell nuclei stain intensely (blue) with DAPI. In sections hybridised with the EUK1195 probe, epithelial cell junctions are apparent. Scale bars: 25 µm.

In addition, proteinase K (5 µg ml^{-1}) was used as a tissue pre-treatment to decrease tissue autofluorescence (Peters, et al., 2011), as described in Section 2.16.3.4. This pre-

treatment was also tested on *D. nodosus*, *F. necrophorum*, *A. pyogenes* and *M. caseolyticus*; the additional pre-treatment had no negative effect on target cell detection/ fluorescence (target cell pixel intensity) (data not shown).

4.3.3.2. *In situ* (tissue) FISH controls.

Additional biopsies were taken from the interdigital space of healthy ovine feet and were subcutaneously inoculated with undiluted culture of either (i) *D. nodosus* (VCS1703A) or (ii) *F. necrophorum* (BS-1) and put in sterile petri dishes and incubated at 37^{o}C for 1 h or 24 h under aerobic conditions to enable cells to multiply/attach to epidermal matrix. The biopsies were then fixed and processed as described in Section 2.16.2.4.

4.3.3.2.1. EUB338 (-I, -II, -III) *in situ* (tissue) controls.

The *D. nodosus* sections were screened separately; first with the EUB338 (-I, -II, -III) probe set and then with the *D. nodosus*-specific probe (in conjunction with the EUK1195 probe and DAPI stain). The sections screened with the EUB338 (-I, -II, -III) probe set were positive (both the 1 h and 24 h biopsies p.i.) and confirmed that the FISH procedure worked effectively. Numerous bacterial cells were detected within the tissue sections incubated for 24 h post-inoculation (p.i.) (Figure 4.10.). The bacteria did not exhibit a specific localisation pattern, however bacteria were observed within and in close proximity to a number of hair follicles (Figure 4.10.). A number of tears were also observed within the tissue sections, likely due to the inoculation procedure and/or increased tissue atrophy due to the incubation period (1 h or 24 h) prior to fixation.

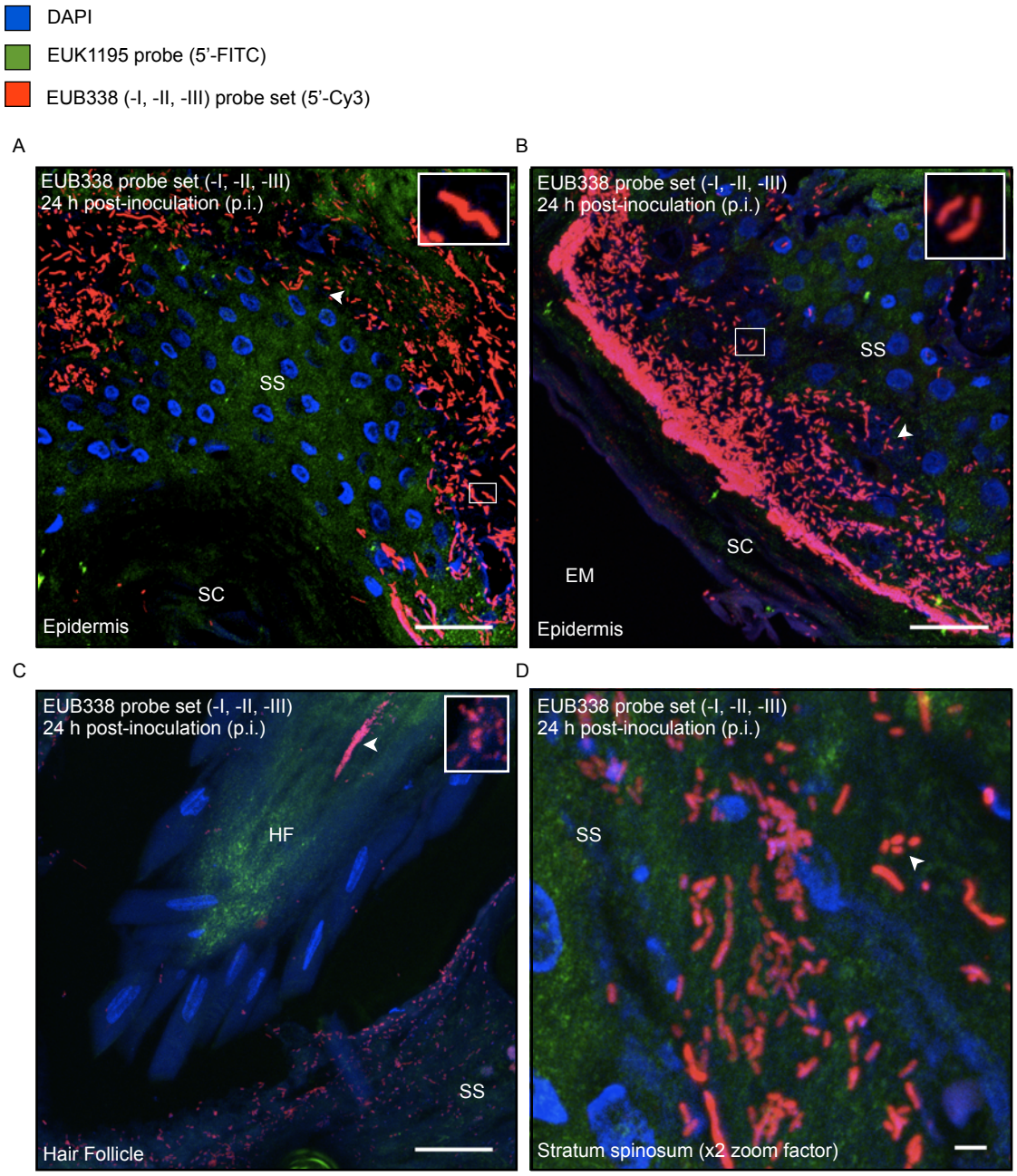

Figure 4.10. Healthy ovine interdigital space biopsies subcutaneously inoculated with *D. nodosus* and screened with EUB338 (-I, -II, -III) probe set (5'-Cy3). Biopsies were incubated at 37ºC post-inoculation (p.i.) for 24 h under aerobic conditions, fixed and processed as described in Section 2.16.2.4. Tissue sections were then stained with DAPI after hybridisation with EUB338 (-I, -II, -III) (5'-Cy3) and EUK1195 (5'-FITC) probes. Epithelial cell nuclei stain blue, epithelial cells green and bacterial cells red (pink; due to subsequent-staining with DAPI). Bacterial cells (with a variety of morphologies) are seen within the stratum spinosum (SS) and localised with hair follicles (HF). Scale bars: 25 µm (A, B, C) and 2.5 µm (D).

4.3.3.2.2. *D. nodosus* and *F. necrophorum in situ* (tissue) controls.

However, the same sections were then screened with the *D. nodosus*-specific probe and were both (1 h and 24 h biopsies p.i.) negative (data not shown), so it is unlikely the bacteria present in the EUB338 (-I -II, -III) screens (Figure 4.10.) were in fact *D. nodosus* cells, but instead bacterial populations that had already been present on the interdigital space biopsies that had multiplied during the 24 h incubation period. Despite this, the tissue sections subcutaneously inoculated with *F. necrophorum* (BS-1) were then screened with the *F. necrophorum*-specific (5'-Alexa Fluor 594) probe. The biopsies that had been incubated for 1 h post-inoculation (p.i.) were negative, however the biopsies that had been incubated for longer (24 h p.i.) were positive. Despite this, the *F. necrophorum* cells only fluoresced weakly with the Alexa-Fluor 594-labelled probe (co-stained with DAPI) (Figure 4.11.). Other bacteria stained by DAPI were also evident.

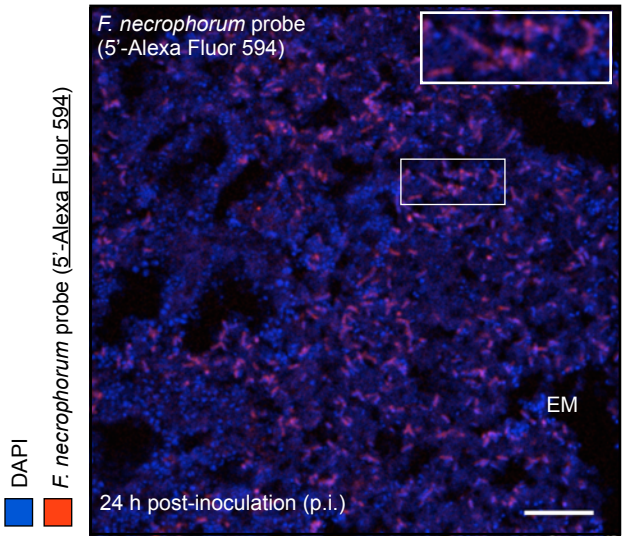

Figure 4.11. Healthy ovine interdigital biopsy subcutaneously inoculated with *F. necrophorum* (BS-1). Biopsies were incubated at 37°C post-inoculation for 24 h under aerobic conditions, fixed and processed as described in Section 2.16.2.4. Sections were then stained with DAPI after hybridisation with *F. necrophorum* (5'-Alexa Fluor 594) and EUK1195 (5'-FITC) probes. Bacterial cells detected within the extracellular milieu (EM). Scale bar: 25 µm.

The *F. necrophorum* cells were detected in the extracellular milieu (EM) within a large tear, rather than within the tissue section itself. The weak staining of the *F. necrophorum* cells and lack of detection of *D. nodosus* cells, indicated that an anaerobic incubation post-inoculation (p.i.) may improve detection. At this point the *F. necrophorum* and *D. nodosus* probes were double-labelled with Cy3 (5' and 3'), because the use of bright carbocyanine dyes (Moter and Göbel, 2000; Amann and Fuchs, 2008) and double labelling (Stoecker, et al., 2010) had been reported to improve detection. The corresponding *in vitro* controls were then repeated (as shown previously). The *in situ* (tissue) controls were then also repeated and after inoculation with undiluted *D. nodosus* (VCS1703A) and *F. necrophorum* (BS-1) were incubated under anaerobic conditions at 37^{o}C for 1 h and 24 h.

A comparison of the target cell fluorescence between single and double labels was however first performed (Figure 4.12.). Two *F. necrophorum* strains (BS-1 and D146) were hybridised with the *F. necrophorum*-specific probe, which had either been labelled with (i) a single 5'-Alexa Fluor 594 fluorphore or (ii) two Cy3 fluorophores 5' and 3'. Target cells, which had been hybridised with the double-labelled *F. necrophorum* probe, had a higher mean target cell fluorescence (a.u.) than those with the single label only (5'-Alexa Fluor 594) and this difference was found to be statistically significant ($p < 0.01$) (Unpaired t-test with Welch's correction, Prism, Graphpad.). It is unknown whether this increase in target cell fluorescence was due to the presence of the double label or because the Cy3 fluorophores were brighter than the Alexa Fluor 594 label. A comparison between single Cy3 and double Cy3 would be required to determine this.

However, the increase in fluorescence intensity was enough to select this probe and fluorophore combination over the previous combination. *D. nodosus* strain VCS1703A was then hybridised with the *D. nodosus*-specific probe, that had been labelled with either (i) a single Cy3 fluorophore (5'-end) or (ii) two Cy3 fluorophores (5'- and 3'-ends). There was no significant increase in the target cell fluorescence between the the single and double Cy3 labels.

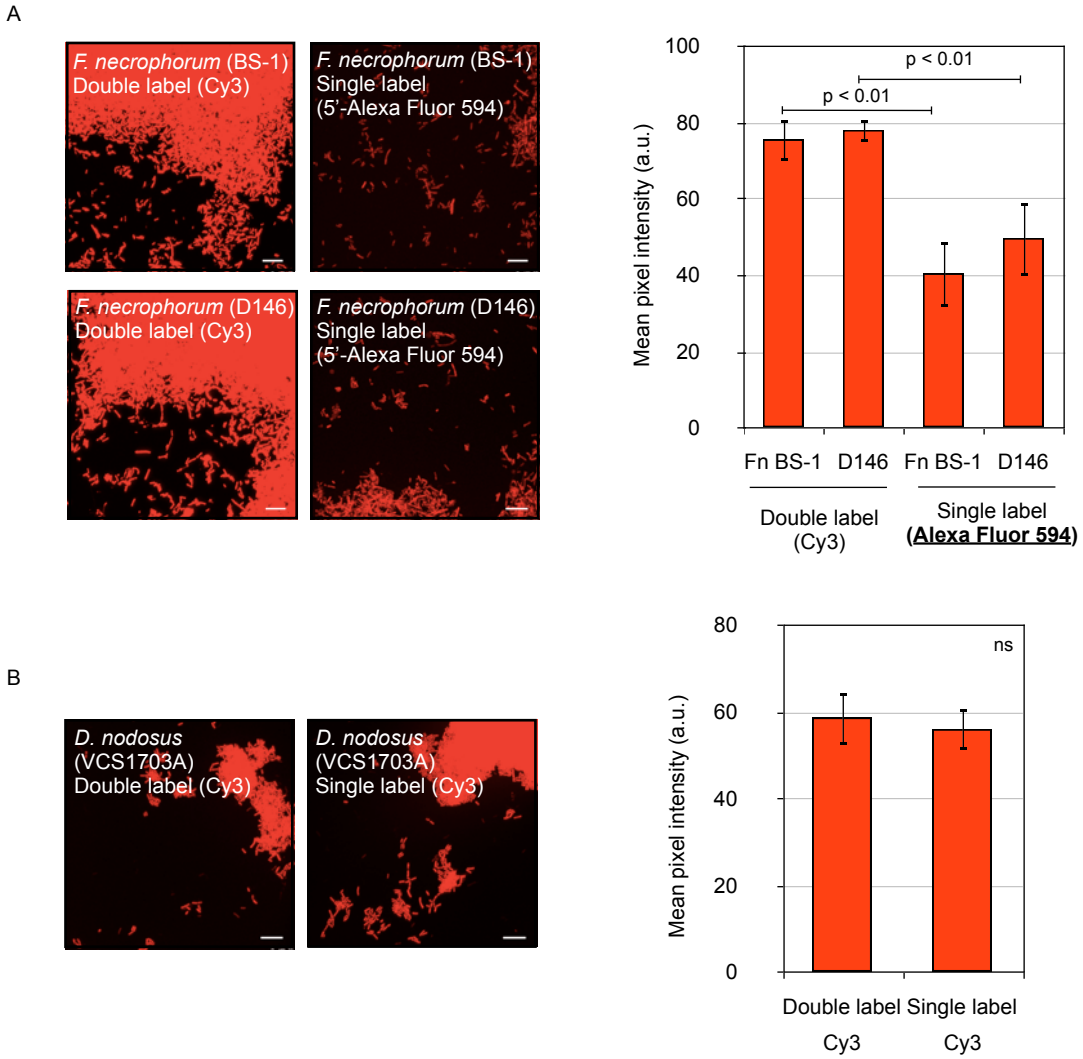

Figure 4.12. Comparison of mean pixel intensity (a.u.) of *F. necrophorum* cells and *D. nodosus* cells labelled with different probe/fluorophore combinations. The *F. necrophorum* probe was labelled with either (i) a single 5'-Alexa Fluor 594 molecule or (ii) a two Cy3 molecules (5' and 3'). The double labelled *F. necrophorum* probe significantly increased the target cell fluorescence ($p < 0.01$) (Unpaired t-test with Welch's correction, one-tailed, Prism, Graphpad) (A). The *D. nodosus* probe was labelled with either (i) a single 5'-Cy3 or (ii) a two Cy3 molecules (5' and 3'). There was no significant difference in target cell fluorescence between the two labels (B). The experiment was performed in duplicate. Scale bars: 10 µm.

However, negative controls were also repeated at this point, and the double-labelled *F. necrophorum* probe produced the same specificity results, whereas the *D. nodosus* probe, started to bind to a number of non-target microorganisms (data not shown), which the single-label probe had not done previously. This phenomenon is thought to occur not because of probe mis-pairing, but because of non-specific interactions with the conjugated (fluorescent) molecule, as previously discussed. The single-labelled *D. nodosus* probe and the double-labelled *F. necrophorum* probe were therefore selected for screening the repeated *in situ* (tissue) controls (with anaerobic incubation).

The first set of secondary punch biopsies were subcutaneously inoculated with *F. necrophorum* (BS-1) and incubated at 37^{o}C for 1 h and 24 h p.i., under anaerobic conditions and were then fixed and processed as described in Section 2.16.2.4. The sections were then screened with the *F. necrophorum* probe (5'- and 3'-Cy3) and EUK1195 probe (5'-FITC) and co-stained with DAPI. All sections were positive for *F. necrophorum* cells, however differences in *F. necrophorum* cell density and morphology were observed between the sections incubated for 1 h and those incubated for 24 h (Figure 4.13.). Despite the 1 h and 24 h p.i. biopsies both being positive for *F. necrophorum*, many more *F. necrophorum* cells were detected within the 24 h p.i. sections, suggesting that the bacteria were not only able to survive, but were able to grow/replicate within this *in situ* setting.

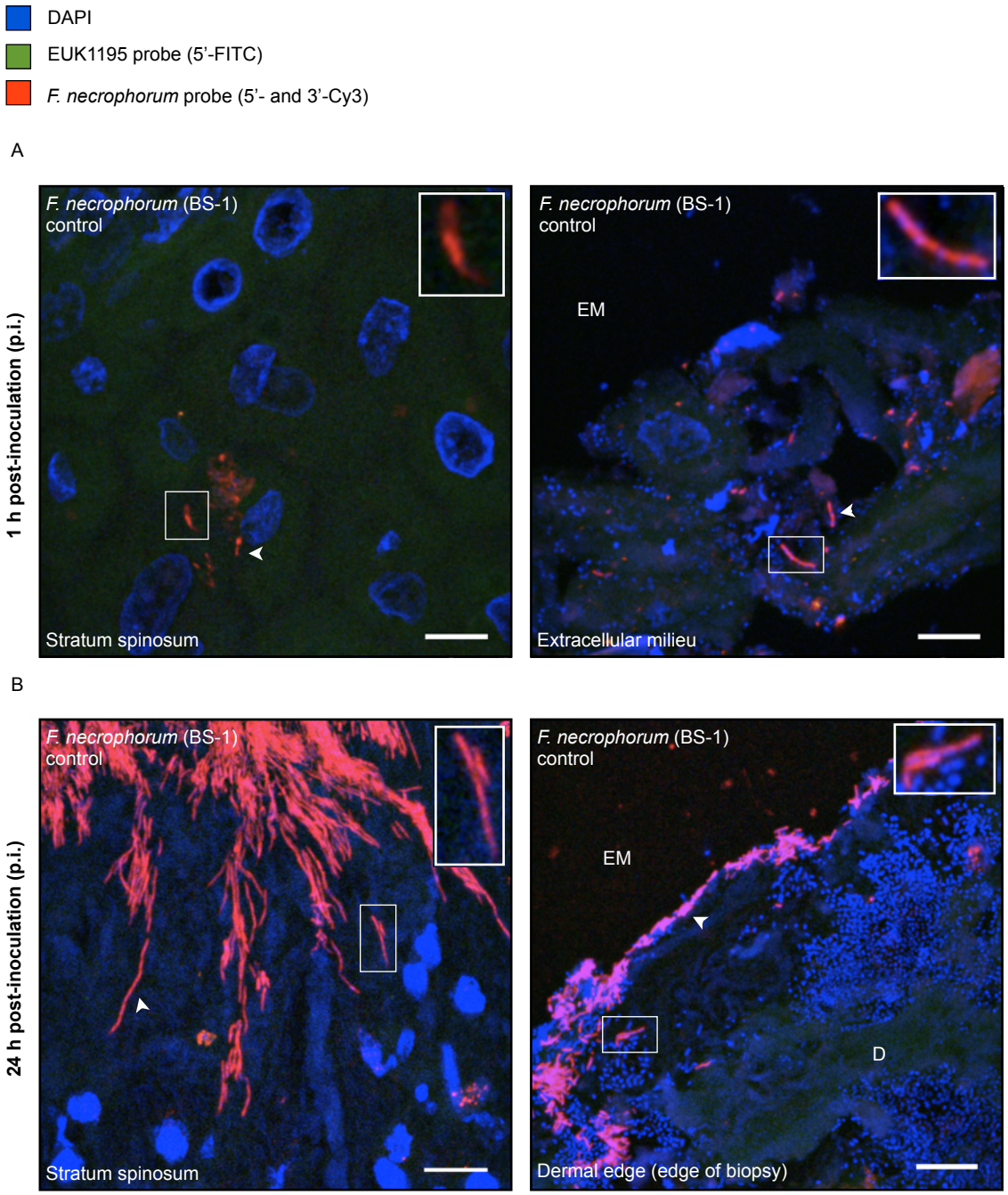

Figure 4.13. *F. necrophorum in situ* (tissue) controls. Healthy ovine interdigital space biopsies were subcutaneously inoculated with *F. necrophorum* (BS-1) cells and incubated under anaerobic conditions at 37°C for 1 h (A) and 24 h (B) prior to fixation and processing (Section 2.16.2.4.). An increase in *F. necrophorum* cell density was observed in the biopsies incubated for 24 h. In addition, *F. necrophorum* filaments were seen invading into tissue with a directionality not observed in the biopsies that were incubated for 1 h only. Epithelial cell nuclei and other bacteria stained with DAPI (blue). Scale bars: 10 µm.

Additionally, the *F. necrophorum* population within some of the 24 h sections (p.i.) appeared to become filamentous, forming unusually long strands. The filamentous forms of *F. necrophorum* were usually found deeper within the epidermis (not only associated with the edges of the biopsy section). Filamentation is described as an unusual increase in cell length, whereby cells continue to grow, but the process of septation ceases. This change in morphology is quite common amongst bacteria and is reported to occur for a number of reasons; as a response to invasion, stress response, intracellular growth or during stationary phase (Humphrey, et al., 2011). *F. necrophorum* (BS-1) cells were then examined briefly *in vitro* under osmotic shock (growth media supplemented with NaCl), which has been shown to cause filamentation in *Listeria monocytogenes* and *Salmonella enterica* serovar Typhimurium (Jørgensen, et al., 1995; Mattick, et al., 2000). *F. necrophorum* (strain BS-1) cells were exposed NaCl present in their growth medium, as described in Section 2.4.3. The cells were then examined after visible growth was observed (3 - 4 d) using light microscopy and then fixed in 4 % (w/v) PFA and hybridised with the *F. necrophorum*-specific oligonucleotide probe. *F. necrophorum* cells appeared to filament in response to osmotic shock and the difference in $\log_{10}$ mean cell length (μm) between treated and non-treated cells was considered significant ($p < 0.01$) using an unpaired t-test with Welch's correction (Prism, Graphpad). This experiment was repeated in duplicate.

This finding highlights that this bacterium may filament in response to a variety of environmental stimuli, providing the microorganism with a number of survival advantages. This phenotype observed in *F. necrophorum* has been reported for a number of *Fusobacterium* species previously, but in response to antibiotics, specifically

mecillinam (Onoe, et al., 1981) and has not been investigated since. Filamentation is generally used as a survival mechanism and therefore may have implications for antibiotic treatment of *F. necrophorum* infections.

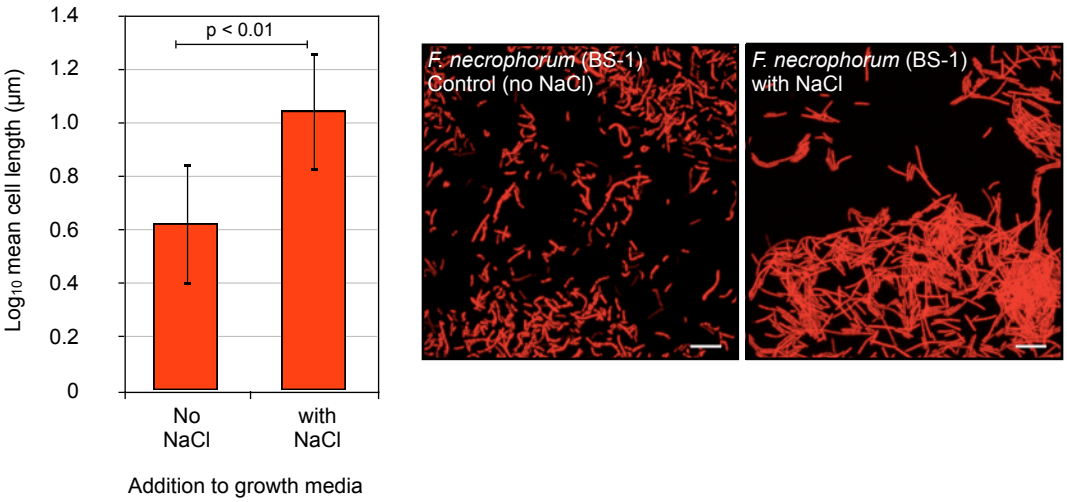

Figure 4.14. *F. necrophorum* filaments in response to high NaCl *in vitro* (osmotic stress). *F. necrophorum* cells appeared to filament in response to NaCl (0.1 M) present in the growth media (as described in Section 2.4.3.), demonstrated by a significant increase in mean $\log_{10}$ cell length (µm) ($p < 0.01$) (Unpaired t-test with Welch's correction, one-tailed, Prism, Graphpad). Experiments were set up in duplicate. A total of fifty *F. necrophorum* cell lengths were measured. Error bars ± SD. Scale bars: 10 µm.

For the *F. necrophorum in situ* (tissue) controls, fluorescent granules (red) that appeared to be associated with epithelial cell nuclei were also observed in the vicinity of the *F. necrophorum* invasion filaments (Figure 4.15.). Images show all planar views: *xy* (centre panels), *xz* (bottom panels) and *yz* (side panels). This type of analysis is one way of using CLSM and the production of z-series to determine the intracellular location of fluorescent objects (Russell, et al., 2008). The granules appear to be associated with the epithelial cell nuclei and from examining all planar views, may in fact be intracellular. The fluorescent granules only appear in close vicinity to the *F. necrophorum* filaments, and were not observed in the *D. nodosus in situ* (tissue) control sections. A number of

studies have reported the production of 'nuclear stress' granules, which appear to be produced in response to stressful conditions, such as viral infection, oxidative stress, etc. (Anderson and Kedersha, 2002; Lindquist, et al., 2010). *F. necrophorum*, along with *F. nucleatum* has been shown to adhere to, invade and replicate within epithelial cells (Gursoy, et al., 2008), however, the intracellular objects do not appear to reflect bacterial cell morphology, but are instead granular, particularly as they appear to autofluoresce in the 'no-probe' tissue controls as well (data not shown). It therefore appears highly likely, that these granules could be auto-fluorescent 'nuclear stress' granules produced by the epithelial cells, in response to the invading *F. necrophorum* filaments or perhaps due to the degraded state of the tissue biopsies (due to removal from the host).

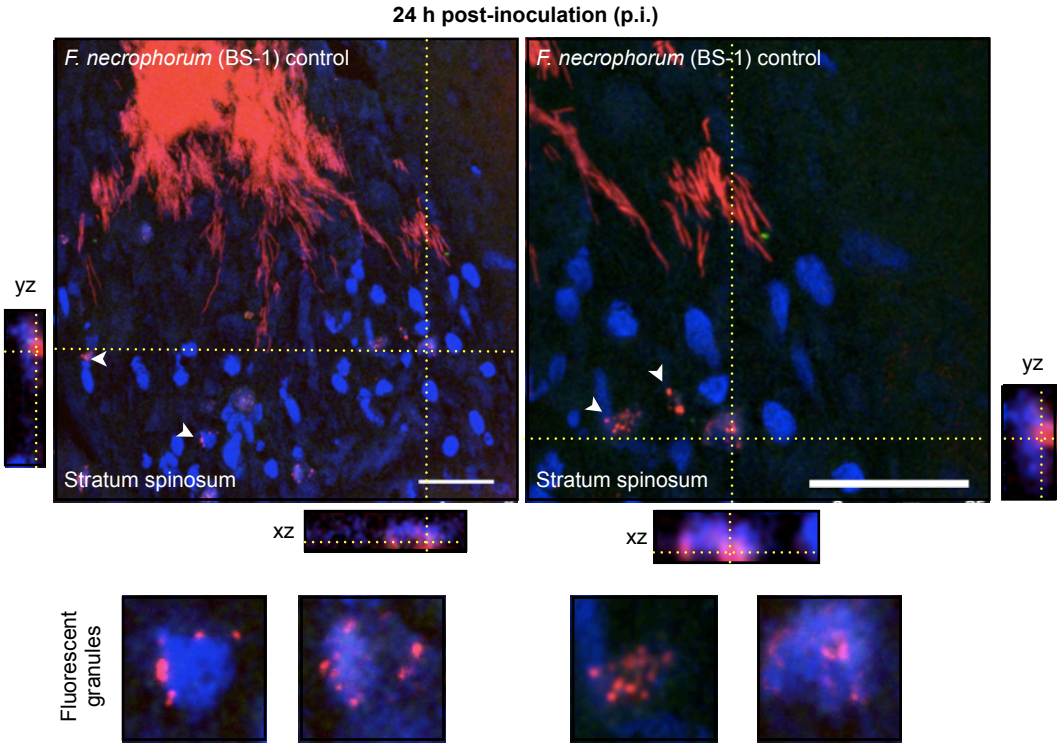

Figure 4.15. *F. necrophorum in situ* (tissue) controls demonstrating the presence of nuclear fluorescent granules. The granules appear to be associated with the epithelial cell nuclei in the vicinity of the *F. necrophorum* invasion filaments. The projections show all planar views: *xy* (centre panels), *xz* (bottom panels) and *yz* (side panels), suggestive of an intracellular localisation. Scale bars: 25µm.

The *D. nodosus in situ* (tissue) controls were also repeated under anaerobic conditions and then screened using the *D. nodosus*-specific probe (5'-Cy3). The biopsies incubated at 37^{o}C for 1 h (p.i.) were negative for *D. nodosus*, however the biopsies incubated for 24 h (p.i.) were positive. A small number of *D. nodosus* cell clusters were detected in the 24 h biopsy sections within the lower epidermal and dermal layers (Figure 4.16.). The difference in the number of cells detected between the *D. nodosus* and *F. necrophorum* tissue controls, correlates with their respective *in vitro* growth, 48 h and 3-4 d, respectively. The *D. nodosus* cells were only detected deeper into the tissue sections examined, however *in vivo* this microorganism reportedly never crosses the epidermal-boundary and localises within the epidermis (Egerton, et al., 1969). This unusual localisation pattern is likely due to the artificial infection process, however the cells appear to be able to survive within the dermal layers *in situ*. Further analysis of non-inoculated biopsy sections would be required to determine the natural localisation patterns of *D. nodosus* and *F. necrophorum*.

Many FISH studies include positive spiked tissue controls, such as those described in Section 4.3.3.2. (Romero, et al., 2005; Boye, et al., 2006; Peters, et al., 2011), however many do not (Hoffman, et al., 2006; Klitgaard, et al., 2008; Trebesius, et al., 2001). The *in situ* (tissue) controls in this chapter, have confirmed that all oligonucleotide probes; the EUB338 (-I, -II, -III) probe set, the *D. nodosus*-specific and the *F. necrophorum*-specific, worked effectively *in situ*. In addition, with the aid of the EUK1195 oligonucleotide probe and DAPI stain, localisation of bacterial populations within the tissue sections was achievable.

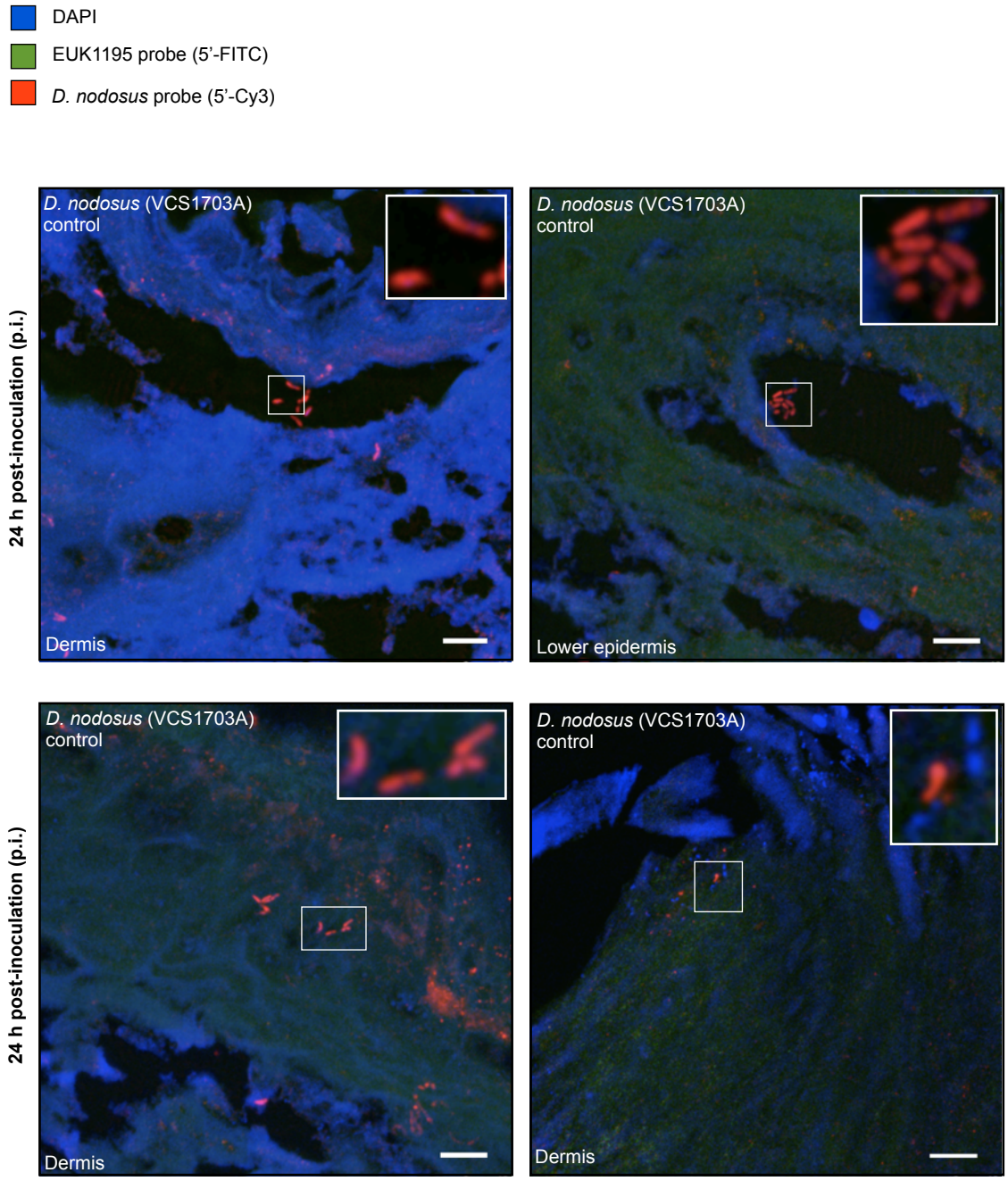

Figure 4.16. *D. nodosus in situ* (tissue) controls. Healthy ovine interdigital space biopsies were subcutaneously inoculated with *D. nodosus* (VCS1703A) cells and incubated under anaerobic conditions at 37°C for 1 h and 24 h prior to fixation and processing. *D. nodosus* cells were only detected in biopsies after 24 h incubation. Small clusters of *D. nodosus* cells were observed in the dermal layers. Tissue and other bacteria stained with DAPI. Scale bars: 10 µm.

4.3.4. Determination of the theoretical detection limit (TDL) of bacterial cells within ovine interdigital space biopsies using FISH.

An estimated TDL would also be useful in determining the lowest concentration of cells within a single biopsy or section, that could be detected. Despite this, many published studies, again, particularly when using tissue biopsies, do not comment on the TDL (Trebesius, et al., 2001; Thimm and Tebbe, 2003; Mallman, et al., 2009). It is particularly difficult to determine a TDL within a tissue biopsy for a number of reasons, firstly it is difficult to achieve an even distribution of the sample throughout the biopsy (in this case approximately 8 mm in diameter) and sections may therefore exhibit an uneven distribution of spiked cells (although this was avoided, by subcutaneously inoculating the spike at multiple sites around the biopsy). Bacteria may also localise preferentially at certain sites, skewing detection. However, an attempt was made to determine a TDL for the detection of *D. nodosus* and *F. necrophorum* cells within circular (8 mm in diameter) ovine foot interdigital space punch biopsies (Figure 4.17.).

The aim of the spiking experiment was to determine when *D. nodosus* and *F. necrophorum* cells could no longer be detected within the biopsies by FISH. The concentrations of the initial *D. nodosus* and *F. necrophorum* cultures were 1.24 x 10^8 *rpoD* and 5.05 x 10^8 *rpoB* copies ml^{-1}, respectively. The cultures were then serially diluted as described in Section 2.16.4.1, to produce 10^{-2}, 10^{-4} and 10^{-6} dilutions. Interdigital space biopsies from healthy sheep were then subcutaneously inoculated with 100 µl of each (including the undiluted culture) at multiple sites, in an attempt to evenly distribute the sample. This resulted in undiluted spikes of 1.24 x 10^7 *rpoD* copies

[absolute] biopsy^{-1} and 5.05 x 10^7 *rpoB* copies [absolute] biopsy^{-1}, as done by Phillips, et al., 2005.

Biopsies were initially incubated for 1 h post-inoculation (p.i.) to enable cells to recover and the biopsies were then fixed. After 1 h, *F. necrophorum* cells were only detected in the biopsy inoculated with undiluted culture (Figure 4.17.). The detection frequency increased however, when biopsies were left for 24 h post-inoculation (p.i.). Despite this, *D. nodosus* cells were only detected in the biopsy inoculated with undiluted culture, whereas the biopsies inoculated with undiluted, 10^{-2} and 10^{-4} dilutions of *F. necrophorum* culture were positive, producing mixed results. A TDL for these assays therefore could not be determined accurately, due to unforeseen difficulties, which will be examined in the Discussion (Section 4.4.).

Although a TDL for FISH-labelled cells in tissue biopsies could not be accurately determined, the FISH procedure itself worked well, as demonstrated by the *in situ* tissue controls (Figure 4.10, Figure 4.13 and Figure 4.16.). In addition, the primary aim of this chapter was to examine the localisation patterns of *D. nodosus* and *F. necrophorum* cells in interdigital space biopsies between different disease states and thus quantification was not a central issue. In conjunction with this, qualitative positive/negative screening could be performed and the determination of absolute bacterial quantities within tissue biopsies was not required, as relative cell counts could be carried out, to highlight the major differences between disease states (H, ID, FR).

A

BIOPSIES 24 H P.I.

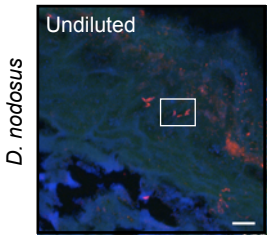

Concentration determined by real-time qPCR (*rpoD*)	Biopsies (1 h p.i.)	Biopsies (24 h p.i.)
Undiluted (1.24 x 10^7 copies [absolute] biopsy^{-1})	negative	**positive**
10^{-2} dilution (~1.24 x 10^5 copies [absolute] biopsy^{-1})	negative	negative
10^{-4} dilution (~1.24 x 10^3 copies [absolute] biopsy^{-1})	negative	negative
10^{-6} dilution (~1.24 x 10^1 copies [absolute] biopsy^{-1})	negative	negative

Punch biopsies produce 130-160 mg biopsies (Calvo-Bado, et al., 2010b).

B

BIOPSIES 24 H P.I.

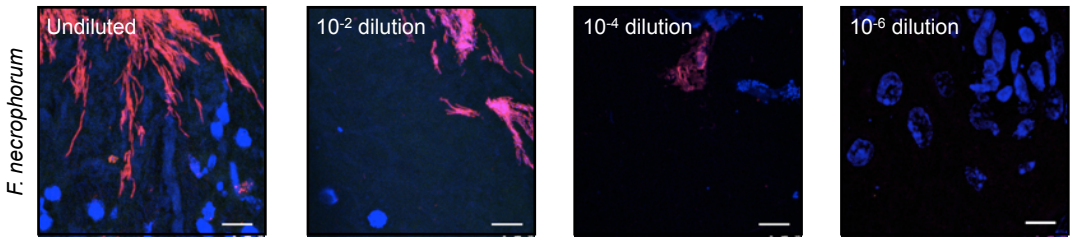

Concentration as determined by real-time qPCR (*rpoB*)	Biopsies (1 h p.i.)	Biopsies (24 h p.i.)
Undiluted (5.05 x 10^7 copies [absolute] biopsy^{-1})	**positive**	**positive**
10^{-2} dilution (~5.05 x 10^5 copies [absolute] biopsy^{-1})	negative	**positive**
10^{-4} dilution (~5.05 x 10^3 copies [absolute] biopsy^{-1})	negative	**positive**
10^{-6} dilution (~5.05 x 10^1 copies [absolute] biopsy^{-1})	negative	negative

Punch biopsies produce 130-160 mg biopsies (Calvo-Bado, et al., 2010b).

Figure 4.17. Determination of TDL for *D. nodosus* and *F. necrophorum* FISH assays. Mixed results were produced for the biopsy spiking experiments. *D. nodosus* (A) and *F. necrophorum* (B) detection limits seemed to vary and were complicated by the 24 h post-inoculation incubation. Scale bars: 10 µm.

4.3.5. Comparison of bacterial counting methods using fluorescent images.

A number of studies have used direct counting of labelled bacterial cells within a sample (Wagner, et al., 1994, Alfreider, et al., 1996; Llobet-Brossa, et al., 1998), which has proved to be successful. However measuring the relative 'bio-volume' of a sample has also been performed (Daims, et al., 2006; Stoecker, et al., 2010), which employs the use of a specific probe (target) and a general population probe (e.g. EUB338) and the relative abundance (%) calculated. For this study however, measuring the relative bio-volume was not suitable, as three dyes/fluorophores were already in use (Cy3, DAPI, FITC) and the fact that *F. necrophorum* was not sufficiently bound by the general bacterial probe set (EUB338-I, -II, -III).

Two counting methods were therefore briefly examined; (i) a manual counting method (Cell Counter plugin) and (ii) an automated counting method, both using the ImageJ software (Abramoff, et al., 2004). The manual counting method (Cell Counter) consisted of highlighting individual bacterial cells with a numbered marker, whereas the automated particle counter employed the use of binary images with an outline detector, which automatically counted the number of objects (given a specific size range) within an image. Both methods proved easy to use and produced similar counts over a range of images tested (data not shown). However, in images with a high number of bacterial cells, or where individual bacteria overlapped or touched, the automated particle counter demonstrated some difficulty in determining cell junctions, despite the additional adjustments made to the threshold or watershed functions. As a result, the automated counter sometimes counted a number of closely localised bacteria as a single bacterium, skewing the counts. The manual particle/cell counting method was therefore chosen

(Figure 4.18.). In summary, the oligonucleotide probes proved effective at detecting the general bacterial population and the *D. nodosus* and *F. necrophorum* communities *in vitro* and *in situ* after some optimisation and were specific for their respective targets. A method for quantifying the number of bacterial cells within individual images was also evaluated.

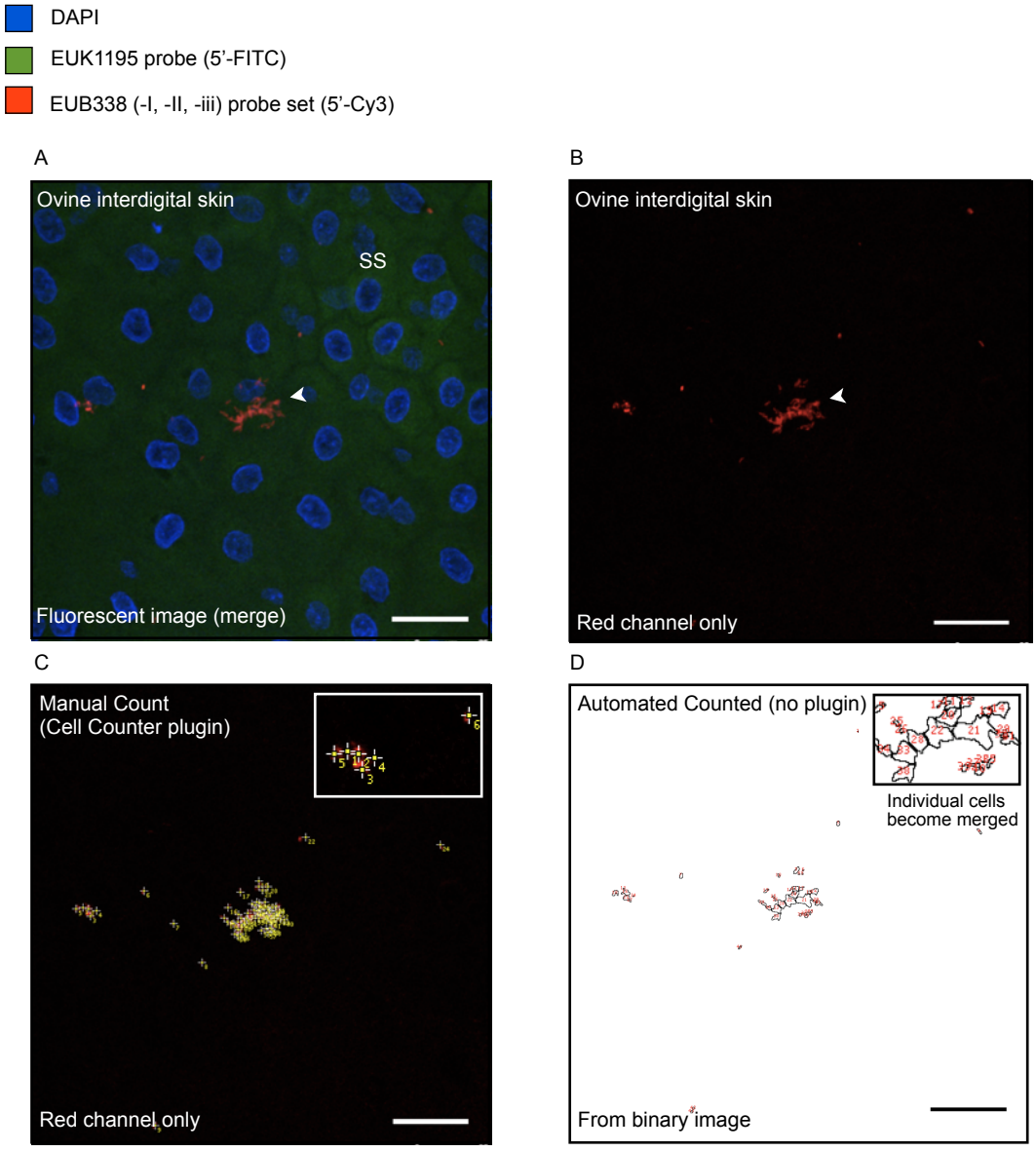

Figure 4.18. Comparison of two particle/cell counting methods for the relative quantification of bacterial cells from fluorescent images. A manual counting method (Cell Counter plugin) compared to an automated counting method (no plugin) using ImageJ. Original fluorescent images (merge) (A) and red-channel only images (B) are shown. The manual counting method (C) proved easier to use when counting overlapping cells or aggregates, when compared to the automated counting method (D). Scale bars: 25 µm.

4.3.6. Interdigital space biopsy screening using FISH.

4.3.6.1. Biopsy collection and ID and FR severity scoring.

Interdigital space biopsies were collected from ovine feet as described in Section 2.5.2.1, from feet presenting with a range of non-experimentally induced disease states. In addition to biopsies, photos, interdigital swabs and severity scores were collected from all four feet of three lambs (Lamb id.: 293, 200 and 358) and three ewes (Ewe id.: 97, 112 and 126). Photos and disease severity scores are shown in Figure 4.19. and Figure 4.20.

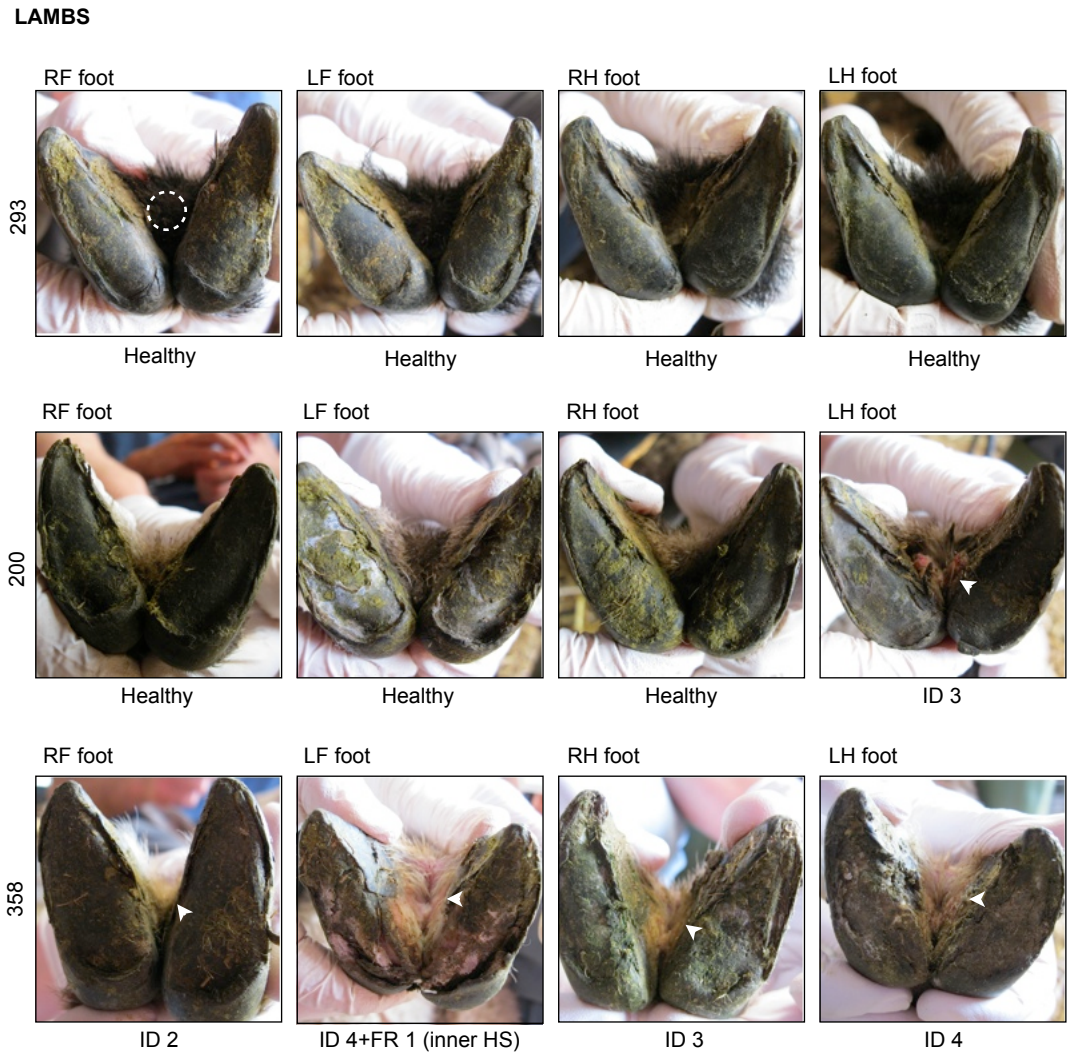

Figure 4.19. Photos for all feet (RF, LF, RH, LH) for Lambs 293, 200 and 358 on day of culling (biopsy collection). Disease severity scores listed underneath each photo and white arrows highlighting regions of ID and/or under-running (FR). Site of interdigital space biopsies indicated with an dashed circle on first image.

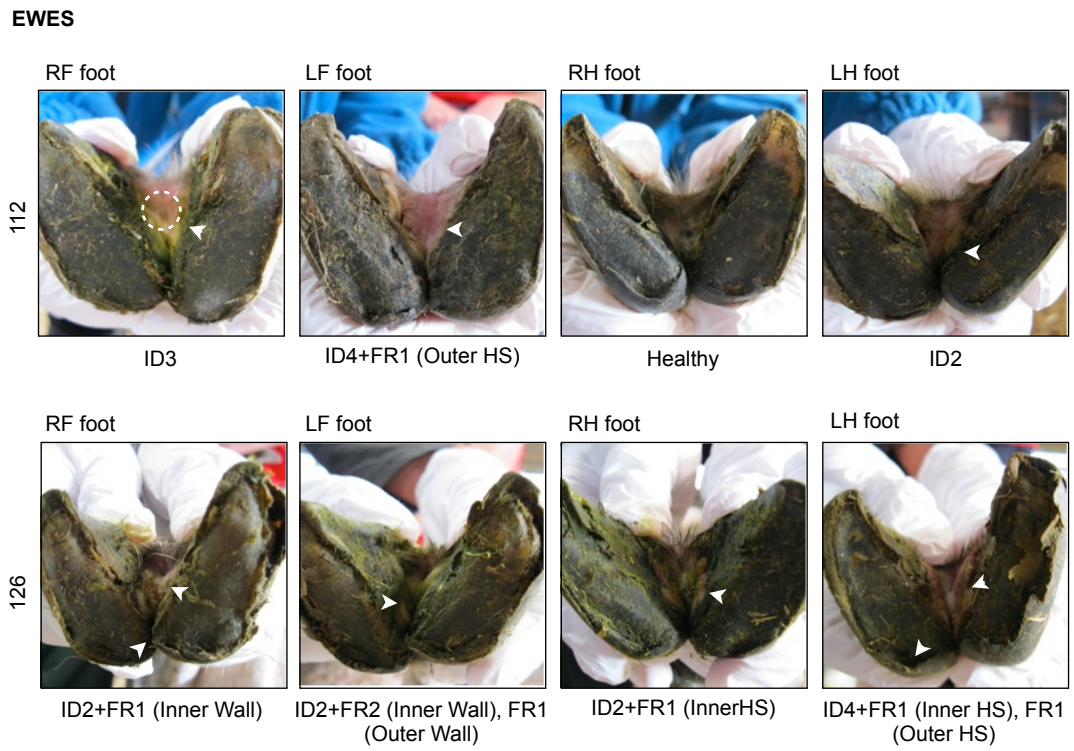

Figure 4.20. Photos for all feet (RF, LF, RH, LH) for Ewes 112 and 126 on day of culling (biopsy collection). Disease severity scores listed underneath each photo and white arrows highlighting regions of ID and/or under-running (FR). No photos were taken for Ewe 97, but all feet were healthy (similar condition to Lamb 293 (Figure 4.19.). Site of interdigital space biopsies indicated with a dashed circle on first image.

Only a single biopsy was taken from each interdigital space due to the small area of the sampling site, as highlighted in Figure 4.19. and Figure 4.20.

4.3.6.2. Overview of the biopsy screening process using FISH.

A total of twenty-four interdigital space biopsies were collected, which were then fixed and processed as described in Section 2.16.5.2. Healthy and diseased tissue biopsies were fixed immediately after collection, in order to avoid negative effects of decomposition on the tissue and bacterial population. Tissue sections were then examined using three separate bacterial probes; the EUB338 (-I, -II, -III) probe set, the *D. nodosus* probe and the *F. necrophorum* probe, in conjunction with the EUK1195 probe and DAPI stain. For quantification analysis, twelve images were taken from each

section (per FISH screen), four of the epidermis, four of the epidermal-dermal boundary and four of the dermis (Figure 4.21.); images for quantification were taken at random within those layers. A total of 849 images were taken (fifteen images could not be taken due to smaller and/or damaged biopsy sections). This number did not include additional images of interest (such as hair follicles), which were taken where appropriate. Bacterial cells were then counted in each image as described in Section 2.19.2. and transformed data presented as +1 $\log_{10}$ number of target cells per field of view (FOV), which was standardised at 25 μm^2, as suggested by Davenport and Curtis (2004).

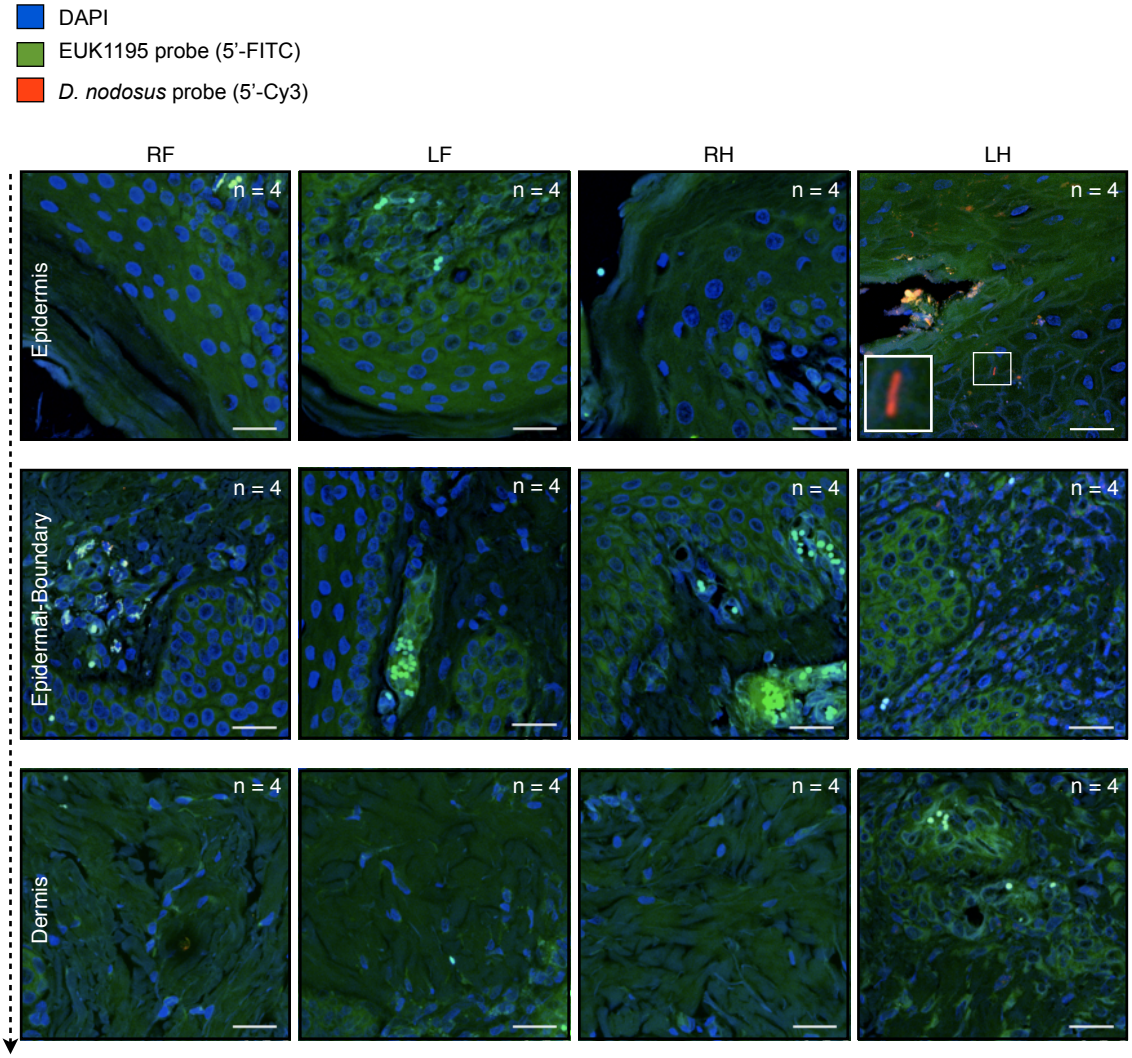

Figure 4.21. Example of FISH screening procedure. The screen above represents the *D. nodosus*-specific FISH screen for Lamb 200 (all four feet; RF, LF, RH, LH). For each foot, twelve images were taken, four of the epidermis (E), four of the epidermal-dermal boundary (EDB) and four of the dermis (D) as indicated (total n = 48 images for each screen). Scale bars: 25 µm.

4.3.6.3. Tissue histology by disease state.

It was observed that the tissue morphology in each section differed considerably, depending on the disease-state of the foot. The outermost epidermal layer (the stratum corneum) was usually absent or only partially intact in biopsies taken from feet presenting with ID only or ID and FR (Figure 4.22.). This suggests that this layer was either (i) removed via sloughing of necrotic tissue, as reported (Egerton, et al., 1969) or (ii) that this layer was instead removed by another means, which disrupted the skin's barrier function and possibly lead to opportunistic infection (or a combination of the two). However, from the data presented here it is unknown whether this process happened pre- or post-infection. All biopsy sections (12/12) collected from healthy feet had an intact stratum corneum (SC), whereas only 16.7 % biopsies taken from feet with ID (1/6) and feet with ID and FR (1/6) had an intact stratum corneum, respectively. All other biopsies sections from diseased feet had either a partial or absent stratum corneum.

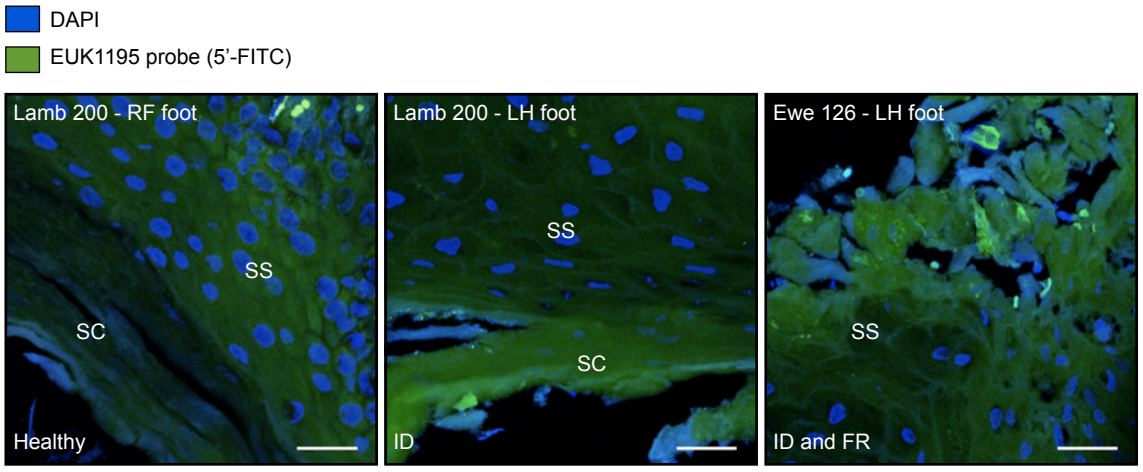

Figure 4.22. Tissue histology by disease state (H, ID and ID and FR). Images represent varying degrees of tissue damage (tissue atrophy); the majority of healthy feet had an intact stratum corneum (SC), whereas this layer was missing or only partially intact for the majority of biopsies from feet with ID and ID and FR. Red channel (Cy3) removed for clarity. Scale bars: 25 μm.

4.3.6.4. Screening of interdigital space biopsies using FISH.

The EUB338 (-I, -II, -III), *F. necrophorum* and *D. nodosus* FISH screens were then carried out for all interdigital space biopsies and a summary of the results is presented in Table 4.5, as percentage of positive biopsies and percentage positive fields of view (FOV) for comparison. *In vitro* (pure culture) positive FISH controls and a 'no-probe' negative tissue control were always carried out in conjunction with the corresponding *in situ* screen.

Table 4.5. Percentage positive interdigital space biopsies and fields of view (FOV) using the EUB338 (-I, -II, -III) probe set, *F. necrophorum*- and *D. nodosus*-specific oligonucleotide probes by foot disease state. Percentage positive biopsies listed first, followed by percentage positive FOVs underneath in bold.

	EUB338 (-I, -II, -III)	***F. necrophorum***	***D. nodosus***
All feet	91.7 % (22/24) **61.0 % (169/277)**	41.7 % (10/24) **9.9 % % (28/284)**	25.0 % (6/24) **5.9 % (17/288)**
Healthy feet	83.3 % (10/12) **63.5 % (87/137)**	8.33 % (1/12) **0.7 % (1/143)**	0 % (0/12) **0 % (0/144)**
Feet with ID	100 % (6/6) **55.1 % (38/69)**	66.7 % (4/6) **17.4 % (12/69)**	50.0 % (3/6) **16.7 % (12/72)**
Feet with ID and FR	100 % (6/6) **62.0 % (44/71)**	83.3 % (5/6) **20.8 % (15/72)**	50.0 % (3/6) **6.9 % (5/72)**

The general bacterial population, labelled with the EUB338 (-I, -II, -III) probe set, was detected on 22/24 of the interdigital biopsies collected; which corresponded to 83.3 % (10/12) of healthy feet and 100.0 % of feet with ID (6/6) and 100 % of feet with ID and FR (6/6). When examining the percentage FOV positive for the domain Bacteria, similar percentages were observed between disease states (H, ID, FR). The EUB338 (-I, -II, -III) probe set acts as a control for false negatives (Moter and Göbel, 2000) and because 100 % of biopsies obtained from feet with ID and feet with ID and FR were positive using this general probe, false negative results due to methodological issues

could be ruled out for the subsequent *F. necrophorum* and *D. nodosus* screens. It should be noted however that biopsies from Ewe 200 LF and RH (healthy feet) were negative for all three screens, including the EUB338 screen, and therefore false negative results due to methodological issues cannot be dismissed. However, the *in vitro* EUB338, *D. nodosus* and *F. necrophorum* FISH controls were positive, suggesting that it was not a problem with the FISH procedure.

D. nodosus cells were significantly more likely to be detected in biopsies from feet with ID ($p < 0.05$) and ID and FR ($p < 0.05$) when compared to healthy feet. When examining FOV, *D. nodosus* cells were again significantly associated with feet with ID ($p < 0.001$) and ID and FR ($p < 0.01$) (although the strength of this associated decreased in FOV from feet with ID and FR) when compared to healthy sheep (Table 4.5.). This is in agreement with the data obtained from the longitudinal study (Chapter 3) and from already published work (Moore, et al., 2005a; Bennett, et al., 2009; Calvo-Bado, et al., 2011b). *F. necrophorum* cells were also significantly more likely to be detected in biopsies from feet with ID ($p < 0.05$) when compared to healthy feet and the strength of this association increased further for feet with ID and FR ($p < 0.01$) when compared to healthy feet. Similarly, *F. necrophorum* cells were significantly associated with FOV obtained from feet with ID ($p < 0.001$) and ID and FR ($p < 0.001$) when compared to healthy feet (Table 4.5.). This is also in agreement with published work (Bennett, et al., 2009). This again highlights a differences in the two communities after FR development, which is consistent with the findings presented in Chapter 3.

D. nodosus was not detected in any of the biopsies taken from healthy ovine feet,

despite a number of feet having had a history of ID and FR. However, a single *F. necrophorum* cell was detected in a healthy foot biopsy (Ewe 112 RH) shown later (Figure 4.27.). Suggesting that *D. nodosus* and *F. necrophorum* could possibly survive within the interdigital space of healthy ovine feet. More healthy foot biopsies (with and without a history of ID and/or FR) would be required for screening in order to determine the frequency at which this occurs. Examples of each screen (EUB338-I, -II, -III, *F. necrophorum* and *D. nodosus*) by foot disease state (H, ID, ID and FR) are shown in Figure 4.23., Figure 4.24. and Figure 4.25.

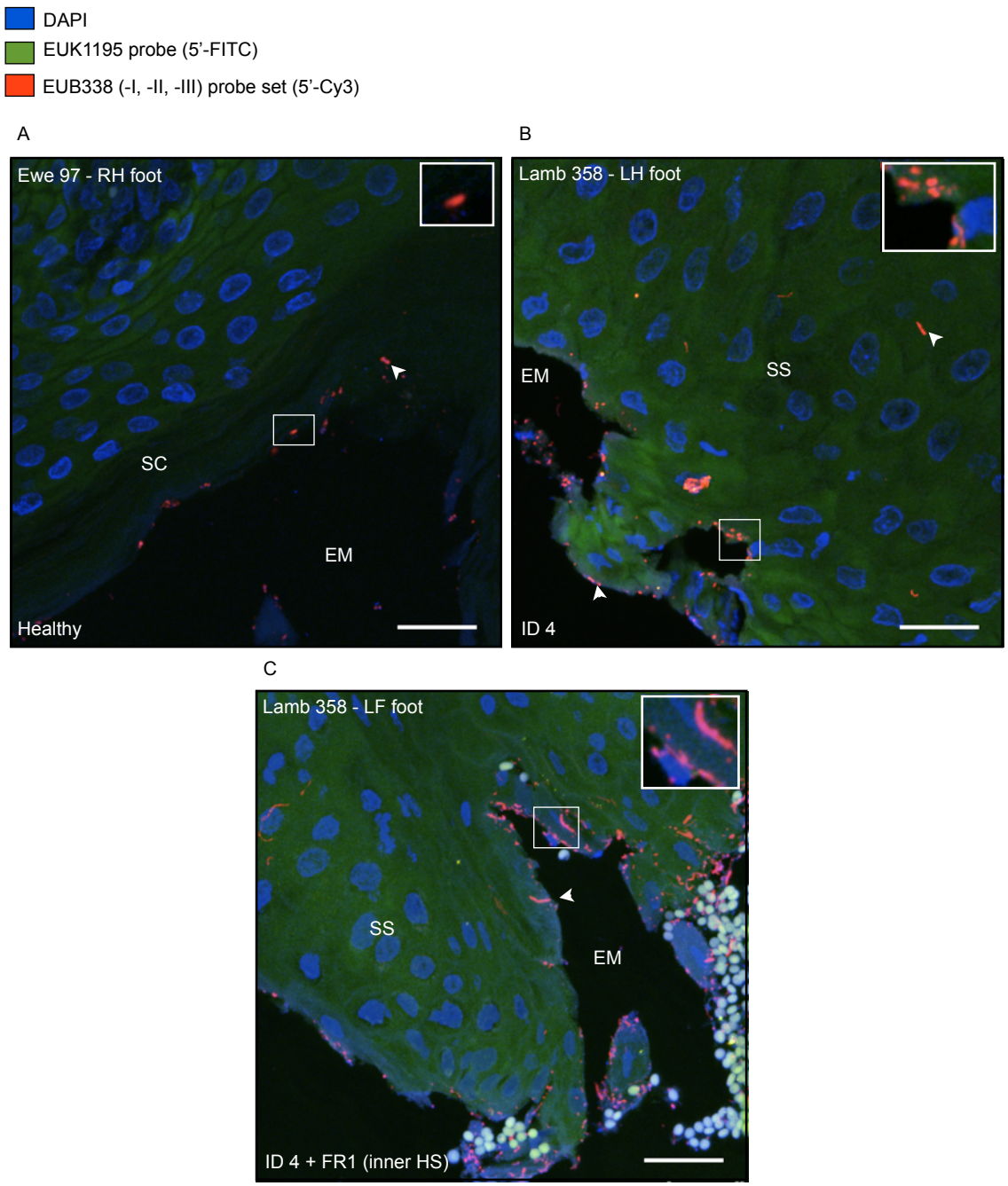

Figure 4.23. Example of EUB338 (-I, -II, -III) screens for sections taken from (A) a healthy foot, (B) a foot with ID only and (C) a foot with both ID and FR. Healthy image taken from Ewe 97 (RH foot); intact stratum corneum (SC), bacterial cells detected, but localisation limited to SC. ID image taken from Lamb 358 (LH foot), which had an ID score of 4; bacterial cells were seen invading into the stratum spinosum (**SS**) and the SC was missing. The ID and FR image was taken from Lamb 358 (LF foot), which had an ID score of 4 and a FR score of 1 (under-running occurred at the inner heel-sole (HS)). Filaments/rods/cocci were seen invading into the stratum spinosum (SS) and the SC was missing. In addition, the presence of white biconcave cells was observed. (Lamb 358). Tissue sections screened with the EUB338 probe set were pre-treated with lysozyme as described in Section 4.3.2.4. Scale bars: 25 µm.

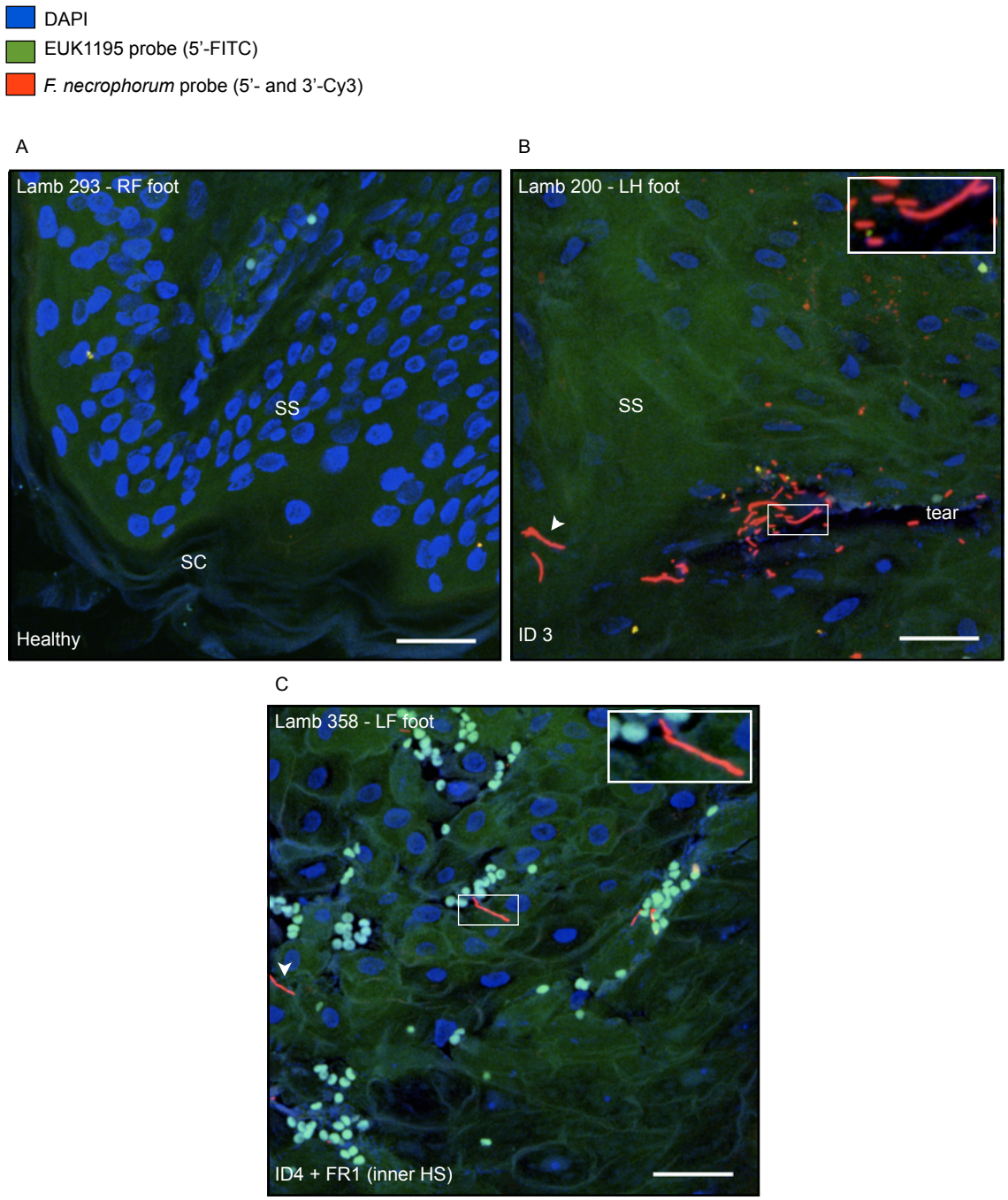

Figure 4.24. Example of *F. necrophorum*-specific screens for sections taken from (A) a healthy foot, (ii) a foot with ID only and (C) a foot with both ID and FR. Healthy image taken from Lamb 293 (RF foot); intact stratum corneum (SC), no *F. necrophorum* cells detected. ID image taken from Lamb 200 (LH foot), which had an ID score of 3; *F. necrophorum* cells were seen invading into the stratum spinosum (SS) within a tear/crevice. ID and FR image taken from Lamb 358 (LF foot), which had an ID score of 4 and a FR score of 1 (under-running occurred at the inner heel-sole (HS)). Filaments/rods were seen invading into the stratum spinosum (**SS**). In addition, the presence of white biconcave cells was observed again. Scale bars: 25 μm.

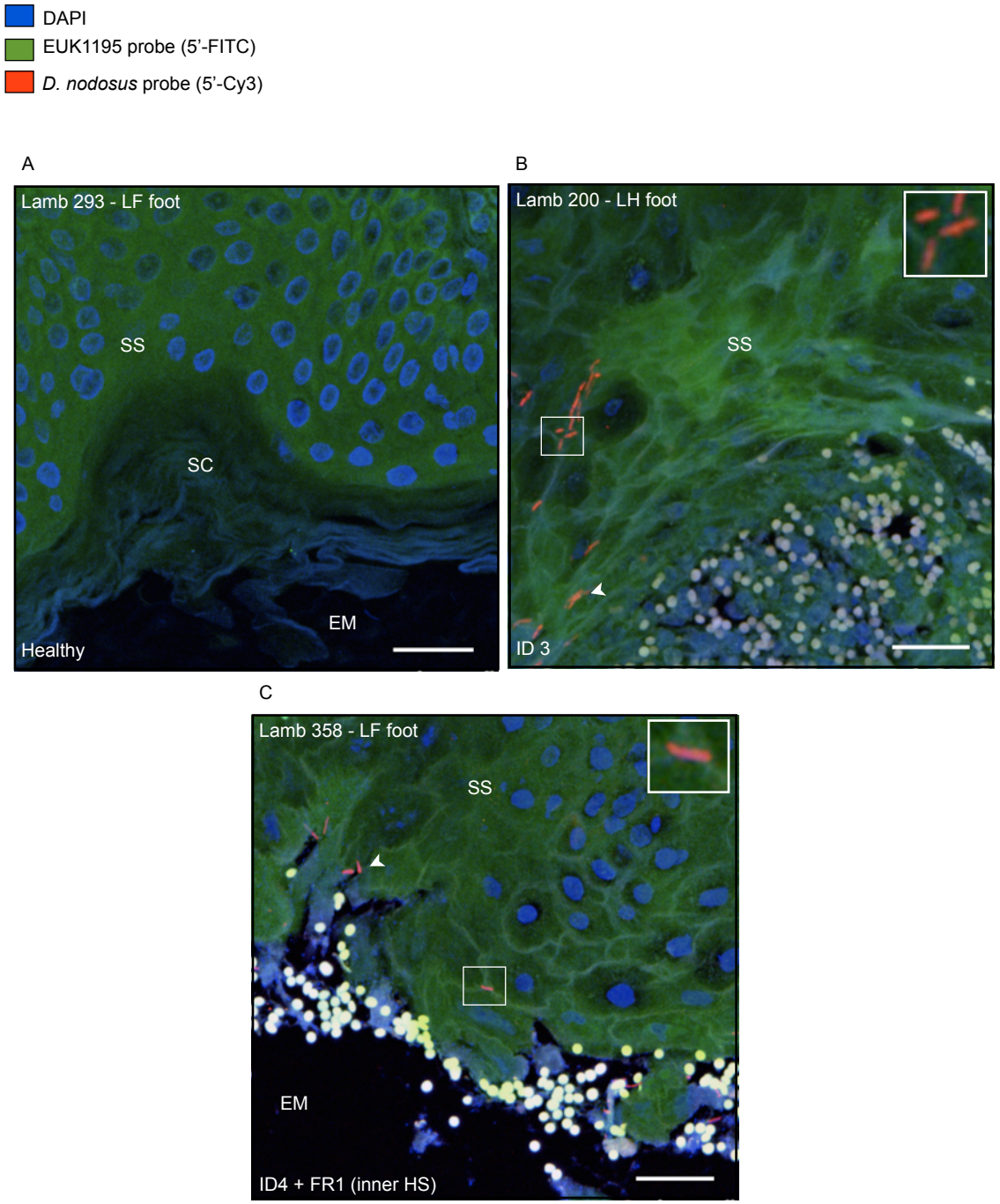

Figure 4.25. Example of *D. nodosus*-specific screens for sections taken from (A) a healthy foot, (B) a foot with ID only and (C) a foot with both ID and FR. Healthy image taken from Lamb 293 (LF foot); intact stratum corneum (SC), no *D. nodosus* cells detected. ID image taken from Lamb 200 (LH foot), which had an ID score of 3; *D. nodosus* cells are seen invading into the stratum spinosum (SS), one after the other. ID and FR image taken from Lamb 358 (LF foot), which had an ID score of 4 and a FR score of 1 (under-running occurred at the inner heel-sole (HS)). *D. nodosus* cells were observed again within the stratum spinosum (SS). In addition, the presence of white biconcave cells was observed again. Scale bars: 25 µm.

4.3.6.5. Bacterial localisation patterns within tissue sections.

The majority of microorganisms detected, irrespective of which screen was used, were located in the epidermal layers; mainly the stratum corneum (SC) and stratum spinosum (SS) (Figure 4.26.). Bacterial cells were less frequently detected at the epidermal-dermal boundary or within the dermal layers. Individual bacterial cells were counted as described in Section 2.19.2, from images representative of the epidermis (E), the epidermal-boundary (EDB) and the dermis (D). Bacterial FISH counts were then +1 $\log_{10}$ transformed and the mean values compared using a one-way ANOVA, with Bonferroni's post-hoc test for multiple pairwise comparisons (Prism, Graphpad). Data were presented as $\log_{10}$ bacterial cell counts per 25 μm^2 image (FOV) (Harmsen, et al., 1999; Apostolou, et al., 2001; Davenport and Curtis, 2004). The one-way ANOVA determined that column means were significantly different ($p < 0.01$) and that there were significantly more EUB338 (-I, -II, -III)-labelled, *D. nodosus* and *F. necrophorum* cells detected within the epidermal layers (E) than in the epidermal-boundary (EDB) ($p < 0.01$) or within the dermis (D) ($p < 0.01$) (Figure 4.26.). But fewer *F. necrophorum* and *D. nodosus* cells were detected overall when compared to the general bacterial population (EUB338-I, -II, -III), even in feet with ID and ID and FR (Figure 4.27.).

The early histo-pathological work (Egerton, et al., 1969; Roberts and Egerton 1969) reported that *D. nodosus* invasion was restricted to the epidermis, whereas *F. necrophorum* cells were seen, on occasion, to enter the dermal layers. In the current study, both *D. nodosus* and *F. necrophorum* were detected within the dermal layers (Figure 4.27.), but only on two occasions. For both screens, only a single cell was detected. The *F. necrophorum* cell was detected within the biopsy collected from the

A

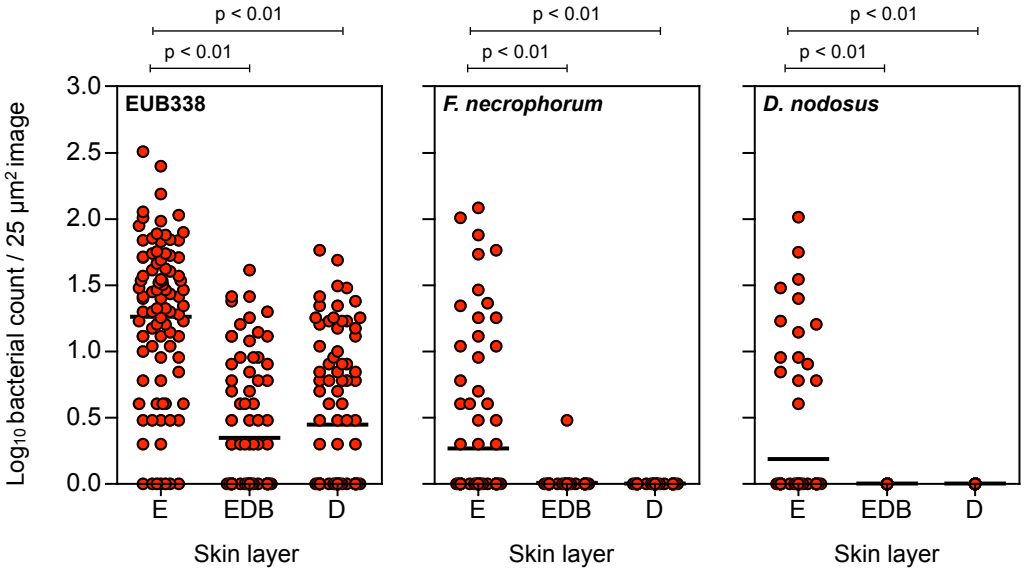

B

	E	EDB	D	E	EDB	D	E	EDB	D
Minimum	0	0	0	0	0	0	0	0	0
25th percentile	0.954	0	0	0	0	0	0	0	0
Mean	1.257	0.347	0.442	0.265	0.005	0	0.183	0	0
75th percentile	1.708	0.699	0.903	0.150	0	0	0	0	0
Maximum	2.508	1.613	1.763	2.083	0.477	0	2.013	0	0
SEM	0.062	0.050	0.056	0.055	0.005	0	0.046	0	0

C

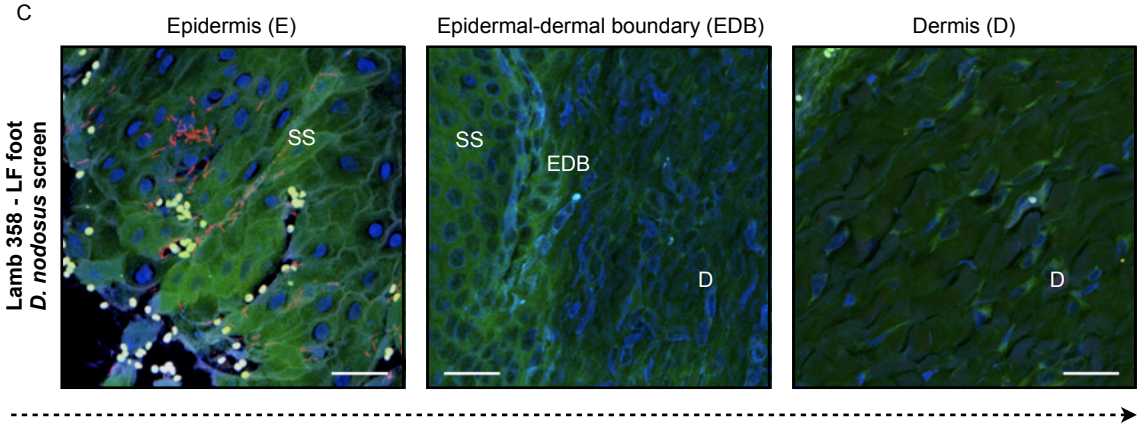

Figure 4.26. Localisation patterns for bacterial populations within ovine interdigital space biopsy sections. The majority of microorganisms were located within the epidermis (E) or on the surface of stratum corneum (SC), fewer cells were seen invading into the epidermal-boundary (EDB) or dermis (D). Data were +1 $\log_{10}$ transformed and mean values analysed using a one-way ANOVA, followed by Bonferroni's post-hoc test. Mean values indicated by bold line (A). Significantly higher bacteria were localised to the epidermal layers (E) than the epidermal-boundary (EDB) ($p < 0.01$) or dermis (D) ($p < 0.01$). Tabulated values (B) and exemplar images (C) of localisation patterns shown (*D. nodosus* screen for Lamb 358 - LF foot). Scale bars: 25 µm.

healthy foot of Ewe 112 (RH), as previously mentioned, whereas the *D. nodosus* cell was detected within the biopsy from a diseased (ID2 +FR1 (inner wall)) foot of Ewe 126 (RF). Providing some evidence that these two pathogens can penetrate the epidermal-boundary and enter the deeper dermal layers, where they may persist and survive.

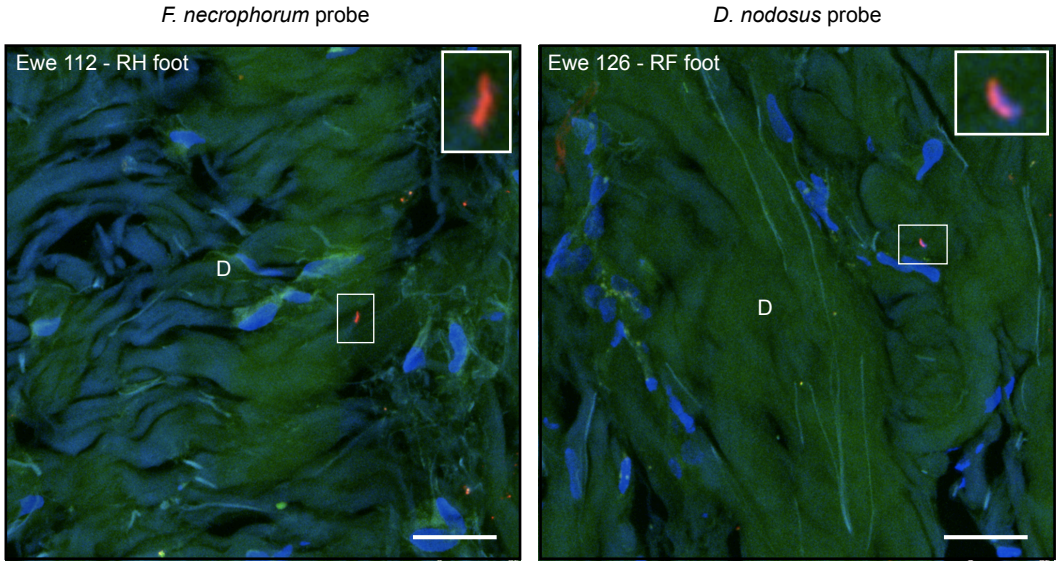

Figure 4.27. *F. necrophorum* and *D. nodosus* observed within the dermis of ovine interdigital skin. The majority of *F. necrophorum* and *D. nodosus* cells were located within the epidermis, however on one occasion a lone *F. necrophorum* cell was detected in the dermis of the healthy foot of Ewe 112 (RH foot) and a single *D. nodosus* cell within the dermis of the RF foot of Ewe 126 (ID2 + FR1 (inner wall)). Scale bars: 25 μm.

4.3.6.6. Bacterial FISH counts in relation to foot disease state.

Bacterial cells counts were also compared between the disease states of feet (H, ID only or ID and FR) for all three FISH screens (Figure 4.28.). The data were again +1 $\log_{10}$ transformed and presented as $\log_{10}$ bacterial cell counts per 25 μm^2 image (FOV) and the mean values for healthy feet, feet with ID and feet with ID and FR were compared using a one-way ANOVA, followed by a Bonferroni's post-hoc test for multiple pairwise comparisons (Prism, Graphpad). The one-way ANOVA determined that

column means differed significantly ($p < 0.01$). The general bacterial population (EUB338-I, -II, -III) exhibited a higher log_{10} mean bacterial count in feet with ID ($p < 0.01$) and those with ID and FR ($p < 0.01$), when compared to healthy feet. But the mean values between feet with ID and ID and FR were not significant ($p > 0.05$). Suggesting that a similar increase in the general bacterial population was observed during both stages of disease.

The log_{10} mean count for *F. necrophorum* cells was significantly higher in feet with ID only, than in healthy feet ($p < 0.05$), and higher still in feet with ID and FR ($p < 0.01$). In conjunction with this, feet presenting with ID and ID and FR were also significantly different ($p < 0.05$) from each other. Suggesting that there was a further increase in *F. necrophorum* cell counts within the epidermal tissue after lesion development. This is consistent with the findings from the longitudinal study (Chapter 3), where *F. necrophorum* (*rpoB*) load increased after the development of FR. Examples of high *F. necrophorum* cell counts observed in biopsies from feet presenting with ID and FR are shown in (Figure 4.29.). Finally, the log_{10} mean count for *D. nodosus* cells was significantly higher in feet presenting with ID only ($p < 0.01$) when compared with healthy feet. Feet presenting with ID and FR were significantly different from feet with ID ($p < 0.05$), but were not considered statistically significant to healthy feet ($p > 0.05$), despite the increase in *D. nodosus* cells. This finding is likely partially because of the small sample size and the fact that *D. nodosus* was not detected in many interdigital space biopsies from feet with FR. However, this finding is consistent with the longitudinal data, where, *D. nodosus* (*rpoD*) load increased in feet presenting with ID (week of disease), providing further support that feet with ID are equally as infectious,

A

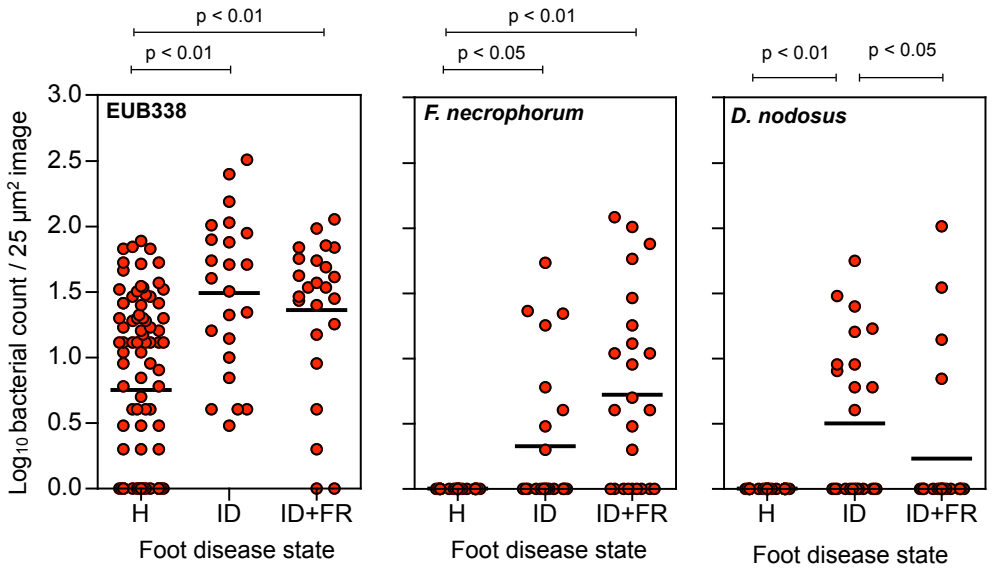

B

	H	ID	ID+FR	H	ID	ID+FR	H	ID	ID+FR
Minimum	0	0.477	0	0	0	0	0	0	0
25th percentile	0	1.000	1.216	0	0	0	0	0	0
Mean	0.747	1.490	1.360	0	0.327	0.720	0	0.501	0.231
75th percentile	1.301	1.949	1.748	0	0.540	1.185	0	0.954	0
Maximum	1.886	2.508	2.053	0	1.732	2.083	0	1.748	2.013
SEM	0.068	0.125	0.119	0	0.112	0.148	0	0.123	0.114

C

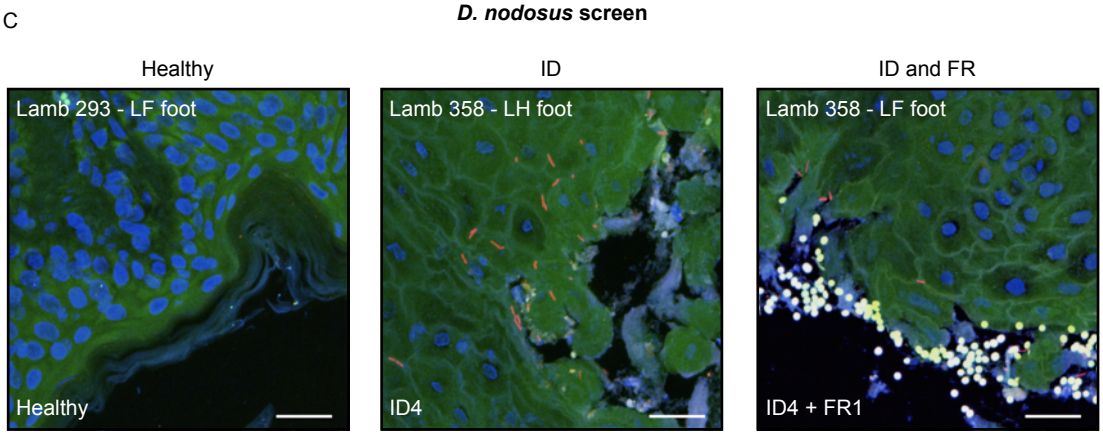

Figure 4.28. Bacterial counts in relation to the disease state of feet (H, ID or ID and FR). The log_{10} mean count for the general bacterial population was significantly higher for feet with ID and ID and FR than healthy feet ($p < 0.01$). The log_{10} mean count for *F. necrophorum* cells in feet with ID was significantly higher than healthy feet ($p < 0.05$) and higher still in feet with ID and FR ($p < 0.01$) (A). The log_{10} mean count for *D. nodosus* cells was significantly higher in feet with ID ($p < 0.01$) than compared to healthy feet or feet with ID and FR ($p < 0.05$) (A). Bacterial counts were +1 log_{10} transformed and column means analysed with a one-way ANOVA, followed by a Bonferonni's post-hoc test for multiple-pairwise comparisons (Prism, Graphpad). Tabulated values (B)and exemplar images (C) are shown. Mean values indicated by bold line. Scale bars: 25 µm.

(assuming *D. nodosus* is shed from the feet) if not more so, than feet with FR.

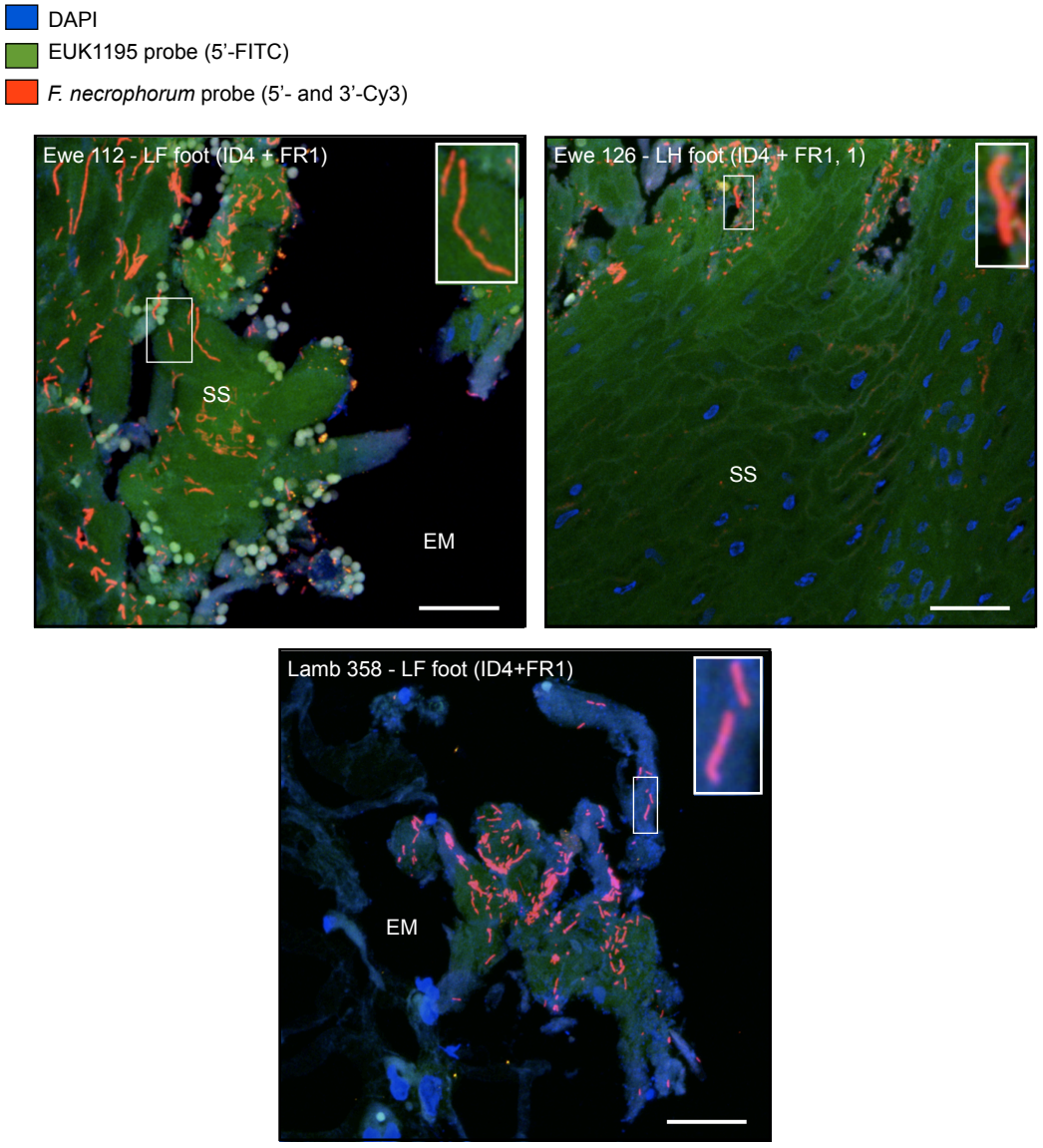

Figure 4.29. Examples of increased *F. necrophorum* cell counts for feet presenting with ID and FR. Increased numbers of filamentous and short *F. necrophorum* rods were observed within biopsies taken from feet with ID and FR. Scale bars: 25 µm.

Large numbers of *D. nodosus* and *F. necrophorum* cells were also detected in flakes of necrotic tissue, as shown in Figure 4.29. for *F. necrophorum*. Suggesting that large quantities of infectious material (containing *D. nodosus* and *F. necrophorum*) may be shed into the environment, during the latter stages of infection, as reported by Beveridge

(1941). Which may have implications for the infectiousness of these individuals.

4.3.6.7. Other observations.

In addition to a significant increase in the general bacterial, *F. necrophorum* and *D. nodosus* populations in diseased tissue (ID and ID and FR), it was also noted that a population of large white (approx. 3-4 μm in diameter) cells appeared in increased numbers in sections from diseased feet that were frequently associated with the *D. nodosus* and *F. necrophorum* populations (Figure 4.30.). The cells appeared white due to emission under all three laser lines (405 nm - blue, 488 nm - green and 561 nm - red). The cells were also similar in appearance to red blood cells (RBCs) in the fluorescent images taken and the corresponding H&E stained sections were then examined under a light microscope. The cells were red/pink in colour and were anucleate, with a characteristic biconcave disc-shape (Canham, 1970) (data not shown). The cell diameter range corresponded to the average reported size of ovine erythrocytes (3.2 μm), which are typically half the size of both human and bovine RBCs (Gaffer, et al., 2003). In addition, RBCs are reported to exhibit strong auto-fluorescence (Young, et al., 1984; Monici, et al., 1995), explaining the emission under all three laser lines.

The RBCs were counted in the same way as the bacterial cells (Section 2.19.2.) and data were +1 $\log_{10}$ transformed and presented as $\log_{10}$ RBC counts per 25 μm^2 image (FOV). Data were then analysed using an unpaired t-test (Prism, Graphpad). A significant difference between the number of RBCs present in diseased (ID only and ID and FR) and healthy tissue sections was observed ($p < 0.05$). Additionally, the RBC count in diseased tissue sections was positively correlated with the number of *F. necrophorum*

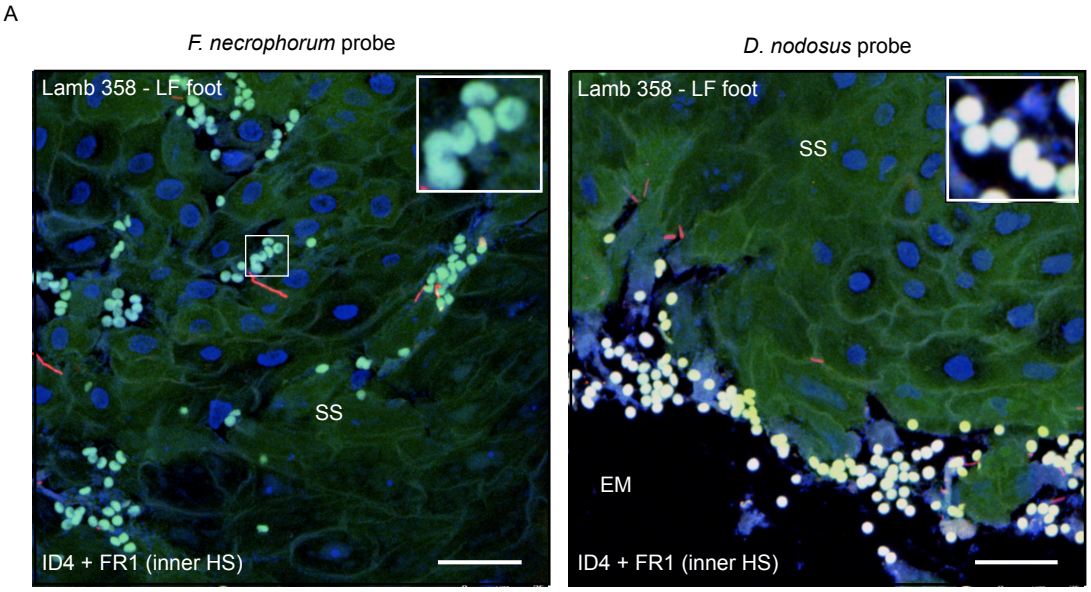

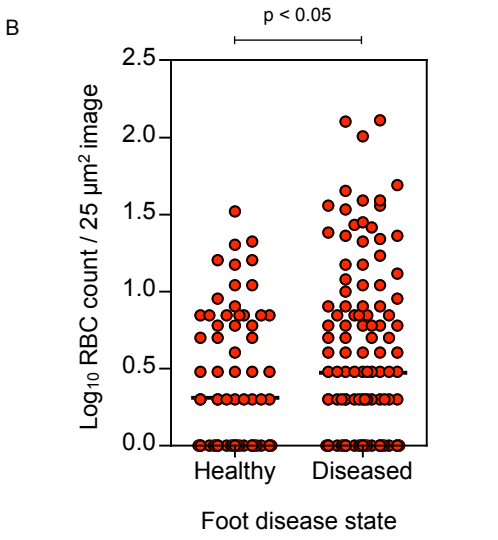

	Healthy	Diseased
Minimum	0	0
25th percentile	0	0
Mean	0.308	0.469
75th percentile	0.699	0.845
Maximum	1.519	2.111
SEM	0.044	0.047

* Values in columns represent $\log_{10}$ RBC count / 25 µm² image.

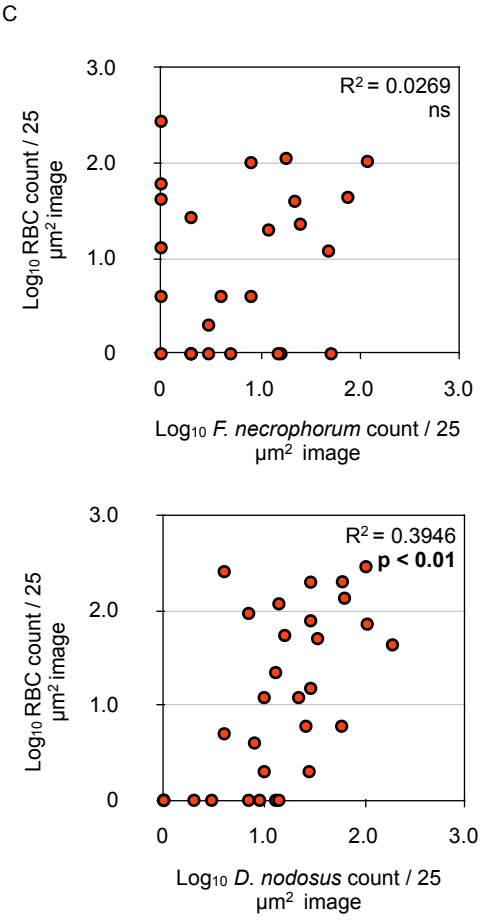

Figure 4.30. Quantification of RBCs in healthy and diseased tissue. (A) Images showing RBC extravasation in diseased tissue. Scale bars: 25 µm. (B) Higher $\log_{10}$ RBC counts in diseased tissue (ID and ID and FR) (unpaired t-test $p < 0.05$) Mean values indicated by bold line with tabulated $\log_{10}$ values. **(**C) Log_{10} RBC counts in relation to either $\log_{10}$ *F. necrophorum* or *D. nodosus* cell counts. Significant positive correlation observed between *D. nodosus* and RBC counts ($R^2 = 0.3946$, $p < 0.01$) (Pearson's correlation).

and *D. nodosus* cells. However, only the correlation with *D. nodosus* cell counts (r = 0.6281) was considered significant ($p < 0.01$) (Pearson's correlation, Prism, Graphpad.), with 39.5 % ($r^2 = 0.3946$) of the variance explained by the two variables (Figure 4.30.).

In addition, images of hair follicles (n = 42) within the interdigital space biopsies were taken, in order to determine if hair follicles may act as an alternative route of bacterial entry, as postulated for the treponemes in bovine digital dermatitis (BDD) (Evans, et al., 2009). Bacterial cells labelled with the EUB338 (-I, -II, -III) probe set were detected within hair follicles, not only within some of the earlier *in situ* controls (Figure 4.10.), but within biopsies collected from healthy and diseased (ID and ID and FR) feet (Figure 4.31.). Despite this, *D. nodosus* and *F. necrophorum* were not detected in any of the hair follicles observed.

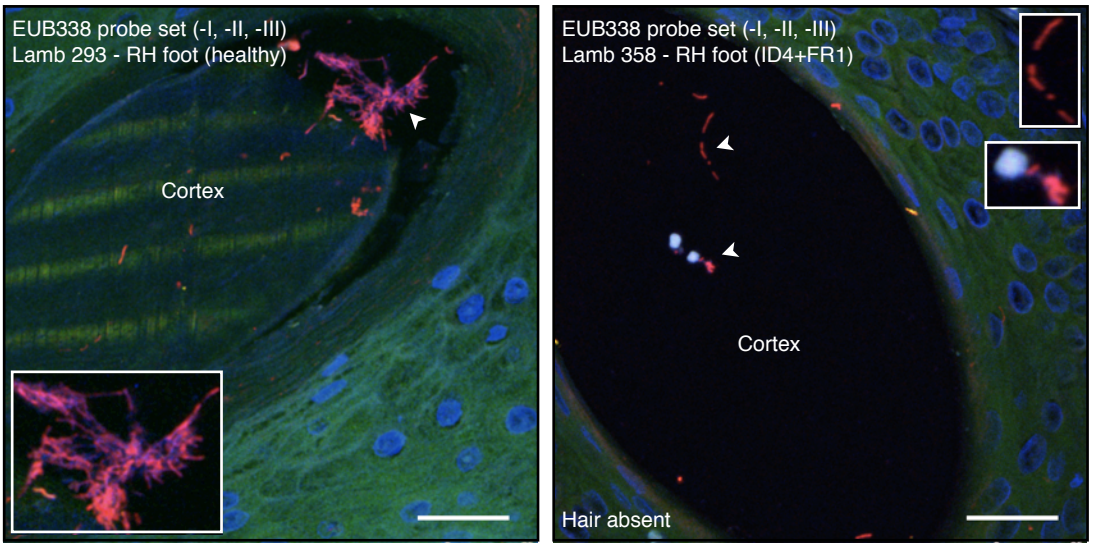

Figure 4.31. Example of EUB338 (-I, -II, -III) labelled bacteria within hair follicles. Bacterial cells are located around the hair cortex, filamentous forms are observed which co-stain with DAPI. Scale bar: 25 µm.

4.3.6.8. Detection and comparison of the surface ('superficial') and 'invasive' *D. nodosus* and *F. necrophorum* populations.

In addition to the interdigital space biopsies, interdigital cotton swabs were also collected from the same feet, before the collection of the biopsies. DNA was extracted from the cotton swabs and analysed using the *F. necrophorum* (*rpoB*) and *D. nodosus* (*rpoD*) quantitative TaqMan® assays as done previously (Chapter 3). The data were then presented as number of *rpoB* or *rpoD* gene copies swab^{-1} (Figure 4.32.). The interdigital space biopsies were considered representative of the 'invasive' bacterial communities present in the ovine interdigital space, whereas the cotton swabs were thought of as representing the superficial bacterial population colonising the interdigital skin or 'surface microflora' (Davies, et al., 2007). The superficial and invasive *D. nodosus* and *F. necrophorum* populations were then qualitatively compared (Table 4.6.).

F. necrophorum and *D. nodosus* were not detected using FISH in biopsies from healthy feet (with one exception), even when belonging to a sheep with other diseased feet, presenting with either ID or ID and FR (Table 4.5.). However, these healthy feet were on occasion positive for 'superficial' *D. nodosus* (*rpoD*) or *F. necrophorum* (*rpoB*), but the bacterial load was usually low (Figure 4.32.); around the TDL of both assays (Chapter 3). The majority of healthy feet also had an intact stratum corneum (barrier) (Figure 4.22.) and therefore these pathogens would be unlikely to penetrate the epidermis. In addition, superficial swabs may have removed any physiologically active *D. nodosus* and *F. necrophorum* cells present from the interdigital skin of healthy feet.

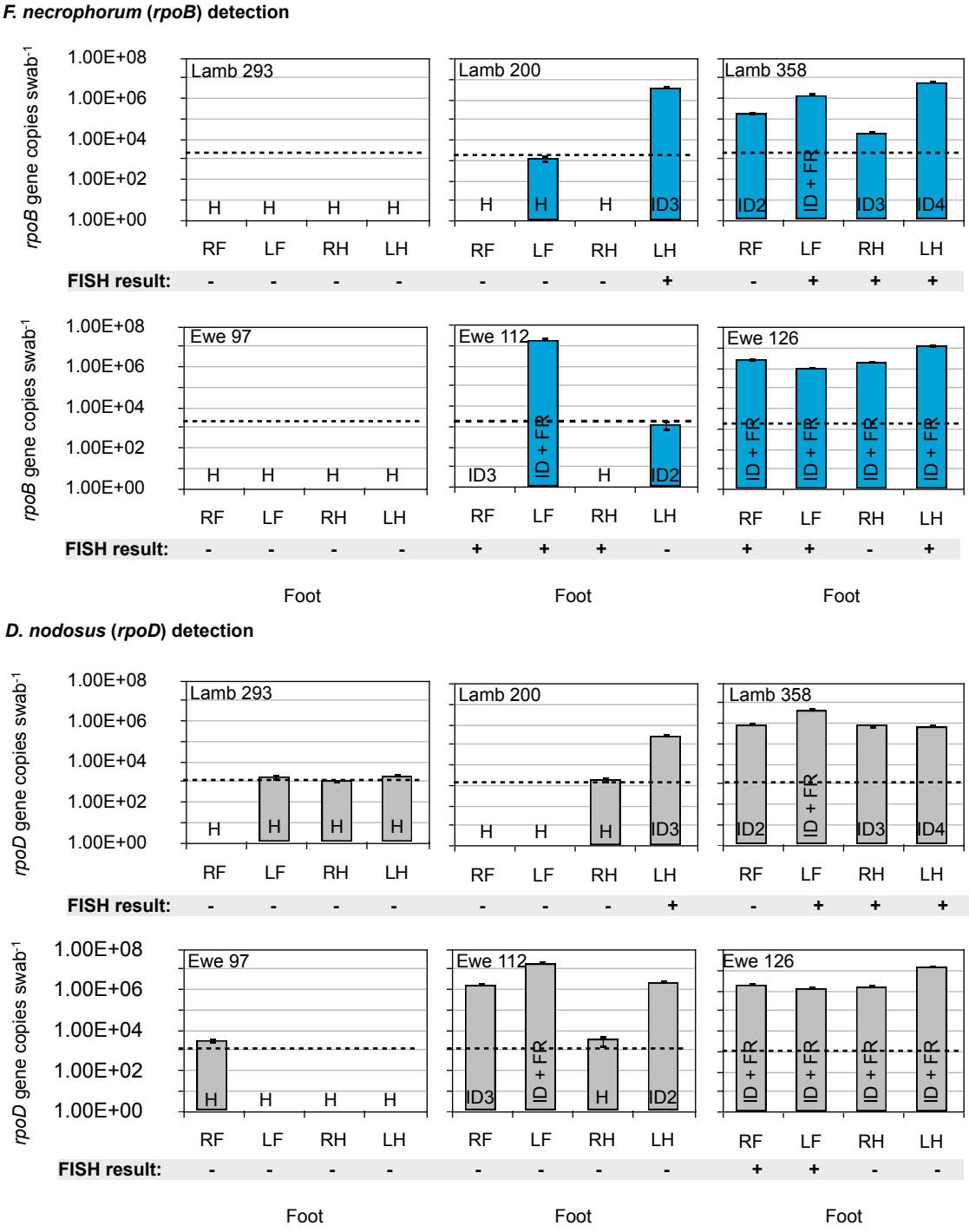

Figure 4.32. Quantification of surface *F. necrophorum* (*rpoB*) and *D. nodosus* (*rpoD*) load from ovine foot swabs collected prior to biopsy sampling. Both *F. necrophorum* (*rpoB*) and *D. nodosus* (*rpoD*) were both detected on the cotton swabs collected from the ovine interdigital spaces (prior to biopsy collection). However, *F. necrophorum* (*rpoB*) and *D. nodosus* (*rpoD*) load were both significantly higher in diseased feet (feet with ID and ID and FR) when compared to healthy feet ($p < 0.01$) (Mann Whitney test, two-tailed, Prism, Graphpad). Data presented as mean values of three technical replicates ± SD. TDLs are shown (dashed line). FISH results (positive/negative) shown in grey and qPCR and FISH results compared by disease severity in Table 4.6.

However, severity scores were examined, in order to explain some of the differences observed between swab (qPCR) and biopsy (FISH) results for diseased feet. Feet with low ID severity scores (ID 1-2) (defined as having < 5 % of the interdigital space inflamed (Kaler, et al., 2011)) were more likely to be positive for *F. necrophorum* and *D. nodosus* by swab (superficial) only. In contrast, feet with higher ID severity scores (ID 3-4) (defined as having either 5-25 % (moderate) or > 25 % (severe) of the interdigital space inflamed and usually accompanied by fetid smell (Kaler, et al., 2011)) were instead more likely to be positive for *F. necrophorum* and *D. nodosus* by both swab (superficial) and biopsy (invasive). This suggests that during mild cases of ID (scores 1-2), *F. necrophorum* and *D. nodosus* are either less likely to have invaded the epidermis or that because < 5 % of the interdigital space is affected by inflammation, the biopsy overlooked the area affected, although this is unlikely as the interdigital space has a small surface area as previously discussed (Figure 4.19 and 4.20.). During more severe stages of ID (scores 3-4) and ID and FR, both *F. necrophorum* and *D. nodosus* were then more likely to have invaded the epidermis (Table 4.6.).

It must be noted, however, that surface *F. necrophorum* (*rpoB*) and *D. nodosus* (*rpoD*) load on feet presenting with ID or ID and FR was significantly higher ($p < 0.01$) than on feet that were healthy (no-ID, no-FR). Bacterial loads (*rpoB* and *rpoD* gene copies $swab^{-1}$) were compared between healthy feet and diseased feet using a Mann Whitney test (non-parametric test), because the data were not normally distributed (D'Agostino & Pearson omnibus normality test). So although invasive cells were less frequently detected in some cases of mild disease, *F. necrophorum* (*rpoB*) and *D. nodosus* (*rpoD*) surface loads were still higher than in healthy feet (Figure 4.32.).

Table 4.6. Detection of *F. necrophorum* and *D. nodosus* by swab (qPCR) and biopsy (FISH) to examine the superficial and invasive populations in relation to disease severity. Feet that were healthy or presented with less severe ID (ID scores 1-2) more likely to be negative by both swab and biopsy or positive by swab only. Feet with higher severity scores (ID scores 3-4) or combined ID and FR scores were instead more likely to be positive by both or biopsy only (these trends are highlighted in blue or grey, respectively).

F. necrophorum

	Healthy	**ID 1-2[a]**	**ID 3-4[b]**	**ID and FR[c]**
Negative by both swab (S) and biopsy (I).	83.3 % (10/12)	0 % (0/0)	0 % (0/0)	0 % (0/0)
Positive by swab (S) only.	8.3 % (1/12)	100 % (2/2)	0 % (0/0)	16.7 % (1/6)
Positive by both swab (S) and biopsy (I) or biopsy (I) only.	8.3 % (1/12)	0 % (0/0)	100 % (4/4)	83.3 % (5/6)

D. nodosus

	Healthy	**ID 1-2[a]**	**ID 3-4[b]**	**ID and FR[c]**
Negative by both swab (S) and biopsy (I).	50.0 % (6/12)	0 % (0/0)	0 % (0/0)	0 % (0/0)
Positive by swab (S) only.	50.0 % (6/12)	100 % (2/2)	25.0 % (1/4)	50.0 % (3/6)
Positive by both swab (S) and biopsy (I) or biopsy (I) only.	0 % (0/0)	0 % (0/0)	75.0 % (3/4)	50.0 % (3/6)

[a]ID scores 1-2 defined as having < 5 % of the interdigital space inflamed.

[b]ID scores 3-4 defined as having either 5-25 % (moderate) or > 25 % (severe) of the interdigital space inflamed and usually accompanied by fetid smell.

[c]ID and FR scores defined as having any combination of ID score with under-running of the hoof horn present.

4.4. Discussion.

In this chapter, a molecular, culture-independent technique (FISH) was used in combination with CLSM for the *in situ* identification, detection, quantification and localisation of *D. nodosus* and *F. necrophorum* in relation to ID and FR presentation. This work represents the first study to use FISH, with the addition of a novel *D.*

nodosus-specific oligonucleotide probe to examine FR in sheep.

The novel *D. nodosus* probe and the *F. necrophorum* probe (Boye, et al., 2006) were both considered specific for their respective targets; neither interacted with the non-target microorganisms tested. In addition, the use of the Cy3-fluorophore produced strong target fluorescent signals (high signal to noise ratio) at the formamide concentrations selected (20 %). Minor adjustments were also made to the permeabilisation step, using lysozyme, to successfully increase target cell detection/ signal intensity for Gram positive bacteria. The EUB338 (-I, -II, -III) probe set did not bind efficiently to *F. necrophorum*, but the probe set has been shown to detect up to 94 % of the domain Bacteria (Amann and Fuchs, 2008) and bound strongly to a number of other bacterial species selected, including *D. nodosus*. Since the start of this work, an additional EUB338 oligonucleotide probe (EUB338-V) has been developed (Vannini, et al., 2010) to further increase the range of bacteria detected. This observation did not effect the study, as a specific *F. necrophorum* probe was used. In addition, a direct counting method was used for the quantification of bacterial cells from 25 μm^2 images. All oligonucleotide probes targeting bacterial species were labelled with either a single or double Cy3 fluorophore. The Cy3 dye is reported to have an increased stability against photobleaching, is very bright and therefore ideal for detecting slow growing species and as very little tissue autofluorescence was observed at this spectral range, the use of Cy3 would avoid any masking of target cell fluorescence (Wessendorf and Brelje, 1992; Moter and Göbel, 2000).

The *in situ* procedure was also confirmed by setting up a number of tissue controls,

whereby undiluted cultures of *F. necrophorum* (BS-1) and *D. nodosus* (VCS1703A) were subcutaneously inoculated into healthy (no-ID, no-FR) interdigital space punch biopsies. This process not only demonstrated that the FISH procedure worked on tissue sections, but revealed that *F. necrophorum* and *D. nodosus* could grow within interdigital space biopsies, as demonstrated by the differences in cell counts between the 1 h and 24 h p.i. samples. Additionally, a number of observations were made regarding the *F. necrophorum in situ* controls. Firstly, that auto-fluorescent nuclear granules were observed in close proximity to the invasive *F. necrophorum* filaments, which were not seen elsewhere within those sections or indeed within the *D. nodosus* control tissue sections. These granules appeared to be intracellular and as such could represent 'nuclear-stress' granules produced by the epithelial cells (Lindquist, et al., 2010), rather than being intracellular *F. necrophorum*, despite reports that *F. necrophorum* attachment to and invasion of epithelial cells can occur (Gursoy, et al., 2008). Intracellular *F. necrophorum* cells were not observed within any of the tissue sections screened. Nuclear stress granules however, have been reported to be produced in response to infection (Lindquist, et al., 2010). The granules detected in this study may have also been produced in response to the tissue degradation.

Secondly, filamentous forms of *F. necrophorum* were seen within some of the interdigital space biopsies and exhibited a directionality not previously observed. This phenotype was also observed briefly in this study under stressful *in vitro* conditions (osmotic shock) and previously in response to antibiotic exposure (mecillinam) (Onoe, et al., 1981). Filamentation can occur naturally (members of actinomycetes) or in response to stressful conditions (Justice, et al., 2004; Humphrey, et al., 2011). This

characteristic can confer a number of advantageous effects, such as protection against grazers (including phagocytes), insensitivity to antibiotics (Justice, et al., 2008) and the ability to evade host immune cells (Justice, et al., 2006). Therefore the filamentation of *F. necrophorum* under stressful *in vitro* conditions (Figure 4.14.) and *in situ* (Figures 4.14, 4.24. and 4.29.) may indicate a survival mechanism and may have implications for antibiotic treatment regimes, however this requires further investigation.

In addition, the *in situ* tissue controls, were an attempt to not only demonstrate that the method worked effectively in tissue samples, but that a TDL could be estimated. Despite this, complications were encountered, when only the undiluted *F. necrophorum* (1 h p.i.) biopsy was positive by FISH. Biopsies were also left for 24 h p.i., which improved *F. necrophorum* (undiluted, 10^{-2} and 10^{-4}) and *D. nodosus* detection (undiluted only). However, a TDL could not be estimated from these results. A number of factors could have contributed to this, firstly, the initial culture concentrations were determined by real-time qPCR analysis, which estimated *rpoD* and *rpoB* copy numbers ml^{-1}, based on DNA content. This may have therefore over-estimated the number of physiologically active intact cells present. In addition, the cells may not have been physiologically active (i.e. low rRNA content), however *D. nodosus* and *F. necrophorum* cells were obtained from plates at 72 h and 48 h, respectively, the same used for the *in vitro* controls, where bright cells were detected. It is therefore more likely that the cells could have been damaged by exposure to oxidative conditions during the inoculation procedure and therefore the cells may have required some time to recover. Additionally, probe penetration was not an issue, as *in vitro* controls demonstrated that the Gram negatives (*D. nodosus* and *F. necrophorum*) were accessible to their specific-probes.

Finally, the inoculum may have been unevenly distributed within the biopsies, although attempts were made to evenly distribute the sample, by using multiple inoculation sites and four sections were screened per spiked biopsy. A TDL may have been estimated by using an aerobic bacterial species with the EUB338 (-I, -II, -III) probe set, to avoid complications of oxidative stress. However, the positive spiked tissue controls worked and a precise TDL was not deemed necessary as direct bacterial cells counts could be compared relatively.

FISH as a method has a number of advantages over other techniques, because it allows for the specific detection, identification and quantification of individual bacterial cells in their natural environment, rather than by using RNA or DNA copy number. However, to date many studies using FISH have remained descriptive, lacking bacterial enumeration and statistical analysis (Bythell, et al., 2002; Boye, et al., 2006; Schmiedel, et al. 2009). Quantification of bacterial populations is intrinsic to the study of microbial ecology and has been shown to be important in understanding mechanisms underlying a number of key biological processes (Davenport and Curtis, 2004; Prosser, et al., 2007). Quantification of the general bacterial population (EUB338-I, -II, -III), *F. necrophorum* and *D. nodosus* communities was therefore considered critical for this study. Images with a standard FOV were taken and randomly selected from the epidermis (E), the epidermal-boundary (EDB) and the dermis (D), producing a total of twelve 25 μm^2 images per tissue section per FISH screen (not including hair follicle images).

Bacterial cells (EUB338-I, -II, -III), along with *D. nodosus* and *F. necrophorum* were more frequently detected within tissue sections from diseased feet (ID or ID and FR), as

previously found with other culture-dependent and culture-independent studies (Moore, et al., 2005a; Bennett, et al., 2009). The majority of microorganisms, irrespective of the oligonucleotide probe used, localised mainly within the epidermis (E), irrespective of disease state and this was significant ($p < 0.01$). However, a surprising number of bacterial cells labelled with the EUB338 (-I, -II, -III) probe set were detected within the epidermal-dermal boundary (EDB) or dermis (D), even from clinically healthy (no-ID, no-FR) feet. However, it cannot be ruled out that these feet did not have another type of bacterial infection on-going or were possibly contaminated. However, if this was due to contamination during the sectioning process, both *D. nodosus* and *F. necrophorum* cells would have been found within the epidermal-boundary (EDB) and dermal (D) layers more frequently and in higher numbers, but they were rarely, if at all, detected within these deeper layers (Figure 4.25.).

Despite the majority of bacteria being localised superficially, on two separate occasions, *F. necrophorum* and and *D. nodosus* were observed within the dermis; the *F. necrophorum* cell within a healthy foot of a sheep with ID and FR and the *D. nodosus* cell within a diseased foot of a sheep with ID and FR. This suggests that occasionally these pathogens may cross the epidermal-boundary (EDB) and enter the dermis (D), where they may persist as a possible reservoir of infection. This did not occur frequently and further investigation may be required. This finding however, does support the view that FR is mainly a superficial disease, whereby the epithelium becomes damaged, allowing opportunistic bacterial invasion. The bacteria elicit an intense inflammatory response, causing sloughing and removal of infected epidermal tissue. The bacteria involved rarely enter the dermal layers. In addition, *D. nodosus* and *F. necrophorum*

were not detected within hair follicles, suggesting that this is not a common route of entry, as discussed for bovine digital dermatitis (BDD) and treponemes (Evans, et al., 2009).

This study found increased cell counts in biopsies from diseased feet (those presenting with ID and ID and FR) in comparison to healthy feet biopsies. For the EUB338 (-I, -II, -III) screens, the mean bacterial count for feet with ID was higher than that for feet with ID and FR, although not significantly higher. The *F. necrophorum* cell counts were elevated in diseased feet when compared to healthy biopsies; those presenting with ID only ($p < 0.05$) and those with ID and FR ($p < 0.01$). The further increase in *F. necrophorum* cell counts in feet presenting with ID and FR is consistent with the earlier findings from the longitudinal study (Chapter 3), where *F. necrophorum* (*rpoB*) load increased after lesion development. In contrast, *D. nodosus* cell counts increased significantly in feet presenting with ID only ($p < 0.01$) when compared to biopsies from healthy (no-ID, no-FR) feet. Very few *D. nodosus* cells were detected in biopsies from feet presenting with ID and FR. This may be because of (i) sloughing of necrotic material, (ii) *D. nodosus* cell migration (perhaps to the coronary band) or (iii) low sample number. However, this still correlates with the findings from the longitudinal study (Chapter 3), where *D. nodosus* (*rpoD*) load increased significantly the week of ID presentation, but did not correlate with FR presentation (week of disease onset). Providing further support for the hypothesis, that feet with ID are infectious and should be treated promptly, in order to reduce further sheep-to-sheep transmission and environmental accumulation. Again correlating with the finding that a high ID prevalence was associated with a stocking density of > 8 ewes/ha (Kaler and Green,

2009). Treatment at this earlier stage also has major implications for improving animal welfare (Wassink, et al., 2010b; Green and Kaler, 2011).

It is known that during acute inflammation, intravascular adhesion and emigration of polymononuclear (PMNs) leukocytes from vessels into surrounding tissues occurs. In addition, haemorrhage or extravasation of RBCs also occurs (Issekutz, et al., 1980). Extravasation of RBCs is particularly common when phagocytosible material (such as microorganisms), initiate the inflammatory response, because PMNs recruited to the site of infection are thought to release proteolytic enzymes that subsequently cause damage to vessel walls, resulting in microvascular haemorrhage. The observation that RBC extravasation occurred in diseased feet and that RBC counts correlated significantly with *D. nodosus* cell counts, may indicate that despite earlier reports (Egerton, et al., 1969), *D. nodosus* may also (in addition to *F. necrophorum*) contribute to the inflammatory response. However, research into the host's immune response to these two pathogens has not yet been performed, but may prove to be invaluable in understanding the disease process.

Finally, the detection of 'superficial' and 'invasive' *F. necrophorum* and *D. nodosus* communities was compared. From these findings, it is now postulated that the superficial and invasive populations also vary at different stages of disease. Firstly, both pathogens were detected using the real-time TaqMan® assays *(rpoB* and *rpoD*) on healthy ovine interdigital skin (superficial) using cotton swabs for the sampling method, usually at a low copy number. It is likely that these feet have encountered environmental *F. necrophorum* and/or *D. nodosus* and the surface of the foot has become contaminated

at a low level. Whereas, a significant increase in *F. necrophorum* (*rpoB*) ($p < 0.01$) and *D. nodosus* (*rpoD*) ($p < 0.01$) load occurred in diseased feet, in comparison to healthy feet.

There was a tendency for feet presenting with severe ID (scores 3-4) to have both invasive and superficial colonisation by *D. nodosus* and *F. necrophorum*, whereas feet presenting with earlier stages of ID (scores 1-2) were unlikely to have invasive communities. In addition, feet presenting with ID and FR were more likely to have invasive and superficial *F. necrophorum*, whereas these same feet tended to have only a superficial colonisation by *D. nodosus* and invasive forms were not detected within the biopsies. The work comparing 'invasive' to 'superficial' bacterial communities is merely descriptive and uses very small numbers of samples, however it may be used to formulate hypotheses for future investigation. For example, the pathogenesis-model put forward by Egerton, et al., (1969), describes a step-by-step process of microbial succession. It is postulated to begin with colonisation with *F. necrophorum*, after damage to the epithelium of interdigital skin, which renders the feet susceptible to subsequent invasion by *D. nodosus*. This then reportedly allows *F. necrophorum* to penetrate deeper layers of the epidermis. It is therefore possible, that by penetrating deeper layers of the epidermis, *F. necrophorum* is shielded to an extent from the sloughing process, although not completely (Figure 4.29.). Whereas *D. nodosus* cells, which are reportedly more superficially localised may be removed after this acute inflammatory response or may migrate deeper into the foot tissue, perhaps as far up as the coronary band (Buller, 2005) (Figure 1.2.). This requires further investigation using whole foot biopsy screening and in addition examining more FOV per section. In

contrast, it may be that *D. nodosus* cells are outcompeted by other microbes at this stage of disease (FR) or that the increased exposure of the epidermis (via the process of sloughing and/or under-running) may increase the levels of oxygen encountered by these cells.

Despite the FISH analysis correlating with aspects of the longitudinal study results (Chapter 3), the FISH work does not provide as clear a pattern of microbial succession, due to the lack of longitudinal sampling. However, interdigital space biopsies could not have been collected over a time series from the same individuals, as the damage inflicted would have allowed opportunistic infection to occur, which would have not only altered the course of disease progression, but would have major implications for animal welfare.

This study represents the first *in situ* analysis of the microbial community associated with FR in sheep. The use of a specific culture-independent method such as FISH combined with the powerful tool of CLSM, has allowed the precise detection, localisation and quantification patterns of *D. nodosus*, *F. necrophorum* and the general bacterial population to be examined, in relation to a range of non-experimentally induced disease states. This work has provided further evidence that feet presenting with ID, not only have an increased *D. nodosus* (*rpoD*) load the week of disease onset, but an increased 'invasive' physiologically active *D. nodosus* population within the deeper layers of the epidermis of the interdigital skin. *F. necrophorum* has again been shown to increase significantly after lesion development, thriving in this altered microenvironment.

CHAPTER 5

5. Environmental distribution of *D. nodosus* and *F. necrophorum*.

5.1. Introduction.

Little is known regarding the environmental distribution of *D. nodosus* and *F. necrophorum*, however, it is thought that *D. nodosus* is unable to persist for long periods of time in the environment and instead uses it as a transitional stage, to transmit between infected and uninfected individuals. *D. nodosus* has been reported to survive, under optimal conditions (warm and damp), for a maximum of 7-10 days on pasture (Whittington, 1995). In addition, FR can occur during the winter in the UK in housed sheep and *D. nodosus* is therefore postulated to be able to survive on bedding; long enough for sheep-to-sheep transmission to occur (Green and George, 2008). To date, no environmental reservoir for *D. nodosus* has been demonstrated.

In contrast, *F. necrophorum* is reported to be ubiquitous in the environment and able to survive in soil (Garcia, et al., 1971; Langworth, 1977). *F. necrophorum* is also a commensal of the alimentary tract (oral cavity, gastrointestinal tract, urogenital tract) of both humans and animals (Hofstad, 2006) and in cases of FR and other 'necrobacilloses', contaminating faecal material is thought to provide the primary source of infection (Roberts and Egerton, 1969; Handeland, et al., 2010). However, the presence of *F. necrophorum* in animal faeces is also reported to be rare, suggesting that this anaerobe is not normally excreted (Smith, et al., 1991; 1993b; Nagaraja, et al., 2005). Additional reports have indicated that diet or perturbation of the normal gut microflora, by the administration of certain types of oral antibiotics may suppress

competing microbes and encourage the intestinal multiplication of *F. necrophorum* and influence the relative frequency of different *Fusobacterium* species (Smith, et al., 1993a; Hofstad, 2006). The frequency of shedding of *F. necrophorum* in ovine faeces has not yet been examined, however, it has been detected from swabs taken from the ovine oral cavity (Bennett, et al., 2009), but the sampling effort, frequency of detection and bacterial load were not reported. *F. necrophorum* has also been detected in the ovine rumen and ruminal material (Edwards, et al., 2005).

The environment acts as either a reservoir of infection, where the microorganism may persist or replicate until a suitable host is found or as a means of transmission via contaminated sources only. It is unknown whether *D. nodosus* and *F. necrophorum* have a specific environmental reservoir or whether they are merely present after a flock becomes colonised and contaminates the surrounding environment.

5.2. Aims.

The aim of this chapter was to examine the distribution and burden of *D. nodosus* and *F. necrophorum* in various environmental samples taken from a farm environment, housing a flock with endemic FR.

The hypotheses were that the environment would become contaminated with *D. nodosus* and *F. necrophorum* to varying degrees, but that faecal material would provide the primary source of *F. necrophorum* and that the ovine foot would instead be the primary reservoir of *D. nodosus*.

5.3. Results.

5.3.1. Study flock (2) and surrounding environment information.

Samples were collected from the farm environment surrounding the second study flock, which was located in Langford, Bristol, UK. The flock were monitored from October 2010 until August 2011. Environmental samples were taken during this period. Sample collection details are listed in Sections 2.5.3., 2.5.4., 2.5.5. and 2.5.6.

5.3.2. Analytical specificity.

The analytical specificity of both assays was previously assessed in Section 3.3.3. of Chapter 3 and were determined to be 100 % specific for their respective targets. However, additional *rpoD* and *rpoB* PCR products amplified from a selection of environmental samples were also cloned using the TOPO TA Cloning® kit and sequenced as described in Section 3.3.3. The sequences obtained revealed the same findings as found in Chapter 3 (data not shown).

5.3.3. Analytical sensitivity.

The *D. nodosus* (*rpoD*) and *F. necrophorum* (*rpoB*) qPCR assays each had a second set of DNA standards, different from those used in Chapter 3; ranging from 7. 89 to 7.89 x 10^6 *rpoD* copies μl^{-1} and 1.44 to 1.44 x 10^7 *rpoB* copies μl^{-1}, respectively. The lowest detected standards for both assays were 7.89 *rpoD* copies μl^{-1} and 14.4 *rpoB* copies μl^{-1}. Calibration standards for the *D. nodosus* (*rpoD*) and *F. necrophorum* (*rpoB*) assays generated R^2 values of ≥ 0.995 and mean slope values of -3.6 (SEM ± 0.04) and -3.5 (SEM ± 0.04), respectively. In addition, the theoretical detection limit (TDL) for each new sample type (faeces, soil and bedding) using the real-time TaqMan® PCR assays

was then established using a series of spiking experiments as detailed in Section 2.9.6.2.

5.3.3.1. Spiking of ovine faeces (estimation of TDL).

Bulk faecal material was collected (Figure 2.1.) and sterilised by autoclaving as described (Section 2.9.6.2.). Sterilised diluted ovine faeces were spiked first with 50 µl of undiluted *D. nodosus* (VCS1703A) culture and 50 µl of each of the six 10-fold dilutions (10^{-1} to 10^{-6}), resulting in approximately 9.06 x 10^{2} to 9.06 x 10^{8} *rpoD* copies g^{-1} faeces. Additional samples of sterilised diluted ovines faeces were then spiked with 50 µl of undiluted *F. necrophorum* (BS-1) culture and 50 µl of each of the six 10-fold dilutions (10^{-1} to 10^{-6}), resulting in approximately 1.90 x 10^{3} to 1.90 x 10^{9} *rpoB* copies g^{-1} [wet wt] faeces. The data are presented as *rpoD* or *rpoB* copies detected g^{-1} faeces and as $\log_{10}$ *rpoD* or *rpoB* copies detected g^{-1} [wet wt] faeces against $\log_{10}$ number of *D. nodosus* or *F. necrophorum* cells added g^{-1} [wet wt] faeces (Figure 5.1.). The lowest detected samples for both the *D. nodosus* and *F. necrophorum* spiking experiments were the 10^{-5} dilutions. Revealing approximate TDLs of 6.18 x 10^{4} *rpoD* copies g^{-1} [wet wt] faeces and 6.09 x 10^{4} *rpoB* copies g^{-1} [wet wt] faeces, respectively. The TDL for faeces was therefore more than 10-fold higher than the detection limit for swab samples (Chapter 3), demonstrating a reduced sensitivity.

5.3.3.2. Spiking of soil (estimation of TDL).

Bulk soil was collected from occupied pasture (Figure 2.1.) and was sterilised by autoclaving as previously described (Section 2.9.6.2.). Tubes containing 0.5 g of sterilised soil were spiked first with 50 µl of undiluted *D. nodosus* (VCS1703A) culture and 50 µl of each of the seven 10-fold dilutions (10^{-1} to 10^{-7}), resulting in approximately

1.01 x 10^2 to 1.01 x 10^9 *rpoD* copies g^{-1} [wet wt] soil. Separate tubes containing 0.5 g of sterilised soil were then spiked with 50 µl of undiluted *F. necrophorum* (BS-1) culture and 50 µl of each of the seven 10-fold dilutions (10^{-1} to 10^{-7}), resulting in approximately 2.21 x 10^0 to 2.21 x 10^7 *rpoB* copies g^{-1} [wet wt] soil. The data are presented as *rpoD* or *rpoB* copies detected g^{-1} [wet wt] soil and as $\log_{10}$ *rpoD* or *rpoB* copies detected g^{-1} [wet wt] soil against $\log_{10}$ number of *D. nodosus* or *F. necrophorum* cells added g^{-1} [wet wt] soil (Figure 5.2.). The lowest detected samples for the *D. nodosus* and *F. necrophorum* spiking experiments were the 10^{-5} and 10^{-4} dilutions, respectively. Revealing approximate TDLs of 3.45 x 10^4 *rpoD* copies g^{-1} [wet wt] soil and 1.09 x 10^4 *rpoB* copies g^{-1} [wet wt] soil, respectively. The variation between the TDLs for the *rpoD* and *rpoB* assays may be partially explained by their respective starting values or intrinsic differences between the two assays. Again the TDL for soil was approximately 10-fold higher than the detection limit for swab samples (Chapter 3), demonstrating a reduced sensitivity.

5.3.3.3. Spiking of bedding (estimation of TDL).

Bedding, which was collected from a housed area (Figure 2.1.) was sterilised by autoclaving as previously described (Section 2.9.6.2.). Tubes containing sterilised bedding (≤ 1.0 g) were spiked first with 1000 µl of undiluted *D. nodosus* (VCS1703A) culture and 1000 µl of each of the seven 10-fold dilutions (10^{-1} to 10^{-7}), resulting in approximately 1.39 x 10^1 to 1.41 x 10^8 *rpoD* copies g^{-1} [wet wt] bedding. Additional sterilised bedding samples were then spiked with 1000 µl of undiluted *F. necrophorum* (BS-1) culture and 1000 µl of each of the seven 10-fold dilutions (10^{-1} to 10^{-7}), resulting in approximately 1.38 x 10^2 to 1.39 x 10^9 *rpoB* copies g^{-1} [wet wt] bedding. The data are

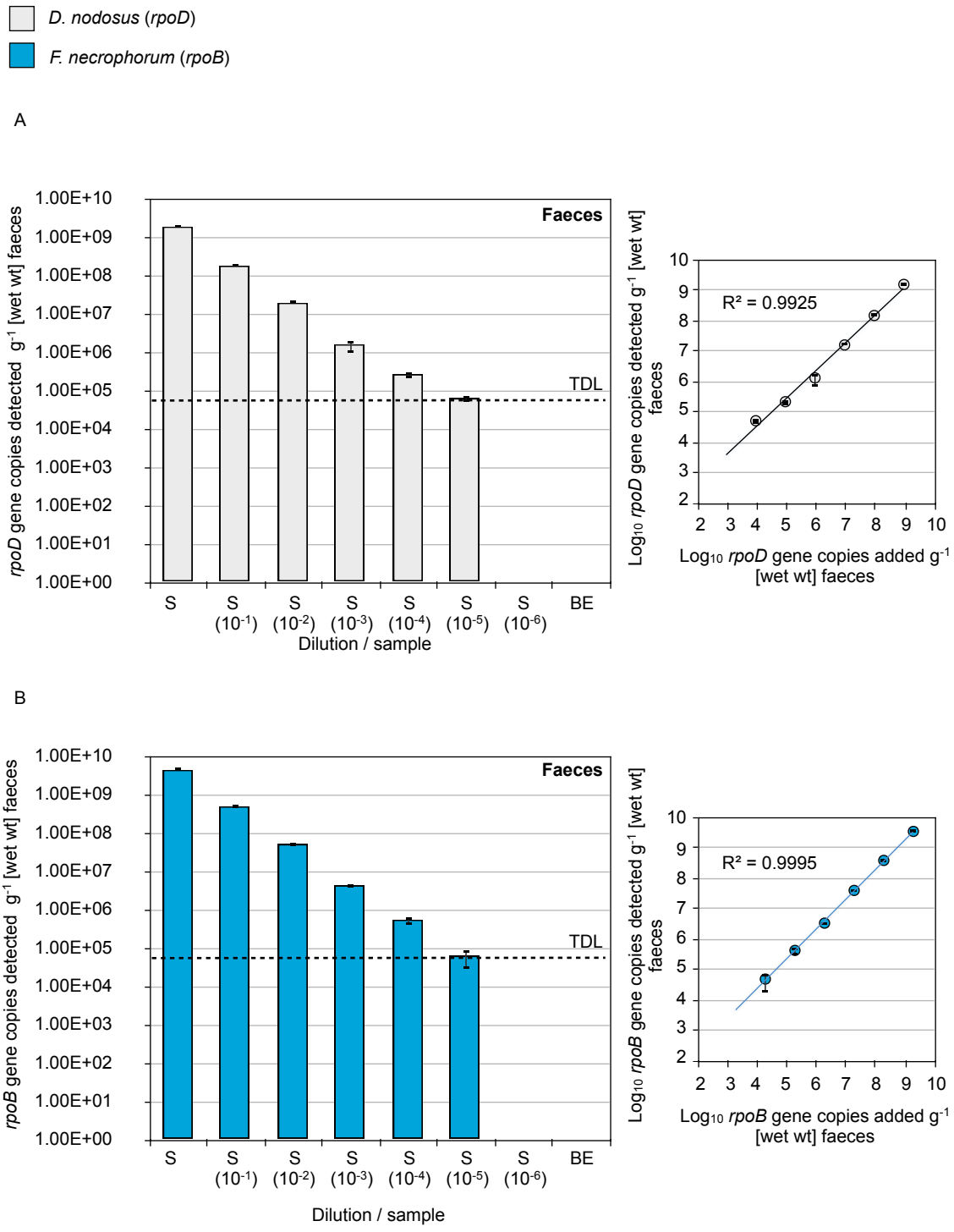

Figure 5.1. Detection of *D. nodsus* (*rpoD*) (A) and *F. necrophorum* (*rpoB*) (B) in faecal samples spiked with undiluted and serially diluted cultures. Spiking experiments were set up as described in Section 2.9.6.2. Data presented as number of *rpoD* and *rpoB* copies detected g^{-1} [wet wt] faeces with approximate TDLs indicated (dashed line). Data also presented as $\log_{10}$ *rpoD* or *rpoB* copies detected g^{-1} [wet wt] faeces against $\log_{10}$ *rpoD* or *rpoB* copies added g^{-1} [wet wt] faeces. Error bars ± SD of three technical replicates. Serial dilutions ranged from (10^{-1} to 10^{-6}) and a blank extraction (BE) (sterilised faeces spiked with sterile water) was included with each set of DNA extractions.

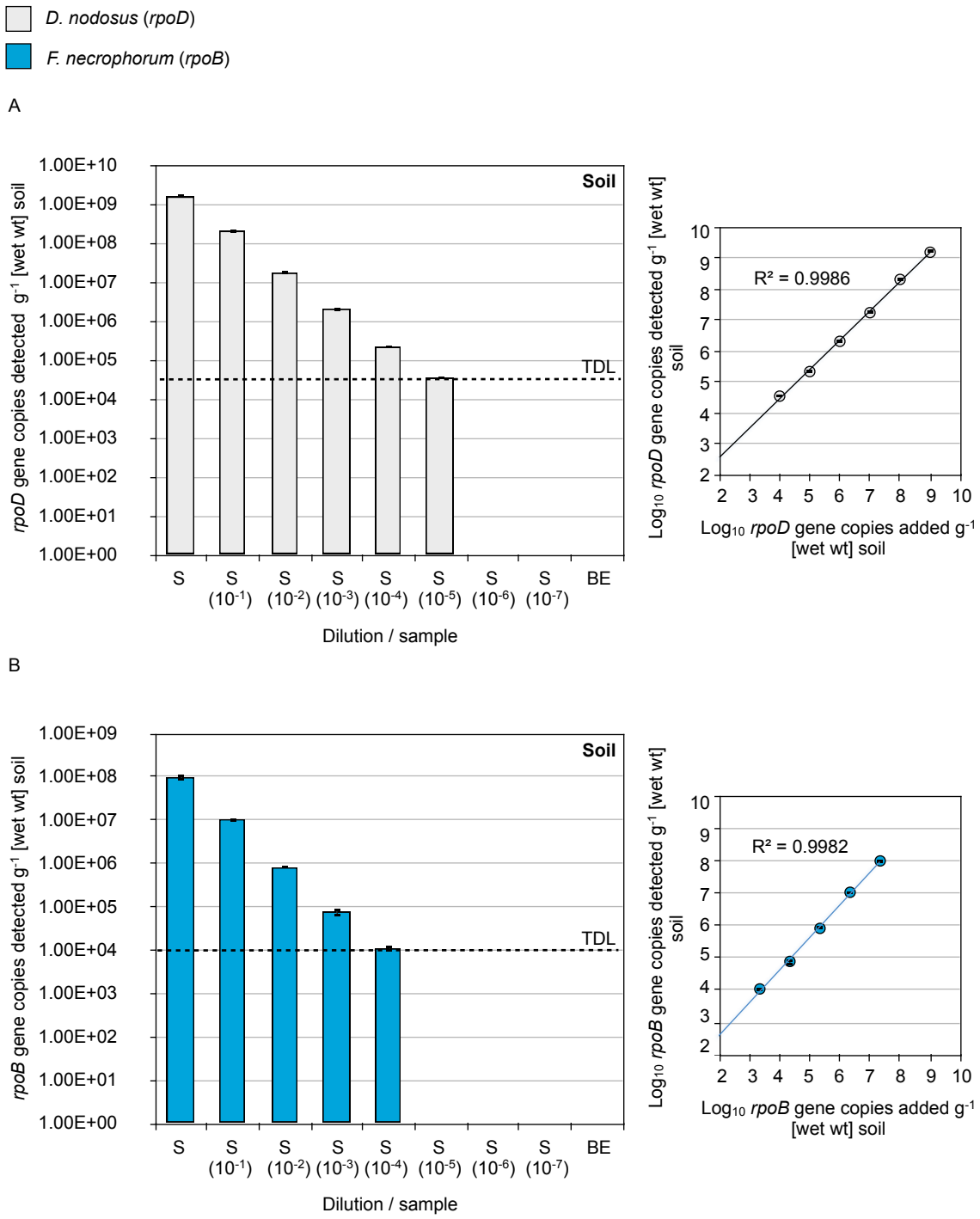

Figure 5.2. Detection of *D. nodsus* (*rpoD*) (A) and *F. necrophorum* (*rpoB*) (B) in soil samples spiked with undiluted and serially diluted cultures. Spiking experiments were set up as described in Section 2.9.6.2. Data presented as number of *rpoD* and *rpoB* copies detected g^{-1} [wet wt] soil with approximate TDLs indicated (dashed line). Data also presented as $\log_{10}$ *rpoD* or *rpoB* copies detected g^{-1} [wet wt] soil against $\log_{10}$ *rpoD* or *rpoB* copies added g^{-1} [wet wt] soil. Error bars ± SD of three technical replicates. Serial dilutions ranged from (10^{-1} to 10^{-7}) and a blank extraction (BE) (sterilised soil spiked with sterile water) was included with each set of DNA extractions.

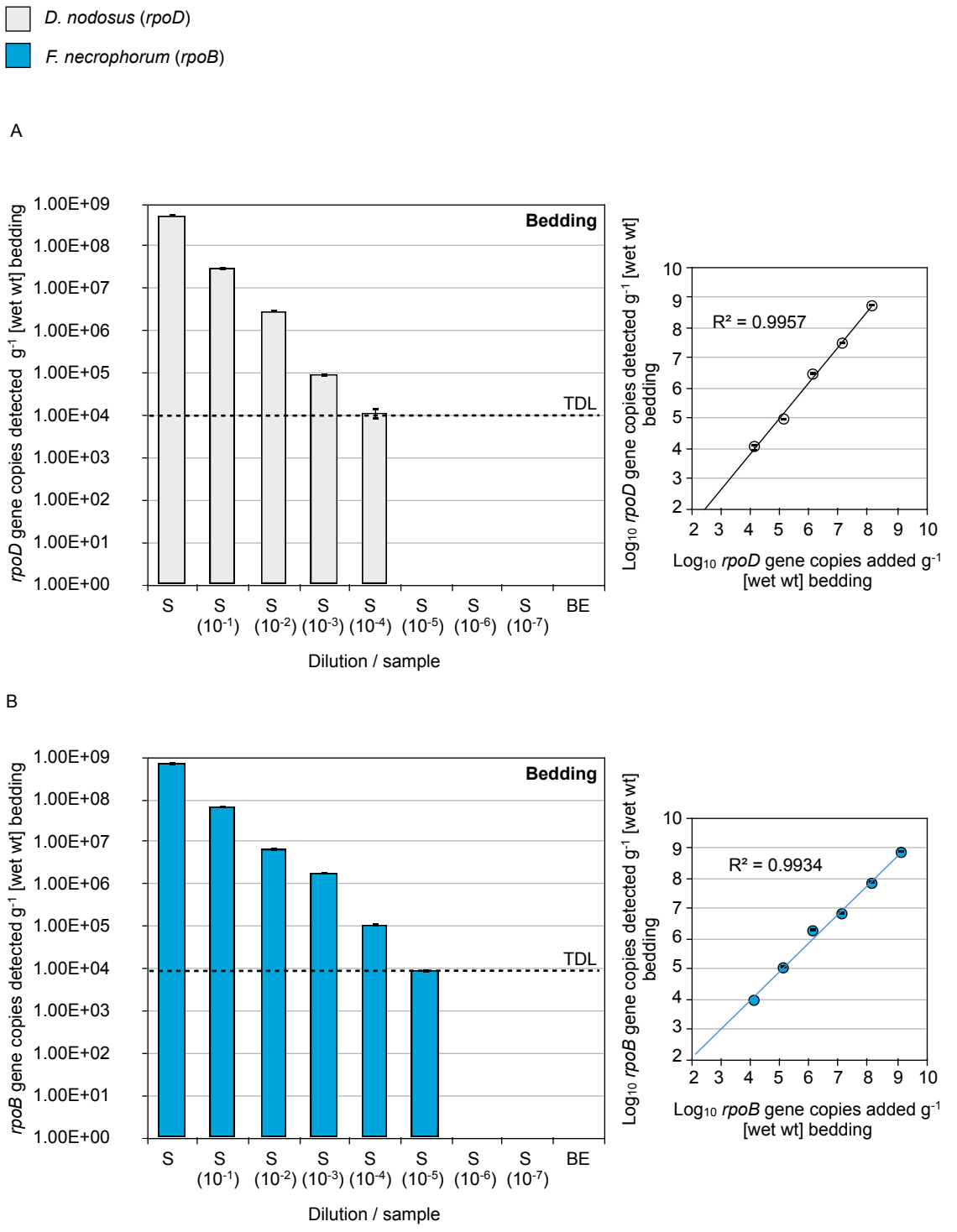

Figure 5.3. Detection of *D. nodsus* (*rpoD*) (A) and *F. necrophorum* (*rpoB*) (B) in bedding samples spiked with undiluted and serially diluted cultures. Spiking experiments were set up as described in Section 2.9.6.2. Data presented as number of *rpoD* and *rpoB* copies detected g^{-1} [wet wt] bedding with approximate TDLs indicated (dashed line). Data also presented as $\log_{10}$ *rpoD* or *rpoB* copies detected g^{-1} [wet wt] bedding against $\log_{10}$ *rpoD* or *rpoB* copies added g^{-1} [wet wt] bedding. Error bars ± SD of three technical replicates. Serial dilutions ranged from (10^{-1} to 10^{-7}) and a blank extraction (BE) (sterilised bedding spiked with sterile water) was included with each set of DNA extractions.

presented as *rpoD* or *rpoB* copies detected g^{-1} bedding and as log_{10} *rpoD* or *rpoB* copies detected g^{-1} bedding against log_{10} number of *D. nodosus* or *F. necrophorum* cells added g^{-1} bedding (Figure 5.3.). The lowest detected samples for the *D. nodosus* and *F. necrophorum* spiking experiments were the 10^{-4} and 10^{-5} dilutions, respectively. Revealing approximate TDLs of 1.15 x 10^4 *rpoD* copies g^{-1} [wet wt] bedding and 9.09 x 10^3 *rpoB* copies g^{-1} [wet wt] bedding, respectively. Demonstrating slightly increased sensitivity when compared to soil or faecal material.

5.3.4. Detection and quantification of *D. nodosus* (*rpoD*) and *F. necrophorum* (*rpoB*).

5.3.4.1 Concrete floor swabs.

Concrete floor (CF) swabs were collected as described in Section 2.5.5. from areas that had been recently occupied by a flock of sheep with endemic FR (Figure 2.1.). DNA was extracted and *D. nodosus* (*rpoD*) and *F. necrophorum* (*rpoB*) loads quantified as performed previously (Chapter 3). *D. nodosus* and *F. necrophorum* were detected on 54.76 % (23/42) and 42.86 % (18/42) of concrete floor (CF) swabs, respectively. Bacterial loads ranged from 10^3 to 10^4 copies $swab^{-1}$ for both the *D. nodosus* (*rpoD*) and *F. necrophorum* (*rpoB*) assays (Figure 5.4.). The load detected from concrete floor (CF) swabs was of a similar range to the load detected on healthy ovine feet (between 10^3-10^4 copies $swab^{-1}$), suggestive of superficial contamination.

Data were not normally distributed (D'Agostino & Pearson omnibus normality test, Prism, Graphpad). However, column medians were compared using a Mann Whitney U test, to determine if there were any differences in *D. nodosus* and *F. necrophorum* loads shed into the environment. No significant differences were found ($p = 0.9496$) between

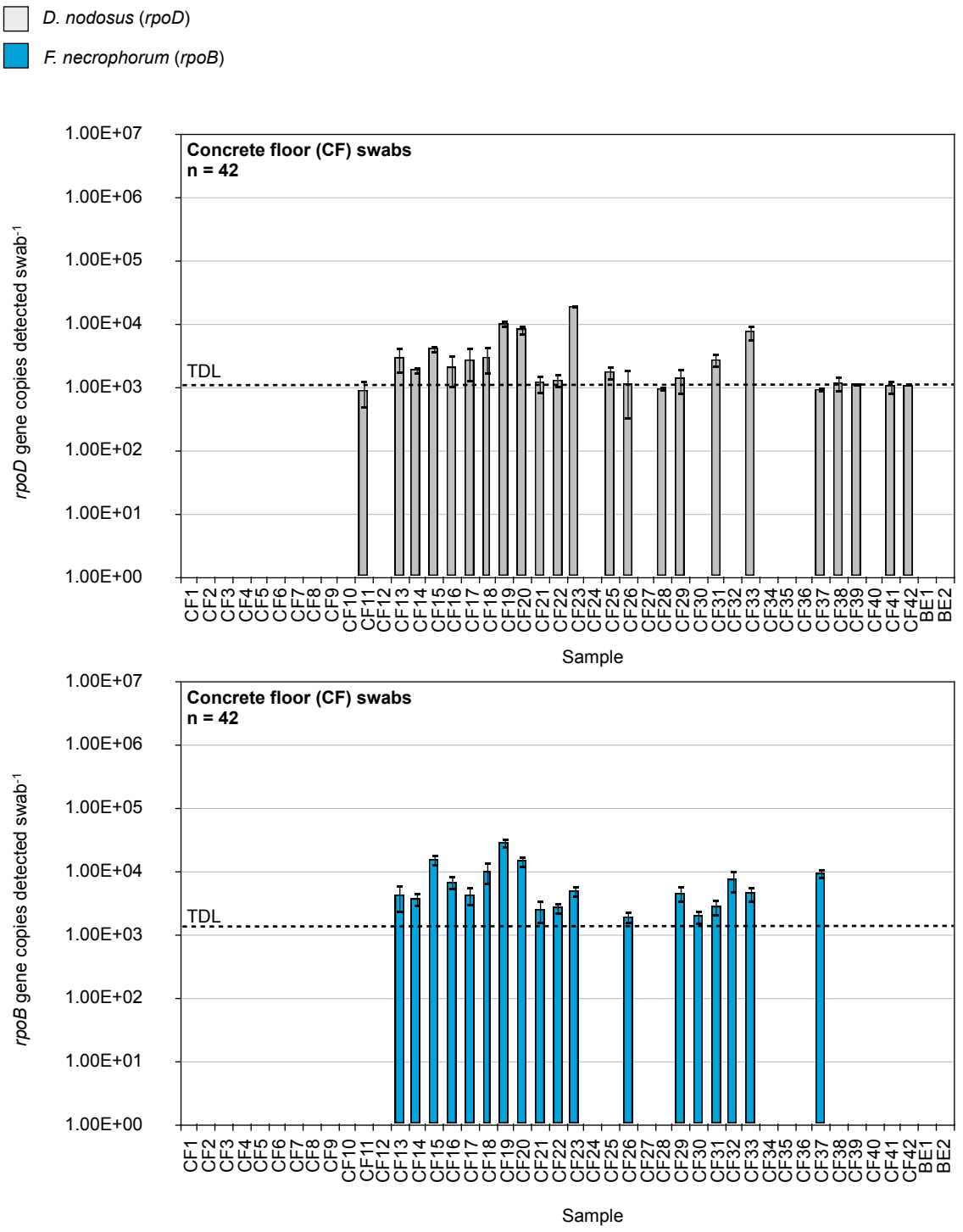

Figure 5.4. Detection and quantification of *D.nodosus* (*rpoD*) and *F. necrophorum* (*rpoB*) load on concrete floor (CF) swabs. Samples collected as described (Section 2.5.5.). A total of 54.76 % (23/42) of samples were positive for *D. nodosus* (*rpoD*) and 42.86 % (18/42) positive for *F. necrophorum* (*rpoB*). Median values for *D. nodosus* and *F. necrophorum* load were not statistically significant ($p > 0.05$) (Mann Whitney U test, Prism, Graphpad). BE swabs were negative for *rpoD* and *rpoB* targets. Error bars ± SD of three technical replicates.

D. nodosus (*rpoD*) and *F. necrophorum* (*rpoB*) load. Blank extraction (BE) swabs were negative for both targets. This demonstrates that both microorganisms were shed into the environment at a similarly low level.

5.3.4.2. Faecal samples.

Ovine faeces were collected as described in Section 2.5.3. from a number of different areas; faeces directly from the sheep (F), faeces from the floor (FF) (Figure 2.1.) and faeces compressed within the interdigital space of the hoof (FH). DNA was then extracted and the *D. nodosus* (*rpoD*) and *F. necrophorum* (*rpoB*) loads quantified. *D. nodosus* and *F. necrophorum* were detected in 24.19 % (15/62) and 9.68 % (6/62) of all faecal samples, respectively. Positive *D. nodosus* (*rpoD*) and *F. necrophorum* (*rpoB*) loads ranged from 10^4 to 10^5 copies g^{-1} [wet wt] faeces (Figure 5.5.). However, neither *F. necrophorum* nor *D. nodosus* were detected in faecal samples obtained directly from the sheep (F), but both were detected in faecal samples collected from the floor (FF) of a housed area. *D. nodosus* (*rpoD*) was detected in 42.86 % of (15/35) samples and *F. necrophorum* (*rpoB*) in 11.43 % (4/35) of samples. In comparison, 28.57 % (2/7) of faeces collected from the interdigital space were positive for *F. necrophorum*.

This suggests that despite previous reports (Roberts and Egerton, 1969), *F. necrophorum* does not appear to be shed in ovine faeces at a detectable level (approximately $\geq 6.00 \times 10^4$ *rpoB* copies g^{-1} [wet wt] faeces) and neither does *D. nodosus*. This demonstrates that faecal material likely becomes contaminated with detectable *F. necrophorum* and *D. nodosus* loads after coming into contact with the environment, acting as a transitory site of infection. This is consistent with reports that

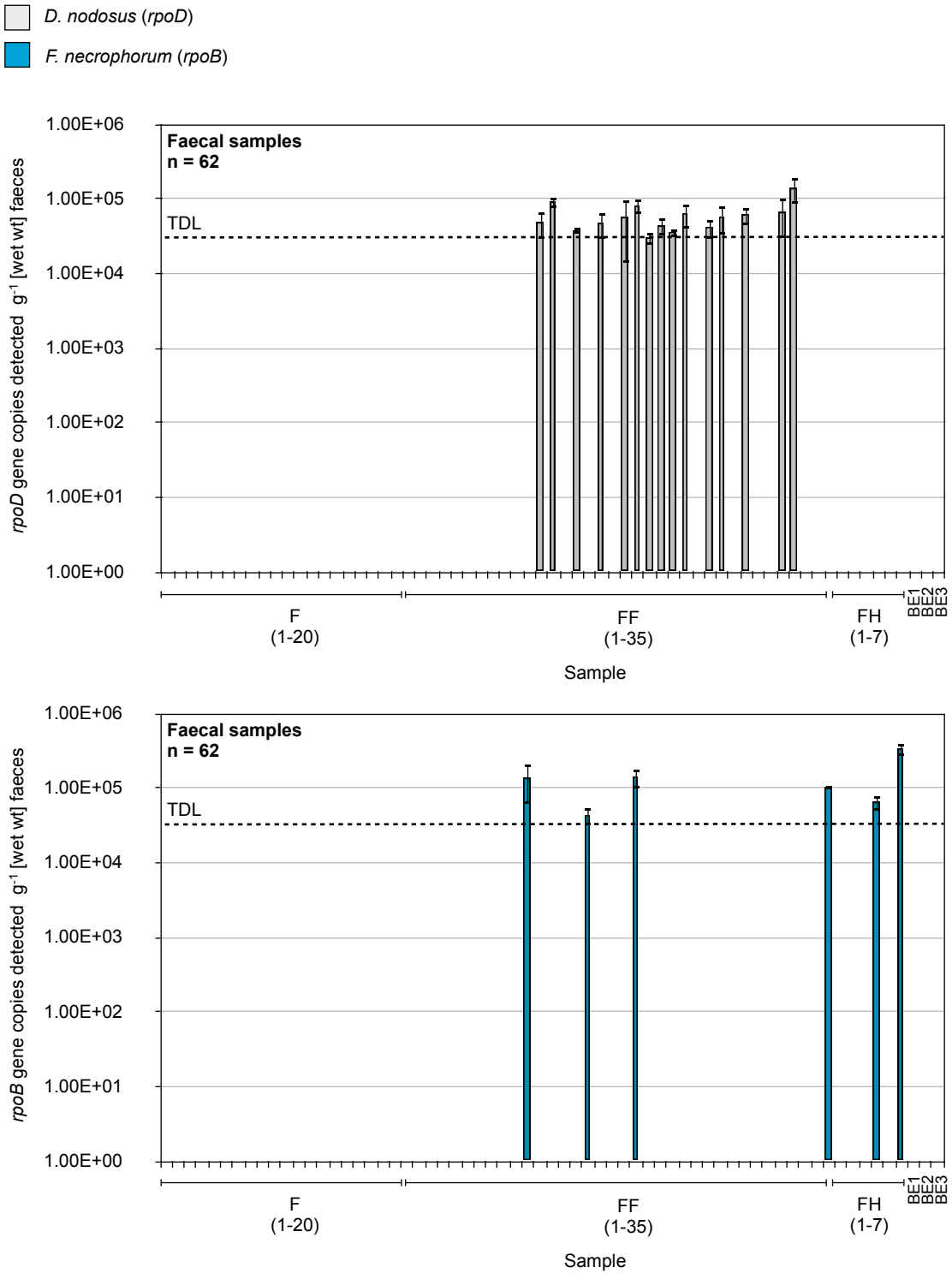

Figure 5.5. Detection and quantification of *D. nodosus* (*rpoD*) and *F. necrophorum* (*rpoB*) load in faecal (F) samples; faeces from sheep (F), faeces from the floor (FF) and faeces from compacted within the hoof (interdigital space) (FH). Samples collected as described (Section 2.5.3.). A total of 24.19 % (15/62) of samples were positive for *D. nodosus* (*rpoD*) and 9.68 % (6/62) positive for *F. necrophorum* (*rpoB*). Median values for *D. nodosus* and *F. necrophorum* loads were not statistically significant ($p > 0.05$) (Mann Whitney U test, Prism, Graphpad). Blank extraction (BE) swabs (1-3) were negative for *rpoD* and *rpoB* gene targets. Error bars ± SD of three technical replicates.

F. necrophorum is rarely excreted in animal faeces (Smith, et al., 1991; 1993a; 1993b). It is unknown however, whether *D. nodosus* or *F. necrophorum* may be shed into the environment at a low level (below the detection limit of these assays). Data were again not normally distributed (D'Agostino & Pearson omnibus normality test, Prism, Graphpad) and column medians were compared using a Mann Whitney U test, to determine if there were differences in the *D. nodosus* and *F. necrophorum* loads shed into the environment. No significant differences were found ($p = 0.1350$) between *D. nodosus* (*rpoD*) and *F. necrophorum* (*rpoB*) load. Blank extraction (BE) swabs were again negative for both targets.

It is widely known that PCR may be inhibited by certain compounds readily associated with environmental samples, such as humic acids and metals and is therefore of concern (Wilson, 1997; Layton, et al., 2006). Samples in this study (faeces, soil and bedding), which were likely to contain high concentrations of humic substances were examined using an internal inhibition control (RD4-GFPpCR®2.1), previously used for monitoring levels of inhibition when detecting *Mycobacterium bovis* from a number of environmental samples (Pontiroli, et al., 2011). The internal inhibition control determined if samples were affected by inhibition and the extent of that inhibition, as described in Section 2.10. The internal inhibition control was first used to screen the faecal samples (Figure 5.6.); the plasmid controls passed the threshold (C_T) at cycle number 21. A difference in sample C_T value was then compared with the no-inhibition control (NIC) value - this difference was termed delta C_T (ΔC_T). Samples with a ΔC_T value of > 0 were affected to some extent by inhibition. Inhibition was considered negligible for all faecal samples. The DNA extraction method with modification for

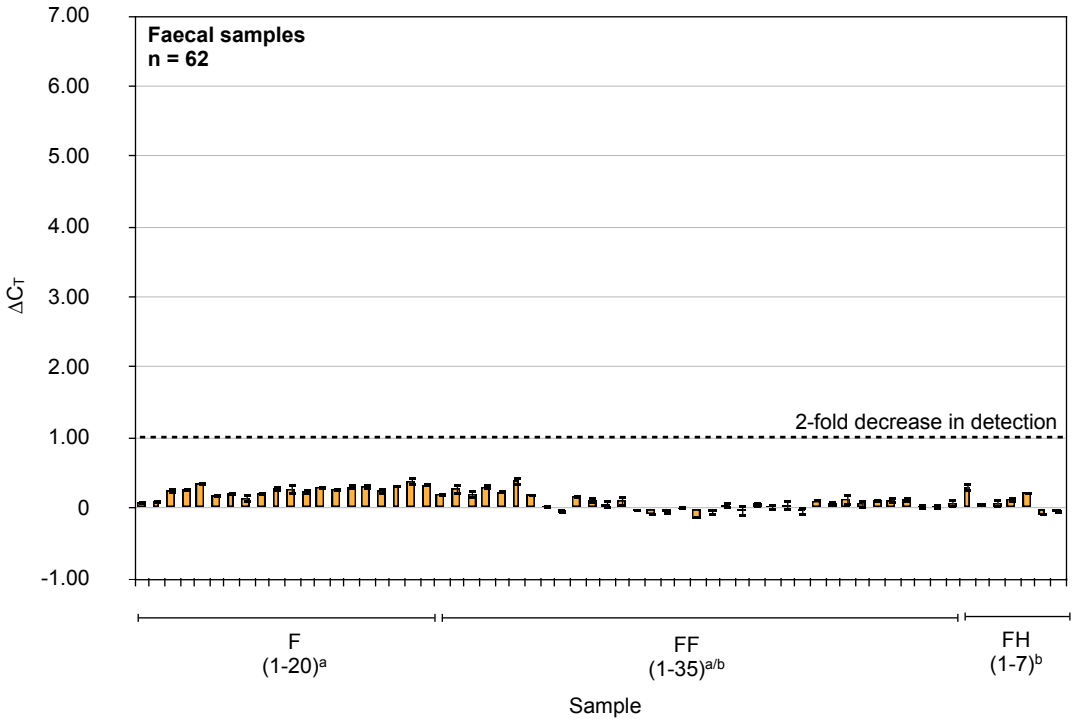

Figure 5.6. RD4 internal inhibition control for faecal samples. Determination of presence and extent of PCR inhibition using the RD4 internal inhibition control. Faecal samples separated into respective categories (F, FF, FH), with ΔC_T values shown. No-inhibition controls containing the plasmid (RD4-GFPpCR®2.1), NIC[a] or NIC[b], produced C_T values of 20.97 and 21.11, respectively. The faecal DNA samples were split over two 96-well plates, each with their own NIC (a or b). ΔC_T values of ≤ 1.0 were indicative of negligible to moderate inhibition, with a ΔC_T value of 1 producing a theoretical 2-fold decrease in detection. Inhibition for the faecal samples shown was negligible. Error bars ± SD of three technical replicates.

faecal samples (Layton, et al., 2006) likely assisted in pre-diluting humic content, resulting in fewer samples suffering with inhibition. ΔC_T values for the faecal samples ranged from -0.14 to 0.39.

5.3.4.3. Soil samples.

Soil (S) samples were collected as described in Section 2.5.3. from a pasture occupied by sheep with ID and/or FR (Figure 2.1.). DNA was then extracted and the *D. nodosus* (*rpoD*) and *F. necrophorum* (*rpoB*) loads were quantified. *F. necrophorum* was not detected in any of the twenty soil samples collected and *D. nodosus* was only detected

in one sample (1/20) and was on the limit of detection. The blank extraction (BE) sample was also negative for both gene targets. This provides further evidence that *D. nodosus* is shed into the environment (Figure 5.7.) and contaminates pasture, as previously described (Whittington, 1995). However, using the RD4 internal inhibition control, it was determined that there were significant levels of inhibition detected in all of the soil samples (Figure 5.8.). and this factor likely contributed to the lack of detection. ΔC_T values for the soil samples ranged from 0.88 to 6.53, demonstrating that the majority of samples were significantly inhibited, which was likely due to soil type; very dark soils are indicative of increased humic content (Mayhew, 2004), which may have contributed to the significant levels of inhibition observed in the samples.

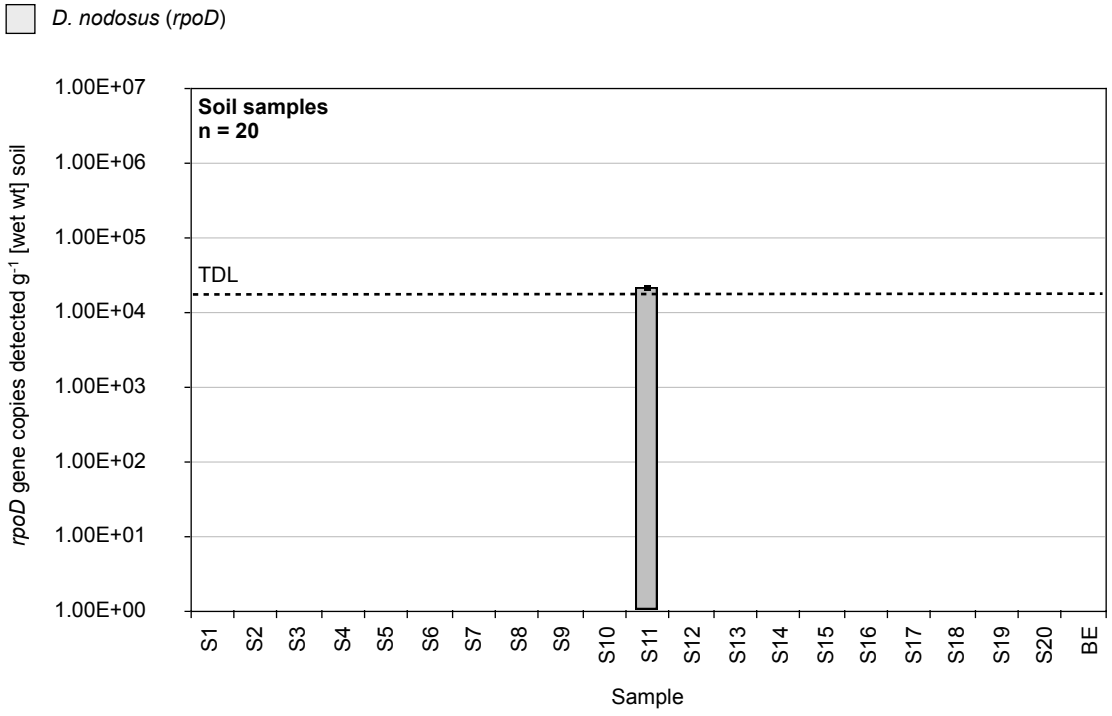

Figure 5.7. Detection and quantification of *D.nodosus* (*rpoD*) in soil (S) samples. Samples collected as described (Section 2.5.3.). *F. necrophorum* was not detected in any of the twenty samples, whilst *D. nodosus* was detected in 1/20 of the soil samples. However, samples were determined to be significantly inhibited (Figure 5.8.). The blank extraction (BE) sample was negative for both *rpoD* and *rpoB* targets. Error bars ± SD of three technical replicates.

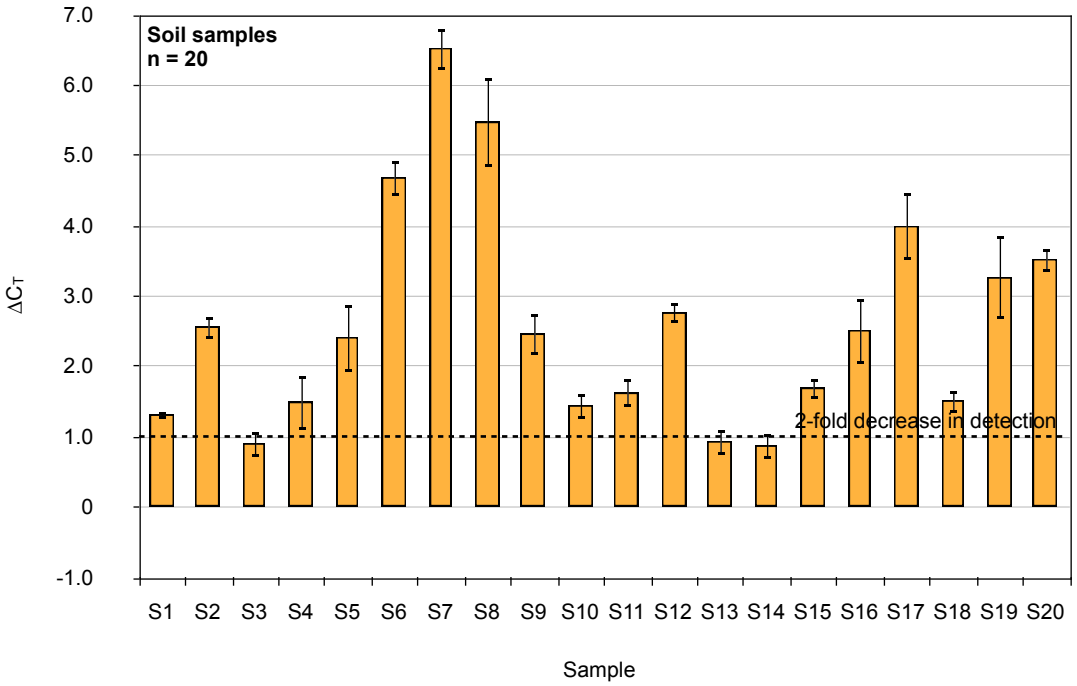

Figure 5.8. RD4 internal inhibition control for soil samples. Determination of presence and extent of PCR inhibition using the RD4 internal inhibition control. ΔC_T values shown for soil samples S1-S20. No-inhibition controls containing the plasmid (RD4-GFPpCR®2.1), NIC^b or NIC^c, produced C_T values of 21.11 and 21.07, respectively. The soil DNA samples were split over two 96-well plates, each with their own NIC (a or b). ΔC_T values of ≤ 1.0 were indicative of negligible to moderate inhibition, with a ΔC_T value of 1 producing a theoretical 2-fold decrease in detection. Inhibition was significant, likely because of soil type (high humic content) and extraction method.

Alterations to the sampling and extraction procedures to improve target detection, whilst decreasing inhibition will be examined in the Discussion (Chapter 6).

5.3.4.4. Bedding samples.

Bedding (B) samples were collected as described in Section 2.5.4. from a housed area occupied by sheep (Figure 2.1.) and from bedding compacted within the interdigital space of the ovine foot. DNA was then extracted and the *D. nodosus* (*rpoD*) and *F. necrophorum* (*rpoB*) loads were quantified. *D. nodosus* (*rpoD*) was detected in 50.00 % (11/22) of bedding samples and *F. necrophorum* (*rpoB*) was detected in 18.18 % (4/22) of bedding samples (Figure 5.9.). *D. nodosus* (*rpoD*) load ranged from 10^4 to 10^6 copies

g^{-1} [wet wt] bedding and *F. necrophorum* (*rpoB*) again ranged from 10^4 to 10^5 copies g^{-1} [wet wt] bedding. Data were again not normally distributed (D'Agostino & Pearson omnibus normality test, Prism, Graphpad) and column medians were compared using a Mann Whitney U test. The median value for *D. nodosus* was significantly higher than that of *F. necrophorum* ($p < 0.05$), this is likely because of an increase in *D. nodosus* (*rpoD*) load particularly in the bedding samples collected from the interdigital space of ovine hoof (BH). The blank extraction (BE) swab was again negative for both targets. The RD4 internal inhibition control indicated that some samples were affected more by inhibition than others, particularly samples collected from the ovine interdigital space (BH) (Figure 5.10.), which were observed to be more contaminated with faecal/soil material (author observation). The *rpoD* and *rpoB* loads detected for certain samples may therefore be underestimates considering the varying levels of inhibition. ΔC_T values for the bedding samples ranged from 0.27 to 2.80, demonstrating reduced inhibition when compared to the soil samples previously described.

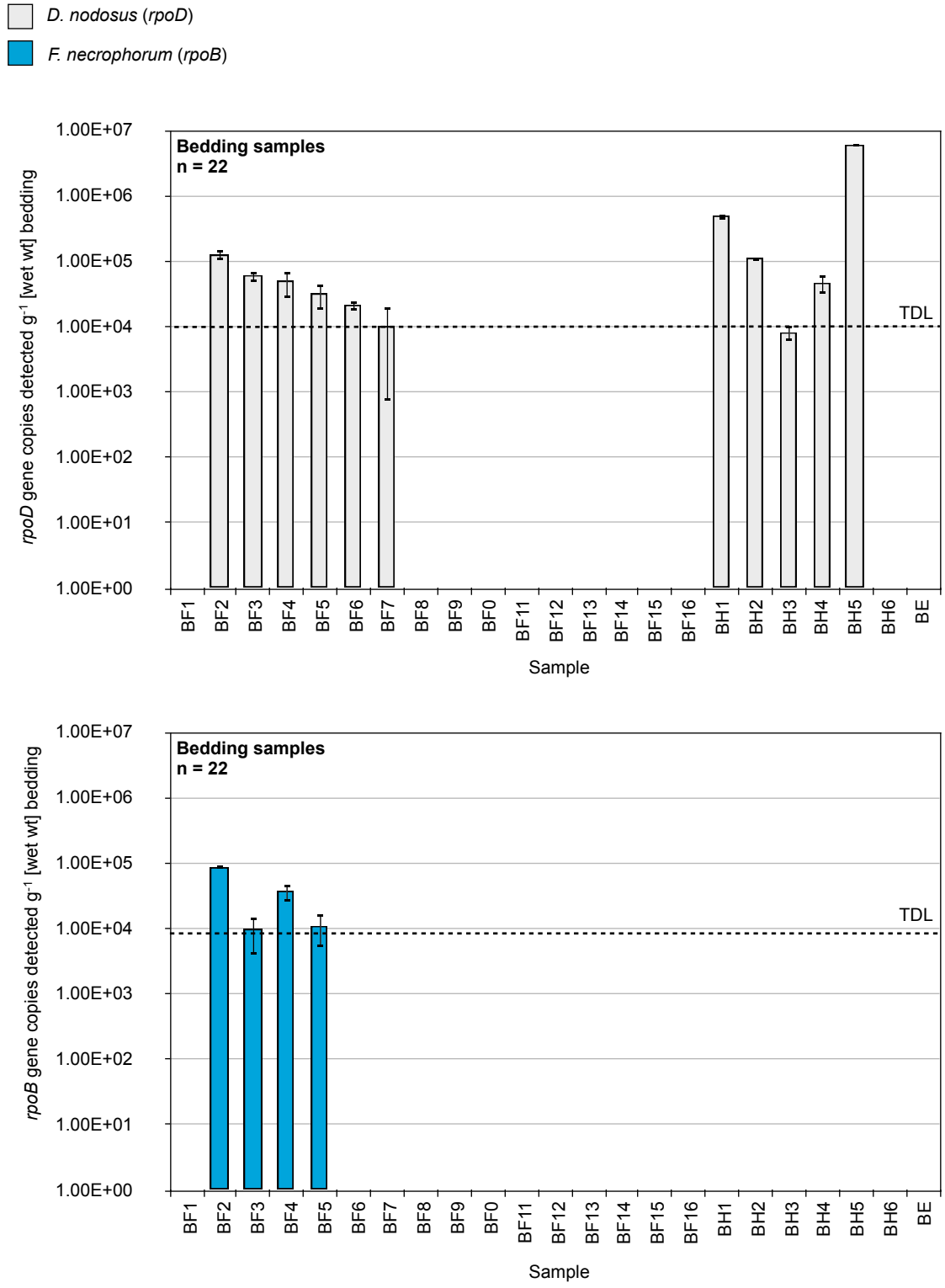

Figure 5.9. Detection and quantification of *D.nodosus* (*rpoD*) and *F. necrophorum* (*rpoB*) load from bedding (B) samples. Samples collected as described (Section 2.5.4.). Bedding collected from the floor (BF) and from compacted within the ovine interdigital space of the hoof (BH). *D. nodosus* (*rpoD*) and *F. necrophorum* (*rpoB*) detected in 50.00 % (11/22) and 18.18 % (4/22) samples, respectively. Levels of inhibition varied. BE swab was negative for *rpoD* and *rpoB* targets. Error bars ± SD of three technical replicates.

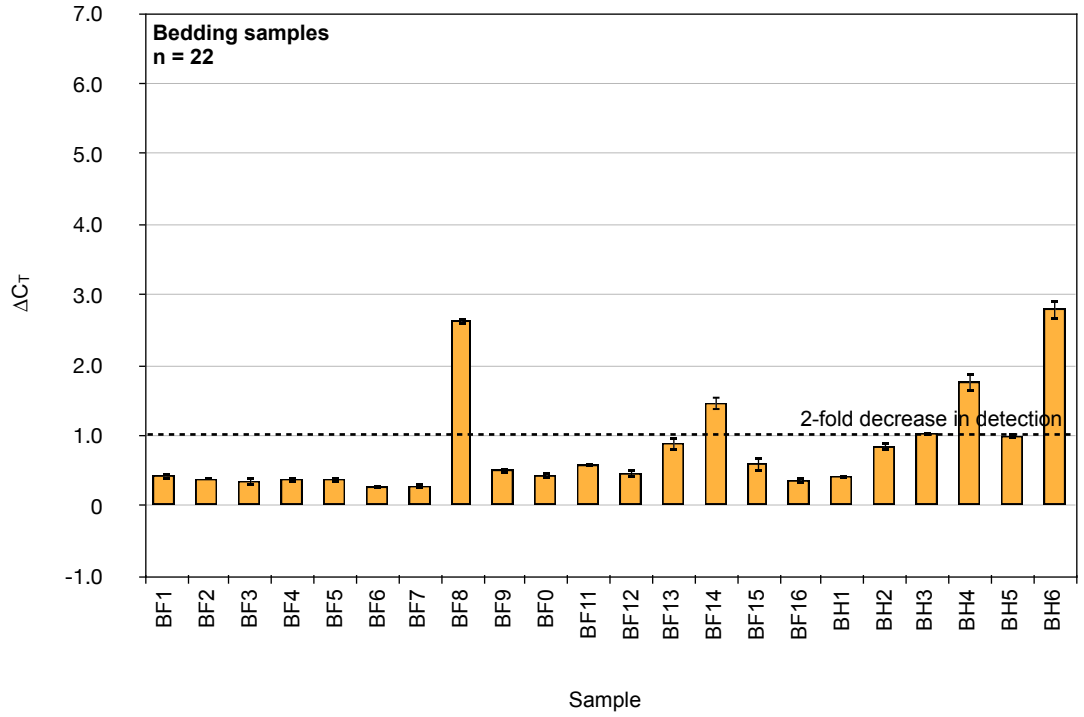

Figure 5.10. RD4 internal inhibition control for bedding samples. Determination of presence and extent of PCR inhibition using the RD4 internal inhibition control. ΔC_T values shown for soil samples S1-S20. No-inhibition controls containing the plasmid (RD4-GFPpCR®2.1), NIC^c or NIC^d, produced C_T values of 21.07 and 21.26, respectively. The bedding DNA samples were split over two 96-well plates, each with their own NIC (a or b). ΔC_T values of ≤ 1.0 were indicative of negligible to moderate inhibition, with a ΔC_T value of 1 producing a theoretical 2-fold decrease in detection. Inhibition was mostly negligible, except in four samples (BF8, BF14, BH4 and BH6), in addition inhibition was higher in samples collected from the interdigital space (BH).

5.3.4.5. Oral cavity samples.

Oral cavity (OC) swabs (cotton and buccal) were collected as described in Section 2.5.6. from the ovine oral cavity (Figure 2.1.). DNA was then extracted and the *D. nodosus* (*rpoD*) and *F. necrophorum* (*rpoB*) loads were quantified. In addition, buccal swabs were fixed as described (Section 2.16.5.1.) and screened using the *D. nodosus*-specific and *F. necrophorum*-specific oligonucleotide probes (FISH) (Chapter 4), to check for intact physiologically active bacterial cells. Both *D. nodosus* (*rpoD*) and *F. necrophorum* (*rpoB*) were detected using the TaqMan® real-time PCR assays (Figure

5.11.). *D. nodosus* (*rpoD*) and *F. necrophorum* (*rpoB*) were detected on 71.43 % (25/35) and 74.29 % (26/35) of the OC swabs, respectively. *D. nodosus* (*rpoD*) load ranged from 10^3 to 10^5 copies swab^{-1} and *F. necrophorum* (*rpoB*) load also ranged from 10^3 to 10^5 copies swab^{-1}. Two separate sampling sets were obtained (n = 15 and n = 20). Data were again not normally distributed (D'Agostino & Pearson omnibus normality test, Prism, Graphpad) and column medians were compared using a Mann Whitney U test. The median value for *D. nodosus* and *F. necrophorum* load were not significantly different (p = 0.2257). Blank extraction (BE) swabs were negative for both targets. In addition, the median *rpoD* copy number swab^{-1} was not significantly different to that of *F. necrophorum* (*rpoB*), a coloniser of the alimentary tract.

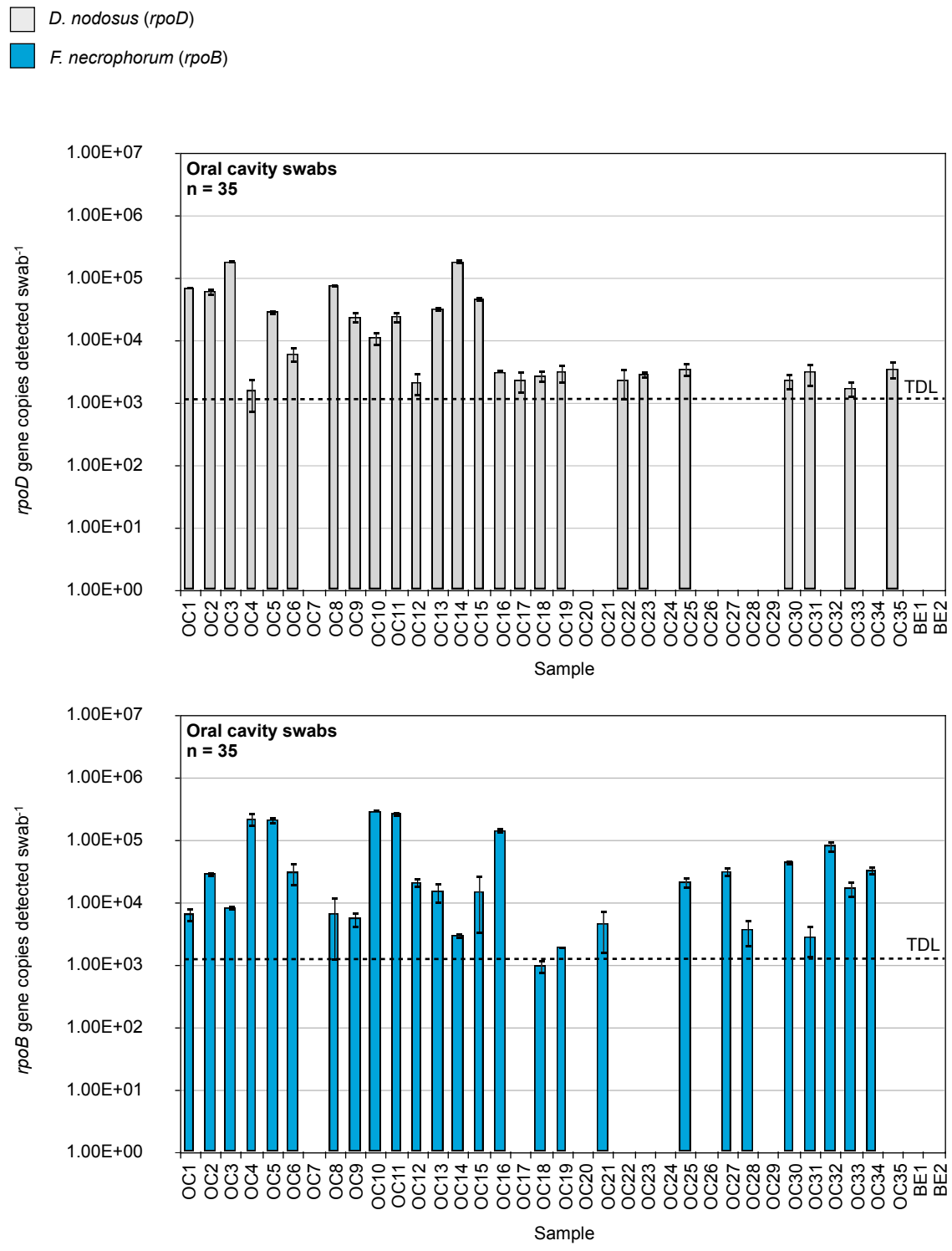

Figure 5.11. Detection and quantification of *D.nodosus* (*rpoD*) and *F. necrophorum* (*rpoB*) load from ovine oral cavity (OC) swabs. Samples collected as described (Section 2.5.6.). *D. nodosus* (*rpoD*) and *F. necrophorum* (*rpoB*) detected in 71.43 % (25/35) and 74.29 % 26/35) samples, respectively. No significant difference between *D. nodosus* (*rpoD*) and *F. necrophorum* (*rpoB*) load ($p > 0.05$). BE samples were negative for *rpoD* and *rpoB* targets. Error bars ± SD of three technical replicates.

5.3.5. Determination of the TDL of bacterial cells from swabs using FISH.

To determine whether physiologically active *D. nodosus* an *F. necrophorum* cells were present within the ovine oral cavity, a FISH assay from buccal swab samples was developed as described in Section 2.16.4.2. and Section 2.16.5.1. A TDL for the assay was determined for one Gram negative bacterium and one Gram positive bacterium, to represent the PFA- and ethanol-fixation protocols, respectively. A series of spiking experiments using *E. coli* (K-12) and *M. caseolyticus* (87) were set up using undiluted and serially diluted (10^{-1} to 10^{-7}) cultures. Undiluted *E. coli* and *M. caseolyticus* cultures initially had an estimated 3.01 x 10^8 and 3.15 x 10^8 cells ml^{-1}, respectively. After fixation cells were diluted with 96 % (v/v) ethanol for storage, resulting in 1.51 x 10^8 and 1.59 x 10^8 cells ml^{-1}, for *E. coli* and *M. caseolyitcus*, respectively. Fluorescently labelled cells were detected in the undiluted, 10^{-1}, 10^{-2} and 10^{-3} dilutions for both fixation methods (Figure 5.12.), revealing an approximate TDL of 1.51 x 10^5 and 1.59 x 10^5 cells ml^{-1}, corresponding to approximately 7.55 x 10^4 and 7.95 10^4 cells $swab^{-1}$, similar to the TDL for other published studies using swabs with FISH (Artz, et al., 2003).

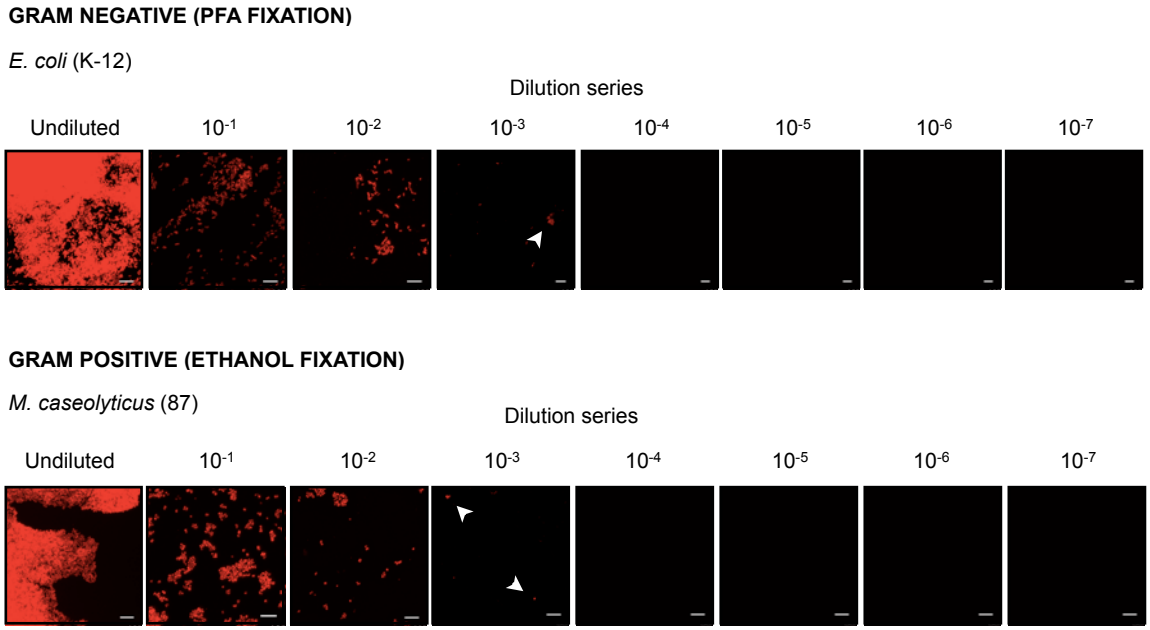

Figure 5.12. Determination of TDL for FISH assay from ovine oral cavity swabs. One gram negative (*E. coli*) and one gram positive (*M. caseolyticus*) were examined, to represent the Gram negative (PFA) and Gram positive (ethanol) fixation protocols, respectively. However, both the undiluted, 10^{-1}, 10^{-2} and 10^{-3} samples were positive for both microorganisms using the EUB338 (-I, -II, -II) probe set. White arrows indicate small clusters/individual cells in the last detectable dilutions. Scale bars: 10 µm.

The FISH analysis was then performed for all (35/35) oral cavity buccal swabs. All swabs were positive using the EUB338 (-I, -II, -III) probe set, which acted as a positive FISH control. However, *F. necrophorum* was only detected from two buccal swabs (OC11 and OC16) (Figure 5.13.), which corresponded with a higher *F. necrophoru*m (*rpoB*) load (Figure 5.11.). This demonstrates that intact physiologically active *F. necrophorum* cells were present within the ovine oral cavity, possibly acting as an alternative reservoir of infection. *D. nodosus* cells were not detected by FISH from any of the samples.

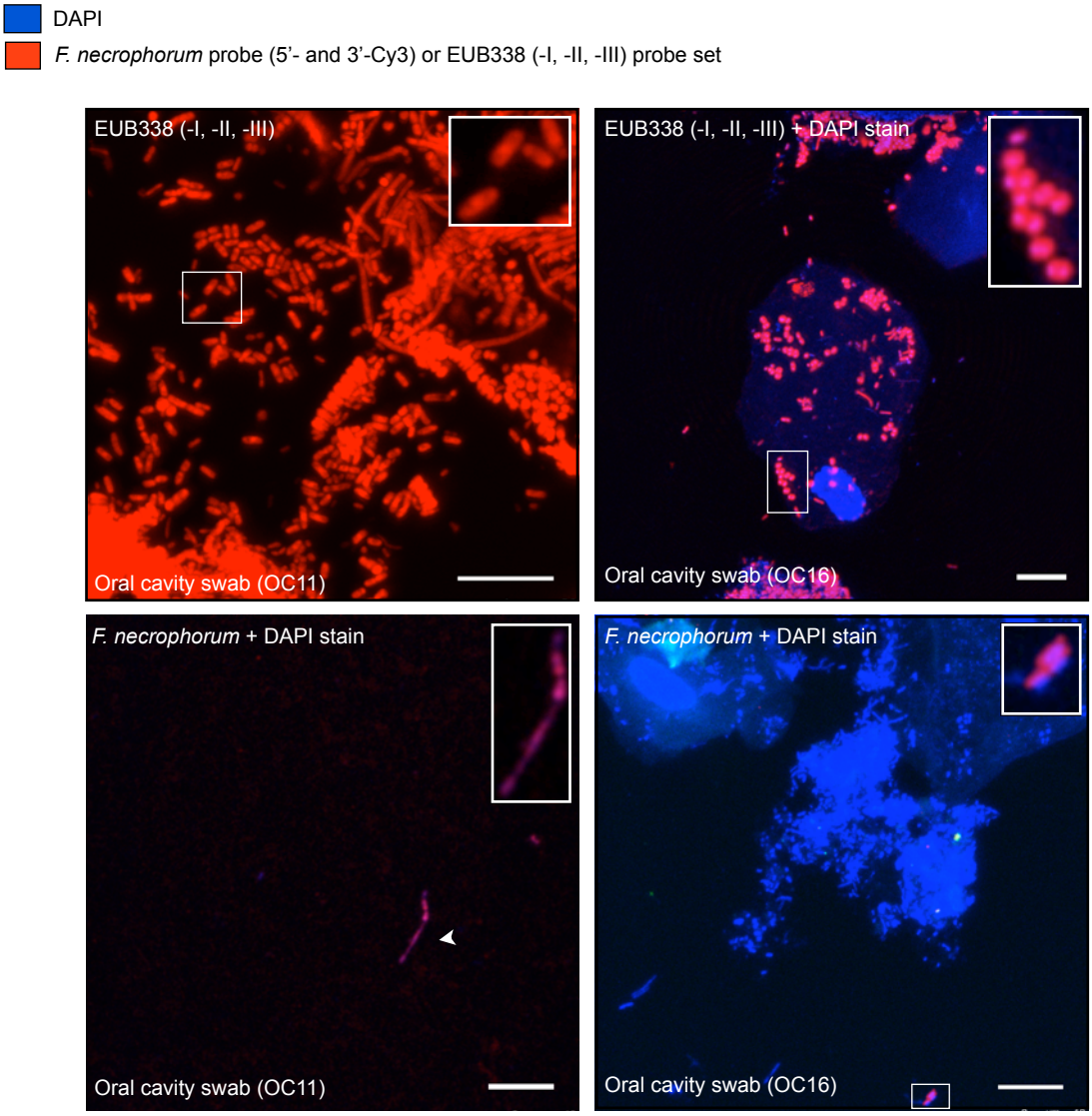

Figure 5.13. Detection of the domain Bacteria and *F. necrophorum* from ovine oral cavity (OC) buccal swabs using FISH. Both OC11 and OC16 swabs were positive for the domain bacteria. Two buccal swabs (OC11 and OC16) were positive for *F. necrophorum* using FISH. From OC11 a lone filamentous *F. necrophorum* cell is observed and for OC16 two small *F. necrophorum* rods were identified at the edge of DAPI-stained bacterial/buccal epithelial cell clump. Buccal epithelial cells and other bacteria were stained by DAPI (DAPI stain was not included for the EUB338-I, -II, -III screen for OC11). Scale bars: 10 µm.

5.3.6. Detection of the genus *Fusobacterium*.

Fusobacterium species were detected using genus-specific primers as detailed in Section 2.8.1. (Table 2.7.). The FUSO1 and FUSO2 primer set targeting the 16S rRNA gene were used as described (Nagano, et al., 2007) and were used to screen a number of positive control strains; *F. necrophorum* (BS-1), *F. necrophorum* subsp. *necrophorum*

(NCTC 10576), *F. necrophorum* subsp. *necrophorum* (ATCC 25286), *F. necrophorum* (R17807), *F. necrophorum* subsp. *funduliforme* (ATCC 51357), *F. nucleatum* (ATCC 25886), *F. simiae* (ATCC 33568) and *F. varium* (AR17443), each of which produced a single band of the expected size (630 bp) and no amplicon was observed for the negative controls, as detailed in Table 3.4. The environmental samples were then screened with the *Fusobacterium* genus primers to determine if any other *Fusobacterium* species were present when *F. necrophorum* was absent and the results are summarised (Table 5.1.). When samples were positive for *F. necrophorum*, the *Fusobacterium* genus screen also produced a single band of the expected size. However, on occasion, when the sample was negative for *F. necrophorum*, the sample was instead positive for the genus only, indicating that other members of the genus *Fusobacterium* were present in some of the environmental samples.

Table 5.1. Percentage positive samples for *F. necrophorum* (*rpoB*) (qPCR assay) and *Fusobacterium* genus (PCR assay) by environmental sample type.

Sample	*F. necrophorum* (*rpoB*) qPCR TaqMan® assay	*Fusobacterium* genus (16S rRNA) PCR assay
1. Concrete floor (CF) swabs	42.86 % (18/42)	47.62 % (20/42)
2. Ovine faecal (F) samples	9.68 % (6/62)	22.58 % (14/62)
3. Soil (S) samples	0.00 % (0/20)	15.00 % (3/20)*
4. Bedding (B) samples	18.18 % (4/22)	45.45 % (10/22)*
5. Oral cavity (OC) swabs	74.29 % (26/35)	100.00 % (35/35)

* Some samples produced double bands; band of correct size extracted as described in Section 2.13. and sent for sequencing and positive results confirmed.

The PCR primer set can not only be used for the detection of the *Fusobacterium* genus, but for identification of the *Fusobacterium* species (Nagano, et al., 2005). PCR products from samples from each category (CF, F, S, B and OC) were purified and sent for

sequencing; sequencing results revealed the presence of *F. russii*, *F. ulcerans*, *F. gonidiaformans*, *F. varium*, *F. equinum*, *F. nucleatum*, and *F. periodonticum*, indicating that other fusobacterial species were present in this environmental setting.

5.4. Discussion.

In this chapter, the distribution and burden of *D. nodosus* and *F. necrophorum* in a farm environment was examined by using two culture-independent methods; qPCR and FISH. The results have highlighted a possible reservoir of infection not previously explored for *D. nodosus*, the causative agent of ovine footrot.

The distribution and bacterial load of *D. nodosus* (*rpoD*) and *F. necrophorum* (*rpoB*) were examined in a range of environmental samples from a farm in Bristol, UK; including ovine faeces, soil, bedding (from a housed area), concrete floor swabs and ovine oral cavity swabs. The theoretical detection limits (TDLs) for each new sample type (faeces, soil and bedding) was determined by setting up a series of spiking experiments; the TDL for the detection of *rpoD* and *rpoB* in faecal material and soil was more than 10-fold higher than that for swabs. However, the TDL for *rpoD* and *rpoB* from bedding was lower (approximately 1.00×10^4 copies g^{-1} [wet wt] bedding). The higher limit of detection (LOD) observed for faecal and soil samples, corresponds with a number of other studies (Bartosch, et al., 2004; Okano, et al., 2004; Pontiroli, et al., 2011).

Both *D. nodosus* (*rpoD*) and *F. necrophorum* (*rpoB*) were successfully amplified from the majority of the environmental sample types obtained and their respective loads were

then quantified. Both *D. nodosus* (*rpoD*) and *F. necrophorum* (*rpoB*) were detected from concrete floor (CF) swabs taken from outside and within a housed area (Figure 2.1.). No significant difference was observed between *D. nodosus* (*rpoD*) and *F. necrophorum* (*rpoB*) load from these swabs. The environmental burden was of a similar range to that detected on healthy ovine feet (10^3 to 10^4 copies swab^{-1}); indicative of superficial contamination. In comparison, neither *D. nodosus* or *F. necrophorum* were detected in ovine faeces (n = 20) obtained before coming into contact with the floor, which was somewhat unexpected, as faecal material was reported to provide the primary source of *F. necrophorum* infection (Roberts and Egerton, 1969). However, later reports did indicate that *F. necrophorum* was in fact rarely excreted in faeces, despite being a coloniser of the alimentary tract (Smith, et al., 1991; 1993b). Smith and colleagues (1993a) postulated that only when the microbial community of the gut was perturbed, via the action of oral antibiotics, did the *F. necrophorum* population become unregulated and subsequently shed into the environment. The sheep in this study (Cohort flock 2) were not administered oral, but parenteral antibiotics, which has also been demonstrated in some circumstances to alter the intestinal microflora of humans and animals (Barza, et al., 1987; Giuliano, et al., 1987; Janczyk, et al., 2007).

It was also hypothesised that the presence of a small number of 'super-shedders' within a population (flock) may exist. However, it could also be that *F. necrophorum* may be shed at a load below the TDL (6.09 x 10^4 *rpoB* copies g^{-1} [wet wt] faeces), and therefore would not have been detected by this method. It would be interesting therefore to determine whether antibiotic treatment and/or diet has a significant effect on the gut microflora of ruminants and whether this in turn causes increased shedding of *F.*

necrophorum, which would have major implications for treatment regimes, if treatment was in fact promoting the multiplication and shedding of this opportunistic pathogen into the surrounding environment.

Both *F. necrophorum* and *D. nodosus* were detected in faecal material collected from the floor (FF) and from compacted within the interdigital space of the ovine foot (FH), suggesting that this material becomes rapidly contaminated once it has come into contact with the floor and/or with colonised feet and may act as a vehicle for transmission. In addition, no difference between *rpoD* and *rpoB* load in faeces was observed.

Although *F. necrophorum* is reportedly ubiquitous in the environment and present in soil (Langworth, 1977; Riordan, et al., 2007), it was not detected in any of the twenty soil samples at a detectable level (above the TDL). However, the majority of soil (S) samples were inhibited, suggesting that this was likely the reason for the lack of detection and therefore no specific conclusions can be drawn. The fact that the majority of the soil samples suffered significantly from inhibition, suggests that the standard method used (FastDNA Spin kit for Soil) was not suitable for this soil type, as other studies have found it to be a suitable extraction method for both faeces and soil (Pontiroli, et al., 2011; Travis, et al., 2011). Less starting material and/or pre-dilution may have to be considered for soil with a high humic content (Mayhew, 2004), perhaps the modification used for the faecal samples (Layton, et al., 2006) in this study could have been used to pre-dilute the soil samples and therefore possible inhibitors. In addition, recent work using sterile cotton swabs to sample the surface of pasture/soil has

demonstrated detection of *D. nodosus* (Calvo-Bado, personal communication), which may provide an alternative sampling method for soil. Despite this, one soil sample (S11) was positive for *D. nodosus* (*rpoD*) and was just above the LOD, despite the sample suffering from moderate inhibition ($\Delta C_t = 1.63$). This theoretically results in more than a 2-fold decrease in detection. This demonstrates that *D. nodosus* is shed onto pasture at a detectable level - however the *rpoD* load g^{-1} [wet wt] soil was likely an underestimate due to the presence of inhibitory compounds. This part of the study should be repeated using a variety of soil types and extraction methods; with or without modifications, to determine which extraction procedure, results in the lowest possible inhibition as performed with other studies (Pontiroli, et al., 2011).

Similarly some of the bedding (B) samples were also affected by inhibition, particularly bedding samples taken from compacted within the interdigital space of the hoof (BH). It was noted that soil/faecal material may have also been present on these samples. Despite this, both *D. nodosus* (*rpoD*) and *F. necrophorum* (*rpoB*) were detected on bedding collected from a housed area, however *D. nodosus* (*rpoD*) load was significantly higher than that of *F. necrophorum* (*rpoB*) - likely because of the increased load observed on BH samples.

The ovine oral cavity has been reported to be positive for *F. necrophorum* (Bennett, et al., 2009), however, the number of samples screened, detection frequency and load were not reported. Surprisingly in the current study, both *D. nodosus* (*rpoD*) and *F. necrophorum* (*rpoB*) were detected on the majority of (> 70 %) of ovine oral cavity (OC) swabs. This highlights that *D. nodosus* (*rpoD*) was just as likely to be detected

from the oral cavity as *F. necrophorum* (*rpoB*), a coloniser of the alimentary tract, which was unexpected. Similarly, the *D. nodosus* (*rpoD*) and *F. necrophorum* (*rpoB*) loads detected on the oral cavity swabs were not significantly different, which was again unexpected. *F. necrophorum* has previously been isolated from the oral cavities of cattle, goats and sheep (Madsen, et al., 1992; Yeruham and Elad, 2004; Bennett, et al., 2009) and humans (Aliyu, et al., 2004). However, this is the first time that *D. nodosus* has been detected within the ovine oral cavity, highlighting either a possible alternative reservoir of infection or transitory route of transmission. Blank extraction (BE) swabs were also negative, so cross-contamination during the extraction procedure can be excluded.

Despite the detection of *D. nodosus* (*rpoD*) using real-time qPCR from the ovine oral cavity, only physiologically active *F. necrophorum* cells were detected by FISH. However, the estimated TDL of the FISH assay from swabs for Gram negative and Gram positive bacteria was determined to be approximately 7.55×10^4 and 7.95×10^4 cells swab^{-1}. However, it remains unknown whether *D. nodosus* is always present in the ovine oral cavity, whether it is viable and able to replicate within the anaerobic crevices in the ovine mouth, acting as a reservoir of infection. Or, whether it occurs after an outbreak of ID and/or FR on a farm, becoming contaminated via the grazing of contaminated pasture. Recently a multiple-locus VNTR (variable number tandem repeat) analysis (MLVA) assay was developed for typing strains of *D. nodosus* using four polymorphic VNTR regions (Russell, et al., unpublished). It would be interesting therefore to determine whether the strains of *D. nodosus* detected on the feet and in the environment were the same strains detected within the ovine oral cavity, or whether

distinct populations exist. This type of analysis would further improve our understanding of disease transmission. In addition, a longitudinal study to examine whether environmental *D. nodosus* and *F. necrophorum* load correlates with an outbreak of FR on a farm would provide additional information regarding which sources were environmental reservoirs and which merely become contaminated after an outbreak.

Finally, a number of environmental samples were positive for the genus *Fusobacterium*, when negative for *F. necrophorum*. When the PCR products were sequenced, *F. russii*, *F. ulcerans*, *F. gonidiaformans*, *F. varium*, *F. equinum*, *F. nucleatum*, and *F. periodonticum* were identified (with *F. nucleatum* and *F. periodonticum* sequences being primarily amplified from oral cavity samples). Of these, the vast majority are involved in some type of opportunistic disease, such as bite wounds, ulcers and oral cavity diseases (Love, et al., 1987; Adriaans and Drasar, 1987; Kolenbrander, et al., 1995; Dorsch, et al., 2001; Ohkusa, et al., 2003). In addition Calvo-Bado, et al., (2011b) also demonstrated the presence of *F. gonidiaformans* in ovine foot biopsies using pyro-sequencing methods. This indicates that other pathogenic fusobacterial species were also present in this environment and may contribute to opportunistic infections of farmed animals.

In summary, this chapter represents the first study to date to examine the distribution and burden of *D. nodosus* and *F. necrophorum* within a farm environment. The use of two culture-independent techniques has highlighted that material present in the environment, such as faeces and bedding may act as a transitory transmission vehicle for *D. nodosus* and *F. necrophorum*. The contaminated farm environment therefore

becomes a potential source of infection for susceptible individuals. In addition, the ovine oral cavity may act as an alternative reservoir of infection of *F. necrophorum* (instead of or in addition to ovine faeces). This study has also revealed the intriguing possibility that the ovine oral cavity may act as an alternative reservoir of *D. nodosus* infection, although it is likely that the ovine foot remains the primary reservoir.

CHAPTER 6

6. General Discussion.

6.1. Overview.

The development and optimisation of two culture-independent techniques are reported for the detection, identification, quantification and localisation of *D. nodosus* and *F. necrophorum* from a range of sample types. Culture-independent techniques were employed to overcome the difficulties associated with the cultivation of fastidious anaerobes (Domann, et al., 2003). The aim of the project was firstly to improve our understanding of the population dynamics involved in the development of ovine FR and secondly, to examine the distribution of *D. nodosus* and *F. necrophorum* in the environment, in an attempt to highlight alternative reservoirs of infection and material, which once contaminated may aid transmission.

6.2. The relative importance of *D. nodosus* and *F. necrophorum* populations in the initiation and development of ID and FR in sheep.

Ovine FR is frequently described as a 'mixed' or poly-microbial disease, whereby damage to the epithelium of the interdigital space allows opportunistic infection with *F. necrophorum* to occur. It is possible that the microbial homeostasis of a healthy foot is negatively affected by this damage, causing a shift in that community (Calvo-Bado, et al., 2011b). This shift may then generate an environment more suited for anaerobic bacteria. *F. necrophorum* is then postulated to generate, via the action of a number of its virulence factors, a more anaerobic microenvironment suitable for fastidious anaerobes,

such as *D. nodosus*. *D. nodosus* is the causative agent of ovine FR, being the only organism able to replicate disease in sheep and having fulfilled Koch's molecular postulates (Beveridge, 1941; Kennan, et al., 2001; 2010). Despite this and recent advances (Calvo-Bado, et al., 2011b) the precise series of microbial succession events, particularly with regard to the specific detection of *D. nodosus* and *F. necrophorum*, have not been examined in detail. The primary aim of this project therefore was to clarify when and where *D. nodosus* and *F. necrophorum* populations become important in the initiation and development of ovine FR, to further define their roles.

The bacterial populations were examined in two different ways, the first by examining the temporal patterns of *D. nodosus* and *F. necrophorum* load in relation to the presentation and development of ID and FR in sheep and the second by examining the spatial distribution of these two microorganisms within interdigital space biopsies, again in relation to disease presentation. These two techniques were used in attempt to complement one another, the first a highly sensitive DNA-based detection method and the second a less sensitive, but equally as informative method for the spatial resolution of physiologically active cells within their natural environment.

The results from Sections 3.3.5. and Section 3.3.6. elucidated the temporal patterns of *D. nodosus* and *F. necrophorum* load in relation to the presentation and development of ID and FR in sheep. A number of other studies have examined the presence of these two microorganisms in relation to disease presentation (La Fontaine, et al., 1993; Moore, et al., 2005a; Bennett, et al., 2009), but are limited by their cross-sectional nature. However, this project demonstrates the first longitudinal study to examine the

progression of disease in relation to *D. nodosus* and *F. necrophorum* load. The results highlight that *D. nodosus* and *F. necrophorum* were more frequently detected in diseased feet and sheep, which corresponds with already published work (Bennett, et al., 2009; Moore, et al., 2005a). However, *D. nodosus* (*rpoD*) load was observed to shift from a 'low-mid' range to a higher range during the progression from a healthy ovine foot to one presenting with ID. In addition, feet with a high *D. nodosus* (*rpoD*) load at this stage, were then more likely to go on to develop FR one week later. Interestingly, the *in situ* results detailed in Sections 4.3.5.4., 4.3.5.5. and 4.3.2.6. also demonstrated the detection of physiologically active *D. nodosus* (Cy3-labelled) cells present in the epidermis of feet presenting with ID. Demonstrating that not only was there an increase in gene (*rpoD*) copy number, but also cell number and that they appeared to be restricted to the epidermal layers.

This demonstrates that despite attitudes towards ID from the UK farming and veterinary communities (Wassink, et al., 2005), this stage of disease should be regarded as that, a 'stage', rather than as a separate disease condition. It indicates that ID is also infectious and that it is unlikely to be solely caused by environmental conditions. This therefore has implications for control and treatment regimes in the UK, as many British farmers do not usually treat affected sheep, until the disease has advanced and the hoof has under-run (Wassink, et al., 2005). The results from this thesis therefore support the clinical epidemiological studies that proposed that treatment should be initiated during stages of ID in order to decrease *D. nodosus* burden on the ovine foot, further sheep-to-sheep transmission and to decrease the incidence of FR on British farms, thereby improving animal welfare. This has also been demonstrated in an observational study

(Green, et al., 2007) and a clinical trial (Wassink, et al., 2010b), where the prompt treatment of sheep with FR (ID only or with under-running) using parenteral and topical antibacterials led to a dramatic decrease in the prevalence and incidence of FR and improved productivity. The work presented in this thesis therefore provides a microbiological explanation for this finding and emphasises the importance of treating sheep promptly. The impact of the results from this thesis is highlighted by the fact that this work was also presented at the Sheep Veterinary Society meeting in 2011 and it was discussed that the advice given to farmers currently on how to treat ovine FR will have to be altered to state to farmers that ID and FR are the same disease and treatment should be applied to all stages.

In the current study, *F. necrophorum* (*rpoB*) load did not increase until after FR had developed and although *F. necrophorum* cells were detected by FISH within the epidermis of both feet presenting with ID and those with FR, *F. necrophorum* cells counts were higher in feet with under-running; possibly indicating that *F. necrophorum* thrives in this altered environment and may aid disease persistence. In comparison, *D. nodosus* was rarely observed in the epidermis of feet with FR and a relatively low number of cells were detected in biopsies from these same feet suggesting that this organism may be shed during the earlier inflammatory process and removed via the sloughing of necrotic tissue; a process previously described (Egerton, et al., 1969). Another hypothesis is that *D. nodosus* may migrate from the interdigital region and settle elsewhere within the ovine foot.

In contrast, *F. necrophorum* is reported to penetrate deeper into the epidermis (Egerton, et al., 1969), possibly avoiding the inflammatory/sloughing process, which may explain the relatively higher numbers of *F. necrophorum* cells detected within FR biopsies. If this is the case, there is an earlier stage in the disease process where feet shed large amounts of infective material (necrotic skin containing *D. nodosus*) into the environment and therefore ideally this stage of disease should be prevented from occurring. Alternatively, *F. necrophorum* may outcompete *D. nodosus* at this stage, or with the increased exposure of the epidermis (via the processes of under-running and sloughing), the *D. nodosus* population may be affected by increased oxygen levels. The findings from this study have contributed to the current model of disease pathogenesis (Figure 6.1.).

*D. nodosu*s cells were not detected in biopsies collected from healthy ovine feet and *F. necrophorum* on only one occasion, which does not correlate with the asymptomatic carriage, albeit at a low level, of *D. nodosus* (*rpoD*) and *F. necrophorum* (*rpoB*) observed in Chapter 3, nor with the isolation of *D. nodosus* cells from asymptomatic sheep (Depiazzi, et al., 1998). However, DNA-based detection methods have a number of limitations and the overestimation of bacterial load (by detecting DNA from non-viable or lysed cells) is one of them (Castillo, et al., 2006), it could therefore be that the qPCR assays detected DNA from non-viable *D. nodosus* and *F. necrophorum* cells present on healthy sheep, possibly overestimating the bacterial load present on these feet. In contrast, the lack of detection by FISH may have been been due to a detection limit issue, although an accurate TDL for the detection of *D. nodosus* and *F. necrophorum* from biopsies was difficult to calculate. A TDL for the detection of

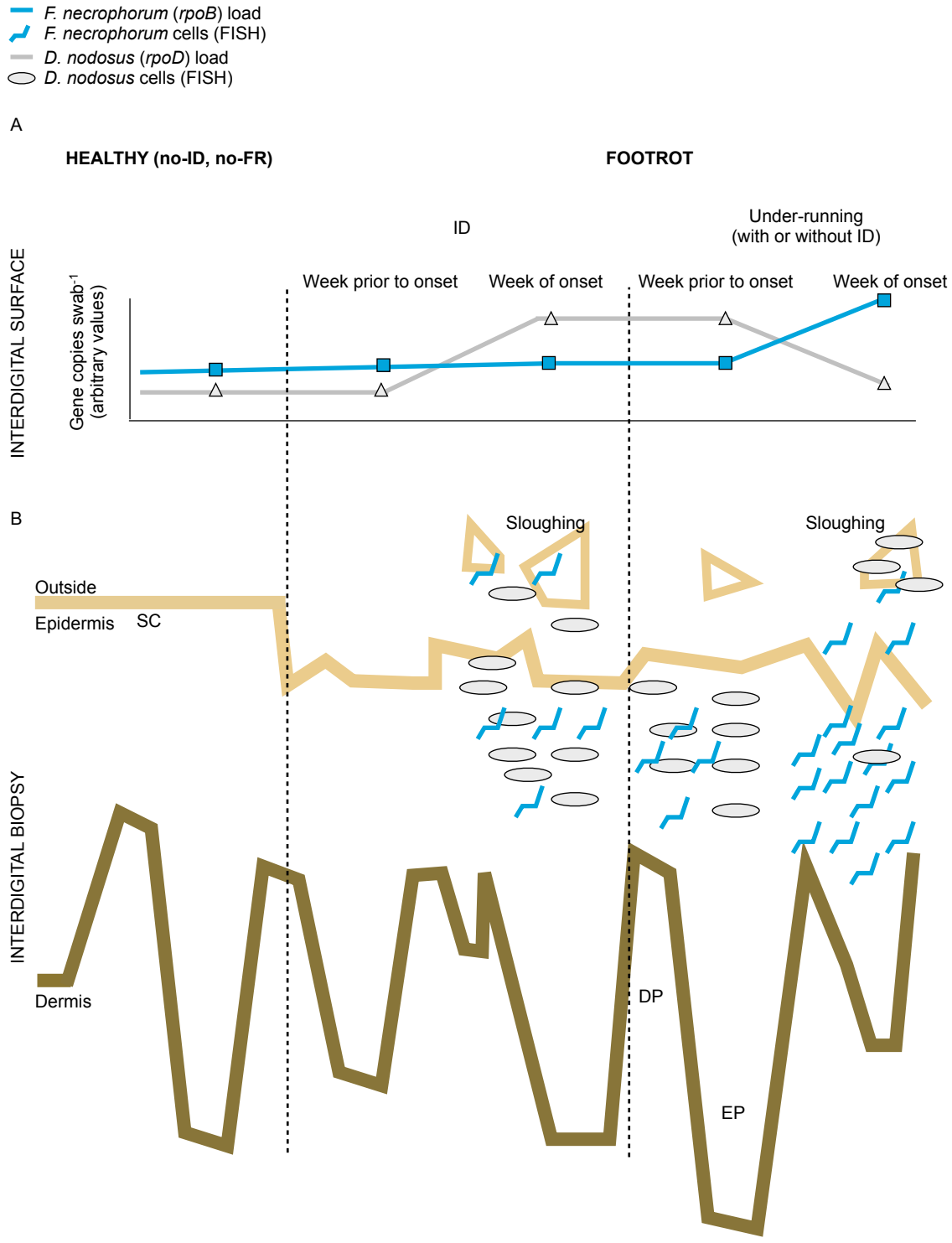

Figure 6.1. Summary of results contributing to the disease pathogenesis model for ovine FR. Stages of disease split into healthy (no-ID, no-FR) and Footrot (ID with and without under-running). The model indicates at which stages of disease the *D. nodosus* and *F. necrophorum* populations fluctuate based on the use of two culture-independent assays; qPCR (A) for sampling the interdigital surface and FISH (B) for screening the interdigital biopsies. SC: stratum corneum, DP: dermal papillae, EP: epidermal pegs.

Gram negative bacteria from swabs however was determined to be approximately 7.55 x 10^4 cells $swab^{-1}$, which corresponds with the upper TDL from other published work (Artz, et al., 2003). The swab method samples the entire surface of the interdigital space, whereas each individual biopsy section covers a only a small area (of the stratum corneum) and therefore *D. nodosus* and *F. necrophorum* cells may have been missed. In addition, *D. nodosus* and *F. necrophorum* cells present on the interdigital spaces of healthy feet, due to nutrient limitation may have been less physiologically active (low rRNA content) and this is one of the main causes of poor or absent FISH signal (Moter and Göbel, 2000).

Finally, it was observed that *F. necrophorum* appeared to filament in response to stressful *in vitro* conditions and in biopsies (*in situ*), however whether this occurs *in vivo* or whether this is an artifact caused by the removal of the biopsy from the host is unknown. This type of response in *F. necrophorum* has only been reported once and in response to exposure to antibiotics (Onoe, et al., 1981), which may have implications for the treatment of FR, if *F. necrophorum* is involved in disease persistence and/or severity. In addition, filamentation may protect *F. necrophorum* against phagocytosis and therefore aid its survival.

6.2.1. Perspectives and future directions.

In order to further the work described in Chapter 3 and Chapter 4, it would be interesting to use pyrosequencing methods to examine the temporal changes of the structure of the total bacterial community present (on the interdigital skin), in relation to the initiation and development of ID and FR, as the work by Calvo-Bado and colleagues

(2011b) was cross-sectional. To determine what population changes, if any, aid the colonisation and invasion of *F. necrophorum* and *D. nodosus* after damage to the interdigital skin. However, a longitudinal study such as this would require non-invasive sampling, such as the swabbing method used in Chapter 3, as invasive biopsy sampling would damage the feet and therefore perturb the existing microbiome. Biopsies would also expose or render the feet susceptible to infection, which would have severe implications for animal welfare.

Despite the findings presented in this thesis, it is still unclear as to what role *F. necrophorum* plays, if any, in the initiation and/or persistence of ovine FR. Sheep infection studies would be useful for determining this, however this type of research is expensive and has a number of ethical issues associated with it. Considering this, it is possible that 3D cell culture models (complex epithelial tissue culture models) could provide an effective alternative to study infectious disease. These types of models not only mimic the morphological and functional features of their corresponding *in vivo* tissues, but provide complex systems in which to study infection without using animal models (Barilla, et al., 2010). In addition, this type of system would allow for easy manipulation, longitudinal sampling and provide more control over the number of biological replicates obtained.

In addition, the hypothesis that *D. nodosus* may migrate elsewhere within the ovine foot when the hoof begins to under-run would need to be examined by screening whole foot biopsies and collection and sectioning of these 'biopsies' has already begun in response to the findings of Chapter 4. The screening of whole foot biopsies may also help

determine whether asymptomatic carriage of *D. nodosus* occurs and may provide more information regarding whether hair follicles may act as an alternative route of bacterial entry.

The ability of *F. necrophorum* to filament in response to *in vitro* and *in situ* conditions, although a very common bacterial response, has not been examined in detail for *F. necrophorum*. It would be interesting therefore to determine what conditions cause filamentation in this microorganism and whether all strains react similarly. The earlier finding that *F. necrophorum* filaments in response to antibiotic treatment may also require further investigation to help determine appropriate antibiotic therapies/ combinations for treatment of *F. necrophorum* infections. Finally, phagocytosis assays could be used to determine whether the filamentation phenotype in *F. necrophorum* enables it to avoid phagocytosis and aid survival (Nagl, et al., 2002), which may have implications for disease pathogenesis.

6.3. The environmental distribution of *D. nodosus* and *F. necrophorum*.

The secondary aim of this project was to use the two culture-independent methods to examine the distribution of *D. nodosus* and *F. necrophorum* in the environment, to highlight possible reservoirs of infection and material which may act as a transitory site of infection (or mode of transmission) once contaminated. Very little is known regarding the environmental distribution of *D. nodosus* and *F. necrophorum*, however it is assumed that both pathogens are transmitted indirectly from infected individual via pasture/bedding, to susceptible individual (Green and George, 2008).

Both *D. nodosus* (*rpoD*) and *F. necrophorum* (*rpoB*) were detected in a range of environmental samples, suggesting that both microorganisms are shed into the environment during an outbreak of FR. However, *F. necrophorum* was not detected as frequently in ovine faeces or soil as expected from the literature (Egerton, et al., 1969). Although, an increase in the detection limit for both faeces and soil and the increased levels of inhibition in soil samples would likely have contributed to the lack of *F. necrophorum (rpoB*) detection. Despite this, *F. necrophorum* (*rpoB*) was detected more frequently in faecal samples collected from the floor (FF) or from compacted within the ovine digits (FH), suggesting that this material becomes contaminated after defaecation and may act as a transitory vehicle of transmission, not only for *F. necrophorum*, but *D. nodosus*. This work however cannot rule out the presence of 'super-shedders' within the population.

Both *D. nodosus* (*rpoD*) and *F. necrophorum* (*rpoB*) were also detected from swabs taken from the ovine oral cavity. This was expected for *F. necrophorum*, as a coloniser of the alimentary tract and because of earlier reports (Bennett, et al., 2009). In contrast, detection of *D. nodosus* (*rpoD*) within the ovine oral cavity was not expected. *D. nodosus* (*rpoD*) load present in the oral cavity was of a similar range to that of *F. necrophorum*; a coloniser of the alimentary tract. In addition, *rpoD* load was considerably higher than that detected on the surrounding floors (concrete floor swabs), suggesting that this was not contamination solely caused by grazing contaminated pasture/straw, but a potential reservoir of infection. The oral cavity has highly anaerobic areas, such as the gingival crevices and it has been reported that more than 50 % of the microbes isolated from this region are obligate anaerobes (Socransky, et al., 1963),

indicating that this environment would be suitable for *D. nodosus* survival, if not growth. In addition, physiologically active *F. necrophorum* cells using FISH, as well as a high *rpoB* load were detected within the ovine oral cavity. Indicating that perhaps the ovine mouth is either the primary source or an additional source of *F. necrophorum* infection, rather than solely faecal material, as previously postulated (Roberts and Egerton, 1969).

6.3.1. Perspectives and future directions.

It has been suggested that *F. necrophorum* is only shed into faeces when the gut microflora are perturbed, for example, via the administration of certain oral antibiotics (Smith, et al., 1993a) or is only excreted by a very few individuals or 'super-shedders' (Smith, et al., 1991). It would be interesting to determine, therefore whether antibiotic treatment and/or diet has any effect on the shedding of *F. necrophorum* into ovine faeces over a longitudinal study or during certain times of year. In addition, increased sampling could be performed, to determine whether 'super-shedders' may exist within a flock or multiple flocks. It was also observed that a minority of sheep during sampling periods had diarrhoea (author observation) and this has been shown to increase bacterial diversity in animal faeces (Chaban, et al., 2010) it would be interesting therefore to determine whether this phenotype and/or antibiotic treatment correlates with the increased shedding of *F. necrophorum* or increased fusobacterial diversity in sheep faeces.

The detection of *D. nodosus* (*rpoD*) within the ovine oral cavity by qPCR, although not by FISH, is still an important observation, particularly as the load present within the

mouth was significantly higher than that in the surrounding environment and sometimes even present on the foot and of a similar load to *F. necrophorum* (*rpoB*) (coloniser of alimentary tract). However, it is unknown whether this microorganism is always present within the ovine oral cavity, or whether it is present only when FR is present on a farm, and the oral cavity then becomes contaminated like the surrounding environment; a longitudinal study would be required to determine this. The detection of *D. nodosus* and/or *F. necrophorum* by culture-dependent methods (if possible) and FISH combined with PMA-qPCR would provide conclusive evidence for their survival within the ovine oral cavity. In addition, understanding whether the *D. nodosus* levels fluctuate in line with the corresponding feet and/or flock health and whether the strains present on ovine feet and within the mouth are distinct or matched populations, would provide further information with regard to disease transmission. The *D. nodosus* populations present on the feet and within the ovine oral cavity could be further examined by using a newly developed MLVA assay for typing *D. nodosus* strains (Russell, et al., unpublished).

6.4. Conclusions.

In summary, the work presented in this thesis has elucidated the temporal patterns associated with *D. nodosus* and *F. necrophorum* load in relation to the initiation and development of ovine FR. The work presented here has highlighted that ID may be the most infectious stage of disease and that feet with a higher *D. nodosus* (*rpoD*) load are more likely to go on to development under-running. In order to reduce the incidence and prevalence of FR in sheep and to improve animal welfare, treatment needs to be initiated earlier. This work was further supported and strengthened by the *in situ* detection of physiologically active *D. nodosus* and *F. necrophorum* cells at the

corresponding stages. Finally, both pathogens were detected in a range of environmental samples, highlighting that faeces in particular, may act as a transitory route of transmission once contaminated and the intriguing possibility that the ovine oral cavity may act as an additional or alternative reservoir of *F. necrophorum* and *D. nodosus* infection. This study has provided an improved understanding of the population dynamics involved in the development of ovine FR by using culture-independent techniques, and the results may have implications for current control and treatment practices not only in the UK, but worldwide.

BIBLIOGRAPHY

Abbott, K. A. and Egerton, J. R. (2003). Eradication of footrot of lesser clinical severity (intermedite footrot). Australian Veterinary Journal. **81** (11): 688-693.

Abbott, K. A. and Lewis, C. J. (2005). Current approaches to the management of ovine footrot. Veterinary Journal **169**: 28-41.

Abramoff, M. D., Magalhaes, P. J. and Ram, S. J. (2004). Image Processing with ImageJ. Biophotonics International. **11** (7): 36-42.

Adriaans, B. and Drasar, B. S. (1987). The isolation of fusobacteria from tropical ulcers. Epidemiology and Infection. **99**: 361-372.

Agosta, S. J., Janz, N. and Brooks, D. R. (2010). How specialists can be generalists: resolving the "parasite paradox" and implications for emerging infectious disease. Zoologia. **27** (2): 151-162.

Ainsworth, T. D., Fine, M., Blackall, L. L. and Hoegh-Guldberg, O. (2006). Fluorescence *in situ* hybridization and spectral imaging of coral-associated bacterial communities. Applied and Environmental Microbiology. **72** (4): 3016-3020.

Alfreider, A., Pernthaler, J., Amann, R., Sattler, B., Wille, A. and Psenner, R. (1996). Community analysis of the bacterial assemblages in the winter cover and pelagic layers of a high mountain lake by *in situ* hybridization. Applied and Environmental Microbiology. **62** (6): 2138-2144.

Aliyu, S. H., Marriott, R. K., Curran, M. D., Parmar, S., Bentley, N., Brown, N. M, Brazier, J. S. and Ludlam, H. (2004). Real-time PCR investigation into the importance of *Fusobacterium necrophorum* as a cause of acute pharyngitis in general practice. Journal of Medical Microbiology. **53** (10): 1029-1035.

Alm, E. W., Oerther, D. B., Larsen, N., Stahl, D. A. and Raskin, L. (1996). The oligonucleotide probe database. Applied and Environmental Microbiology. **62** (10): 3557-3559.

Altmann, D., Stief, P., Amann, R., de Beer, D. D. and Schramm, A. (2003). Brief report *in situ* distribution and activity of nitrifying bacteria in freshwater sediment. Environmental Microbiology. **5**: 798-803.

Altschul, S. F., Madden, T. L., Schaffer, A. A., Zhang, J., Zhang, Z., Miller, W. and Lipman, D. J. (1997). Gapped BLAST and PSI-BLAST: a new generation of protein database search programs. Nucleic Acids Research. **23** (17): 3389-3402.

Amann, R. I., Krumholz, L. and Stahl, D. A. (1990). Fluorescent-oligonucleotide probing of whole cells for determinative, phylogenetic, and environmental studies in microbiology. Journal of Bacteriology. **172** (2): 762-770.

Amann, R. and Fuchs, B. M. (2008). Single-cell identification in microbial communities by improved fluorescence *in situ* hybridization techniques. Nature Reviews Microbiology. **6** (5): 339-348.

Anderson, P. and Kedersha, N. (2002). Stressful initiations. Journal of Cell Science. **115** (16): 3227-3234.

Apostolou, E., Pelto, L., Kirjavainen, P. V., Isolauri, E., Salminen, S. J. and Gibson, G. R. (2001). Differences in the gut bacterial flora of healthy and milk-hypersensitive adults, as measured by fluorescence *in situ* hybridization. FEMS Immunology and Medical Microbiology. **30**: 217-221.

Artz, L. A., Kempf, V. A. J. and Autenrieth, I. B. (2003). Rapid screening for *Streptococcus agalactiae* in vaginal specimens of pregnant women by fluorescent *in situ* hybridization. Journal of Clinical Microbiology. **41** (5): 2170-2173.

Arya, M., Shergill, I. S., Williamson, M., Gommersall, L., Arya, N. and Patel, H. R.

H. (2005). Basic principles of real-time quantitative PCR. Expert Review of Molecular Diagnostics. **5** (2): 209-219.

Barrila, J., Radtke, A. L., Crabbé, A., Sarker, S. F., Herbst-Kralovetz, M. M., Ott, C. M. and Nickerson, C. A. (2010). Organotypic 3D cell culture models: using the rotating wall vessel to study host-pathogen interactions. Nature Reviews. Microbiology. **8** (11): 791-801.

Bartosch, S., Fite, A., Macfarlane, G. T. and McMurdo, M. E. T. (2004). Characterization of bacterial communities in feces from healthy elderly volunteers and hospitalized elderly patients by using real-time PCR and effects of antibiotic treatment on the fecal microbiota. Applied and Environmental Microbiology. **70** (6): 3575-3581.

Barza, M., Giuliano, M., Jacobus, N. V. and Gorbach, S. L. (1987). Effect of broad-spectrum parenteral antibiotics on "colonization resistance" of intestinal microflora of humans. Antimicrobial Agents and Chemotherapy. **31** (5): 723-727.

Baschong, W., Suetterlin, R. and Laeng, R. H. (2001). Control of autofluorescence of archival formaldehyde-fixed paraffin-embedded tissue in confocal laser scanning microscopy (CLSM). Journal of Histochemistry and Cytochemistry. **49** (12): 1565-1571.

Behrens, S., Rüland, C., Inacio, J., Huber, H., Fonseca, A., Spencer-Martins, I., Fuchs, B. M. and Amann, R. (2003). *In situ* accessibility of small-Subunit rRNA of members of the domains Bacteria, Archaea, and Eucarya to Cy3-labeled oligonucleotide probes. Applied and Environmental Microbiology. **69** (3): 1748-1758.

Bennett, G., Hickford, J., Sedcole, R. and Zhou, H. (2009). *Dichelobacter nodosus*, *Fusobacterium necrophorum* and the epidemiology of footrot. Anaerobe. **15** (4): 173-176.

Beveridge, W. I. B. (1941). Foot-rot in sheep: a transmissable disease due to infection

with *Fusiformis nodosus* (n. sp.): studies on its cause, epidemiology and control. CSIRO Australian Bulletin. **140**: 1-56.

Bhat, M. A., Wani, S. A., Hussain, I., Magray, S. N. and Muzafar, M. (2012). Identification of two new serotypes within serogroup B of *Dichelobacter nodosus*. Anaerobe. **18** (1): 91-95.

Billington, S. J., Johnston, J. L. and Rood, J. I. (1996). Virulence regions and virulence factors of the ovine footrot pathogen, *Dichelobacter nodosus*. FEMS Microbiology Letters. **145** (2): 147-156.

Boye, M., Aalbaek, B. and Agerholm, J. S. (2006). *Fusobacterium necrophorum* determined as abortifacient in sheep by laser capture microdissection and fluorescence *in situ* hybridization. Molecular and Cellular Probes. **20** (6): 330-336.

Buller, N. (2005). "Molecular epidemiology, clonality and virulence of *Dichelobacter nodosus,* the agent of ovine footrot." PhD thesis, University of Murdoch, Australia.

Buttner, M. P., Cruz-Perez, P. and Stetzenbach, L. D. (2001). Enhanced detection of surface-associated bacteria in indoor environments by quantitative PCR. Applied and Environmental Microbiology. **67** (6): 2564-2570.

Bythell, J. C., Barer, M. R., Cooney, R. P., Guest, J. R., O'Donnell, A. G., Pantos, O. and Le Tissier, M. D. A. (2002) Histopathological methods for the investigation of microbial communities associated with disease lesions in reef corals. Letters in Applied Microbiology. **34** (5): 359-364.

Caldwell, D. E., Korber, D. R. and Lawrence, J. R. (1992). Imaging of bacterial cells by fluorescence exclusion using scanning confocal laser microscopy. Journal of Microbiological Methods. **15** (4): 249-261.

Calvo-Bado, L. A., Green, L. E., Medley, G. F., Ul-Hassan, A., Grogono-Thomas, R., Buller, N., Kaler, J., Russell, C. L., Kennan, R. M., Rood, J. I. and Wellington,

E. M. H. (2011a). Detection and diversity of a putative novel heterogeneous polymorphic proline-glycine repeat (Pgr) protein in the footrot pathogen *Dichelobacter nodosus*. Veterinary Microbiology. **147**: 358-366.

Calvo-Bado, L. A., Oakley, B. B., Dowd, S. E., Green, L. E., Medley, G. F., Ul-Hassan, A., Bateman, V., Gaze, W., Witcomb, L., Grogono-Thomas, R., Kaler, J., Russell, C. L. and Wellington, E. M. H. (2011b). Ovine pedomics: the first study of the ovine foot 16S rRNA-based microbiome. The ISME Journal. **5** (9): 1426-1437.

Canham, P. B. (1970). The minimum energy of bending as a possible explanation of the biconcave shape of the human red blood cell. Journal of Theoretical Biology. **26** 61-81.

Cartlet, J., Jarlier, V., Harbarth, S., Voss, A., Goossens, H., Pittet, D. and the Participants of the 3rd World Heathcare-Associated Infections Forum. (2012). Ready for a world without antibiotics? The Pensières Antibiotic Resistance Call to Action. Antimicrobial Resistance and Infection Control. **1**: 11.

Case, R. J., Boucher, Y., Dahllöf, I., Holmström, C., Doolittle, W. F. and Kjelleberg, S. (2007). Use of 16S rRNA and *rpoB* genes as molecular markers for microbial ecology studies. Applied and Environmental Microbiology. **73** (1): 278-288.

Castillo, M., Martín-Orúe, S. M., Manzanilla, E. G., Badiola, I., Martín, M. and Gasa, J. (2006). Quantification of total bacteria, enterobacteria and lactobacilli populations in pig digesta by real-time PCR. Veterinary Microbiology. **114**: 165-170.

Chaban, B., Ngeleka, M. and Hill, J.E. (2010). Detection and quantification of 14 Campylobacter species in pet dogs reveals in an increase in species richness in feces of diarrheic animals. BMC Microbiology. **10**: 73.

Chabert, P., Flandrin, P. and Huzard, J. B. (1791). Instructions et observations sur les maladies des animaux domestiques. Veuve Vallat-la-Chapelle, Paris, France. Cited

by Buller, N. (2005). “Molecular epidemiology, clonality and virulence of *Dichelobacter nodosus,* the agent of ovine footrot.” PhD thesis, University of Murdoch, Australia.

Chamberlain, A. N., Halablab, M. A., Gould, D. J. and Miles, R. J. (1997). Distribution of bacteria on hands and the effectiveness of brief and thorough decontamination procedures using non-medicated soap. Zentralblatt für Bakteriologie: International Journal of Medical Microbiology, Virology, Parasitology and Infectious Diseases. **285**: 565-575.

Cheetham, B. F., Tattersall, D. B., Bloomfield, G. A., Rood, J. I. and Katz, M. E. (1995). Identification of a gene encoding a bacteriophage-related integrase in a *vap* region of the *Dichelobacter nodosus* genome. Gene. **162**: 53-58.

Cheetham, B. F., Tanjung, L. R., Sutherland, M., Druitt, J., Green, G., McFarlane, J., Bailey, G. D., Seaman, J. T. and Katz, M. E. (2006). Improved diagnosis of virulent ovine footrot using the *intA* gene. Veterinary Microbiology. **116** (1-3): 166-174.

Christie-Oleza, J. A., Fernandez, B., Nogales, B., Bosch, R. and Armengaud, J. (2012). Proteomic insights into the lifestyle of an environmentally relevant marine bacterium. The ISME Journal. **6**: 124-135.

Chua, A. S. M., Onuki, M., Satoh, H. and Mino, T. (2006). Examining substrate uptake patterns of *Rhodocyclus*-related PAO in full-scale EBPR plants by using the MAR-FISH technique. Water Science and Technology. **54** (1): 63-70.

Chukurian, C. J. (2009). Method of the Histochemical Stains & Diagnostic Application. [online]. Available at: <http://www.urmc.rochester.edu/path/zqu/StainsManual/index.html>. [Accessed 11 June 2010].

Claxton, P. D., Ribeiro, L. A. and Egerton, J. R. (1983). Classification of *Bacteroides nodosus* by agglutination tests. Australian Veterinary Journal. **60** (11): 331-334.

Claxton, P. D. (1989). Antigenic classification of *Bacteroides nodosus*. In: Egerton, J.R., Yong, W. K. and Riffkin, G. G., eds (2004). Footrot and foot abscess of ruminants. CRC Press, Boca Raton. 155-166.

Contreras, P. J., Urrutia, H., Sossa, K. and Nocker, A. (2011) Effect of PCR amplicon length on suppressing signals from membrane-compromised cells by propidium monoazide treatment. Journal of Microbiological Methods. **87** (1): 89-95.

Cross, R. F. (1978). Influence of environmental factors on transmission of ovine contagious foot rot. Journal of the American Veterinary Medical Association. **173**: 1567-1568.

Daims, H., Brühel, A., Amann, R., Schleifer, K.-H. and Wagner, M. (1999). The domain-specific probe EUB338 is insufficient for the detection of all bacteria: development and evaluation of a more comprehensive probe set. Systematic and Applied Microbiology. **22**: 434-444.

Daims, H., Lücker, S. and Wagner, M. (2006). daime, a novel image analysis program for microbial ecology and biofilm research. Environmental Microbiology. **8** (2): 200-213.

Darveau, R. P. (2010). Periodontitis: a polymicrobial disruption of the host homeostasis. Nature Reviews Microbiology. **8**: 481-490.

Davenport, R. J. and Curtis, T. P. (2004). Quantitative fluorescence *in situ* hybridisation (FISH): statistical methods for valid cell counting. In: G. A. Kowalchuk, F. J. de Bruijn, I. M. Head, A. D. Akkermans and J. D. van Elsas, eds. (2004). Molecular Microbial Ecology Manual (volume 1). New York: Springer. 1487-1516.

Davies, C. E., Hill, K. E., Newcombe, R. G., Stephens, P., Wilson, M. J., M.R.C. Path, Harding, K. G., FRCS and Thomas, D. W. (2007). A prospective study of the

microbiology of chronic venous leg ulcers to reevaluate the clinical predictive value of tissue biopsies and swabs. Wound Repair and Regeneration. **15**: 17-22.

de Gasparin, A.-E.-P. (1821) Des maladies contagieuses des bêtes á laine. Huzard, Paris, France. Cited by Buller, N. (2005). "Molecular epidemiology, clonality and virulence of *Dichelobacter nodosus,* the agent of ovine footrot." PhD thesis, University of Murdoch, Australia.

Degraves, F. J., Gao, D. and Kaltenboeck, B. (2003) High-sensitivity quantitative PCR Platform. BioTechniques. **34**: 106-115.

Depiazzi, L. J., Richards, R. B., Henderson, J., Rood, J. I., Palmer, M. and Penhale, W. J. (1991). Characterisation of virulent and benign strains of *Bacteroides nodosus*. Veterinary Microbiology. **26**: 151-160.

Depiazzi, L. J., Roberts, W. D., Hawkins, C. D., Palmer, M. A., Pitman, D. R., McQuade, N. C., Jelinek, P. D., Devereaux, D. J. and Rippon, R. J. (1998) Severity and persistence of footrot in Merino sheep experimentally infected with a protease thermostable strain of *Dichelobacter nodosus* at five sites. Australian Veterinary Journal. **76** (1): 32-38.

Dewhirst, F. E., Paster, B. J., La Fontaine, S. and Rood, J. I. (1990). Transfer of *Kingella indologenes* (Snell and Lapage 1976) to the genus *Suttonella* gen. nov. as *Suttonella indologenes* comb. nov.; transfer of *Bacteroides nodosus* (Beveridge 1941) to the genus *Dichelobacter* gen. nov. as *Dichelobacter nodosus* comb. nov.; and assignment of the genera *Cardiobacterium*, *Dichelobacter*, and *Suttonella* to *Cardiobacteriaceae* fam. nov. in the gamma division of *Proteobacteria* based on 16S ribosomal ribonucleic acid sequence comparisons. International Journal of Bacteriology. **40**: 426-433.

Dhungyel, O. P., Lehmann, D. R. and Whittington, R. J. (2008). Pilot trials in

Australia on eradication of footrot by flock specific vaccination. Veterinary Microbiology. **132** (3-4): 364-371.

Dhungyel, O. P. and Whittington, R. J. (2009). Modulation of inter-vaccination interval to avoid antigenic competition in multivalent footrot (*Dichelobacter nodosus*) vaccines in sheep. Vaccine. **28** (2): 470-473.

Domann, E., Hong, G., Imirzalioglu, C., Turschner, S., Kühle, J., Watzel, C., Hain, T., Hossain, H. and Chakraborty, T. (2003) Culture-independent identification of pathogenic bacteria and polymicrobial infections in the genitourinary tract of renal transplant recipients. Journal of Clinical Microbiology. **41** (12): 5500-5510.

Dormans, J., Burger, M., Aguilar, D., Hernandez-Pando, R., Kremer, K., Roholl, P., Arend, S. M. and van Soolingen, D. (2004) Correlation of virulence, lung pathology, bacterial load and delayed type hypersensitivity responses after infection with different *Mycobacterium tuberculosis* genotypes in a BALB/c mouse model. Clinical and Experimental Immunology. **137**: 460-468.

Dorsch, M., Love, D. N. and Bailey, G. D. (2001). *Fusobacterium equinum* sp. nov., from the oral cavity of horses. International Journal of Systematic and Evolutionary Microbiology. **51**: 1959-1963.

Dykhuizen, D. and Davies, M. (1980). An experimental model: bacterial specialists and generalists competing in chemostats. Ecology. **61** (5): 1213-1227.

EBLEX Ltd. (2008). EBLEX Sheep Manual 7: Target Lameness for Better Returns. [online]. Available at: <http://www.eblex.org.uk/documents/content/returns/brp_1_sheepsbrp_manual_7_-_target__lameness_for_better_returns.pdf> [Accessed 12 January 2011].

Edwards, A. M., Dymock, D. and Jenkinson, H. F. (2003), From tooth to hoof: treponemes in tissue-destructive diseases. Journal of Applied Microbiology. **94**:

767-780.

Edwards, J. E., McEwan, N. R., McKain, N., Walker, N. and Wallce, R. J. (2005). Influence of flavomycin on ruminal fermentation and microbial populations in sheep. Microbiology. **151**: 717-725.

Egerton, J. R. and Parsonson, I. M. (1966). Parenteral antibiotic treatment of ovine footrot. Australian Veterinary Journal. **42** (3): 97-98.

Egerton, J. R., Roberts, D. S. and Parsonson, I. M. (1969). The aetiology and pathogenesis of ovine foot-rot. I. A histological study of the bacterial invasion. Journal of Comparative Pathology. **79**: 207-217.

Egerton, J. R. and Burrell, D. H. (1970). Prophylactic and therapeutic vaccination against ovine foot-rot. Australian Veterinary Journal. **46** (11): 517-522.

Egerton, J. R. and Roberts, D. S. (1971). Vaccination against ovine foot-rot. Journal of Comparative Pathology. **81**: 179-185.

Egerton, J. R. (1973). Surface and somatic antigens of *Fusiformis nodosus*. Journal of Comparative Pathology. **83**: 151-159.

Egerton, J. R. (1989). Footrot of cattle, goats and deer. In: Egerton J. R., Yong, W. K. and Riffkin, G.G., eds. (1989). Footrot and foot abscess of ruminants. CRC Press, Boca Raton. 47-56.

Egerton, J. R. , Ghimire, S. C., Dhungyel, O. P., Shrestha, H. K., Joshi, H. D., Joshi, B. R., Abbott, K. A. and Kristo, C. (2002). Eradication of virulent footrot from sheep and goats in an endemic area of Nepal and an evaluation of specific vaccination. Veterinary Record. **151**: 290-295.

Eickhorst, T. and Tippkötter, R. (2008). Improved detection of soil microorganisms using fluorescence *in situ* hybridization (FISH) and catalyzed reporter deposition (CARD-FISH). Soil Biology and Biochemistry. **40**: 1883-1891.

Elias, P. M. (2005). Stratum corneum defensive functions: an integrated view. The Journal of Investigative Dermatology. **125**: 183-200.

Evans, N. J., Brown, J. M., Demirkan, I., Singh, P., Getty, B., Timofte, D., Vink, W. D., Murray, R. D., Blowey, R. W., Birtles, R. J., Hart, C. A. and Carter, S. D. (2009). Association of unique, isolated treponemes with bovine digital dermatitis lesions. Journal of Clinical Microbiology. **47** (3): 689-696.

Falkow, S. (2004). Molecular Koch's postulates applied to bacterial pathogenicity - a personal recollection 15 years later. Nature Reviews Microbiology. **2**: 67-72.

Fitzpatrick, J., Scott, M. and Nolan, A. (2006). Assessment of pain and welfare in sheep. Small Ruminant Research. **62**: 55-61.

Fredricks, D. N., Fiedler, T. L., Thomas, K. K., Mitchell, C. M. and Marrazzo, J. M. (2009). Changes in vaginal bacterial concentrations with intravaginal metronidazole therapy for bacterial vaginosis as assessed by quantitative PCR. Journal of Clinical Microbiology. **47** (3): 721-726.

Freedman, D. (1997). From association to causation via regression. Advances in Applied Mathematics. **18**: 59-110.

Fuchs, B. M., Wallner, G., Beisker, W., Schwippl, I., Ludwig, W., and Amann, R. (1998). Flow cytometric analysis of the *in situ* accessibility of *Escherichia coli* 16S rRNA for fluorescently labeled oligonucleotide probes. Applied and Environmental Microbiology. **64** (12): 4973-4982.

Fujita, H., Eishi, Y., Ishige, I., Saitoh, K., Takizawa, T., Arima, T. and Koike, M. (2002). Quantitative analysis of bacterial DNA from *Mycobacteria* spp., *Bacteroides vulgatus*, and *Escherichia coli* in tissue samples from patients with inflammatory bowel diseases. Journal of Gastoenterology. **37** (7): 509-516.

Gaffar, F. R., Franssen, F. F. J. and Vries, E. D. (2003). *Babesia bovis* merozoites

invade human, ovine, equine, porcine and caprine erythrocytes by a sialic acid-dependent mechanism followed by developmental arrest after a single round of cell fission. International Journal for Parasitology. **33**: 1595-1603.

Ganter, R. (2008). Veterinary consultancy and health schemes in sheep: Experiences and reflections from a local German outlook. Small Ruminant Research. **76**: 55-67.

Garcia, M. M., Neil, D. H. and McKay, K. A. (1971). Application of immunofluorescence to studies of the ecology of *Sphaerophorus necrophorus*. Applied Microbiology. **21** (5): 809-814.

Ghimire, S. C., Egerton, J. R., Dhungyel, O. P. and Joshi, H. D. (1998). Identification and characterisation of serogroup M among Nepalese isolates of *Dichelobacter nodosus*, the transmitting agent of footrot in small ruminants. Veterinary Microbiology. **62**: 217-233.

Ghimire, S. C., Egerton, J. R. and Dhungyel, O. P. (1999). Transmission of virulent footrot between sheep and goats. Australian Veterinary Journal. **77** (7): 450-453.

Ghimire, S. C. and Egerton, J. R. (1999). PCR-RFLP of outer membrane proteins gene of *Dichelobacter nodosus*: a new tool in the epidemiology of footrot. Epidemiology and Infection. **122**: 521-528.

Giovannoni, S. J., DeLong, E. F., Olsen, G. J. and Pace, N. R. (1988). Phylogenetic group-specific oligodeoxynucleotide probes for identification of single microbial cells. Journal of Bacteriology. **170** (2): 720-726.

Giuliano, M., Barza, M., Jacobus, V. and Gorbach, S. L. (1987). Effect of broad-spectrum parenteral antibiotics on composition of intestinal microflora of humans. Antimicrobial Agents and Chemotherapy. **31** (2): 202-206.

Glöckner, F. O., Amann, R., Alfreider, A., Pernthaler, J., Psenner, R., Trebesius, K. and Schleifer, K.-H. (1996). An *in situ* hybridization protocol for detection and

identification of planktonic bacteria. Systematic and Applied Microbiology. **19** (3): 403-406.

Goddard, P., Waterhouse, T., Dwyer, C. and Stott, A. (2006). The perception of the welfare of sheep in extensive systems. Small Ruminant Research. **62** (3): 215-225.

Gohier, J. B. (1813-1816) Mémoires et observations sur la chirurgie et la médecine vétérinaires. Chez Lions, Lyon, France. Cited by Buller, N. (2005). "Molecular epidemiology, clonality and virulence of *Dichelobacter nodosus,* the agent of ovine footrot." PhD thesis, University of Murdoch, Australia.

Gorbach, S. L. and Bartlett, J. G. (1974). Anaerobic infections (part II). New England Journal of Medicine. **290**: 1237-1245.

Gradin, J. L. and Schmitz, J. A. (1977). Selective medium for isolation of *Bacteroides nodosus*. Journal of Clinical Microbiology. **6** (3): 298-302.

Gradin, J. L., Sonn, A. E. and Petrovska, L. (1993). Serogrouping of Bacteroides nodosus isolates from 62 sources in the United States. American Journal of Veterinary Research. **54** (7): 1069- 1073.

Graham, N. P. H. and Egerton, J. R. (1968) Pathogenesis of ovine foot-rot: the role of some environmental factors. Australian Veterinary Journal. **44** (5): 235-240.

Green, L. E., Wassink, G. J., Grogono-Thomas, R., Moore, L. J. and Medley, G. F. (2007). Looking after the individual to reduce disease in the flock: a binomial mixed effects model investigating the impact of individual sheep management of footrot and interdigital dermatitis in a prospective longitudinal study on one farm. Preventive Veterinary Medicine. **78**: 172-178.

Green, L. E. and George, T. R. N. (2008). Assessment of current knowledge of footrot in sheep with particular reference to *Dichelobacter nodosus* and implications for elimination or control strategies for sheep in Great Britain. The Veterinary Journal. **175**:

173-180.

Green, L. E. and Kaler, J. (2011). A clinical trial comparing oxytetracycline, foot trimming and fluxixine meglumine on time to recovery in sheep with footrot. Livestock. **1**: 44-48.

Grogono-Thomas, R., Wilsmore, A. J., Simon, A. J. and Izzard, K. A. (1994). The use of long-acting oxytetracycline for the treatment of ovine footrot. British Veterinary Journal. **150**: 561-568.

Grogono-Thomas, R. and Johnston, A. M. (1997). A study of ovine lameness. MAFF Final Report. MAFF open contract OC59 45K. London, DEFRA Publications.

Gursoy, U. K., Könönen, E. and Uitto, V.-J. (2008). Intracellular replication of fusobacteria requires new actin filament formation of epithelial cells. APMIS: acta pathologica, microbiologica, et immunologica Scandinavica: **116** (12): 1063-1970.

Gurung, R. B., Dhungyel, O. P., Tshering, P. and Egerton, J. R. (2006). The use of an autogenous *Dichelobacter nodosus* vaccine to eliminate clinical signs of virulent footrot in a sheep flock in Bhutan. The Veterinary Journal. **172**: 356-363.

Hackett, S. J., **Guiver, M., Marsh, J., Sills, J. A., Thomson, A. P. J., Kaczmarski, E. B. and Hart, C. A.** (2002). Meningococcal bacterial DNA load at presentation correlates with disease severity. Archives of Disease in Childhood. **86**: 44-46.

Hagedorn, T. (2007). [photograph]. Winning the war on sheep footrot. Sheep Canada. 5-9.

Hall, V., Duerden, B. I., Magee, J. T., Ryley, H. C. and Brazier, J. S. (1997). A comparative study of *Fusobacterium necrophorum* strains from human and animal sources by phenotypic reactions, pyrolysis mass spectrometry and SDS-PAGE. Journal of Medical Microbiology. **46**: 865-871.

Han, X., Kennan, R. M., Parker, D., Davies, J. K. and Rood, J. I. (2007). Type IV

fimbrial biogenesis is required for protease secretion and natural transformation in *Dichelobacter nodosus*. Journal of Bacteriology. **189** (14): 5022-5033.

Han, X., Kennan, R. M., Davies, J. K., Reddacliff, L. A., Dhungyel, O. P., Whittington, R. J., Turnbull, L., Whitchurch, C. B. and Rood, J. I. (2008). Twitching motility is essential for virulence in *Dichelobacter nodosus*. Journal of Bacteriology. **190** (9): 3323-3335.

Handeland, K., Boye, M., Bergsjø, B., Bondal, H., Isaksen, K. and Agerholm, J. S. (2010). Digital necrobacillosis in Norwegian wild tundra reindeer (*Rangifer tarandus tarandus*). Journal of Comparative Pathology. **143** (1): 29-38.

Harmsen, H. J. M., Gibson, G. R., Elfferich, P., Raangs, G. C., Wildeboer-veloo, A. C. M., Argaiz, A., Roberfroid, M. B. and Welling, G. W. (1999). Comparison of viable cell counts and fluorescence *in situ* hybridization using specific rRNA-based probes for the quantification of human fecal bacteria. FEMS Microbiology Letters. **183** 125-129.

Harro, J. M., Peters, B. M., O'May, G. A., Archer, N., Kerns, P., Prabhakara, R. and Shirtliff, M. E. (2010). Vaccine development in *Staphylococcus aureus*: taking the biofilm phenotype into consideration. FEMS Immunology and Medical Microbiology, **59**: 306-323.

Hill, A. B. (1965). The environment and disease: association or causation? Journal of the Royal Society of Medicine. **58**: 295-300.

Hill, A. T., Campbell, E. J., Hill, S. L., Bayley, D. L. and Stockley, R. A. (2000). Association between airway bacterial load and markers of airway inflammation in patients with stable chronic bronchitis. The American Journal of Medicine. **109**: 288-295.

Hill, A. E., Dhungyel, O. P. and Whittington, R. J. (2010). Diagnostic sampling

strategies for virulent ovine footrot: simulating detection of *Dichelobacter nodosus* serogroups for bivalent vaccine formulation. Preventive Veterinary Medicine. **95** (1-2): 127-136.

Hoffmann, F., Rapp, H. T. and Reitner, J. (2006). Monitoring microbial community composition by fluorescence *in situ* hybridization during cultivation of the marine cold-water sponge *Geodia barretti*. Marine Biotechnology. **8** (4): 373-379.

Hofstad, T. O. R. (2006). The Genus *Fusobacterium*. Prokaryotes. **7**: 1016-1027.

Humphrey, S., MacVicar, T., Stevenson, A., Roberts, M., Humphrey, T. J. and Jepson, M. A. (2011). SulA-induced filamentation in *Salmonella enterica* serovar Typhimurium: effects on SPI-1 expression and epithelial infection. Journal of Applied Microbiology. **111**: 185-196.

Hughes, L. A., Williams, N., Clegg, P., Callaby, R., Nuttall, T., Coyne, K., Pinchbeck, G. and Dawson, S. (2012). Cross-sectional survey of antimicrobial prescribing patterns in UK small animal veterinary practice. Preventive Veterinary Medicine. **104**: 309-316.

Hunt, J. D., Brown, L. E., Wood, P. R., Stewart, D. J. and Jackson, D. C. (1996). Manipulation of the helper T cell response to influence antigenic competition occurring with a multivalent vaccine. Immunology and Cell Biology. **74**: 81-89.

Hurtado, M. a., Píriz, S., Valle, J., Jimenez, R. and Vadillo, S. (1998). Aetiology of ovine footrot in Spain. The Veterinary Record. **142**: 60-63.

Inácio, J., Ludwig, W., Spencer-Martins, I. and Fonseca, A. (2010). Assessment of phylloplane yeasts on selected Mediterranean plants by FISH with group- and species-specific oligonucleotide probes. FEMS Microbiology Ecology. **71** (1): 61-72.

Inoue, T., Kanoe, M., Goto, N., Matsumura, K. and Nakano, K. (1985). Chemical and biological properties of lipopolysaccharides from *Fuobacterium necrophorum*

biovar A and biovar B strains. Japanese Journal of Veterinary Science. **47** (4): 639-645.

Issekutz, A. C., Movat, K. W. and Movat, H. Z. (1980). Enhanced vascular permeability and haemorrhage-inducing activity of zymosan-activated plasma. Clinical and Experimental Immunology. **41** (3): 505-511.

Janczyk, P., Piper, R., Souffrant, W. B., Bimczok, D., Rothkotter, H.-J. and Smidt, H. (2007). Parenteral long-acting amoxicillin reduces intestinal bacterial community diversity of piglets even 5 weeks after the administration. The ISME Journal. **1**: 180-183.

Jaton, K., Bille, J. and Greub, G. (2006). A novel real-time PCR to detect *Chlamydia trachomatis* in first-void urine or genital swabs. Journal of Medical Microbiology. **55** 1667-1674.

Jiménez, R., Píriz, S., Martin-Palomino, P., Mateos, E. and Vadillo, S. (2003). Aetiology of ovine footrot in the Portuguese region of Alto Alentejo. Journal of Veterinary Medicine, Series B. **50** (3): 118-120.

Jiménez, R., Píriz, S., Mateos, E. and Vadillo, S. (2004). Minimum inhibitory concentrations for 25 selected antimicrobial agents against *Dichelobacter nodosus* and *Fusobacterium* strains isolated from footrot in sheep of Portugal and Spain. Journal of Veterinary Medicine. **51**: 245-248.

Johnson, I. and Spence, M. T. Z. (2010). Molecular Probes Handbook, A Guide to Fluorescent Probes and Labeling Technologies. [online] Available at: <http:// www.invitrogen.com/site/us/en/home/References/Molecular-Probes-The-Handbook.html> [Accessed 23 September 2011].

Jørgensen, F., Stephens, P. J. and Knøchel, S. (1995). The effect of osmotic shock and subsequent adaptation on the thermotolerance and cell morphology of *Listeria monocytogenes*. Journal of Applied Microbiology. **79** (3): 274-281.

Justice, S. S., Hung, C., Theriot, J. A., Fletcher, D. A., Anderson, G. G., Footer, M. J. and Hultgren, S. J. (2004). Differentiation and developmental pathways of uropathogenic *Escherichia coli* in urinary tract pathogenesis. Proceedings of the National Academy of Sciences. **101** (5): 1333-1338.

Justice, S. S., Hunstad, D. A., Seed, P. C. and Hultgren, S. J. (2006). Filamentation by *Escherichia coli* subverts innate defenses during urinary tract infection. Proceedings of the National Academy of Sciences. **103** (52): 19884-19889.

Justice, S. S., Hunstad, D. A., Cegelski, L. and Hultgren, S. J. (2008). Morphological plasticity as a bacterial survival strategy. Nature Reviews Microbiology. **6** (2): 162-168.

Kaler, J. and Green, L. E. (2008). Naming and recognition of six foot lesions of sheep using written and pictorial information: a study of 809 English sheep farmers. Preventive Veterinary Medicine. **83** (1): 52-64.

Kaler, J. and Green, L. E. (2009). Farmers' practices and factors associated with the prevalence of all lameness and lameness attributed to interdigital dermatitis and footrot in sheep flocks in England in 2004. Preventive Veterinary Medicine. **92**: 52-59.

Kaler, J., Medley, G. F., Grogono-Thomas, R., Wellington, E. M. H., Calvo-Bado, L. A., Wassink, G. J., King, E. M., Moore, L. J., Russell, C. and Green, L. E. (2010). Factors associated with changes of state of foot conformation and lameness in a flock of sheep. Preventive Veterinary Medicine. **97**: 237-244.

Kaler, J., George, T. R. N. and Green, L. E. (2011). Why are sheep lame? Temporal associations between severity of foot lesions and severity of lameness in 60 sheep. Animal Welfare. **20**: 433-438.

Kaler, J., Wani, S. A., Hussain, I., Beg, S. A., Makhdoomi, M., Kabli, Z. A. and Green, L. E. (2012). A clinical trial comparing parenteral oxytetracyline andenrofloxacin on time to recovery in sheep lame with acute or chronic footrot in

Kashmir, India. BMC Veterinary Research. **8**: 1-7.

Katz, M. E., Wright, C. L., Gartside, T. S., Cheetham, B. F., Doidge, C. V., Moses, E. K. and Rood, J. I. (1994). Genetic organization of the duplicated *vap* region of the *Dichelobacter nodosus* genome. Journal of Bacteriology. **176** (9): 2663-2669.

Kawaji, S., Begg, D. J., Plain, K. M. and Whittington, R. J. (2011). A longitudinal study to evaluate the diagnostic potential of a direct faecal quantitative PCR test for Johne's disease in sheep. Veterinary Microbiology. **148**: 35-44.

Kemp, P. F., Lee, S. and LaRoche, J. (1993). Estimating the growth rate of slowly growing marine bacteria from RNA content. Applied and Environmental Microbiology, **59** (8): 2594-2601.

Kennan, R. M., Dhungyel, O. P., Whittington, R. J., Egerton, J. R. and Rood, J. I. (2001). The Type IV fimbrial subunit gene (*fimA*) of *Dichelobacter nodosus* is essential for virulence, protease secretion, and natural competence. Journal of Bacteriology. **183** (15): 4451-4458.

Kennan, R. M., Dhungyel, O. P., Whittington, R. J., Egerton, J. R. and Rood, J. I. (2003). Transformation-mediated serogroup conversion of *Dichelobacter nodosus*. Veterinary Microbiology. **92** (1-2): 169-178.

Kennan, R. M., Wong, W., Dhungyel, O. P., Han, X., Wong, D., Parker, D., Rosado, C. J., Law, R. H. P., McGowan, S., Reeve, S. B., Levina, V., Powers, G. A., Pike, R. N., Bottomley, S. P., Smith, A. I., Marsh, I., Whittington, R. J., Whisstock, J. C., Porter, C. J. and Rood, J. I. (2010). The subtilisin-like protease AprV2 is required for virulence and uses a novel disulphide-tethered exosite to bind substrates. PLoS Pathogens. **6** (11): e1001210.

Klitgaard, K., Boye, M., Capion, N. and Jensen, T. K. (2008) Evidence of multiple *Treponema* phylotypes involved in bovine digital dermatitis as shown by 16S rRNA

gene analysis and fluorescence *in situ* hybridization. Journal of Clinical Microbiology. **46** (9): 3012-3020.

Knoblaugh, S., Randolph-Habecker, J. and Rath, S. (2011). Necropsy and Histology. In: P. M. Treuting, S. M. Dintzis, C. W. Frevert, D. Liggitt and K. S. Montine, eds. (2011). Comparative Anatomy and Histology, A Mouse and Human Atlas. London, UK: Academic Press. 15-37.

Kobayashi, H., Oethinger, M., Tuohy, M. J., Hall, G. S. and Bauer, T. W. (2009). Improving clinical significance of PCR: use of propidium monoazide to distinguish viable from dead *Staphylococcus aureus* and *Staphylococcus epidermidis*. Journal of Orthopaedic Research. **27** (9): 1243-1247.

Kobayashi, K., Sudiarta, I. P., Kodama, T., Fukushima, T., Ara, K., Ozaki, K. and Sekiguchi, J. (2012). Identification and characterization of a novel polysaccharide deacetylase C (Pda C). Journal of Biological Chemistry. **287**: 9765-9776.

Kolenbrander, P. E., Parrish, K. D., Andersen, R. N. and Greenberg, E. P. (1995). Intergenic coaggregation of oral Treponema spp. with Fusobacterium spp. and intragenic coaggregation among Fusobacterium spp. Infection and Immunity. **63** (12): 4584-4588.

König, U., Nyman, A.-K. J. and Verdier, K. D. (2011). Prevalence of footrot in Swedish slaughter lambs. Acta Veterinaria Scandinavica. **53**: 27.

Kristensen, L. H. and Prag, J. (2000). Human necrobacillosis, with emphasis on Lemierre's syndrome. Clinical Infectious Diseases. **31** (2): 524-532.

Kumer, G. L. and Kiernan, J. A. (Dako) (2010). Special Stains and H&E [pdf] Available at: <http://www.histosense.net/Connectionv14.pdf#page=14> [Accessed 11 June 2010].

Kutter, S., Hartmann, A. and Schmid, M. (2006). Colonization of barley (*Hordeum*

vulgare) with *Salmonella enterica*. FEMS Microbiology Ecology. **56**: 262-271.

Laflamme, C., Gendron, L., Turgeon, N., Filion, G., Ho, J. and Duchaine, C. (2009). Rapid detection of germinating *Bacillus cereus* cells using fluorescent *in situ* hybridisation. Journal of Rapid Methods and Automation of Microbiology. **17**: 80-102.

La Fontaine, S., Egerton, J. R. and Rood, J. I. (1993). Detection of *Dichelobacter nodosus* using species-specific oligonucleotides as PCR primers. Veterinary Microbiology. **35** (1-2): 101-117.

Langworth, B. F. (1977). *Fusobacterium necrophorum*: its characteristics and role as an animal pathogen. Bacteriological Reviews. **41** (2): 373-390.

Layton, A., McKay, L., Williams, D., Garrett, V., Gentry, R. and Sayler, G. (2006). Development of *Bacteroides* 16S rRNA gene TaqMan-based real-time PCR assays for estimation of total, human, and bovine fecal pollution in water. Applied and Environmental Microbiology. **72** (6): 4214-4224.

Lechtenberg, K. F., Nagaraja, T. G. and Chengappa, M. M. (1998). Antimicrobial susceptibility of *Fusobacterium necrophorum* isolated from bovine hepatic abscesses. American Journal of Veterinary Research. **59** (1): 44-47.

Lefmann, M., Schweickert, B., Buchholz, P., Göbel, U. B., Ulrichs, T., Seiler, P., Theegarten, D. and Moter, A. (2006). Evaluation of peptide nucleic acid-fluorescence *in situ* hybridization for identification of clinically relevant mycobacteria in clinical specimens and tissue sections. Journal of Clinical Microbiology. **44** (10): 3760-3767.

Lindquist, M. E., Lifland, A. W., Utley, T. J., Santangelo, P. J. and Crowe, Jr. J. E. (2010). Respiratory syncytial virus induces host RNA stress granules to facilitate viral replication. Journal of Virology. **84** (23): 12274-12284.

Llobet-Brossa, E., Rosselló-Mora, R. and Amann, R. (1998). Microbial community composition of Wadden Sea sediments as revealed by fluorescence *in situ* hybridization.

Applied and Environmental Microbiology. **64** (7): 2691-2696.

Lopez, C., Pons, M. N. and Morgenroth, E. (2005). Evaluation of microscopic techniques (epifluorescence microscopy, CLSM, TPE-LSM) as a basis for the quantitative image analysis of activated sludge. Water Research. **39**: 456-468.

Love, D. N., Cato, E. P., Johnson, J. L., Jones, R. F. and Bailey, M. (1987). Deoxyribonucleic acid hybridization among strains of Fusobacteria isolated from soft tissue infections of cats: comparison with human and animal type strains from oral and other sites. International Journal of Systematic Bacteriology. **37** (1): 23-26.

Loy, A., Arnold, R., Tischler, P., Rattei, T., Wagner, M. and Horn, M. (2008). probeCheck - a central resource for evaluating oligonucleotide probe coverage and specificity. Environmental Microbiology. **10** (10): 2894-2898.

Lund, M., Nordentoft, S., Pedersen, K. and Madsen, M. (2004). Detection of *Campylobacter* spp. in chicken fecal samples by real-time PCR. Journal of Clinical Microbiology. **42** (11): 5125-5132.

Madsen, M., Sørensen, G. H., Aalbaek, B., Hansen, J. W. and Bjørn, H. (1992). Summer mastitis in heifers: studies on the seasonal occurrence of *Actinomyces pyogenes*, *Peptostreptococcus indolicus* and Bacteroidaceae in clinically healthy cattle in Denmark. Veterinary Microbiology. **30**: 243-255.

Mallmann, C., Siemoneit, S., Schmiedel, D., Petrich, A., Gescher, D. M., Halle, E., Musci, M., Hetzer, R., Göbel, U. B. and Moter, A. (2009). Fluorescence *in situ* hybridization to improve the diagnosis of endocarditis: a pilot study. Clinical Microbiology and Infection. **16**: 767-773.

Mao-Jones, J., Ritchie, K. B., Jones, L. E. and Ellner, S. P. (2010). How microbial community composition regulates coral disease development. PLoS Biology. **8** (3): e1000345.

Marsh, H. and Tunnicliff, E. A. (1934). Montana State College Agricultural Experiment Station Bulletin, No. 285.

Marshall, D. J., Walker, R. I., Cullis, B. R. and Luff, M. F. (1991). The effect of footrot on body weight and wool growth of sheep. Australian Veterinary Journal. **68** (2): 45-49.

Mattick, J. S., Anderson, B. J., Cox, P. T., Dalrymple, B. P., Bills, M. M., Hobbs, M. and Egerton, J. R. (1991). Gene sequences and comparison of the fimbrial subunits representative of *Bacteroides nodosus* serotypes A to I: class I and class II strains. Molecular Microbiology. **5** (3): 561-573.

Mattick, K. L., Jörgensen, F., Legan, J. D., Cole, M. B., Porter, J., Lappin-Scott, H. M. and Humphrey, T. J. (2000). Survival and filamentation of *Salmonella enterica* Serovar Enteritidis PT4 and *Salmonella enterica* Serovar Typhimurium DT104 at low water activity. Environmental Microbiology. **66** (4): 1274-1279.

Mayhew, L. (2004). Humic Substances in Biological Agriculture. ACRES USA, **34** (1&2). Available at: <http://www.acresusa.com/toolbox/reprints/Jan04_Humic %20Substances.pdf>. [Accessed February 24 2011].

McKern, N. M., O'Donnell, I. J., Stewart, D. J. and Clark, B. L. (1985). Primary structure of pilin protein from *Bacteroides nodosus* strain 216: comparison with the corresponding protein from strain 198. Journal of General Microbiology. **131**: 1-6.

Mohler, J. R. and Washburn, H. J. (1905) Foot-rot of sheep: its nature, cause and treatment. Government Printing Office. Washington, DC, USA. Available at: <http:// www.archive.org/stream/footrotofsheepit00mohliala/ footrotofsheepit00mohliala_djvu.txt> [Accessed 20 December 2011].

Monici, M., Pratesi, R., Bernabei, P. A., Caporale, R., Ferrini, P. R., Croce, A. C., Balzarini, P. and Bottiroli, G. (1995). Natural fluorescence of white blood cells:

spectroscopic and imaging study. Journal of Photochemistry and Photobiology. **30**: 29-37.

Moore, L. J., Wassink, G. J., Green, L. E. and Grogono-Thomas, R. (2005a). The detection and characterisation of *Dichelobacter nodosus* from cases of ovine footrot in England and Wales. Veterinary Microbiology. **108**: 57-67.

Moore, L. J., Woodward, M. J. and Grogono-thomas, R. (2005b) The occurrence of treponemes in contagious ovine digital dermatitis and the characterisation of associated *Dichelobacter nodosus*. Veterinary Microbiology. **111**: 199-209.

Morgan, K. (1987) Footrot. In Practice. **9**: 124-129.

Moses, E. K., Good, R. T., Sinistaj, M., Billington, S. J., Langford, C. J. and Rood, J. I. (1995). A multiple site-specific DNA-inversion model for the control of OmpI phase and antigenic variation in *Dichelobacter nodosus*. Molecular Microbiology. **17** (1): 183-196.

Moter, A. and Göbel, U. B. (2000). Fluorescence *in situ* hybridization (FISH) for direct visualization of microorganisms. Journal of Microbiological Methods. **41**: 85-112.

Munford, R. S. (2008). Sensing gram-negative bacterial lipopolysaccharides: a human disease determinant? Infection and Immunity. **76** (2): 454-465.

Myers, G. S. A., Parker, D., Al-Hasani, K., Kennan, R. M., Seemann, T., Ren, Q., Badger, J. H., Selengut, J. D., Deboy, R. T., Tettelin, H., Boyce, J. D., McCarl, V. P., Han, X., Nelson, W. C., Madupu, R., Mohamoud, Y., Holley, T., Fedorova, N., Khouri, H., Bottomley, S. P., Whittington, R. J., Adler, B., Songer, J. G., Rood, J. I. and Paulsen, I. T. (2007). Genome sequence and identification of candidate vaccine antigens from the animal pathogen *Dichelobacter nodosus*. Nature Biotechnology. **25** (5): 569-575.

Nagai, S., Kanoe, M. and Toda, M. (1984). Purification and partial characterisation of

Fusobacterium necrophorum hemagglutinin. Zentralblatt für Bakteriologie: International Journal of Medical Microbiology, Virology, Parasitology and Infectious Diseases. **258** (2-3): 232-241.

Nagano, Y., Watabe, M., Porter, K. G., Coulter, W. A., Millar, B. C., Elborn, J. S., Goldsmith, C. E., Rooney, P. J., Loughrey, A. and Moore, J. E. (2007). Development of a genus-specific PCR assay for molecular detection, confirmation and identification of *Fusobacterium* spp. British Journal of Biomedical Science. **64** (2): 74-77.

Nagaraja, T. G. and Lechtenberg, K. F. (2007). Liver abscesses in feedlot cattle. Veterinary Clinics of North America: Food Animal Practice. **23** (2): 351-369.

Nagaraja, T. G., Narayanan, S. K., Stewart, G. C. and Chengappa, M. M. (2005). *Fusobacterium necrophorum* infections in animals: Pathogenesis and pathogenic mechanisms. Anaerobe. **11**: 239-246.

Nagl, M., Kacani, L., Müllauer, B., Lemberger, E.-M., Stoiber, H., Sprinzl, G. M., Schennach, H. and Dierich, M. P. (2002). Phagocytosis and killing of bacteria by professional phagocytes and dendritic cells. Clinical and Vaccine Immunology. **9** (6): 1165-1168.

Narayanan, S. K., Nagaraja, T. G., Chengappa, M. M. and Stewart, G. C. (2002). Leukotoxins of gram-negative bacteria. Veterinary Microbiology. **84** (4): 337-356.

Naylor, R. D., Martin, P. K., Jones, J. R. and Burnell, M. C. (1998). Isolation of spirochaetes from an incident of severe virulent ovine footrot. Veterinary Record. **143**: 690-691.

Nestle, F. O., Meglio, P. D., Qin, J.-Z. and Nickoloff, B. J. (2009). Skin immune sentinels in health and disease. Immunology. **9**: 679-691.

Neumann, M. and Gabel, D. (2002). Simple method for reduction of autofluorescence in fluorescence microscopy. Journal of Histochemistry and Cytochemistry. **50** (3):

437-439.

Nieuwhof, G. J. and Bishop, S. C. (2005). Costs of the major endemic diseases of sheep in Great Britain and the potential benefits of reduction in disease impacts. Animal Science. **81**: 57-67.

Nocker, A., Cheung, C.-Y. and Camper, A. K. (2006). Comparison of propidium monoazide with ethidium monoazide for differentiation of live vs. dead bacteria by selective removal of DNA from dead cells. Journal of Microbiological Methods. **67**: 310-320.

Nocker, A., Sossa-Fernandez, P., Burr, M. D. and Camper, A. K. (2007). Use of propidium monoazide for live/dead distinction in microbial ecology. Applied and Environmental Microbiology. **73** (16): 5111-5117.

Nogva, H. K., Rudi, K., Naterstad, K., Holck, A. and Lillehaug, D. (2000). Application of 5'-nuclease PCR for quantitative detection of *Listeria monocytogenes* in pure cultures, water, skim milk, and unpasteurized whole milk. Applied and Environmental Microbiology. **66** (10): 4266-4271.

Ohkusa, T., Okayasu, I., Ogihara, T., Morita, K., Ogawa, M. and Sato, N. (2003). Induction of experimental ulcerative colitis by *Fusobacterium varium* isolated from colonic mucosa of patients with ulcerative colitis. Gut. **52**: 79-83.

Ohtani, F. (1970). Selective media for the isolation of non-sporulating gram-negative anaerobic rods. 2. Distribution of non-sporulating gram-negative anaerobic rods in the feces of normal human beings. Nihon Saikingaku Zasshi. **25** (5): 292-299. Cited by Tan, Z. L., Nagaraja, T. G. and Chengappa, M. M. (1996) *Fusobacterium necrophorum* infections: virulence factors, pathogenic mechanism and control measures. Veterinary Research Communications. 20: 113-140.

Okano, Y., Hristova, K. R., Leutenegger, C. M., Jackson, L. E., Denison, R. F.,

Gebreyesys, B., Lebauer, D. and Scow, K. M. (2004). Application of real-time PCR to study effects of ammonium on population size of ammonia-oxidizing bacteria in soil. Applied and Environmental Microbiology. **70** (2): 1008-1016.

Olson, M. E., Gard, M. S., Gradin, J. and Morck, D. W. (1998). Serological classification and virulence determination of *Dichelobacter nodosus* isolated from Alberta and British Columbia sheep. Canadian Journal of Veterinary Research. **62**: 33-37.

Onoe, T., Umemoto, T., Sagawa, H. and Suginaka, H. (1981). Filament formation of *Fusobacterium nucleatum* cells induced by mecillinam. Antimicrobial Agents and Chemotherapy. **19** (3): 487-489.

Palmer, M. A. (1993). A gelatin test to detect activity and stability of proteases produced by *Dichelobacter* (*Bacteroides*) *nodosus*. Veterinary Microbiology. **36**: 113-122.

Parajuli, B. and Goddard, P. J. (1989). A comparison of the efficacy of footbaths containing formalin or zinc sulphate in treating ovine foot-rot under field conditions. British Veterinary Journal. **145** (5): 467-472.

Parker, D., Kennan, R. M., Myers, G. S., Paulsen, I. T., Songer, J. G. and Rood, J. I. (2006). Regulation of type IV fimbrial biogenesis in *Dichelobacter nodosus*. Journal of Bacteriology. **188** (13): 4801-4811.

Parsonson, I. M., Egerton, J. R. and Roberts, D. S. (1967). Ovine interdigital dermatitis. Journal of Comparative Pathology. **77**: 309-313.

Pathak, S., Awuh, J. A., Leversen, N. A., Flo, T. H. and Asjo, B. (2012). Counting Mycobacteria in infected human cells and mouse tissue: a comparison between qPCR and CFU. PloS one. **7** (4): e34931.

Perry-O'Keefe, H., Rigby, S., Oliveira, K., Sørensen, D., Stender, H., Coull, J. and

Hyldig-Nielsen, J. J. (2001). Identification of indicator microorganisms using a standardized PNA FISH method. Journal of Microbiological Methods. **47**: 281-292.

Peters, I. R., Helps, C. R., Willi, B., Hofmann-Lehmann, R., Gruffydd-Jones, T. J., Day, M. J. and Tasker, S. (2011). Detection of feline haemoplasma species in experimental infection by *in-situ* hybridisation. Microbial Pathogenesis. **50** (2): 94-99.

Phillips, R., Horsfield, C., Kuijper, S., Lartey, A., Tetteh, I., Etuaful, S., Nyamekye, B., Awuah, P., Nyarko, K. M., Osei-Sarpong, F., Lucas, S., Kolk, A. H. J. and Wansbrough-Jones, M. (2005). Sensitivity of PCR targeting the *IS2404* insertion sequence of *Mycobacterium ulcerans* in an assay using punch biopsy specimens for diagnosis of buruli ulcer. Journal of Clinical Microbiology. **43** (8): 3650-3656.

Pimentel-Elardo, S., Wehrl, M., Friedrich, A. B., Jensen, P. R. and Hentschel, U. (2003). Isolation of planctomycetes from *Aplysina* sponges. Aquatic Microbial Ecology. **33**: 239-245.

Píriz, D. S., Manzano, J. V., Cuenca, V., Vadillo, M. S. (1990a). Susceptibilities of *Bacteroides* and *Fusobacterium* spp. from foot rot in goats to 10 β-lactam antibiotics. Antimicrobial Agents and Chemotherapy. **34** (4): 657-659.

Píriz, D. S., Manzano, J. V., Cuenca, V., Vadillo, M. S. (1990b). *In-vitr*o antimicrobial susceptibility of *Bacteroides* and *Fusobacterium* isolated from footrot in goats. British Veterinary Journal. **14** (5): 437-442.

Píriz, D. S., Cuenca, V. R., Valle, M. J. and Vadillo, M. S. (1990c). Isolation and identification of anaerobic bacteria from ovine foot rot in Spain. Research in Veterinary Science. **49** (2): 245-247.

Píriz, D. S., Cuenca, V. R., Vadillo, M. S., Manzano, J. V. and Vadillo, M. S. (1991). Comparative in vitro susceptibility of *Bacteroides* and *Fusobacterium* isolated from footrot in sheep to 28 antimicrobial agents. Journal of Veterinary Pharmacology and

Therapeutics. **14** (2): 185-192.

Píriz, S., Hurtado, M. A., Valle, J., Mateos, E. M., Martin-Palomino, P., and Vadillo, S. (1996). Bacteriological study of footrot in pigs: a preliminary note. Veterinary Record. **139**: 17-19.

Pontiroli, A., Travis, E. R., Sweeney, F. P., Porter, D., Gaze, W. H., Mason, S., Hibberd, V., Holden, J., Courtenay, O. and Wellington, E. M. H. (2011). Pathogen quantitation in complex matrices: a multi-operator comparison of DNA extraction methods with a novel assessment of PCR inhibition. PloS one. **6** (3): e17916.

Poulsen, L. K., Ballard, G. and Stahl, D. A. (1993). Use of rRNA fluorescence *in situ* hybridization for measuring the activity of single cells in young and established biofilms. Applied and Environmental Microbiology. **59** (5): 1354-1360.

Prosser, J. I., Bohannan, B. J. M., Curtis, T. P., Ellis, R. J., Firestone, M. K., Freckleton, R. P., Green, J. L., Green, L. E., Killham, K., Lennon, J. J., Osborn, A. M., Solan, M., van der Gast, C. J. and Young, J. P. W. (2007). The role of ecological theory in microbial ecology. Nature Reviews Microbiology. **5**: 384-392.

Raadsma, H. W., O'Meara, T. J., Egerton, J. R., Lehrbach, P. R. and Schwartzkoff, C. L. (1994). Protective antibody titres and antigenic competition in multivalent *Dichelobacter nodosus* fimbrial vaccines using characterised rDNA antigens. Veterinary Immunology and Immunopathology. **40**: 253-274.

Rabash, J., Carlton, C., Browne, W. J., Healy, M. and Cameron, B. (2005). MLwiN Version 2.02. Centre for multilevel modelling. University of Bristol.

Ramirez, S., Hild, T. G., Rudolph, C. N., Sty, J. R., Kehl, S. C., Havens, P., Henrickson, K. and Chusid, M. J. (2003). Increased diagnosis of Lemierre Syndrome and other *Fusobacterium necrophorum* infections at a children's hospital. Pediatrics. **112** (5): e380-e380.

Rampersad, J., Johnson, J., Brown, G., Samlal, M. and Ammons, D. (2008) Comparison of polymerase chain reaction and bacterial culture for *Salmonella* detection in the Muscovy duck in Trinidad and Tobago. Revista Panam Salud Publica. **23** (4): 264-267.

Riordan, T. (2007). Human infection with *Fusobacterium necrophorum* (Necrobacillosis), with a focus on Lemierre's Syndrome. Clinical Microbiology Reviews. **20** (4): 622-659.

Roberts, D. S. (1968). The pathogenic synergy of *Fusiformis necrophorus* and *Corynebacterium pyogenes*. I. The influence of the leucocidal exotoxin of *F. necrophorus*. British Journal of Experimental Pathology. **48** (6): 665-673.

Roberts, D. S. and Egerton. J. R. (1969). The aetiology and pathogenesis of ovine foot-rot. II. The pathogenic association of *Fusiformis nodosus* and *F. necrophorus*. Journal of Comparative Pathology. **79**: 217-227.

Rogers, G. B., Caroll, M. P. and Bruce K. D. (2009). Studying bacterial infections through culture-independent approaches. Journal of Medical Microbiology. **58**: 1401-1418.

Romero, C., Hamdi, A., Valentine, J. F. and Naser, S. A. (2005). Evaluation of surgical tissue from patients with Crohn's Disease for the presence of *Mycobacterium avium* subspecies *paratuberculosis* DNA by *in situ* hybridization and nested polymerase chain reaction. Inflammatory Bowel Disease. **11** (2): 116-125.

Ruder, C. A., Sasser, R. G., Williams, R. J., Ely, J. K., Bull, R. C. and Butler, J. E. (1981). Uterine infections in the postpartum cow. Theriogenology, **15** (6): 573-580.

Russell, C. L., Smith, E. M., Calvo-Bado, L. A., Kaler, J., Medley, G. F., Green, L. E., Wellington, E. M. H., Moore, L. J. and Grogono-Thomas, R. (in press). Development of a Multiple Locus VNTR Analysis method for typing *Dichelobacter*

nodosus, the causal agent of footrot in sheep.

Russell, B. H., Liu, Q., Jenkins, S. A., Tuvim, M. J., Dickey, B. F. and Xu, Y. (2008). *In vivo* demonstration and quantification of intracellular *Bacillus anthracis* in lung epithelial cells. Infection and Immunity. **76** (9): 3975-3983.

Salyers, A. A. and Whitt, D. D. (2002) An Uneasy Truce: Never Underestimate the Power of Bacteria. In: Bacterial Pathogenesis A Molecular Approach. Washington DC: ASM Press. 3-15.

Santelli, C. M., Orcutt, B. N., Banning, E., Bach, W., Moyer, C. L., Sogin, M. L., Staudigel, H. and Edwards, K. J. (2008). Abundance and diversity of microbial life in ocean crust. Nature Letters. **453**: 653-656.

Saukkoriipi, A., Kaijalaninen, T., Kuisma, L., Ojala, L. and Leinonen, M. (2003). Isolation of pneumococcal DNA from nasopharyngeal samples for real-time, quantitative PCR: comparison of three methods. Molecular Diagnostics. **7** (1): 9-15.

Sbordone, L. and Bortolaia, C. (2003). Oral microbial biofilms and plaque-related diseases: microbial communities and their role in the shift from oral health to disease. Clinical Oral Investigations. **7**: 181-188.

Schmiedel, D., Epple, H.-J., Loddenkemper, C., Ignatius, R., Wagner, J., Hammer, B., Petrich, A., Stein, H., Göbel, U. B., Schneider, T. and Moter, A. (2009). Rapid and accurate diagnosis of human intestinal spirochetosis by fluorescence *in situ* hybridization. Journal of Clinical Microbiology. **47** (5): 1393-1401.

Schramm, A., Fuchs, B. M., Nielsen, J. L., Tonolla, M. and Stahl, D. A. (2002). Fluorescence *in situ* hybridization of 16S rRNA gene clones (Clone-FISH) for probe validation and screening of clone libraries. Environmental Microbiology. **4** (11): 713-720.

Schwartzkoff, C. L., Egerton, J. R., Stewart, D. J., Lehrbach, P. R., Elleman, T. C.

and Hoyne, P. A. (1993). The effects of antigenic competition of the efficacy of multivalent footrot vaccines. Australian Veterinary Journal. **70** (4): 123-126.

Sha, B. E., Zariffard, M. R., Wang, Q. J., Chen, H. Y., Bremer, J., Cohen, M. H. and Spear, G. T. (2005). Utility of amsel criteria, nugent score and quantitative PCR for *Gardnerella vaginalis*, *Mycoplasma hominis* and *Lactobacillus* spp. for diagnosis of bacterial vaginosis in human immunodeficiency virus-infected women. **43** (9): 4607-4612.

Simeonov, A. and Nikiforov, T. (2002). Single nucleotide polymorphism genotyping using short, fluorescently labelled locked nucleic acid (LNA) probes and fluorescence polarisation detection. Nucleic Acid Research. **30**: e91.

Skerman, T. M. (1975). Determination of some *in vitro* growth requirements of *Bacteroides nodosus*. Journal of General Microbiology. **87**: 107-119.

Smith, G. R., Till, D., Wallace, L. M. and Noakes, D. E. (1989). Enhancement of the infectivity of *Fusobacterium necrophorum* by other bacteria. Epidemiology and Infection. **102**: 447-458.

Smith, G. R., Barton, S. A. and Wallace, L. M. (1991). A sensitive method for isolating *Fusobacterium necrophorum* from faeces. Epidemiology and Infection. **106** 311-317.

Smith, G. R. and Thornton, E. A. (1993a). Effect of disturbance of the gastrointestinal microflora on the faecal excretion of *Fusobacterium necrophorum* biovar A. Epidemiology and Infection. **110**: 333-337.

Smith, G. R. and Thornton, E. A. (1993b). The prevalence of *Fusobacterium necrophorum* biovar A in animal faeces. Epidemiology and Infection. **110**: 327-331.

Smith, G. R. and Thornton, E. A. (1997). Classification of human and animal strains of *Fusobacterium necrophorum* by their pathogenic effects in mice. Journal of Medical

Microbiology. **46**: 879-882.

Smith-Vaughan, H., Byun, R., Nadkarni, M., Jacques, N. A., Hunter, N., Halpin, S., Morris, P. S. and Leach, A. J. (2006). Measuring nasal bacterial load and its association with otitis media. BMC Ear, Nose and Throat Disorders. **6** (10): 1-9.

Socranksy, S. S., Gibbon, R. J., Dale, A. C., Bortnick, L., Rosenthal, E. and Macdonald, J.B. (1963). The microbiota of the gingival crevice area of man. I. Total microscopic and viable counts of specific organisms. Archives of Oral Biology. **8**: 275-280.

Srinivasan, S., Liu, C., Mitchell, C. M., Fiedler, T. L., Thomas, K. K., Agnew, K. J., Marrazzo, J. M. and Fredricks, D. N. (2010). Temporal variability of human vaginal bacteria and relationship with bacterial vaginosis. PloS one. **5** (4): e10197.

Stelzel, M., Conrads, G., Pankuweit, S., Maisch, B., Vogt, S., Moosdorf, R. and Flores-de-Jacoby, L. (2002). Detection of *Porphyromonas gingivalis* DNA in aortic tissue by PCR. Journal of Periodontology. **73** (8): 868-870.

Stewart, D. J. (1989). Footrot of Sheep. In: J. R.Egerton, W. K. Yong and G. G. Riffin, eds. Footrot and Foot Abscess of Ruminants. Florida: CRC Press: 5-46.

Stoecker, K., Dorninger, C., Daims, H. and Wagner, M. (2010). Double labeling of oligonucleotide probes for fluorescence *in situ* hybridization (DOPE-FISH) improves signal intensity and increases rRNA accessibility. Applied and Environmental Microbiology. **76** (3): 922-926.

Takada, T., Matsumoto, K. and Nomoto, K. (2004). Development of multi-color FISH method for analysis of seven *Bifidobacterium* species in human feces. Journal of Microbiological Methods. **58**: 413-421.

Tan, Z. L., Nagaraja, T. G. and Chengappa, M. M. (1992). Factors affecting the leukotoxin activity of *Fusobacterium necrophorum*. Veterinary Microbiology. **32**:

15-28.

Tan, Z. L., Nagaraja, T. G., Chengappa, M. M. and Smith, J. S. (1994). Biological and biochemical characterization of *Fusobacterium necrophorum* leukotoxin. American Journal of Veterinary Research. **55** (4): 515-521.

Tan, Z. L., Nagaraja, T. G. and Chengappa, M. M. (1996) *Fusobacterium necrophorum* infections: virulence factors, pathogenic mechanism and control measures. Veterinary Research Communications. **20**: 113-140.

Tanjung, L. R., Whittle, G., Shaw, B. E., Bloomfield, G. A., Katz, M. E. and Cheetham, B. F. (2009). The *intD* mobile genetic element from *Dichelobacter nodosus*, the causative agent of ovine footrot, is associated with the benign phenotype. Anaerobe. **15** (5): 219-224.

Taylor, M. W., Schupp, P. J., Dahllof, I., Kjelleberg, S. and Steinberg, P. D. (2003). Host specificity in marine sponge-associated bacteria, and potential implications for marine microbial diversity. Environmental Microbiology. **6** (2): 121-130.

Thimm, T. and Tebbe, C. C. (2003). Protocol for rapid fluorescence in situ hybridization of bacteria in cryosections of microarthropods. Applied and Environmental Microbiology. **69** (5): 2875-2878.

Thomas, J. H. (1958). A simple medium for the isolation and cultivation of *Fusiformis nodosus*. Australian Veterinary Journal. **34** (12): 411.

Thurnheer, T., Gmür, R. and Guggenheim, B. (2004). Multiplex FISH analysis of a six-species bacterial biofilm. Journal of Microbiological Methods. **56**: 37-47.

Travis, E. R., Gaze, W. H., Pontiroli, A., Sweeney, F. P., Porter, D., Mason, S., Keeling, M. J. C., Jones, R. M., Sawyer, J., Aranaz, A., Razaldos, E. C., Cork, J., Delahay, R. J., Wilson, G. J., Hewinson, R. G., Courtenay, O. and Wellington, E. M. H.. (2011). An inter-laboratory validation of a real time PCR assay to measure host

excretion of bacterial pathogens, particularly of Mycobacterium bovis. PLoS one. **6** (11): e27369.

Trebesius, K., Adler, K., Vieth, M., Stolte, M. and Hass, R. (2001). Specific detection and prevalence of *Helicobacter heilmannii*-like organisms in the human gastric mucosa by fluorescent *in situ* hybridization and partial 16S ribosomal DNA sequencing. Journal of Clinical Microbiology. **39** (4): 1510-1516.

Van der Woude, M. W. and Bäumler, A. J. (2004). Phase and antigenic variation in bacteria. Clinical Microbiology Reviews. **17** (3): 581-611.

Vannini, C., Ferrantini, F., Schleifer, K.-H., Ludwig, W., Verni, F. and Petroni, G. (2010). "*Candidatus anadelfobacter veles*" and "*Candidatus cyrtobacter comes*," two new *Rickettsiales* species hosted by the protist ciliate *Euplotes harpa* (*Ciliophora, Spirotrichea*). Applied and Environmental Microbiology. **76** (12): 4047-4054.

Vatn, S., Hektoen, L., Høyland, B. Reiersen, A., Kampen, A.H. and Jørgensen, H. J. (2012). Small Ruminant Research. In Press.

Verstraelen, H., Verhelst, R., Claeys, G., Temmerman, M. and Vaneechoutte, M. (2004). Culture-independent analysis of vaginal microflora: the unrecognized association of *Atopobium vaginae* with bacterial vaginosis. American Journal of Obstetrics and Gynecology. **191**: 1130-1132.

Von Wissman, B., Klinc, C., Schulze, R., Wolf, A., Schreiner, H., Rabsch, W., Prager, R. and Hautmann, W. (2012). Outbreak of salmonellosis after a wedding part, Bavaria, Germany, summer 2010: the importance of implementing food safety concepts. Euro Surveillance. **17** (6): 20076.

Wagner, M., Erhart, R., Manz, W., Amann, R., Lemmer, H., Wedi, and. & Schleifer, K.-H. (1994). Development of an rRNA-targeted oligonucleotide probe specific for the genus *Acinetobacter* and its application for *in situ* monitoring in

activated sludge. Applied and Environmental Microbiology. **60** (3): 792-800.

Walberg, M., Gaustad, P. and Steen, H. B. (1999). Uptake kinetics of nucleic acid targeting dyes in *S. aureus*, *E. faecalis* and *B. cereus*: a flow cytometric study. Journal of Microbiological Methods. **35**: 167-176.

Wallner, G., Amann, R. and Beisker, W. (1993). Optimizing fluorescent *in situ* hybridization with rRNA-targeted oligonucleotide probes for flow cytometric identification of microorganisms. Cytometry. **14**: 136-143.

Wani, S. A., Samanta, I. and Kawoosa, S. (2007). Isolation and characterization of *Dichelobacter nodosus* from ovine and caprine footrot in Kashmir, India. Research in Veterinary Science. **83**: 141-144.

Wassink, G. J., Grogono-Thomas, R., Moore, L. J. and Green, L. E. (2003). Risk factors associated with the prevalence of footrot in sheep from 1999 to 2000. Veterinary Record. **152**: 351-358.

Wassink, G. J., Grogono-Thomas, R., Moore, L. J. and Green, L. E. (2004). Risk factors associated with the prevalence of interdigital dermatitis in sheep from 1999 to 2000. Veterinary Record. **154**: 551-555.

Wassink, G. J., Moore, L. J., Grogono-Thomas, R. and Green, L. E. (2005). Footrot and interdigital dermatitis in sheep: farmers' practices, opinions and attitudes. Veterinary Record. **157**: 761-766.

Wassink, G. J., Green, L. E., Moore, L. J. and Grogono-Thomas, R. (2006) Footrot and interdigital dermatitis in sheep. Veterinary Record. **158**: 71-72.

Wassink, G. J., George, T. R. N., Kaler, J. and Green, L. E. (2010a). Footrot and interdigital dermatitis in sheep: Farmer satisfaction with current management, their ideal management and sources used to adopt new strategies. Preventive Veterinary Medicine. **96**: 65-73.

Wassink, G. J., King, E. M., Grogono-Thomas, R., Brown, J. C., Moore, L. J. and Green, L. E. (2010b). A within farm clinical trial to compare two treatments (parenteral antibacterials and hoof trimming) for sheep lame with footrot. Preventive Veterinary Medicine. **96**: 93-103.

Wessendorf, M. W. and Brelje, T. C. (1992). Which fluorophore is brightest? A comparison of the staining obtained using fluorescein, tetramethylrhodamine, lissamine rhodamine, Texas Red, and cyanine 3.18. Histochemistry. **98**: 81-85.

Westmacott, D. and Perkins, H. R. (1979). Effects of lysozyme on *Bacillus cereus* 569: rupture of chains of bacteria and enhancement of sensitivity to autolysins. Journal of General Microbiology. **115**: 1-11.

Whiley, H., Taylor, M. and Bentham, R. (2011). Detection of *Legionella* species in potting mixes using fluorescent *in situ* hybridisation (FISH). Journal of Microbiological Methods. **86** (3): 304-309.

Whittington, R. J. (1995). Observations of the indirect transmission of virulent ovine footrot in sheep yards and its spread in sheep on unimproved pasture. Australian Veterinary Journal. **72** (4): 132-134.

Wilson, I. G. (1997). Inhibition and facilitation of nucleic acid amplification. Applied and Environmental Microbiology. **63** (10): 3741-3751.

Winter, A. C. (2008). Lameness in sheep. Small Ruminant Research. **76**: 149-153.

Wu, H.-J., Wang, A. H.-J. and Jennings, M. P. (2008). Discovery of virulence factors of pathogenic bacteria. Current Opinion in Chemical Biology. **12**: 1-9.

Yeruham, I. and Elad, D. (2004). Necrotizing stomatitis associated with *Fusobacterium necrophorum* in two goats. Journal of Veterinary Medicine. **51**: 46-47.

Youatt, W. (1837). Sheep: their breeds, management and diseases. London, UK.: Baldwin and Cradock. 523. Cited by Buller, N. (2005). “Molecular epidemiology,

clonality and virulence of *Dichelobacter nodosus,* the agent of ovine footrot." PhD thesis, University of Murdoch, Australia.

Young, J.-D., Ko, S. S. and Cohn, Z. A. (1984). The increase in intracellular free calcium associated with IgG gamma 2b/gamma 1 Fc receptor-ligand interactions: role in phagocytosis. Proceedings of the National Academy of Sciences. **81**: 5430-5434.

Young, K.D. (2006). The selective value of bacterial shape. Microbiology and Molecular Biology Reviews. **70** (3): 660-703.

Zhang, F., Nagaraja, T. G., George, D. and Stewart, G. C. (2006). The two major subspecies of *Fusobacterium necrophorum* have distinct leukotoxin operon promoter regions. Veterinary Microbiology. **112**: 73-78.

Zhou, H. and Hickford, J. G. (2000). Extensive diversity in New Zealand *Dichelobacter nodosus* strains from infected sheep and goats. Veterinary Microbiology. **71**: 113-123.